University of Milano-Bicocca
Department of Biotechnology and Biosciences
Doctoral thesis in Life Sciences – Cycle XXIX

An integrated approach to study Ras-dependent cancer metabolic rewiring in mouse fibroblasts

Gaia De Sanctis
ID 709575

Academic Year 2015-2016

SCUOLA DI DOTTORATO
UNIVERSITÀ DEGLI STUDI DI MILANO-BICOCCA

Department of Biotechnology and Biosciences

PhD program in Life Sciences, Cycle XXIX

Curriculum in Industrial Biotechnology

AN INTEGRATED APPROACH TO STUDY RAS-DEPENDENT CANCER METABOLIC REWIRING IN MOUSE FIBROBLASTS

Surname DE SANCTIS Name GAIA

Registration number 709575

Tutor and Supervisor: Dr. ELENA SACCO

Coordinator: Prof. MARCO VANONI

ACADEMIC YEAR 2015/2016

“Nothing in life is to be feared, it is only to be understood. Now is the time to understand more, so that we may fear less.”

Marie Curie

ABSTRACT

Cancer cells adapt their metabolism to meet the energetic and biosynthetic demands associated to their enhanced growth. Metabolic alterations in cancer are under direct control of oncogenes such as *ras*, and include the increase in glucose and glutamine consumption, decreased mitochondrial activity and increase in ROS production. Since molecules out of many cascades of interconnected biochemical pathways are involved in oncogenesis, cancer is a Systems Biology disease, requiring the integration of the knowledge derived from experimental results through mathematical models.

Here we study the effect of *K-ras* oncogene activation in NIH3T3 mouse fibroblasts on transport and metabolism of cysteine and methionine, the two proteinogenic sulphur-containing amino acids. While methionine may act as a precursor for cysteine synthesis, cysteine is in turn a precursor for the biosynthesis of antioxidant glutathione. We show that cysteine limitation and deprivation cause apoptotic cell death in both normal and *K-ras*-transformed fibroblasts (NIH-RAS), due to accumulation of reactive oxygen species and a decrease in reduced glutathione. Only cysteine-containing glutathione partly rescues the cell growth defect induced by limiting cysteine, showing that mouse fibroblasts use cysteine mainly in the synthesis of glutathione and require an exogenous cysteine source for protein synthesis. On the contrary, methionine limitation and deprivation

have only a cytostatic effect on mouse fibroblasts, unaffected by glutathione. NIH-RAS cells -but not their parental NIH3T3- are extremely sensitive to methionine limitation. This fragility correlates with decreased expression of the Slc6a15 gene -encoding the nutrient transporter SBAT1, known to exhibit a strong preference for methionine- and decreased methionine uptake. Remarkably, expression of the ortholog human gene SLC6A15 is mostly down-regulated in the NCI-60 human cancer cells. An exception is represented by melanoma cells, in which SLC6A15 is highly up-regulated. Thus, therapeutic regimens of cancer involving modulation of methionine metabolism could be more effective in cells with limited methionine transport capability.

We next study glutamine roles in metabolism and redox homeostasis in *K-ras*-transformed NIH3T3 mouse fibroblasts (NIH-RAS), by complementing glutamine deprivation with dimethyl-α-ketoglutarate (AKG) and nonessential amino acids (NEAA). The combination AKG+NEAA only partly rescues glutamine deprivation and weakly activates mTOR pathway. This substitution results in low levels of nucleotides and the non-use of reductive carboxylation of AKG –predicted by ENGRO model– to synthesize lipids, whose content is lower due to downregulated expression of genes involved in lipogenesis that correlates with lower NADPH levels.

Thus, in NIH-RAS cells glutamine is essential as a carbon and nitrogen source for biosynthesis (amino acids, nucleotides and glutathione) and as a signaling molecule.

We successfully exploit an integrated, Systems Biology approach to study nutritionally-perturbed transformed cells, pushing forward a system-level understanding of complex diseases like cancer.

RIASSUNTO

Le cellule tumorali adattano il loro metabolismo per far fronte alle richieste energetiche e biosintetiche associate alla loro maggiore crescita. Le alterazioni metaboliche nel cancro sono sotto il controllo diretto di oncogeni come ras e includono l'aumento del consumo di glucosio e glutammina, una ridotta attività mitocondriale e un aumento nella produzione di specie reattive dell'ossigeno (ROS). Poiché molecole appartenenti a molteplici cascate di vie biochimiche interconnesse sono coinvolte nel processo di oncogenesi, il cancro è una malattia che necessita di essere studiata attraverso la Biologia dei Sistemi e che richiede l'integrazione della conoscenza derivante dai risultati sperimentali all'interno di modelli matematici.

In questa tesi viene studiato l'effetto dell'attivazione dell'oncogene K-ras in fibroblasti murini NIH3T3 sul trasporto e sul metabolismo di cisteina e metionina, i due amminoacidi solforati utilizzati nella sintesi proteica. Mentre la metionina può fungere da precursore per la sintesi della cisteina, la cisteina, a sua volta, è un precursore per la biosintesi dell'antiossidante glutatione. I dati qui riportati mostrano che la limitazione e la deprivazione di cisteina causano la morte cellulare per apoptosi sia nelle cellule normali sia in quelle trasformate da K-ras (NIH-RAS), a causa dell'accumulo di specie reattive dell'ossigeno e di una diminuzione del glutatione ridotto. Soltanto il glutatione, che contiene la

cisteina nella sua struttura, complementa parzialmente il difetto di crescita indotto dalla limitazione di cisteina, evidenziando così che i fibroblasti murini utilizzano la cisteina soprattutto per la sintesi del glutatione e richiedono una fonte esterna di cisteina per la sintesi proteica. Al contrario, la limitazione e la deprivazione di metionina hanno soltanto un effetto citostatico sui fibroblasti murini, il quale non viene eliminato dal glutatione. Le cellule NIH-RAS, ma non le cellule NIH3T3 da cui derivano, sono estremamente sensibili alla limitazione da metionina. Tale fragilità correla con una ridotta espressione del gene Slc6a15, che codifica per il trasportatore di nutrienti SBAT1, noto per possedere una forte preferenza per la metionina, e con una ridotta internalizzazione della metionina. Di notevole interesse è il fatto che l'espressione del gene ortologo umano SLC6A15 è per la maggior parte downregolato nelle cellule tumorali umane che costituiscono il pannello NCI-60. Un'eccezione è rappresentata dalle cellule di melanoma, nelle quali il gene SLC6A15 è fortemente upregolato. Le terapie antitumorali che prevedono la modulazione del metabolismo della metionina potrebbero, dunque, essere più efficaci nelle cellule che possiedono limitate capacità di trasporto della metionina.

In seguito viene presentato lo studio dei ruoli della glutammina nel metabolismo e nell'omeostasi redox in fibroblasti murini trasformati da K-ras (NIH-RAS), tramite la complementazione della deprivazione di glutammina con dimetil-α-chetoglutarato (AKG) e amminoacidi non

essenziali (NEAA). La combinazione AKG+NEAA complementa la deprivazione di glutammina e attiva il pathway di mTOR soltanto parzialmente. Tale sostituzione ha, come conseguenza, una riduzione dei livelli di nucleotidi e, come predetto dal modello ENGRO, il mancato utilizzo della carbossilazione riduttiva dell'AKG per la sintesi dei lipidi. Il contenuto lipidico, inoltre, è minore a causa di una ridotta espressione dei geni coinvolti nella sintesi lipidica, che correla con livelli inferiori di NADPH.

Nelle cellule NIH-RAS, dunque, la glutammina è essenziale come fonte di carbonio e di azoto per la biosintesi degli amminoacidi, dei nucleotidi e del glutatione, oltre che come molecola coinvolta nella biosegnalazione.

E' stato utilizzato con successo un approccio integrato di Biologia dei Sistemi per lo studio delle cellule trasformate cresciute in perturbazione nutrizionale, utile nella comprensione a livello di sistema di malattie complesse come il cancro.

INDEX

1. INTRODUCTION

1.1 Cancer cell biology

Mammalian cells require proliferation to sustain embryogenesis, growth and functioning of most tissues. The first studies on cell proliferation focused on signal transduction pathways, by which cells start and maintain cell cycle. However, metabolism also plays an important role in cell cycle during doubling of total biomass (proteins, lipids and nucleic acids) [1]. When specific alterations in metabolism occur, cells over-proliferate and acquire malignant properties.

Indeed, cancer is defined as a set of diseases in which cells become abnormal and start an uncontrolled proliferation that leads them to invade nearby tissues [2]. Cancer is a major cause of morbidity and mortality, with approximately 14 million new cases and 8 million cancer-related deaths in 2012, affecting populations in all countries and all regions. Prostate and breast cancers are the most common sites in men and women, respectively, together with lung and colorectal cancers (**Figure 1.1**).

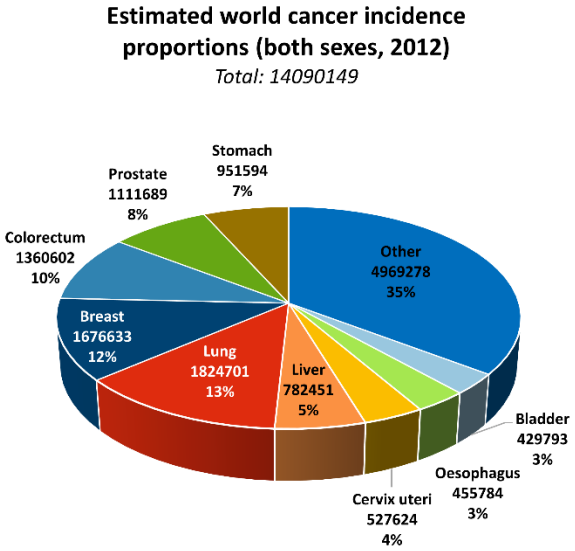

Figure 1.1 Estimated world cancer incidence. Adapted from World Cancer Report 2014. *The figure reports estimated world cancer incidence proportions by major sites, in both sexes combined, in men, and in women, 2012.*

While a high heterogeneity exists among more than 100 types of cancer, tumors also show some similarities, known as “hallmarks of cancer” and first outlined by Hanahan and Weinberg [3]. The mechanisms that integrate signal transduction and cell metabolism are largely conserved between normal and cancer cells. While in the first ones extracellular stimulation is required to initiate signaling, cancer cells often have mutations that chronically alter metabolic pathways, allowing them to maintain a metabolic phenotype of biosynthesis independently of normal physiologic constraints [1,4,5]. For example, activating mutations in the *RAS* signaling pathway controlling proliferative signals are frequently found in a variety of cancers [6]. Besides enhanced proliferative signals,

cancer progression also requires the inactivation of tumor suppressor genes, such as *TP53* or *RB* [7,8], that negatively control cell proliferation. Moreover, cancer cells must circumvent the inherent cell death program of apoptosis, which serves as a natural barrier to cancer development. Indeed, tumor cells adopt a variety of strategies to evade this process, such as induction of antiapoptotic regulators (BCL-2, BCL-xL) or downregulation of proapoptotic factors (BAX, BIM, PUMA) [9,10,11]. Senescence and crisis are the two main mechanisms that limit replicative potential in healthy tissues, by maintaining cells in a resting but viable state and by involving cell death, respectively. The enzyme telomerase confers to cancer cells the resistance to both senescence and crisis [12] and renders them immortalized. To spread into an organism, however, cancer cells also need nutrients and oxygen as well as the ability to evacuate metabolic wastes and carbon dioxide efficiently. Angiogenesis is the process that allows the formation of new vessels to fulfill these requirements. In tumors, angiogenesis remains activated, following for example the upregulation of VEGF, a pro-angiogenic signal [13]. This causes normally quiescent vasculature to continually sprout new vessels and sustain the expansion of malignancy [14]. Indeed, cancer cells spread in the organism in a multistep process of invasion and metastasis. The first step of the process is the local invasion, which evolves in the intravasation into nearby blood and lymphatic vessels. The transit of cancer cells through the lymphatic and hematogenous system is followed by

extravasation and formation of micrometastases that grow into macroscopic tumors in a process called colonization [15]. During invasion and metastasis, cancer cells develop alterations in their shape as well as in their attachment to other cells and to the extracellular matrix [16].

Two new hallmarks of cancer emerged over the last years [17] (**Figure 1.2**). First, the capacity of cancer cells to evade the immune system, which is responsible for detecting and eliminating the vast majority of incipient cancer cells and nascent tumors. Second, the reprogramming of cancer metabolism. Indeed, to achieve all the above-mentioned hallmarks, cancer cells must reorganize the metabolic network at the service of an increased demand of energy and macromolecules to sustain cell proliferation and tumorigenesis [18].

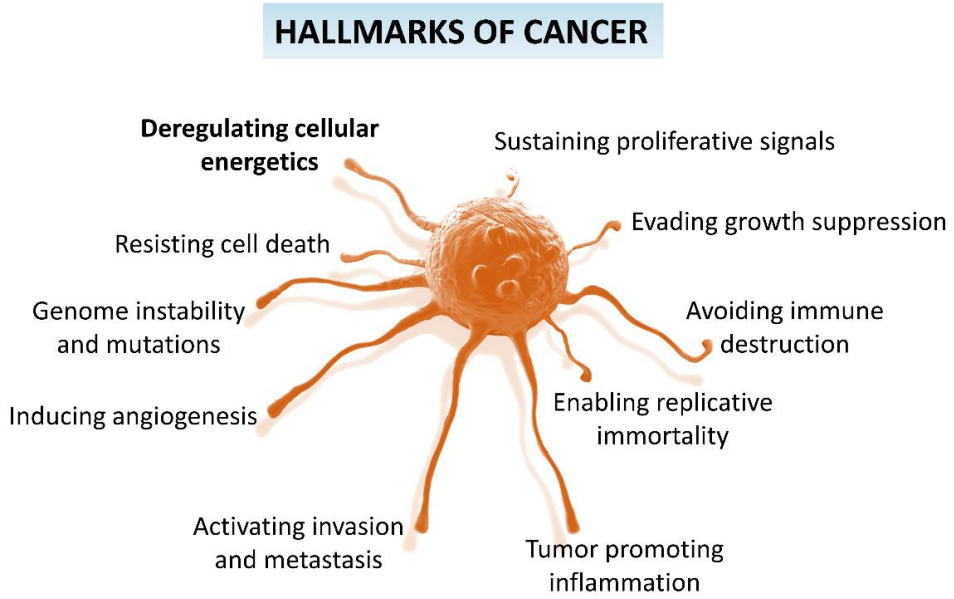

Figure 1.2 Hallmarks of cancer. Adapted from [17]. *Besides the six hallmark capabilities originally proposed in [3], two additional hallmarks of cancer are involved in the pathogenesis of cancers. One involves the capability to modify, or reprogram, cellular metabolism in order to most effectively support neoplastic proliferation. The second allows cancer cells to evade immunological destruction. Additionally, two consequential characteristics of neoplasia are genomic instability and thus mutability, which endow cancer cells with genetic alterations that drive tumor progression. Inflammation by innate immune cells designed to fight infections and heal wounds can instead support multiple hallmark capabilities, thereby manifesting the tumor-promoting consequences of inflammatory responses.*

Metabolic reprogramming offers tumor cells the possibility either to grow at higher rates than normal cells or to proliferate during harsh conditions [19]. The studies of Otto Warburg in the 1920s first highlighted the link between metabolic alterations and oncogenesis, by showing that cancer cells ferment glucose to lactate at high rates even in the presence of oxygen [20] (**Figure 1.3**).

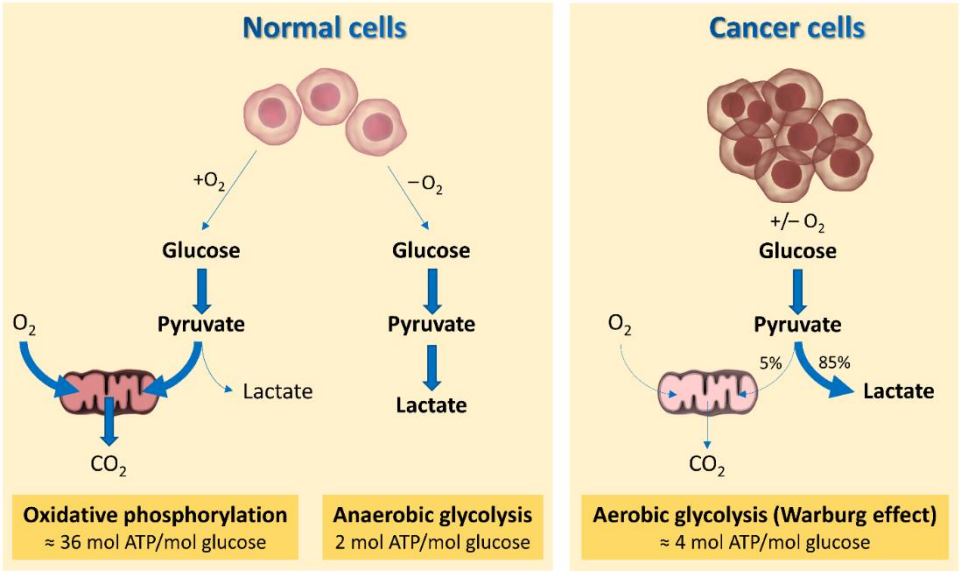

Figure 1.3 The Warburg effect. Adapted from [21]. *Schematic representation of the differences between oxidative phosphorylation, anaerobic glycolysis, and aerobic glycolysis (Warburg effect). In the presence of oxygen, normal cells first metabolize glucose to pyruvate via glycolysis and then completely oxidize most of that pyruvate in the mitochondria to CO_2 during the process of oxidative phosphorylation. Oxygen is the final electron acceptor that completely oxidizes the glucose. When oxygen is limiting, cells can redirect the pyruvate generated by glycolysis away from mitochondrial oxidative phosphorylation by generating lactate (anaerobic glycolysis), but this process results in minimal ATP production when compared with oxidative phosphorylation. Cancer cells tend to convert most glucose to lactate regardless of whether oxygen is present (aerobic glycolysis).*

Warburg postulated that the diversion of glucose to fermentation rather than respiration was due to a damage in mitochondria, already known to be the respiratory center of the cells by this time. However, following studies showed that the changes in mitochondrial respiration that are sometimes present in cancers may not always be the leading injury for tumorigenesis [22,23].

Besides glucose, there are other important metabolites contributing to cancer growth and progression. For example, citrate and aspartate, two

TCA intermediates, are diverted to lipid and aspartate biosynthesis, respectively. These intermediates need to be replenished through the process known as "anaplerosis" (**Figure 1.4**), in which glutamine is involved in many cancer cell types [24,25,26,27]. Glutamine is utilized to produce ATP and for biosynthesis; as such, many cancer cells show glutamine dependence, being sensitive to its withdrawal [28,29].

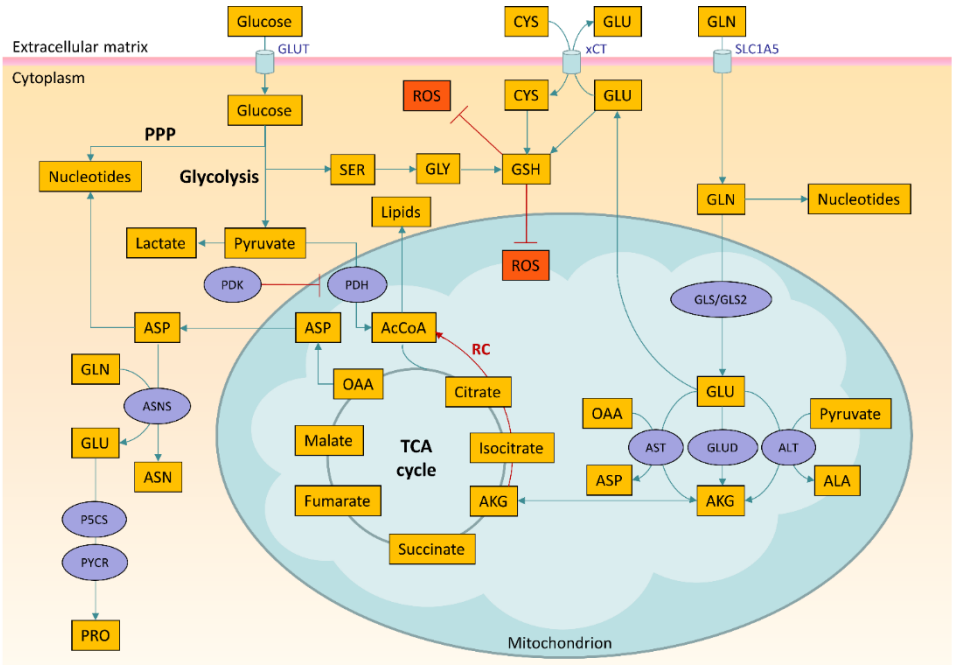

Figure 1.4 Main metabolic and biosynthetic cell fates of glutamine. Adapted from [30]. *Glutamine enters the mammalian cell through transporters such as SLC1A5 (also known as ASCT2). Glutamine itself can contribute to nucleotide biosynthesis, or is converted to glutamate by glutaminase (GLS or GLS2). Glutamate can contribute to the synthesis of glutathione and has many other metabolic fates in the cell. Glutamate is converted to α-ketoglutarate (AKG) through one of two sets of enzymes, glutamate dehydrogenase (GLUD1 or GLUD2) or aminotransferases. Whereas the by-product of GLUD is NH_4^+, the by-product of aminotransferase reactions is other amino acids. Aminotransferases may be present in either the cytoplasm or the mitochondria. AKG enters the tricarboxylic acid (TCA) cycle and can provide energy for the cell. Malate exiting the TCA cycle can*

produce pyruvate and NADPH for reducing equivalents, and oxaloacetate (OAA) can be converted into aspartate to support nucleotide synthesis. Alternatively, AKG can proceed backwards through the TCA cycle, in a process called reductive carboxylation (RC) to produce citrate, which supports synthesis of acetyl-CoA and lipids.

1.2 Metabolic rewiring in cancer

Metabolic reprogramming consists of the enhancement or suppression of metabolic pathways in cancer cells compared to normal tissues as a result of tumorigenic mutations and/or other factors [19].

Although tumors display a vast heterogeneity in terms of genetics and histology, in all the different cancer types a limited set of pathways is commonly induced to support the enhanced growth [31], likely due to their regulation by signaling pathways that are generally perturbed in cancer cells. Normal cells, upon stimulation by growth factors, activate phosphatidylinositol 3-kinase (PI3K) and its downstream pathways AKT and mammalian target of rapamycin (mTOR), thus promoting anabolism that involves increased glycolytic flux and fatty acid synthesis through activation of hypoxia-inducible factor–1 (HIF-1) and sterol regulatory element–binding protein (SREBP), respectively [32]. Cancer cells often have mutations that allow the PI3K-AKT-mTOR network to reach high levels of signaling with minimal dependency on extrinsic stimulation by growth factors [33]. Many of the best characterized oncogenes and tumor suppressors lie in the PI3K-AKT-mTOR network, and aberrant activation of this pathway is among the most frequent alterations observed in a diverse set of cancers.

Another commonly deregulated pathway in cancer is gain of function of MYC oncogene by chromosomal translocations, gene amplification and single-nucleotide polymorphisms. MYC increases the expression of many genes that support anabolic growth, including transporters and enzymes involved in glycolysis, fatty acid synthesis, glutaminolysis, serine metabolism and mitochondrial metabolism [34]. Oncogenes like K-ras, which is frequently mutated in lung, colon and pancreatic cancers and which is described in the next paragraph, cross-talks with PI3K and MYC pathways to promote carcinogenesis. Besides oncogenes, tumor suppressors such as the p53 transcription factor can also regulate metabolism [35]. The p53 protein–encoding gene *TP53* (tumor protein p53) is mutated or deleted in 50% of all human cancers. Recent studies indicate that p53 tumor-suppressive actions might be independent of the canonical p53 activities (i.e. execution of DNA repair, cell cycle arrest, senescence and apoptosis) but rather dependent on metabolism regulation and oxidative stress [36,37]. Loss of p53 increases glycolytic flux to promote anabolism and redox balance, two key processes that promote tumorigenesis [35].

1.2.1 *K-RAS* oncogene-driven metabolic rewiring in cancer

As reported above, metabolic alterations in cancer, as well as changes in nutrient uptake, are reported to be under direct control of oncogenes such as *RAS* or *MYC* [1,17,21,28,38,39,40,41].

In humans, *RAS* gene encodes four distinct but highly homologous 21-kDa Ras proteins: H-Ras, N-Ras, K-Ras4A and K-Ras4B (the last two proteins being alternative splice variants of the *K-RAS* gene). Activation of the *K-RAS* proto-oncogene [42,43,44,45] has a great incidence in human tumors, as reported in the catalogue of somatic mutations in cancer (COSMIC) [46]. Particularly, *RAS* gene is mutated in approximately 30% of human tumors [47,48] and *K-RAS* isoform is the most frequently mutated among the three isoforms in malignancies, with a mutation rate in all tumors estimated to be 25-30%. In contrast, mutations in *N-RAS* and *H-RAS* are less common (8 and 3% mutation rate, respectively) [47,48]. K-Ras oncoproteins are important clinical targets for anti-cancer therapy [49] and several strategies have been explored in order to inhibit aberrant Ras signaling, as reviewed in [50,51,52,53].

Ras proteins act as transducers that couple cell surface receptors to intracellular effectors and alternate between on and off conformation that are conferred by binding of GTP or GDP, respectively [54] (**Figure 1.5**). Under physiological conditions, the transitions between these two states is finely regulated by guanine nucleotide exchange factors (GEFs), which promote the activation of Ras by stimulating GDP for GTP exchange, and by GTPase activating proteins (GAPs), which accelerate Ras-mediated GTP hydrolysis [55]. Altering this fine balance by deregulation of either GAP or GEF activity may result in hypo- or hyper-activation of downstream

pathway(s), so that overexpression of a GEF or inactivation of a GAP may both result in cell transformation [41,54].

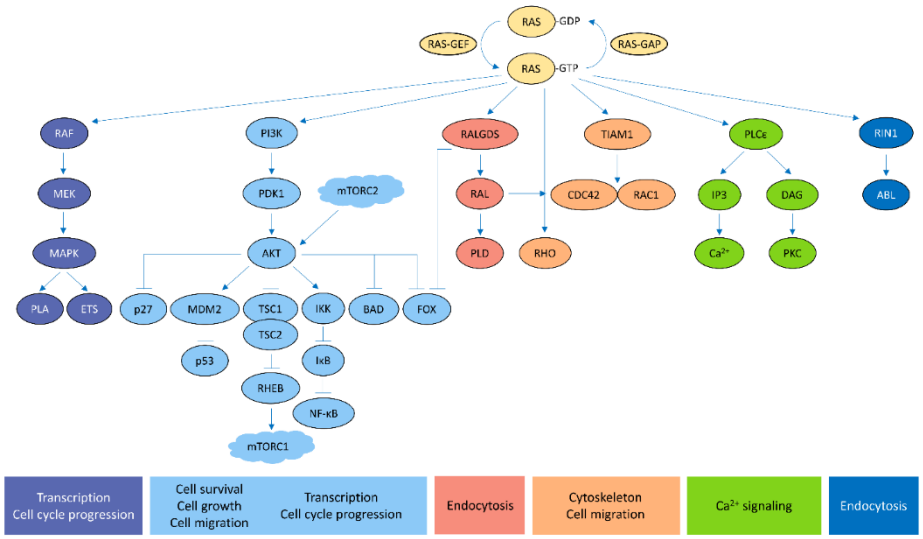

Figure 1.5 Ras signalling pathways. Adapted from [56]. *Active (farnesylated, membrane-bound and GTP-bound) RAS modulates a number of signalling pathways. Oncogenic RAS mutations tend to lock RAS in its GTP-bound state, resulting in constitutive RAS signalling. The major RAS effector pathways are shown. The two best-studied pathways that are activated by RAS are the RAF–MEK–MAPK signalling cascade and the PI3K–AKT pathway. The RAF–MEK–MAPK pathway ultimately activates the ETS family of transcription factors, which induce multiple genes that promote cell cycle progression and cell migration. Likewise, AKT phosphorylates multiple cellular proteins, leading to the inhibition of several tumour suppressors (such as p27, p53, tuberous sclerosis 1 (TSC1), TSC2 and BCL-2 antagonist of cell death (BAD)) or leading to the activation of several oncogene products. RAS also activates other small GTPases such as RALA and RALB. CDC42, cell division cycle 42; DAG, diacylglycerol; FOX, forkhead transcription factor; GAP, GTPase-activating protein; GEF, guanine nucleotide exchange factor; IKK, IκB kinase; IP3, inositol-1,4,5-trisphosphate; mTORC, mTOR complex; NF-κB, nuclear factor-κB; PDK1, phosphoinositide-dependent kinase 1; PKC, protein kinase C; PLA, phospholipase A; PLCε, phospholipase Cε; PLD, phospholipase D; RALGDS, RAL guanine nucleotide dissociation stimulator; RHEB, RAS homologue enriched in brain; RIN1, RAS and RAB interactor 1; TIAM1, T cell lymphoma invasion and metastasis 1.*

Inactivation of Ras activity by GAPs is the predominant target of the most common somatic mutations that are found in the oncogenic variants of Ras alleles. Oncogenic substitutions in residues G12 and G13 of Ras

prevent the formation of Van der Waals bonds between Ras and the GAP through esteric hindrance, perturbing the proper orientation of the catalytic glutamine Q61 in Ras, which results in the pronounced attenuation of GTP hydrolysis [57]. The outcome of these substitutions is the persistence of the GTP-bound state of Ras and, as a consequence, the permanent activation of a multitude of Ras-dependent downstream effectors pathways. These effectors are involved in many aspects of the tumor phenotype such as promotion of proliferation, suppression of apoptosis, metabolic reprogramming, remodeling of the microenvironment, evasion of the immune response and metastasis [55]. Although Ras modulates different metabolic processes in the cell, regulation of glycolysis is one of the most important metabolic effects (**Figure 1.6**). Its main effect on metabolism is targeted to glycolysis by upregulating HIF1α, considered one of the main regulators of glycolysis, and glucose transporter expression [58,59,60]. Additionally, Ras family proteins act upstream PI3K/Akt/mTOR pathway, which is a regulatory axis with deep effects on aerobic glycolysis and cellular biosynthesis. This pathway has been shown to stimulate cell growth and ATP production by regulating the activity and expression of key glycolytic enzymes and nutrient transporters, enabling increased uptake of glucose, amino acids and other nutrients [61,62,63,64].

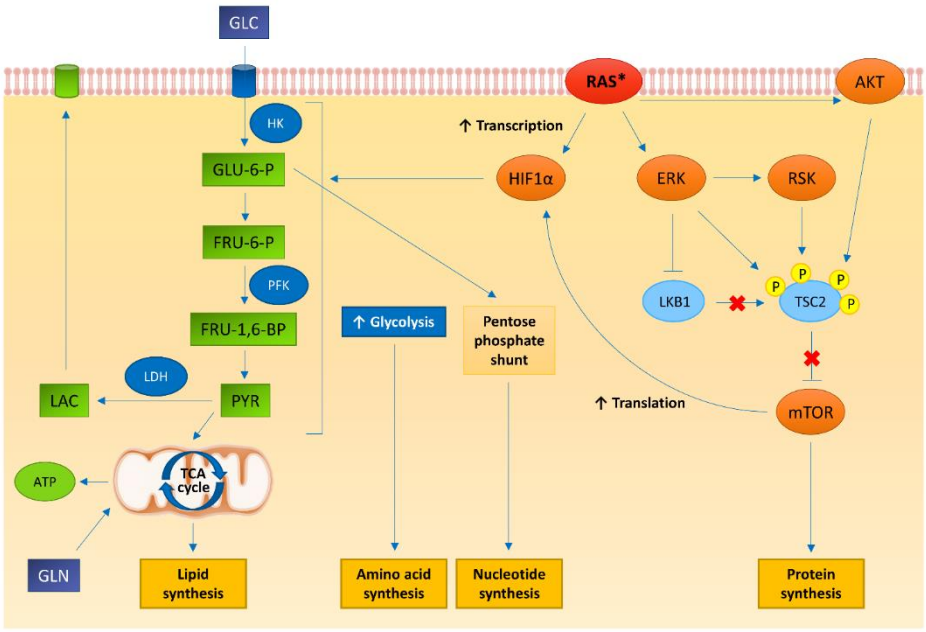

Figure 1.6 Ras effects on metabolism. Adapted from [55]. *ERK and PI3K signalling downstream of oncogenic RAS converge to activate mTOR by inhibiting its negative regulators tuberin (TSC2) and liver kinase B1 (LKB1)–AMP-activated protein kinase (AMPK). TSC2 can be directly phosphorylated by both ERK and ERK-activated ribosomal protein S6 kinase (RSK), as well as by AKT, and, likewise, RAF–ERK1 or RAF–ERK2 signalling disrupts the LKB1–AMPK checkpoint. This leads to mTOR–eukaryotic translation initiation factor 4 (eIF4)-dependent translation of hypoxia-inducible factor 1α (HIF1α). Activated RAS can also result in the transcriptional upregulation of* HIF1A. *Increased levels of HIF1α augment multiple steps in glycolytic metabolism. The upregulation of hexokinase (HK) facilitates the conversion of glucose to glucose-6-phosphate, a glycolytic intermediate that is used in pentose phosphate pathway-dependent nucleotide synthesis. Higher levels of phosphofructokinase (PFK) lead to an enhanced glycolytic flux and the production of pyruvate, which, in conjunction with the oncogenic RAS-dependent increase in lactose dehydrogenase (LDH) levels, can allow glycolysis to persist by regenerating NAD+, a necessary cofactor for glycolytic reactions. In addition, some of the pyruvate can enter the tricarboxylic acid (TCA) cycle where its conversion to citrate generates intermediates that are necessary for the synthesis of fatty acids and non-essential amino acids. The asterisk represents the mutational activation of RAS.*

Oncogenic activation of *K-RAS* contributes to the acquisition of the hyper-glycolytic phenotype (the previously described Warburg effect [65]) due to enhancement in glucose transport and aerobic glycolysis [66,67]. *K-RAS* oncogene activation also correlates with down-regulated expression of

mitochondrial genes, altered mitochondrial morphology and production of large amount of reactive oxygen species (ROS) associated with mitochondrial metabolism [68,69].

1.2.2 Redox homeostasis and ROS detoxification

Reactive oxygen species (ROS) are waste by-products of the oxidative metabolism that must be either excreted or neutralized. ROS have a toxic effect when their concentration increases, leading to oxidative stress. However, ROS are essential for many biological functions, such as cell growth and differentiation, enzyme regulation or inflammation, and they regulate many signal transduction pathways involved in these processes (**Figure 1.7**). They are produced either inside the cells (internal sources) or by environmental agents (external sources). Sources of internal oxidative stress include peroxisomes and enzymes, like the detoxifying enzymes of the P450 complex, xanthine oxidase complexes, and the NADPH oxidase complexes. Most of these enzymes operate in the mitochondria, which are the main sources of oxidative stress.

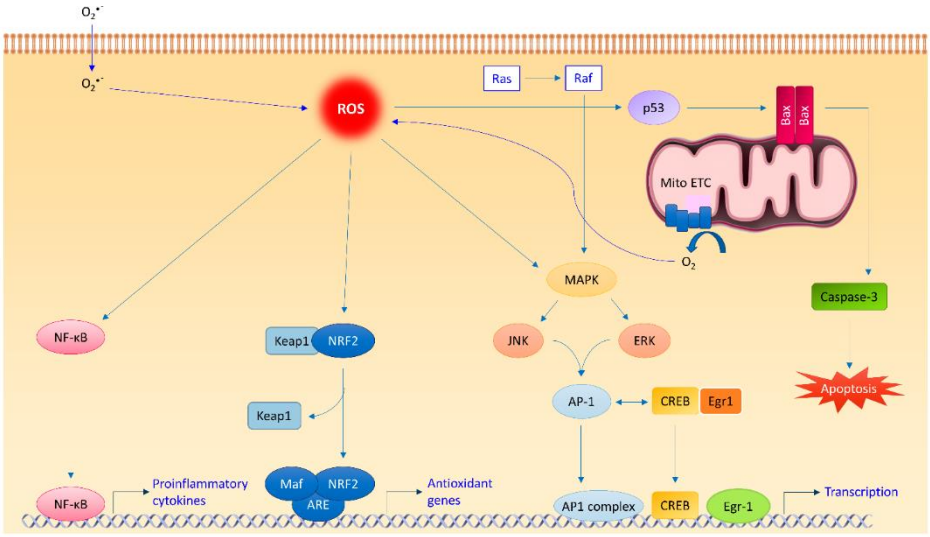

Figure 1.7 ROS effects in the cell. Inspired by [70]. *Reactive oxygen species (ROS) production enhances the phosphorylation (P) of inhibitor of NF-κB (IκB). This leads to the ubiquitylation (Ub) of IκB and its subsequent degradation by the proteasome. Nuclear factor-κB (NF-κB) is then released and translocates to the nucleus to initiate transcription. ROS production also leads to MAPK and NRF2 activation, thus promoting the activation of specific gene transcription.*

A moderate increase in ROS can promote cell proliferation and differentiation, whereas excessive amount of ROS can damage many molecules, including DNA, RNA, lipids and proteins, inducing senescence and/or cell death [71] (**Figure 1.8**). Thus, a fine regulation of ROS –through the modulation of their generation and elimination by scavenging systems– is necessary [72].

ROS scavengers include superoxide dismutases, glutathione peroxidase, peroxiredoxins, glutaredoxins, thioredoxins or catalase. Abnormal cancer cell growth is associated with increase in ROS and reflects a disruption of redox homeostasis, due to either an elevation of ROS production or to a decrease of ROS-scavenging capacity, resulting in oxidative stress.

Signaling events mediated by oxidative stress have been reported to affect all aspects of cancer cell behaviour, including cell cycle progression and proliferation, cell survival and apoptosis, energy metabolism, cell morphology, motility and adhesion, angiogenesis, and tumor stemness [73].

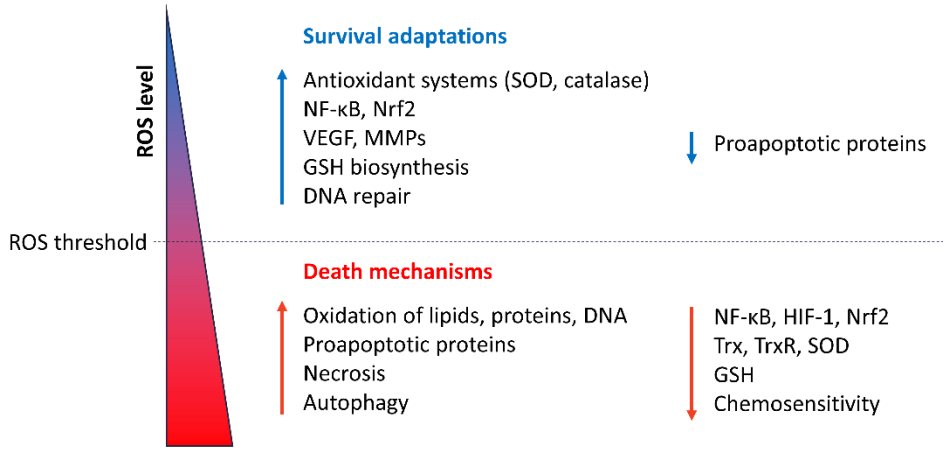

Figure 1.8 ROS levels and cancer. Inspired by [74]. *The effect of ROS on cell fate depends on the level at which ROS are present. Low levels of ROS provide a beneficial effect, supporting cell proliferation and survival pathways. However, once levels of ROS become excessively high, they cause detrimental oxidative stress that can lead to cell death. To counter such oxidative stress, a cell uses antioxidants that prevent ROS from accumulating at high levels. In a cancer cell, aberrant metabolism and protein translation generate abnormally high levels of ROS. Through additional mutations and adaptations, a cancer cell exerts tight regulation of ROS and antioxidants in such a way that the cell survives and the levels of ROS are reduced to moderate levels. This extraordinary control of ROS and the mechanisms designed to counter it allow the cancer cell to avoid the detrimental effects of high levels of ROS, but also increase the chance that the cell will experience additional ROS-mediated mutagenic events and stress responses that promote tumorigenesis.*

Among the signaling pathways involved are the MAPK pathway or PI3K/AKT pathway [75]. As cancer cells with increased oxidative stress are likely to be more vulnerable than normal cells to further ROS insults induced by exogenous agents [76], this opens new possibilities for

therapeutic intervention [77]. For example, breast tumors show persistent ROS generation [78,79], and markers of constitutive oxidative stress have been detected in samples from *in vivo* breast carcinomas [80]. Despite the clear implications of ROS in tumorigenesis, the precise mechanisms leading to oxidative stress in cancer cells remain unclear. However, some intrinsic and extrinsic mechanisms are demonstrated to cause oxidative stress during cancer development and disease progression. Oncogene activation, aberrant metabolism, mitochondrial dysfunction, and loss of p53 are intrinsic factors known to cause increased ROS production in cancer cells. Moreover, the expression of genes associated with tumor transformation, such as RAS, BCR-ABL and c-MYC, were found to induce ROS production [68,81]. In H-Ras^{V12}-transformed NIH3T3 fibroblasts, a large amount of superoxide was generated through the activation of the membrane associated ROS-producing enzyme NADPH oxidase (NOX) [82]. In addition to the intrinsic mechanisms, extrinsic ones such as inflammatory cytokines, imbalance of nutrients and hypoxic environment could also affect intracellular redox homeostasis [83]. As cancer cells are continuously exposed to high levels of ROS, oxidative stress may exert selective pressure to enrich the population of cells that are able to resist it. Among the acquired resistance mechanisms, for instance, oncogenic H-Ras-transformed cells (which exhibited increased superoxide and hydrogen peroxide levels) were shown to express higher levels of antioxidant enzymes such as peroxiredoxin-3 and

thioredoxin peroxidase compared to their non-tumorigenic parental cells [84]. The enhanced antioxidant potential is likely to serve as a key mechanism to evade ROS-induced apoptosis, as evidenced by the resistance to hydrogen peroxide-induced cell death that was observed in the H-Ras-transformed cells [84]. In keeping with these findings, Ras-transformed cells were also found to be more sensitive to glutathione depletion, which leads to ROS accumulation and cell death [81]. Also, an increase of the flux through the oxidative branch of PPP [85] as well as the overexpression of the NADPH producing enzyme G6PD has been reported in K-Ras-transfected NIH3T3 cells [85,86]. Thus, oncogenic signals stimulate both the formation of ROS to enhance proliferation and the promotion of antioxidant mechanisms to minimize oxidative damage. The mechanisms of redox regulation involve multiple signaling pathways which employ several antioxidant-sensitive transcription factors such as nuclear factor-κB (NF-κB), nuclear factor (erythroid-derived 2)-like 2 (NRF2), c-JUN, and HIF1, which in turn lead to an increased expression of antioxidant molecules such as superoxide dismutase (SOD), catalase, thioredoxin and reduced glutathione (GSH).

Of particular interest in redox homeostasis maintenance is the role of NRF2 transcription factor, which induces the expression of many cytoprotective genes in response to oxidative stress. NRF2 target genes are mainly involved in glutathione synthesis, elimination of ROS, xenobiotic metabolism, and drug transport [87]. Interestingly, an increase

in NRF2 levels is frequently detected in various types of human cancers, resulting in an overactivation of its target genes that provide cells with additional capabilities of malignance [88,89,90,91]. The regulation of NRF2 by oncogene-dependent signaling has been recently described [92,93]. Therein, *K-RAS* is reported to activate NRF2 transcription through the MEK-ERK-JUN signaling pathway and to reduce ROS levels in primary fibroblasts. Metabolic genes involved in PPP and NADPH production also represent a significant portion of the genes regulated by NRF2 [94]. Moreover, NRF2 promotes glutamine consumption by enhancing glutaminolysis and glutathione synthesis. Overall, these findings indicate that NRF2 acts as a link between redox homeostasis maintenance and anabolic metabolism, pointing out the intimate collaboration between carbon metabolism and ROS detoxification systems.

1.3 Nutrient modulation through amino acid deprivation in cancer

As previously mentioned, cancer cells rewire their metabolism to meet an increased demand of energy and macromolecules necessary to sustain cell proliferation and tumorigenesis. This renders cancer cells particularly addicted to some nutrients compared to normal cells and offers a therapeutic opportunity to fight cancer. Indeed, nutrient intake in cancer patients can be modulated in order to reduce (or eliminate) from the diet those molecules to which cancer cells show dependency. Among the

nutrients that tumors consume in large quantity are some amino acids, like glutamine and sulfur amino acids methionine and cysteine.

1.3.1 Glutamine

1.3.1.1 Glutamine metabolism

Oncogenic activation of *K-RAS* also allows cells to make extensive anaplerotic usage of glutamine, rendering them addicted to this amino acid and to glutaminolysis. Glutamine is the most abundant amino acid in blood [95], composed by an amine functional group. Although it is considered a non-essential amino acid, most proliferating and tumor cells rely on it to grow. The amine group is lost when glutamine is converted to alpha-ketoglutarate (AKG), and is used to synthesize nucleotides, hexosamines (that glycosylate growth factor receptors and promote their localization to the cell surface) and non-essential amino acids (NEAA), all of which are necessary for cell growth. Moreover, the oxidation of AKG to oxaloacetate generates reducing equivalents that can be used to produce energy [26]. Glutamine also modulates redox homeostasis and can influence the activity of signal transduction pathways [25].

While the high demand for glucose shown by tumor cells was already known from the 1920s, the need for glutamine of proliferating cells was discovered 30 years later. Indeed, in 1955, Eagle observed that glutamine consumption rate was about 10-fold higher than that of all other amino acids. Moreover, the tested cell lines could not proliferate without

glutamine and most of them were neither viable [96]. In 1971, Kovacevic demonstrated that some of the carbon atoms of glutamine could be found in the carbon dioxide released by the cells, proving that cells may use glutamine as a fuel [97]. Besides being an anaplerotic precursor, glutamine can also be catabolized in a process known as glutaminolysis (**Figure 1.4**). During this process, glutamine generates glutamate, aspartate, pyruvate, lactate, CO_2, citrate and alanine. In the first step, glutamine is converted to glutamate and ammonia by glutaminase (GLS). Then, glutamate is oxidized into AKG, either by glutamate dehydrogenase (GDH), generating ammonia and mitochondrial NADH or NADPH [98], or by transaminases.

Besides being oxidized into AKG, glutamic acid is the primary nitrogen donor for the synthesis of the NEAAs [99,100]. The amine group of glutamic acid is transferred to α-ketoacids by transaminases. The α-ketoacids used to synthesize NEAAs are the carbon catabolites of glucose or glutamine: pyruvate, 3-phosphoglycerate, oxaloacetate and glutamic acid gamma-semialdehyde, which are respectively used to synthesize alanine, serine, aspartate, and ornithine. Serine is a precursor for glycine and cysteine biosynthesis, aspartate is a precursor for asparagine biosynthesis, and ornithine is a precursor for arginine biosynthesis. Glutamic acid is the carbon and nitrogen source for the synthesis of proline. Tyrosine, being directly produced from phenylalanine, is the only NEAA that does not derive from glucose or glutamine.

The second major route of glutamine metabolism, reductive carboxylation (RC), occurs in cell lines under hypoxic stress or disrupted mitochondrial functioning, and has been shown to take place in Ras-transformed cells [24,68,101,102,103,104]. In these conditions, glutamine-derived α-ketoglutarate preferentially undergoes reductive metabolism through the TCA cycle to isocitrate and then citrate, where it can then be converted to acetyl-CoA for lipid synthesis [105,106,107]. Mass action controls induction of this pathway via situations that perturb the citrate-to-α-ketoglutarate ratio, such as oxidative energetic stress. Indeed, *in vitro* studies of IDH1 indicate that a high ratio of NADPH/$NADP^+$ and low citrate concentration activate the reductive carboxylation reaction [108]. This is supported by data demonstrating that interrupting the supply of mitochondrial NADPH by silencing the nicotinamide nucleotide transhydrogenase (NNT) suppresses reductive carboxylation [109]. NNT, a mitochondrial transmembrane protein, catalyzes the transfer of a hydride ion from NADH to $NADP^+$ to generate NAD^+ and NADPH. Together, these observations suggest that reductive carboxylation is modulated in part through the balance of substrate/products and the mitochondrial redox state. As the inhibition of reductive carboxylation might selectively suppress growth of tumor cells subjected to hypoxia or with defects in oxidative metabolism, targeting glutamine metabolism through GLS inhibition is considered a potential therapeutic strategy under such

circumstances, especially in combination with other anticancer drugs [104,110,111].

1.3.1.2 Glutamine transport

The elevated glutamine influx of some cancer cells is accomplished by the upregulation of glutamine transporters, which normally allow cells to use exogenous glutamine [112].

Glutamine transporters can be sodium-dependent or sodium-independent (**Figure 1.9**).

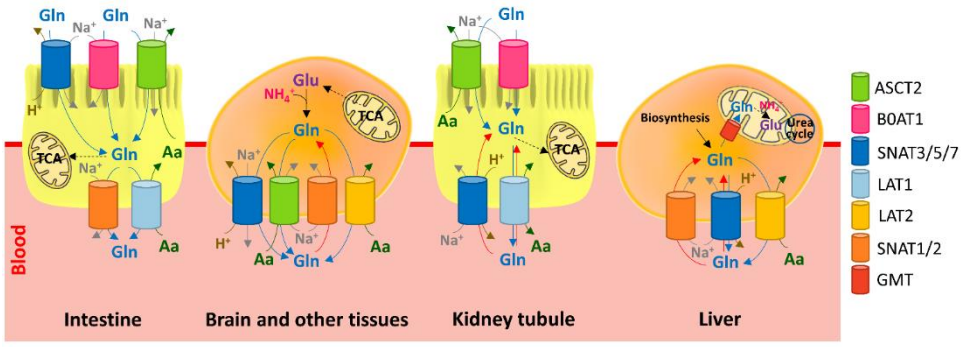

Figure 1.9 Glutamine transporters. Adapted from [113]. *Interplay among epithelial polarized cells (apical membrane is depicted as brush-border; basolateral membrane is in contact with blood) and other cells. Glutamine transporters are indicated with different colors. Arrows indicate glutamine fluxes from (red) or toward (blue) blood or from lumen to epithelial cells (blue); gray arrows indicate sodium fluxes; brown and green arrows indicate proton and other amino acid fluxes, respectively.*

Sodium-dependent transporters include System A (alanine-preferring), System N (that exhibit preference for amino acids with nitrogen in their side-chains) and System ASC amino acid transporter-2 (ASCT2), while System L transporters (leucine-preferring) are included among the sodium-independent transporters and have been extensively studied

[114]. Sodium-coupled neutral amino acid transporter 1 (SNAT1) is the most significant glutamine transporter among System A transporters and is implicated in neuronal glutamine uptake [115], while SNAT2 is expressed in most tissue, including adipose [115,116,117]. However, System N transporters have the highest affinity for glutamine [114,117] and include SNAT3, expressed in a variety of tissues [115,117]. Glutamine uptake via ASCT2 triggers leucine uptake by a parallel leucine/glutamine antiport catalyzed by L-type amino acid transporter 1 (LAT1) [112]. Both LAT1 and LAT2 are involved in glutamine absorption [114,116,117], and LAT1 also modulates signaling through the mammalian target of rapamycin (mTOR) pathway, suggesting a link between LAT1 and cancer [113].

1.3.1.3 Glutamine activates mTOR pathway

Another role of glutamine is to activate a master regulator of protein translation, the mammalian target of rapamycin complex 1 (mTORC1) (**Figure 1.10**). This evolutionarily conserved complex activates protein translation and inhibits macroautophagy (the random sequestration and delivery of cytoplasm to the lysosome/vacuole) in the presence of large amounts of amino acids and growth factors [118]. Indeed, mTORC1 acts by phosphorylating multiple downstream targets, including the p70 ribosome protein S6 kinase (S6K1), the eukaryotic translation initiation

factor 4E-binding protein (4E-BP1) and the autophagy-associated kinase ULK1 (Atg1) [119,120].

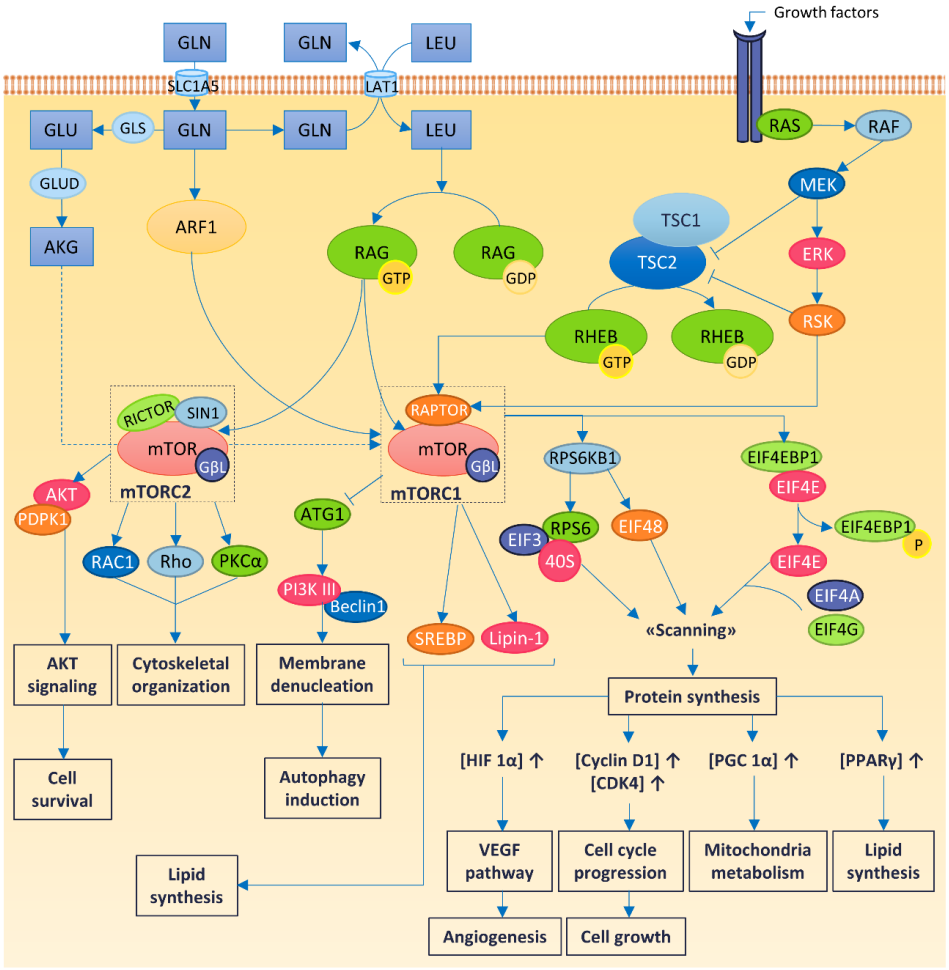

Figure 1.10 Mammalian target of rapamycin (mTOR) pathway. *The mechanistic target of rapamycin (mTOR) is an atypical serine/threonine kinase that is present in two distinct complexes. The first, mTOR complex 1 (mTORC1), is composed of mTOR, Raptor, GβL, and DEPTOR and is inhibited by rapamycin. It is a master growth regulator that senses and integrates diverse nutritional and environmental cues, including growth factors, energy levels, cellular stress, and amino acids. It couples these signals to the promotion of cellular growth by phosphorylating substrates that potentiate anabolic processes such as mRNA translation and lipid synthesis, or limit catabolic processes such as autophagy. The small GTPase Rheb, in its GTP-bound state, is a*

necessary and potent stimulator of mTORC1 kinase activity, which is negatively regulated by its GAP, the tuberous sclerosis heterodimer TSC1/2. Most upstream inputs are funneled through Akt and TSC1/2 to regulate the nucleotide-loading state of Rheb. In contrast, amino acids signal to mTORC1 independently of the PI3K/Akt axis to promote the translocation of mTORC1 to the lysosomal surface where it can become activated upon contact with Rheb. This process is mediated by the coordinated actions of multiple complexes, notably the v-ATPase, Ragulator, the Rag GTPases, and GATOR1/2. The second complex, mTOR complex 2 (mTORC2), is composed of mTOR, Rictor, GβL, Sin1, PRR5/Protor-1, and DEPTOR. mTORC2 promotes cellular survival by activating Akt, regulates cytoskeletal dynamics by activating PKCα, and controls ion transport and growth via SGK1 phosphorylation.

Moreover, in cancer cells with constitutively high rates of fatty acid synthesis, mTORC1 signaling via its effector S6K activates a transcriptional program that includes both SREBP-1 and the related protein SREBP-2, which regulates transcription of genes in fatty acid and sterol biosynthesis [121]. Both SREBP-1 and SREBP-2 are required for mTORC1-mediated cell proliferation. The mechanism of SREBP activation by mTORC1 is incompletely understood but involves nuclear entry of the phosphatidic acid phosphatase Lipin-1, which enhances nuclear SREBP abundance and activity on the promoters of lipogenic genes [122].

The role of amino acids in the activation of mTORC1-dependent signaling has been widely described in literature [123,124]. Of the EAAs, mTORC1-signaling appears to respond most acutely to leucine; however, glutamine is also necessary for maximal mTOR activation [112,123,125]. Particularly, a portion of the glutamine that enters the cell through the SLC1A5 (or ASCT2) glutamine importer is rapidly exported through the bidirectional amino acid transporter SLC7A5 (or LAT1) in exchange for the uptake of extracellular EAAs, suggesting that glutamine uptake and export is required for EAA activation of mTORC1 [126].

1.3.1.4 Glutamine promotes resistance to cell death

Although many cancer cells require glutamine for survival, cells with enhanced expression of Myc oncoproteins are particularly sensitive to glutamine deprivation [28,29,127]. In these cells, glutamine deprivation induces depletion of TCA cycle intermediates, depression of ATP levels, delayed growth, diminished glutathione pools, and apoptosis (**Figure 1.11**). In 2008, Wise and colleagues observed that the glutamine-derived AKG was able to rescue MYC-transformed cells from apoptotic cell death upon glutamine withdrawal [28], making AKG an essential component of glutamine-dependent cell survival. This effect correlates with the ability of AKG to replenish the TCA cycle by providing oxaloacetate (OAA). Indeed, OAA condenses with acetyl-CoA to produce citrate, thus maintaining the TCA cycle and sustaining *de novo* fatty acid biosynthesis. Cheng and co-authors also demonstrated that increased expression of pyruvate carboxylase (the enzyme that catalyzes the conversion of pyruvate into OAA) can also render MYC-transformed cells resistant to glutamine depletion-induced cell death [128]. Overall, these data indicate that glutamine maintains cell survival primarily by supporting the anaplerosis of the TCA cycle.

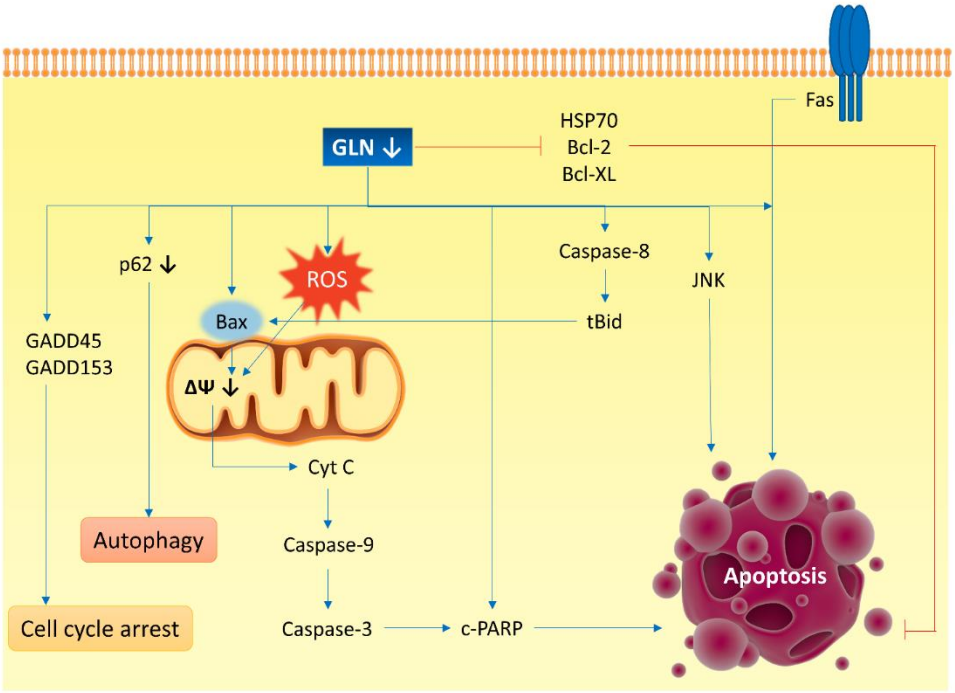

Figure 1.11 Glutamine and apoptosis. Inspired by [129]. *Glutamine deprivation makes cells sensitive to Fas ligand, TNF-α and heat shock-mediated apoptosis. Glutamine deprivation induces apoptosis through extrinsic or intrinsic pathway, which is dependent on cell type and cell condition. Cyt c, cytochrome c; C-PARP, cleaved-PARP; t-Bid, truncated Bid; ΔΨ, mitochondrial membrane potential; GADD, growth arrest and DNA damage-induced genes; ROS, reactive oxygen species; JNK, c-Jun N-terminal kinase; HSP70, heat shock protein 70. ⊥, inhibiting effect; bold arrow, decreased p62 and ΔΨ after glutamine deprivation.*

1.3.1.5 The need for glutamine differs among tumors

One important consideration is that not all cancer cells need an exogenous supply of glutamine. For example, a panel of lung cancer cell lines [130] and breast cancer cells [131] showed significant variability in their response to glutamine deprivation, with some cells displaying almost total independence. Resistance to glutamine deprivation is associated with the

ability to synthesize glutamine *de novo* and/or to rely on alternative pathways of anaplerosis [128,131].

This variability renders essential to develop ways to predict which tumors would be more sensitive to the inhibition of glutamine metabolism, like methods to image or otherwise quantify glutamine metabolism *in vivo* [132]. Approaches for glutamine-based imaging that do not require a specimen of the tumor include a number of glutamine analogues compatible with PET [133]. Labeled analogues of glutamate are also taken up by some tumors [134,135] and one of these has been evaluated in small clinical trials involving patients with several types of cancer [134,136]. This analogue enters the cell through the cystine/glutamate exchange transporter (xC^- transport system), linked to glutathione biosynthesis [137], and has high tumor detection rates and good tumor-to-background ratios in hepatocellular carcinoma and lung cancer.

1.3.1.6 Pharmacological inhibition of glutamine metabolism in cancer

One of the most studied approach to inhibit glutamine metabolism consists in the use of amino acid analogues (**Figure 1.12**).

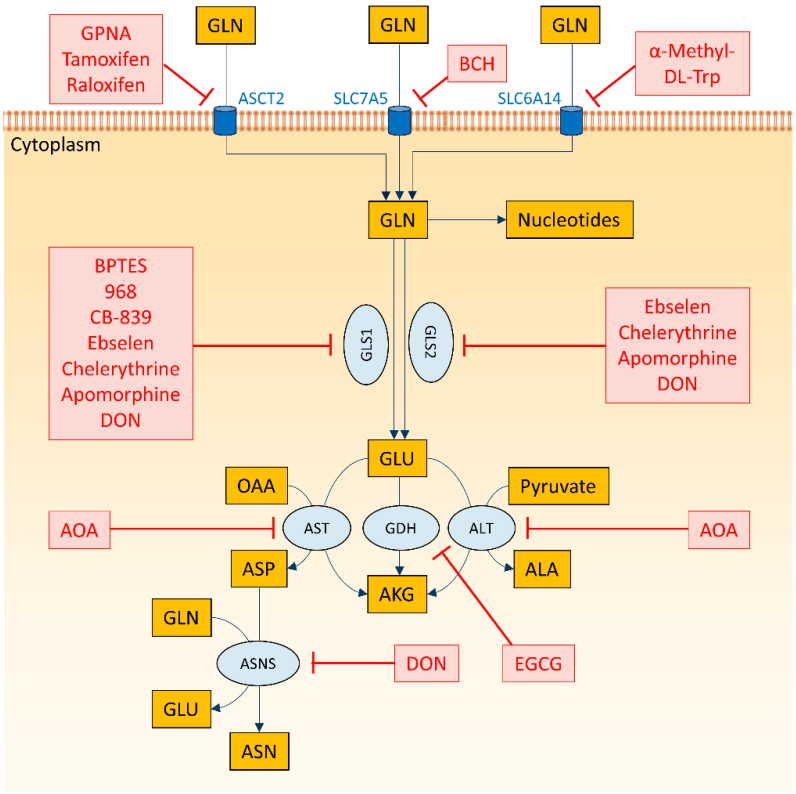

Figure 1.12 Targeting glutamine metabolism. Adapted from [138]. *Glutamine is imported via different transporters, which are the target of some inhibitors, and then enters a complex metabolic network to promote cell survival and growth. Inhibitors that target various aspects of glutamine metabolism are shown in red.*

However, the well-studied acivicin, 6-diazo-5-oxo-L-norleucine (DON) and azaserine showed gastrointestinal toxicity, myelosuppression and neurotoxicity [139]. Thus, methods directed at specific nodes of glutamine metabolism have been recently developed. ASCT2, the Na^+-dependent neutral amino acid transporter encoded by *SLC1A5*, is largely expressed in lung cancer cells and transports the majority of glutamine in those cells.

The compound γ-L-glutamyl-p-nitroanilide (GPNA) inhibits this transporter and limits the growth of lung cancer [140]. Moreover, GPNA can enhance the uptake of drugs imported via the monocarboxylate transporter MCT1. Suppressing glutamine uptake with GPNA improves MCT1 stability and stimulates uptake of the glycolytic inhibitor 3-bromopyruvate [141].

Another way to block glutamine metabolism is to inhibit glutaminase (GLS). Compound 968 inhibits the transformation of fibroblasts by oncogenic Rho GTPases and delays the growth of GLS-expressing lymphoma xenografts [142]. Bis-2-(5-phenylacetamido-1,2,4-thiadiazol-2-yl)ethyl sulfide (BPTES) also strongly inhibits GLS isoforms encoded by *GLS* [143], impairing ATP levels and growth rates of P493 lymphoma cells [144].

No effective, specific inhibitors yet exist to target the flux from glutamate to α-ketoglutarate. Aminooxyacetate (AOA) inhibits aminotransferases nonspecifically, but millimolar doses are usually needed to obtain this effect in cultured cells. Nevertheless, AOA was effective in neuroblastomas in mice and in breast adenocarcinoma xenografts [145,146]. AOA treatment also showed a cytotoxic effect on a glutamine-dependent MYC-amplified glioblastoma cell line *in vitro* while having no significant effect on a paired Myc-deficient line [28]. Epigallocatechin gallate (EGCG), a green tea polyphenol, is able to inhibit GDH [147]. It has been successfully employed to kill glutamine-addicted cancer cells during

glucose deprivation or glycolytic inhibition [148,149] and to suppress growth of neuroblastoma xenografts [146].

A set of Food And Drug Administration (FDA)-approved anti-cancer drugs used to target cancer metabolism (including glutamine metabolism) is reported in Supplementary Information, Chapter 5.2.

1.3.2 Sulfur amino acid metabolism

Besides glutamine transporters, all amino acid transporters are being receiving attention from scientific community as potential drug targets for cancer treatment, given the increased demand of cancer cells for these nutrients to support their enhanced cell growth [150,151]. Selective blockers of these transporters might be effective in preventing the entry of important amino acids into tumor cells, thus essentially starving these cells to death. Here we focus on the two proteinogenic sulfur amino acids, methionine and cysteine (**Figure 1.13**).

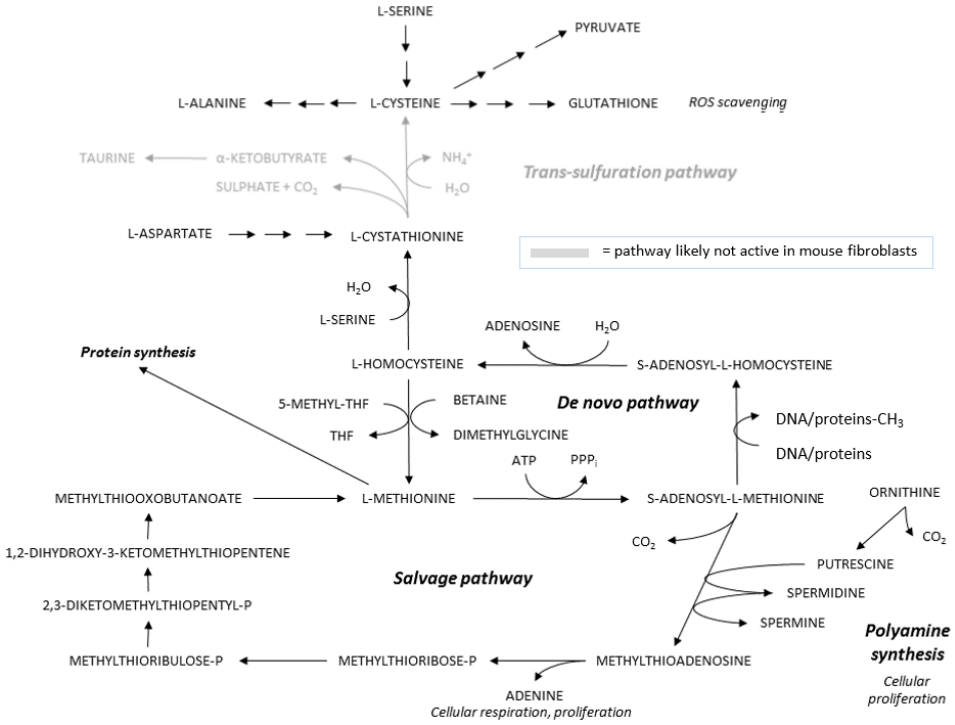

Figure 1.13 Sulfur amino acid metabolism. From [152]. *Methionine is partitioned between protein synthesis,* de novo *and recycling pathway, where it is converted to S-adenosylmethionine (SAM). SAM is converted to S-adenosylhomocysteine (SAH) during methylation of DNA and a large range of proteins and other molecules. SAH is then hydrolyzed to homocysteine (Hcy) in a reversible reaction. In the trans-sulfuration pathway, Hcy is metabolized to form cystathionine, which is the immediate precursor to cysteine. Besides from methionine, cysteine can be synthesized from serine. The sulfur is derived from methionine, which is converted to homocysteine through the intermediate SAM. Cystathionine beta-synthase then combines homocysteine and serine to form the asymmetrical thioether cystathionine. The enzyme cystathionine gamma-lyase converts the cystathionine into cysteine and alpha-ketobutyrate. The trans-sulfuration pathway is not active in all cells, and in human is active essentially only in cells from splanchnic organs. Mouse embryonic fibroblasts are not able to convert methionine into cysteine: for this reason, the trans-sulfuration reaction is highlighted in grey.*

1.3.2.1 Methionine

Methionine is an essential amino acid required for normal growth and development in mammals [153]. The intracellular level of methionine

depends on the balance between synthesis (through the *de novo* synthetic pathway), recycle (through the *salvage* pathway), consumption (in biosynthesis of proteins) and its transport. An important metabolite of methionine is S-adenosylmethionine (SAM), the principal methyl donor in the cell. SAM is required for methylation of DNA, RNA, proteins (including histones [154]) and lipids by the enzymes methyltransferases. Moreover, SAM is involved in biosynthesis of polyamines, which have far-ranging effects on nuclear and cell division, and methionine salvage pathway [155].

Some cancers show methionine dependence, a feature firstly noted in xenograft rodents in response to a methionine-free diet [156]. Since then normal cells have been reported to be more resistant to external methionine limitation [155,157]. Methionine dependence might be correlated with inability of methionine-restricted cells to cope with demand for SAM, a major methionine product [155]. This "SAM-checkpoint" may protect cellular integrity and maintain epigenetic stability, since it stops cell cycle progression when intracellular SAM concentrations are insufficient to sustain the methylation reactions necessary for normal cell physiology [155]. Several drugs that target the enzymes that are involved in the post-translational modifications of histones and DNA, cell survival, proliferation and stem cell function [154,158,159] are being evaluated pre-clinically or in early-stage clinical trials [160].

Both a deficiency and an excess of the dietary levels of methionine can result in either genomic instability, which leads to diseases such as cancer, or changes in gene expression, which lead to alterations in metabolism [161], including improvement of hepatic lipid and glucose metabolism and induction of adiposity resistance [161]. Some cancer cells show a high activity of the methionine cycle that promotes chemo-resistance and evasion from apoptosis [162], whereas normal cells are relatively resistant to dietary methionine restriction: therapies to block the methionine cycle in transformed cells may thus represent a safe and effective strategy to fight cancer [162,163]. Dietary methionine restriction, used alone or in combination with other treatments, impaired cancer growth and carcinogenesis in human patients [164,165] or in rodents [166,167,168]. However, one *caveat* is that methionine restriction must be closely regulated, because methionine is an essential amino acid and a long use of diets extremely poor in methionine could be extremely toxic and cause death. Dietary methionine restriction (achievable in humans with a predominantly vegan diet) may have an additive healthy effect if combined with calorie restriction, by limiting glucose [168]. The potential of methionine depletion in enhancing the anti-cancer effect of chemotherapeutic agents on drug-resistant tumors and cell lines has also been reported [169].

We recently demonstrated that sensitivity to methionine limitation of mouse fibroblasts and expression of the SBAT1-encoding *Slc6a15* gene (a

methionine transporter) are regulated by the activation state of Ras [152], resulting in decreased methionine uptake in K-Ras-transformed mouse fibroblasts. *Slc6a15* and its human ortholog - *SLC6A15* - belong to a large family (over 450 members) of solute carrier proteins (SLCs) controlling import/export of nutrients, cofactors, ions and many drugs. While many SLCs have not yet been characterized, a quarter of their encoding genes has been associated with human diseases and 26 different SLCs are the targets of known drugs, or drugs in development [170,171].

Remarkably, expression of the human *SLC6A15* gene is mostly down-regulated in the NCI-60 cells panel, the US National Cancer Institute (NCI) panel of 60 human cancer cell lines grown in culture [172]. An exception is represented by melanoma cells, in which *SLC6A15* is highly up-regulated. Therefore, the use of methionine uptake as a marker for proliferative activity in substitution of fluoro-deoxyglucose [173,174], or therapeutic use of dietary methionine restriction would benefit from knowledge of the expression of methionine transporters. Particularly, therapeutic regimens of cancer involving modulation of methionine metabolism could be more effective in cells with limited methionine transport capability.

1.3.2.2 Cysteine

Cysteine is a sulfur-containing, semi-essential proteinogenic amino acid [175]. It can be synthesized in humans to some extent; as such, it is

classified as conditionally essential, since it may become temporarily essential when synthesis during rapid growth or critical illness is insufficient [175]. Cysteine is a precursor for the tripeptide glutathione, an important intracellular antioxidant that reduces reactive oxygen species (ROS), thereby protecting cells from oxidative stress [176]. The systemic availability of oral glutathione (GSH) is negligible; so it must be biosynthesized from its constituent amino acids, cysteine, glycine, and glutamic acid, the first being the limiting substrate [177]. Furthermore, cysteine is a precursor for the production of taurine, another antioxidant, and sulfate [163]. At least in liver, glutathione also acts as cysteine storage, from which this amino acid can be mobilized if required to maintain protein synthesis under nutritional stress [178]. Under normal physiological conditions, cysteine can usually be synthesized *de novo* from homocysteine in humans if a sufficient quantity of methionine is available. Glutathione content in tumor cells has particular importance in the regulation of DNA synthesis, growth, and multidrug and radiation resistance [179]. As the half-life of intracellular glutathione is short, a lack of cysteine can lead to glutathione depletion, which in turn determines growth arrest and reduction in therapy resistance. Thus, glutathione might be a good target in cancer therapy [180], and cysteine/cystine deprivation of tumor cells has been proposed as treatment against a variety of cancers [181,182,183,184]. The x_c^- cystine/glutamate antiporter is one of the main plasma membrane transporter for cystine and

glutamate and is essential for cystine uptake in cancer cells. This transporter was first described in 1980 as a Na^+-independent transport system for L-cystine and L-glutamate in human fibroblasts [185]. The x_c^- transporter has also proven to be implicated in glutathione-based chemoresistance [186,187,188]. As such, the inhibition of x_c^- transporter to generate cystine/cysteine depletion may reveal a valuable therapeutic strategy [183,184,189].

Some cancers are unable to synthesize cysteine [182], likely due to a deficiency in the last enzyme in the transsulfuration pathway, γ-cystathionase [181]. Thus, cystine/cysteine is an essential amino acid for such cancers and its uptake from the external is vital for their growth and viability [179]. In addition, some cells show a low uptake capability for cystine due to lack of cystine transporter expression, like lymphoid cells. As such, in the absence of endogenous pathways for cysteine synthesis, these cells are mainly dependent on uptake of extracellular cysteine [182].

1.4 A mouse fibroblast model to study Ras-dependent metabolic rewiring in cancer

The identification of the networks underlying a considered system [39] is achievable by using a defined, genetically tractable model both for normal and transformed cells in which the transformed phenotype can be switched on and off by specific molecular events.

Normal mouse fibroblasts (NIH3T3) are largely employed for their indefinite growth in culture, retention of contact inhibition, and ease of transformation due to mutations or expression of introduced genes [41]. These cells and their derived cells stably expressing oncogenic *K-ras* mutant (NIH-RAS) proved to be a valid cellular model for studying Ras-dependent transcriptional reprogramming [191] and metabolic rewiring [101,192,193]. Indeed, several reports found coherent correlation between the results obtained in this cellular model with findings in tumor tissues and animal models [194,195,196,197]. The Ras-dependent transformation phenotypes of NIH-RAS cells (like the ability to overcome contact inhibition when plated in soft agar [41]) can be down-regulated by over-expressing a dominant negative mutant of RasGRF1 with Ras sequestering properties, called GEF-DN, extensively characterized in our laboratory [50,198,199] (**Figure 1.14**).

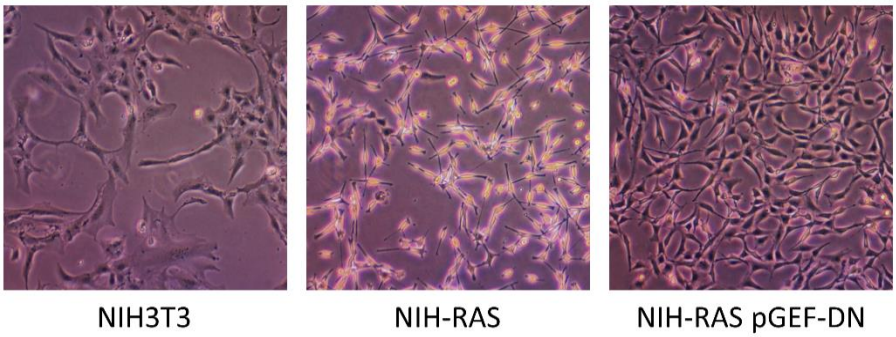

Figure 1.14 Our cellular model to study K-ras-induced transformation. *Left: normal NIH3T3 mouse fibroblasts; middle: NIH3T3 cells transformed by an activated form of the K-ras oncogene; right: K-ras-transformed NIH3T3 fibroblasts that stably overexpress the GEF-DN.*

Particularly, a single amino acid change within the catalytic domain of RasGRF1 turns this molecule into a dominant negative protein. GEF-DN is able to efficiently displace wild-type GEF from $p21^{ras}$ and to originate a stable Ras–GEF binary complex due to the reduced affinity of the nucleotide-free Ras–GEF complex for the incoming nucleotide [200]. This Ras sequestering property can be utilized to attenuate Ras signal transduction pathways in *K-ras*-transformed mouse fibroblasts, since GEF-DN expression down-regulates Ras activity both *in vitro* and *in vivo* and induces a reversion of the transformed phenotype on the basis of morphology, anchorage-independent growth and reduction of Ras-dependent tumor formation in nude mice [198]. Thus, the use of three cell lines (normal NIH3T3, transformed NIH-RAS and reverted NIH-RAS GEF-DN) allows to directly assess the role played by Ras activation in any given studied phenotype.

1.5 The study of cancer metabolism with a Systems Biology approach

Since the process of mapping and sequencing the human genome began, new technologies have made possible to obtain a huge number of molecular measurements within a tissue or cell. These technologies can be applied to a biological system of interest to get a snapshot of the underlying biology at a resolution never reached before. The scientific fields associated with measuring such biological molecules in a high-throughput way are called "*-omics*" and include proteomics,

transcriptomics, genomics, metabolomics, lipidomics and epigenomics, which correspond to global analyses of proteins, RNA, genes, metabolites, lipids and methylated DNA or modified histone proteins in chromosomes, respectively (**Figure 1.15**).

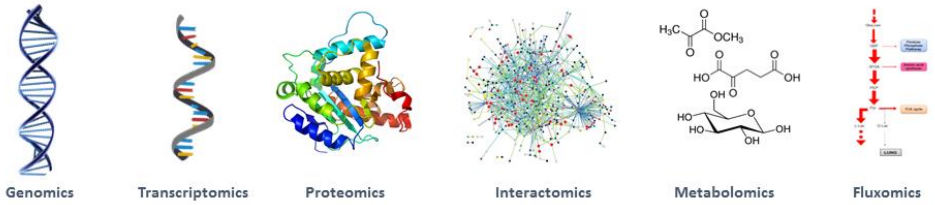

Figure 1.15 Omic technologies for Systems biology. From [201]

One common reason for conducting *-omic* research is to achieve a comprehensive understanding of the complex biological system under study [39]. Another common goal of *-omic* studies is to associate the *omics*-based molecular measurements with a clinical outcome of interest, such as prostate cancer survival time, risk of breast cancer recurrence, or response to therapy. The rationale is that, by taking advantage of *omics*-based measurements, there is the potential to develop a more accurate predictive or prognostic model of a particular condition or disease.

1.5.1 Main types of *-omic* data

Genomics Complete or partial DNA sequence of the genome of an organism (that remains essentially constant over time) can be assayed using various experimental platforms, including single nucleotide polymorphism (SNP) chips and DNA sequencing technology. SNP chips are

arrays of thousands of oligonucleotide probes that bind to specific DNA sequences in which nucleotide variants are known to occur. Genomic analysis also can detect insertions and deletions and copy number variation, referring to loss of or amplification of the expected two copies of each gene (one from the mother and one from the father at each gene locus). Personal genome sequencing is a more recent and powerful technology, which allows for direct and complete sequencing of genomes and transcriptomes.

Transcriptomics The transcriptome is the complete set of RNA transcripts from DNA in a cell or tissue. The transcriptome includes ribosomal RNA (rRNA), messenger RNA (mRNA), transfer RNA (tRNA), micro RNA (miRNA), and other non-coding RNA (ncRNA). In humans, only 1.5-2% of the genome is represented in the transcriptome as protein-coding genes. The two dominant classes of measurement technologies for the transcriptome are microarrays and RNA sequencing (RNAseq). Microarrays are based on oligonucleotide probes that hybridize to specific RNA transcripts. RNAseq is a much more recent approach, which allows for direct sequencing of RNAs without the need for probes. Transcriptomic data allowed to quantify and characterize global gene expression profiles of various cancer types [202,203], showing a differential expression of several genes between normal and transformed cells [204,205].

Proteomics The proteome is the complete set of proteins expressed by a cell, tissue, or organism. It is inherently quite complex because proteins can undergo posttranslational modifications (glycosylation, phosphorylation, acetylation, ubiquitylation, and many other modifications to the amino acids comprising proteins), have different spatial configurations and intracellular localizations, and interact with other proteins as well as other molecules. This complexity can lead to challenges in proteomics-based test development. The proteome can be assayed using mass spectrometry and protein microarrays [206,207]. Unlike RNA transcripts, proteins do not have obvious complementary binding partners, so the identification and characterization of capture agents is critical to the success of protein arrays. Proteomic approaches allowed the identification of proteins specifically expressed in transformed cells that could be used as cancer biomarkers [208,209,210].

Epigenomics The epigenome consists of reversible chemical modifications to the DNA, or to the histones that bind DNA, and produce changes in the expression of genes without altering their base sequence. Epigenomic modifications can occur in a tissue-specific manner, in response to environmental factors, or in the development of disease states, and can persist across generations. The epigenome can vary substantially among different cell types within the same organism. Biochemically, epigenetic changes that are measured at high-throughput level belong to two categories: methylation of DNA cytosine residues at CpG and multiple

kinds of modifications of specific histone proteins in the chromosomes (histone marks). RNA editing, the molecular process through which some cells can make discrete changes to specific nucleotide sequences within a RNA molecule after it has been generated by RNA polymerase, is another mechanism for epigenetic changes in gene expression, measured primarily by transcriptomic methods [211].

Metabolomics The metabolome is the complete set of small molecule metabolites found within a biological sample (including metabolic intermediates and end products). The metabolome is dynamic and can vary within a single organism and among organisms of the same species due to many factors such as changes in diet, stress, physical activity, pharmacological effects and disease. The components of the metabolome can be measured with mass spectrometry [212] as well as by nuclear magnetic resonance spectroscopy [213]. This method also can be used to study the lipidome [214], which is the complete set of lipids in a biological sample.

Metabolomics is the youngest of the *-omics* technologies and is able to concurrently identify thousands of metabolites, generated by the enzymatic reactions of specific metabolic pathways. As the different amounts of metabolites obtained under perturbed experimental conditions reflect the changes in enzyme activity, metabolomics allows to obtain a biochemical snapshot of the physiological and pathological state of a cell or an organism. Metabolic profiling provides a complete

functional picture of the biochemistry that connects the genome —via transcription and translation— to a particular phenotype through the interaction between the cell and the environment. For this reason, metabolomics applications have recently found a valuable use in clinical field, to identify new biomarkers in neurological, cardiovascular and cancer diseases [215].

Fluxomics Metabolomics, however, only provides a picture of the metabolite concentrations in the cell in a particular moment. The complete metabolic picture is a consequence of the transformation and transport of metabolites throughout metabolic reactions and transport processes, which are finely regulated at different levels. To complement metabolomics-derived information, the analysis of flux distributions and the changes associated to them are explored at cellular level with fluxomics [216,217].

Similar to genome, transcriptome, proteome, and metabolome, the fluxome is the complete set of metabolic fluxes in a cell. Nevertheless, unlike the others, the fluxome is a dynamic representation of the phenotype. This is due to the fluxome resulting from the interactions of the metabolome, genome, transcriptome, proteome, post-translational modifications and the environment [218]. Metabolic flux refers to the rate of metabolite conversion in a metabolic network: for a reaction, this rate is a function of both enzyme abundance and enzyme activity. Enzyme concentration is itself a function of transcriptional and translational

regulation in addition to the stability of the protein. Enzyme activity is affected by the kinetic parameters of the enzyme, the substrate concentrations, the product concentrations, and the effector molecules concentration. The genomic and environmental effects on metabolic flux are what determine healthy or diseased phenotype. Fluxomics describes the various approaches that seek to determine the rates of metabolic reactions within a biological entity. While metabolomics can provide instantaneous information on the metabolites in a biological sample, fluxomics describes metabolism as a dynamic process, since metabolic fluxes determine the cellular phenotype [219].

Two important technologies for flux analysis are ^{13}C-fluxomics and Flux Balance Analysis (FBA), the latter treated in the next paragraph. In ^{13}C-fluxomics, metabolic precursors are enriched with ^{13}C before being introduced to the system. Using an imaging technique, such as mass spectrometry or nuclear magnetic resonance spectroscopy, the level of incorporation of ^{13}C into metabolites can be measured and, with stoichiometry, the metabolic fluxes can be estimated [220].

As many reactions compete for common substrates, not only a single reaction or a small portion of the metabolic network must be considered. Thus, a complete study of cancer metabolism is achieved by pairing biochemical information with transcriptomic and proteomic data. Therefore, the study of metabolism is commonly addressed from an integrated perspective that aims to consider the metabolic network in its

entirety. To this end, Systems biology [221,222] is the conceptual and operative approach needed to extract and integrate information from this huge amount of different -*omic* data [216,223,224]. The systems biology approach systematically organizes, integrates and rationalizes the different -*omic* data through statistical analysis, computer aided modeling and visualization. It requires different scientific competencies so to give them structure, improve the understanding of emergent properties and their design principles and gain ability to predict the behavior of a system and to exploit it for applicative purposes [201].

1.5.2 Metabolic modeling

According to the Systems Biology paradigm, the biological system of interest needs to be formally described with a mathematical model. Two key features of modeling are the possibility to formulate *in vivo*-testable hypotheses and to integrate different experimental (wet lab) data, especially those measured with high-throughput techniques as transcriptomics, proteomics and metabolomics. In this context, there is a need for models able to analyze the regulatory features of metabolism, as well as to give structure and predictive power to post-genomic data.

Metabolism can be described with mathematical models defined at different levels of detail, ranging from *genome-wide models*, which include several thousands of reactions and metabolites, to *toy models*, which consider only a few reactions, passing through *core models*, usually characterized by hundreds of reactions and metabolites. The scale of the

model depends on the nature of the biological system under examination and the experimental data that are available or measurable for that system. Particularly, the analysis of the model is expected to increase the current knowledge on the system, thanks to novel predictions on its functioning and to their experimental validation. In this phase, initial experimental data are necessary to define a plausible mathematical model, since they can aid to discriminate among different hypotheses on the structure of the system. Moreover, the modeler has to identify the proper *level of abstraction* necessary to formally describe the components of the system and their mutual interactions and choose the most appropriate *mathematical formalism*. In this regard, dynamical models -usually defined as systems of differential equations- are considered the most likely candidates to achieve a detailed comprehension of cellular processes. However, the usual lack of quantitative parameters represents a limit to a wide applicability of this approach for large metabolic networks. Thus, the common practice for the computational investigation of metabolism usually relies on constraint-based models, which will be briefly treated in this thesis.

1.5.2.1. From wet lab to dry lab

1.5.2.1.1. Reconstruction of metabolic network

The starting point to develop a computational model of metabolism is the reconstruction of the network of metabolites and reactions in a cell [225].

This metabolic network can be represented as a graph, in which a number of components, called *nodes* (= metabolites), are interconnected through *edges* (= metabolic reactions). Such formal representations usually rely on genomic and literature data, possibly integrated with data obtained from laboratory experiments. Network reconstructions can vary in size and in levels of abstraction, according to the scope of their formulation.

One of the main purposes in the reconstruction of *genome-wide (GW) models* is to summarize all the current knowledge concerning metabolic processes at the level of single gene annotation, trying to consider every single reaction that is known to occur within an organism. The curation of GW models became possible after the development of high-throughput and *-omics* technologies [226], able to generate large amounts of quantitative data about living systems [227]. Thus, GW models are the result of the integration of different kinds of information about metabolism. Being extended and complex, GW metabolic network reconstructions often derive from a community effort, which may require many years of work [228].

At the opposite extreme, *toy models* have a simple structure and include a limited number of components, in order to just highlight some major regulatory properties and easily identify the most relevant components of the system. *Core models (CMs)* stay in between toy and GW models. They can cover in molecular details only one or a few simple pathways, or summarize information about several pathways, by including only those

elements that are assumed to be essential to unravel the regulatory features and/or the dynamic behavior of the phenomenon under study.

1.5.2.1.2. Ensemble Modeling approach

Ensemble modeling (EM) aims at the investigation of the model behavior under different perturbations. EM consists in a large set of candidate models, based on elementary reactions characterized by mass-action kinetics, that achieve a certain steady state flux distribution in a given experimental condition. This strategy allows to capture the behavior of enzymatic reactions, in the case of complete knowledge of reference fluxes, or enzyme and metabolite concentrations in the whole network.

EM is more appropriate than other approaches to directly account for uncertainties, especially in the case of models with large numbers of unknown parameters, and when some parameters are not completely identifiable with the available experimental data [229]. Once the ensemble of models is produced, additional experimental data obtained in perturbation experiments are acquired and used to iteratively reduce the set of candidate models, resulting in an increasingly predictive subset of models.

Being the main input of the models in the ensemble, the lack of experimental measurements or the ability of calculating the steady state fluxes can reduce the applicability of EM.

1.5.2.2 From models to *in silico* data: Flux Balance Analysis

Constraint-based modeling relies on the idea that all the expressed phenotypes of a given biological system must satisfy a number of constraints, which can be of physicochemical, spatial or environmental type. Accordingly, by restricting the space of all possible system's states, it is possible to determine the functional states that a metabolic network can or cannot achieve. The fundamental assumption of constraint-based modeling is that, regardless of the environmental condition, the organism will reach a quasi-steady state that satisfies the given constraints.

The starting point of constraint-based modeling is the stoichiometric matrix, which contains the stoichiometric values of the reactants and products of each reaction in the metabolic network: each row in the matrix corresponds to a metabolite, each column corresponds to a reaction. The null space of this matrix mathematically represents the mass balances for each intracellular metabolite, and expresses all those flux distributions that can be achieved by the metabolic network at steady state. Additional constraints, such as irreversibility or capacity constraints, are incorporated to further restrict the solution space, by specifying the maximum and minimum values of the flux through any given reaction. Capacity constraints are usually set according to experimental records and are recommended at least for nutrient intake reactions.

FBA [230] allows to select a single flux distribution within the obtained feasible solution space, by assuming that the cell behavior is optimal with

respect to a specified objective (represented according to an *objective function* (OF)), and by calculating the optimal flux distribution by means of an optimization routine.

Thus, the inputs of FBA are the stoichiometric matrix, the specification of the flux boundaries for each reaction and the OF, whereas the output is the quantification of the flux through each reaction.

Thanks to the advantages of a modeling approach that does not require information about kinetic parameters, FBA has recently received increasing attention in Systems Biology, to gain novel knowledge about the physiological state of a cell [231,232]. As a general remark, solutions obtained with FBA are only as good as the constraints used to identify them and the rightness of the OF (knowledge about the true OF that drives the evolution is often limited). Moreover, a major limit of FBA is that it is not suited for the investigation of the system dynamics, as it disregards information on metabolic concentrations and kinetic parameters.

Despite these challenges, FBA has significant potential to support the interpretation of metabolic data, and there have been many innovative developments to improve its predictive capabilities [233,234].

1.5.2.3. Model validation

Any *in silico* metabolic model must undergo a validation process to confirm its capability to reproduce the behavior and properties of the biological system under study in different conditions.

The evaluation of a model proceeds through the analysis of its behavior, which allows to detect problems in its reconstruction, according to an iterative process of tuning, simulation and validation. Errors in a metabolic reconstruction are more likely to occur within large-scale models, which are typically investigated with constraint-based approaches. Some known issues that can affect the validity of a metabolic reconstruction are the presence of dead-end metabolites (i.e., metabolites that are only produced or consumed within the network) or the existence of network gaps [225], which are missing reactions that should connect some metabolites.

Metabolic models might be evaluated qualitatively (e.g., to assess their capability to generate all the precursor metabolites and all the metabolites that the organism produces/degrades) and quantitatively, by comparing the model behavior with various experimental observation such as secretion products and gene essentiality.

The strategy of *gene deletion analysis* deserves particular attention as it might be exploited either to validate a model, or to infer novel experimental hypotheses after model validation. This method consists in simulating the inhibition of a metabolic gene by excluding from the model the reactions associated to that gene.

2. AIM OF THE THESIS

Cancer cells rewire their metabolism to sustain enhanced proliferation and survival, rendering them dependent on constant supply of nutrients and energy. Besides the well-studied altered glucose metabolism, over the last years increased utilization of amino acids has emerged as another key feature of cancer cell metabolism. In parallel, recent advances in the comprehension of tumorigenesis have revealed that cancer is a complex disease and cannot be unraveled by simply investigate genetic mutations of cancer cells. In this context, targeting dysregulated metabolic pathways that support tumorigenesis and cancer cell growth requires both the advancement of experimental technologies for exhaustive measurement of *-omics* as well as the advancement of robust computational methods for accurate analysis of the generated data. Such system-level perspective of cancer metabolism may help in the identification of novel selective drug targets.

In this regard, the work here presented has the following main objectives:

1) Study the effect of *K-ras* proto-oncogene activation in NIH3T3 mouse fibroblasts on transport and metabolism of the proteinogenic sulfur amino acids, cysteine and methionine, by using the approach of nutritional perturbation. Possibly extend the findings to human cancer cells in the perspective of novel

anticancer strategies dealing with sulfur amino acid metabolism, which may involve the approach of dietary methionine restriction;

2) Investigate the roles that glutamine has in promoting the enhanced proliferation of *K-ras*-transformed NIH3T3 mouse fibroblasts, by substituting it with nonessential amino acids (NEAA) as nitrogen source and alpha-ketoglutarate (AKG) as carbon source and exploiting an integrated, Systems biology approach, which makes use of *–omics* technologies and metabolic modeling to analyze the behavior of nutritionally-perturbed cells.

3. RESULTS

3.1 K-Ras Activation Induces Differential Sensitivity to Sulfur Amino Acid Limitation and Deprivation and to Oxidative and Anti-Oxidative Stress in Mouse Fibroblasts

Gaia De Sanctis[1,2], Michela Spinelli[1,2], Marco Vanoni[1,2] and Elena Sacco[1,2*]

[1]*SYSBIO, Centre of Systems Biology, Milan, Italy*
[2]*Department of Biotechnology and Biosciences, University of Milano-Bicocca, Piazza della Scienza 2, 20126 Milan, Italy*

[*]Corresponding author
E-mail: elena.sacco@unimib.it

Published as:

De Sanctis G, Spinelli M, Vanoni M, Sacco E (2016) K-Ras Activation Induces Differential Sensitivity to Sulfur Amino Acid Limitation and Deprivation and to Oxidative and Anti-Oxidative Stress in Mouse Fibroblasts. PLoS ONE 11(9): e0163790.
doi:10.1371/journal.pone.0163790

Abstract

Background

Cancer cells have an increased demand for amino acids and require transport even of non-essential amino acids to support their increased proliferation rate. Besides their major role as protein synthesis precursors, the two proteinogenic sulfur-containing amino acids, methionine and cysteine, play specific biological functions. In humans, methionine is essential for cell growth and development and may act as a precursor for cysteine synthesis. Cysteine is a precursor for the biosynthesis of glutathione, the major scavenger for reactive oxygen species.

Methodology and Principal Findings

We study the effect of K-ras oncogene activation in NIH3T3 mouse fibroblasts on transport and metabolism of cysteine and methionine. We show that cysteine limitation and deprivation cause apoptotic cell death (cytotoxic effect) in both normal and K-ras-transformed fibroblasts, due to accumulation of reactive oxygen species and a decrease in reduced glutathione. Anti-oxidants glutathione and MitoTEMPO inhibit apoptosis, but only cysteine-containing glutathione partially rescues the cell growth defect induced by limiting cysteine. Methionine limitation and deprivation has a cytostatic effect on mouse fibroblasts, unaffected by glutathione. K-ras-transformed cells – but not their parental NIH3T3 - are extremely sensitive to methionine limitation. This fragility correlates with decreased expression of the Slc6a15 gene - encoding the nutrient transporter SBAT1,

known to exhibit a strong preference for methionine - and decreased methionine uptake.

Conclusions and Significance

Overall, limitation of sulfur-containing amino acids results in a more dramatic perturbation of the oxido-reductive balance in K-ras-transformed cells compared to NIH3T3 cells. Growth defects induced by cysteine limitation in mouse fibroblasts are largely – though not exclusively – due to cysteine utilization in the synthesis of glutathione, mouse fibroblasts requiring an exogenous cysteine source for protein synthesis. Therapeutic regimens of cancer involving modulation of methionine metabolism could be more effective in cells with limited methionine transport capability.

Introduction

Activation of the *K-ras* proto-oncogene [1,2,3,4] has a great incidence in human tumors, as reported in the catalogue of somatic mutations in cancer (COSMIC) [5]. *K-ras* activation occurs in 22% of all tumors, prevalently in pancreatic carcinomas (about 90%), colorectal carcinomas (40–50%), and lung carcinomas (30–50%), as well as in biliary tract malignancies, endometrial cancer, cervical cancer, bladder cancer, liver cancer, myeloid leukemia and breast cancer. K-Ras oncoproteins are important clinical targets for anti-cancer therapy [6] and several strategies have been explored in order to inhibit aberrant Ras signaling, as reviewed in [7,8,9,10].

The acquisition of important hallmark traits of cancer cells, including enhanced cell growth and survival, rely on deep changes in metabolism driven by oncogene activation [11,12,13,14,15]. Oncogenic activation of *K-ras* contributes to the acquisition of the hyper-glycolytic phenotype (also known as Warburg effect, from the pioneering studies of Warburg [16]) due to enhancement in glucose transport and aerobic glycolysis [17,18]. *K-ras* oncogene activation also correlates with down-regulated expression of mitochondrial genes, altered mitochondrial morphology and production of large amount of reactive oxygen species (ROS) associated with mitochondrial metabolism [19,20]. Furthermore, *K-ras* activation allows cells to make extensive anaplerotic usage of glutamine, the more concentrated amino acid in human plasma [21]. In Ras-

transformed cells, glutamine is largely utilized through reductive carboxylation that results in a non-canonical tricarboxylic acid cycle (TCA) pathway [19,22,23,24,25,26]. These metabolic changes render Ras-transformed cells addicted to glutamine, and to glutaminolysis, and offer new therapeutic opportunities. Indeed, glutamine metabolism restriction and targeted cancer therapeutics directed against glutamine transporters or glutaminolysis can be used to limit tumor cell proliferation and survival without affecting normal cells [27,28,29].

Besides glutamine transporters, all amino acid transporters are being receiving attention from scientific community as potential drug targets for cancer treatment, given the increased demand of cancer cells for these nutrients to support their enhanced cell growth [30,31]. Selective blockers of these transporters might be effective in preventing the entry of important amino acids into tumor cells, thus essentially starving these cells to death.

Methionine is an essential amino acid required for normal growth and development in mammals [32]. The intracellular level of methionine depends on the balance between synthesis (through the *de novo* synthetic pathway), recycle (through the *salvage* pathway), consumption (in biosynthesis of proteins) and its transport. An important metabolite of methionine is S-adenosylmethionine (SAM), the principal methyl donor in the cell. SAM is required for methylation of DNA, RNA, proteins (including histones [33]) and lipids by the enzymes methyltransferases. Moreover,

SAM is involved in biosynthesis of polyamines, which have far-ranging effects on nuclear and cell division, and methionine salvage pathway [34]. SAM gives its activated methyl group in methylation reactions, being converted to S-adenosylhomocysteine, which is reversibly hydrolyzed to homocysteine (S1 Fig). Depending on demand, homocysteine metabolism can be either directed toward the re-methylation pathway to regenerate methionine (thus increasing methylation potential) or toward antioxidant synthesis in the trans-sulfuration pathway [34]. In the first catabolic step of trans-sulfuration, homocysteine may be condensed to serine to form cystathionine, which in turn may be converted to cysteine [35].

Cysteine is a sulfur-containing, semi-essential proteinogenic amino acid. It can be synthesized in humans to some extent; as such, it is classified as conditionally essential, since it may become temporarily essential when synthesis during rapid growth or critical illness is insufficient [36]. Cysteine is a precursor for the tripeptide glutathione, an important intracellular antioxidant that reduces reactive oxygen species (ROS), thereby protecting cells from oxidative stress [37]. The systemic availability of oral glutathione (GSH) is negligible; so it must be biosynthesized from its constituent amino acids, cysteine, glycine, and glutamic acid, the first being the limiting substrate [38]. Furthermore, cysteine is a precursor for the production of taurine, another antioxidant, and sulfate [39]. At least in liver, glutathione also acts as cysteine storage, from which this amino acid can be mobilized if required to maintain protein synthesis under

nutritional stress [40]. Under normal physiological conditions, cysteine can usually be synthesized *de novo* from homocysteine in humans if a sufficient quantity of methionine is available.

Normal mouse fibroblasts (NIH3T3) and their derived cells stably expressing oncogenic K-*ras* mutant (NIH-RAS) proved to be a valid cellular model for studying Ras-dependent transcriptional reprogramming [41] and metabolic rewiring [23,42,43]. The Ras-dependent transformation phenotypes of NIH-RAS cells can be down-regulated by over-expressing a dominant negative mutant of RasGRF1 with Ras sequestering properties, extensively characterized in our laboratory [7,44,45]. We use these cell lines to study the effect of *K-ras* proto-oncogene activation on transport and metabolism of the proteinogenic sulfur amino acids, cysteine and methionine.

We show that cysteine limitation and deprivation increase ROS level and decrease reduced glutathione, eventually leading to apoptotic cell death. Through the complementary use of anti-oxidants glutathione and MitoTEMPO (a cysteine non-containing reducing agent) and inhibitors of *de novo* biosynthesis of reduced glutathione, we show that growth defects induced by cysteine limitation in mouse fibroblasts are largely – though not exclusively – due to cysteine utilization in the synthesis of glutathione and that mouse fibroblasts require an exogenous cysteine source for protein synthesis. Methionine limitation and deprivation is cytostatic and unaffected by glutathione. Limitation of sulfur-containing amino acids

perturbs the oxidoreductive balance, particularly in *K-ras*-transformed cells that display selective growth fragility to a moderate reduction in methionine supply. Such nutritional fragility correlates with Ras activation, decreased expression of the *Slc6a15* gene -encoding the methionine transporter SBAT1- and reduced methionine uptake.

Results

Methionine limitation reduces growth of Ras-transformed mouse fibroblasts more than growth of normal cells

First, we analyzed cell proliferation of normal NIH3T3 and Ras-transformed NIH-RAS mouse fibroblasts under standard growth condition (0.2 mM Cys, 0.2 mM Met), limitation (1/8: 0.025 mM; 1/4: 0.05 mM; 1/2: 0.1 mM) and deprivation of cysteine or methionine. Both cell lines were unable to grow in the absence of either methionine or cysteine (Fig 1A-B, open squares), demonstrating that both sulfur amino acids are essential for cell proliferation of mouse fibroblasts, which are not able to synthesize neither cysteine nor methionine each from the other.

Growth of NIH-RAS cells was more severely inhibited by methionine limitation than that of NIH3T3 cells. In $Met_{1/2}$ condition (Fig 1A-B, light triangles, and Fig 1D) the mass duplication time (MTD) of NIH-RAS cells was 1.5 longer than that of NIH3T3 (S1 Table). More stringent methionine limitation ($Met_{1/8}$) resulted in almost complete arrest of cell proliferation of both cell lines (Fig 1A, dark filled triangles, and S1 Table). Fig 1C-D show cell proliferation data 30 and 72 hours after methionine limitation, highlighting enhanced sensitivity of transformed NIH3T3 cells to methionine limitation. Note that NIH-RAS cells grown in $Met_{1/2}$ condition are still largely viable after 72 hours, unlike the cells grown in $Met_{1/8}$ condition (Fig 1D). Under methionine limitation NIH-RAS cells were also

severely hampered in *foci* formation ability (Fig 1E). Notably the major sensitivity of Ras-transformed cells to methionine limitation was fully reverted by the over-expression of a dominant negative mutant of the Ras-specific guanine nucleotide exchange factor RasGRF1 (RasGRF1^{W1056E}, that we refer to as GEF-DN), endowed with Ras sequestering properties (Fig 1C-D, S2-3 Fig).

All together, these data indicate that Ras hyper-activation enhances sensitivity to methionine limitation in mouse fibroblasts.

As shown in Figure 1B and in S1 Table the cell proliferation behavior under cysteine limitation and deprivation was quite similar in NIH3T3 and NIH-RAS cells. In $Cys_{1/2}$ condition both cell lines grew as well as in standard medium (S4A Fig, S1 Table), while further reduction of cysteine ($Cys_{1/4}$) increased the MDT of both NIH3T3 and NIH-RAS cells, even if slightly more in transformed cells (Fig 1B, S1 Table). Cysteine limitation strongly reduced *foci* formation ability of NIH-RAS cells (Fig 1E).

Fig 1 Proliferation under methionine and cysteine deprivation and limitation.

Cell proliferation of NIH3T3 and NIH-RAS cells grown in media supplemented with different concentrations of methionine and glutathione (A) or cysteine and glutathione (B) and counted daily for 72 h of growth under conditions indicated. Plotted data are mean +/- standard deviation computed from at least three independent experiments. (C-D)

Cell proliferation of NIH3T3, NIH-RAS and NIH-RAS pGEF-DN cells grown for 30 h (C) and 72 h (D) under conditions indicated. (E) *Foci* formation of NIH-RAS cells grown for 9 days under conditions indicated. *P<0.05; **P<0.01 (Student's *t*-test).

Cysteine mainly acts as a precursor of glutathione, whose excess mostly affects normal cells

Apoptotic and necrotic cell death can be assayed by FACS after staining with Annexin V-FITC and propidium iodide (PI). After limitation or deprivation of cysteine for 30 hours, apoptotic cells significantly increased in both cell lines, the effect being stronger in cysteine-deprived cells (Fig 2A). Supplementation of cysteine to cells grown for 72 hours in cysteine-free medium did not result in any significant growth recovery, reinforcing the notion that cysteine deprivation exerted a cytotoxic effect (cell death) in both NIH3T3 and NIH-RAS cell lines (Fig 2E).

Glutathione is the most important endogenous antioxidant in mammalian cells, and the major redox buffer responsible for redox homeostasis [46,47]. It acts as a ROS scavenger through its oxidation to GSSG. The reduced form (GSH) is restored at the expenses of NADPH. The intracellular concentration of GSH depends on a dynamic balance between synthesis, consumption rate (metabolism), and its transport.

We measured ROS (by FACS analysis of DCFDA-stained cells, Fig 2B), endogenous total (GSH+GSSG) and reduced (GSH) glutathione levels (by an enzymatic assay, Fig 2C) in NIH3T3 and NIH-RAS cells in standard

medium and 48 h after perturbing cysteine metabolism. In keeping with literature data [19,45,48,49], in standard medium NIH-RAS cells showed a 1.7-fold higher ROS level than NIH3T3 (Fig 2B), accompanied by a moderate decrease in total glutathione and a significant decrease in reduced glutathione (Fig 2C). Cysteine limitation and deprivation induced an increase in ROS levels, the effect being stronger in NIH-RAS cells (Fig 2B). Under cysteine limitation, total glutathione levels (GSH+GSSG) were lower than in standard condition (Fig 2C), consistently with the notion that cysteine availability is rate-limiting for GSH synthesis [50,51,52,53]. The high cell mortality under cysteine deprivation hindered the measurement of glutathione levels.

To investigate whether mouse fibroblasts are dependent on cysteine for growth, or whether the growth defects are the result of the oxidative stress on the cells, we took two complementary approaches. First, we modulated the oxidative response of cysteine-depleted cells with either cysteine-containing (GSH) or cysteine-non-containing (MitoTEMPO) anti-oxidants. Second, we blocked glutathione *de novo* biosynthesis of standard or cysteine-limited cells with buthionine sulfoximine (BSO), that blocks the activity of gamma-glutamylcysteine synthetase (γ-GCT) required for the formation of the glutathione precursor gamma-glutamylcysteine from glutamate and cysteine [47].

Supplementing GSH to cysteine-free medium (-Cys+GSH growth condition) partially restored cell proliferation (Fig 1A, Fig 1C-D) in both

NIH3T3 and NIH-RAS cell lines and the ability to form *foci* in NIH-RAS cells (Fig 1E). Also, supplementation of GSH significantly reduced apoptosis induced by cysteine withdrawal and fully restored ROS levels to basal (Fig 2A-B). Compared to NIH3T3, NIH-RAS cells require a higher GSH concentration both to recover cell survival and growth as well as to show the "anti-oxidative stress" (Fig 2D), phenomenon described in [54]. The reduced sensitivity to both positive and negative effects of GSH is most likely the result of the lower GSH content of Ras-transformed cells (Fig 2C). Supplementation of MitoTEMPO in cysteine-free medium reduced apoptosis to the same levels observed after GSH addition (Fig 2A), but could not rescue cell proliferation under cysteine deprivation (S4B Fig).

In both NIH3T3 and NIH-RAS cell lines, BSO treatment severely down-regulated glutathione accumulation (Fig 2C) and reduced proliferation (S4C Fig). Concurrently, both ROS accumulation (Fig 2B) and the fraction of apoptotic cells increased (Fig 2A). These effects appear stronger in NIH-RAS than in NIH3T3 cells. They are dramatically enhanced by growth in limiting cysteine, which results in the death of most cells within 30 h from the treatment (Fig 2A). Cell death in BSO-treated cells grown in the absence of cysteine was essentially caused by oxidative stress, since almost all cells were strongly positive to DCFDA staining, as shown by fluorescence-microscopy analysis (S4D Fig). In these conditions ca 90% and 50% of NIH-RAS and NIH3T3 cells, respectively, are apoptotic after 30 h of treatment (Fig 2A). All together, these data confirm the major

dependence of NIH-RAS from cysteine availability for the maintenance of proper GSH levels, redox homeostasis and cell viability, and on the other hand suggest that NIH3T3 cells less recur to the *de novo* synthesis of GSH to maintain redox homeostasis and favorable growth conditions.

Fig 2 Viability and redox state under cysteine deprivation and limitation. (A) Representative dot plots for NIH3T3 and NIH-RAS cells stained with Annexin V-FITC and propidium iodide and analyzed by FACS after 30 h of growth under conditions indicated. Q1 = quadrant 1, healthy cell; Q2 = quadrant 2, early apoptotic cells; Q3 = quadrant 3, late apoptotic cells; Q4 = quadrant 4, necrotic cells. MitoTEMPO and buthionine sulfoximine (BSO) were used at the concentration of 10 μM and 100 μM, respectively. The values reported for each quadrant are the mean +/- standard deviation of three independent experiments. (B) Relative ROS levels in NIH3T3 and NIH-RAS cells grown for 48 h under conditions indicated as determined by DCFDA (2',7'-dichlorodihydrofluorescein diacetate) staining. Each bar represents the mean of at least three independent experiments with error bars representing the standard deviation. (C) Reduced and total glutathione levels (measured as described in [55]) in NIH3T3 and NIH-RAS cells grown for 48 h under conditions indicated. Each bar represents the mean of at least three independent experiments with error bars representing the standard deviation. (D) Cell proliferation of NIH3T3 and NIH-RAS cells grown for 48 h in cysteine-free medium supplemented with

different concentrations of glutathione. Plotted data are mean +/- standard deviation computed from at least three independent experiments. *P<0.05; **P<0.01 (Student's *t*-test). (E) Crystal violet staining of NIH3T3 and NIH-RAS cells plated at the density of 9000 cells/cm^2, grown for 72 h under cysteine deprivation and then for 48 h in standard medium.

Ras-transformed mouse fibroblasts show lower expression of a gene encoding a methionine-transporting solute carrier and reduced methionine uptake than normal cells

Contrary to the behavior of cells perturbed by cysteine limitation or deprivation, methionine perturbation only weakly enhanced apoptosis in cells, slightly more in NIH-RAS cells (Fig 3A). Methionine limitation and deprivation increased ROS levels, methionine limitation having a significantly stronger effect in NIH-RAS cells (Fig 3B). As a likely consequence, GSH levels under limiting methionine were lower than in standard medium (Fig 3C) and inversely correlated with ROS levels (Fig 3D). By contrast, total glutathione levels (GSH+GSSG) under limiting methionine were similar to those found in standard condition, consistently with the presence in the medium of the glutathione precursor cysteine (Fig 3C). The high cell mortality under methionine deprivation hindered the measurement of glutathione levels. These results demonstrated that changes in ROS and reduced glutathione levels under

methionine limitation (and, likely, in methionine deprivation) do not depend on alterations in glutathione biosynthesis. It is noteworthy that supplementation of 4 mM GSH to cells growing in methionine-free medium (-Met+GSH growth condition) resulted in decreased ROS levels in both cell lines (Fig 3B), however, neither NIH3T3 nor NIH-RAS cells were able to grow (Fig 1A,C-D), and NIH-RAS cells did not form *foci* (Fig 1E).

A GSH *versus* ROS plot (Fig 3D) confirms that GSH and ROS levels are inversely correlated (which is not unexpected) and further shows that limitation of sulfur-containing amino acids results in a more dramatic decrease of GSH as a function of ROS concentration in NIH-RAS compared to NIH3T3 cells.

Supplementation of methionine to cells grown for 72 hours in methionine-free medium resulted in a significant growth recovery, reinforcing the notion that methionine deprivation exerted a cytostatic effect (arrest of cell proliferation) in both NIH3T3 and NIH-RAS cell lines (Fig 3E).

We analyzed genome-wide transcriptional profiling datasets for NIH3T3 and NIH-RAS cells (available in NCBI GEO database; accession GSM741354-GSM741361 for NIH3T3 cells and GSM741368-GSM741375 for NIH-RAS cells), previously obtained in our laboratory with an MG_U74Av2 Affymetrix Gene Chip [41] to identify the pattern of expression of genes encoding solute carriers [56]. The expression of four of these genes was significantly altered in Ras-transformed *versus* normal cells (S5 Fig). One of these genes is *Slc6a15* that encodes SBAT1, an amino

acid transporter exhibiting strong preference for branched chain amino acids and methionine [57,58]. RT-PCR analysis of the expression of these four genes in normal and transformed fibroblasts (Fig 4A) validated Affymetrix results, clearly indicating that in NIH-RAS cells the expression of *Slc6a15* is down-regulated. Notably, over-expression in NIH-RAS cells of the Ras inhibitor GEF-DN determined a significant increase in the expression of *Slc6a15* (S3C Fig). Consistently with the strong, but not always complete reversion of Ras-dependent phenotypes induced by GEF-DN expression [45], up-regulation of *Slc6a15* expression is strong, but possibly not complete compared to NIH3T3 cells. Our data thus indicate that sensitivity to methionine limitation (S3A-B Fig) and expression of the SBAT1-encoding *Slc6a15* gene (S3C Fig) are regulated by the activation state of Ras.

To confirm that methionine transport is impaired in NIH-RAS cells as suggested by transcriptional analysis, we assayed methionine uptake in NIH3T3 and NIH-RAS cells by using a ^{35}S-methionine incorporation assay. NIH-RAS cells showed a significantly reduced incorporation of ^{35}S-methionine per unit of protein in both exponential and confluent growth conditions (Fig 4B). The combined transcriptional and biochemical analyses therefore suggest that down-regulation of *Slc6a15* gene expression and ensuing decreased methionine transport activity in Ras-transformed cells could be the reason for their higher sensitivity to methionine limitation.

Fig 3 Viability and redox state under methionine deprivation and limitation.

(A) Representative dot plots for NIH3T3 and NIH-RAS cells stained with Annexin V-FITC and propidium iodide and analyzed by FACS after 30 h of growth under conditions indicated. Q1 = quadrant 1, healthy cell; Q2 = quadrant 2, early apoptotic cells; Q3 = quadrant 3, late apoptotic cells; Q4 = quadrant 4, necrotic cells. The values reported for each quadrant are the mean +/- standard deviation of three independent experiments. (B) Relative ROS levels in NIH3T3 and NIH-RAS cells grown for 48 h under conditions indicated as determined by DCFDA (2',7'-dichlorodihydrofluorescein diacetate) staining. Each bar represents the mean of at least three independent experiments with error bars representing the standard deviation. (C) Reduced and total glutathione levels (measured as described in [55]) in NIH3T3 and NIH-RAS cells grown for 48 h under conditions indicated. Each bar represents the mean of at least three independent experiments with error bars representing the standard deviation *P<0.05; **P<0.01 (Student's *t*-test). (D) Negative correlation between reduced glutathione levels and ROS levels in NIH3T3 and NIH-RAS cells grown under conditions indicated. Linear regression curves are not parallel with a 99.9% confidence interval; Student's *t*-test. (E) Crystal violet staining of NIH3T3 and NIH-RAS cells plated at the density of 9000 cells/cm^2, grown for 72 h under methionine deprivation and then for 48 h in standard medium.

Fig 4 Methionine transport and solute carrier expression in mouse fibroblasts and in NCI-60 panel.

(A) Semiquantitative RT-PCR results for NIH3T3 and NIH-RAS cells grown for 48 h in standard medium performed in triplicate on genes showing at least a two-fold change between NIH-RAS *vs* NIH3T3 cells in each of the two Affymetrix independent experiments (S5 Fig). (B) Labeled amino acid (^{35}S-methionine) uptake rate in exponential and confluent cells (48 and 72 h of growth in standard medium, respectively), measured after 20'-40'-60' (for exponential cells) and after 30'-50'-60' (for confluent cells) of labeling with 0.025 mCi/ml ^{35}S-Met. Radioactivity values, expressed as CCPM (corrected counts per minute), were normalized on total protein content and plotted against labeling time. Results are mean +/- standard deviation of three independent experiments. **P<0.01; ***P<0.001 (Student's *t*-test). (C) The mRNA expression data for the NCI-60 human tumor cell lines were retrieved from CellMiner relational database [59]. These expression data were inputted in CIMminer [60] to generate a heat map, as described in Materials and Methods. Here are highlighted the names of the genes whose expression was statistically different between NIH3T3 and NIH-RAS cells, with a particular emphasis on the data related to *SLC6A15* gene. (D) Concept map of cysteine and methionine metabolism in NIH3T3 and NIH-RAS cells.

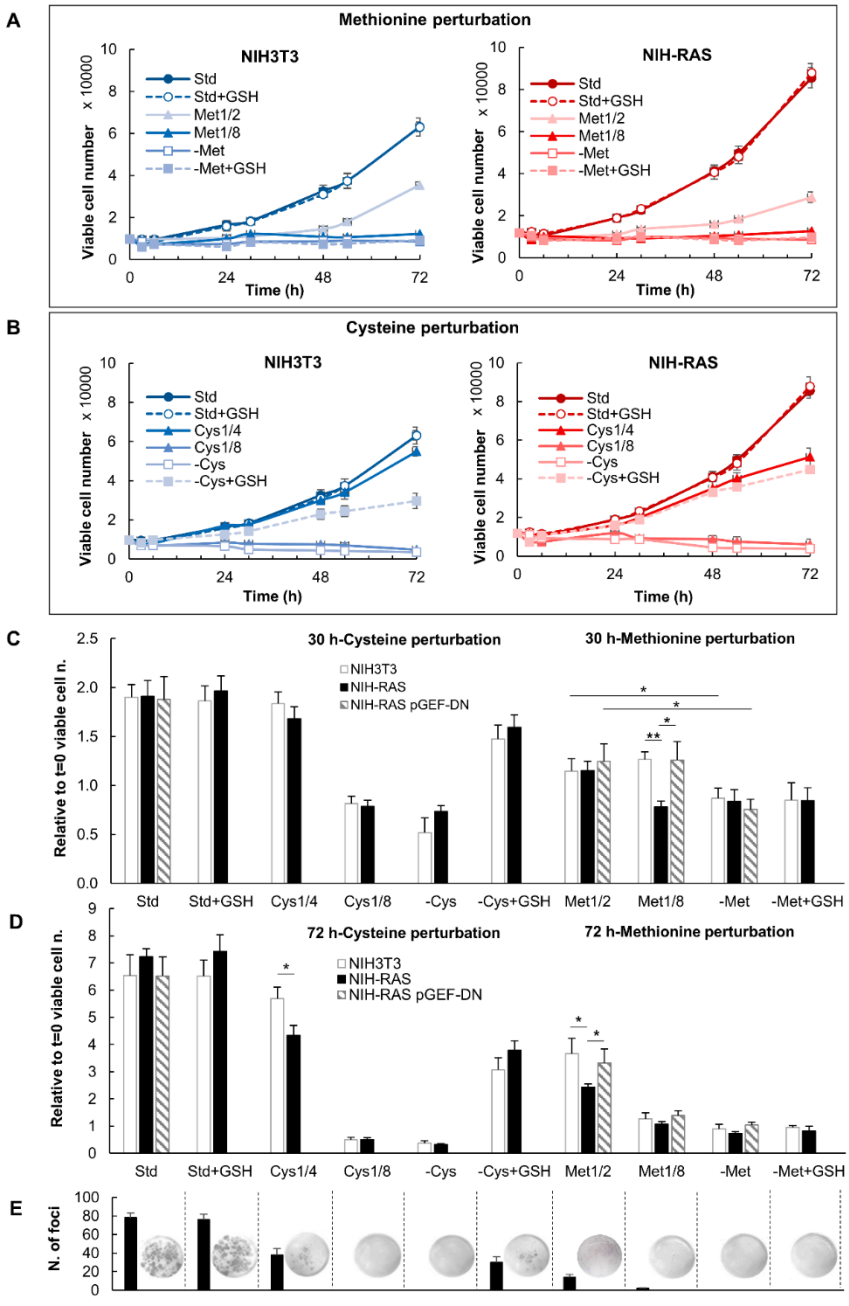
A
Methionine perturbation
NIH3T3
NIH-RAS
Viable cell number x 10000
Time (h)
Std
Std+GSH
Met1/2
Met1/8
-Met
-Met+GSH
B
Cysteine perturbation
Cys1/4
Cys1/8
-Cys
-Cys+GSH
C
30 h-Cysteine perturbation
30 h-Methionine perturbation
NIH3T3
NIH-RAS
NIH-RAS pGEF-DN
Relative to t=0 viable cell n.
D
72 h-Cysteine perturbation
72 h-Methionine perturbation
E
N. of foci

Figure 1

A
NIH3T3
NIH-RAS
Std
Std+BSO
Cys1/4
Cys1/4+BSO
Cys1/8
Cys1/8+BSO
-Cys
-Cys+GSH
-Cys+MitoTEMPO
0.34 ±0.06% 1.58 ±0.07% 2.90 ±0.21% 5.41 ±0.43% 2.64 ±0.23% 7.98 ±1.66% 13.33 ±1.16% 46.18 ±1.90% 8.03 ±1.60% 8.93 ±1.32% 14.22 ±1.35% 51.29 ±2.03% 17.02 ±1.16% 33.76 ±0.11% 1.84 ±0.07% 3.19 ±0.13% 0.63 ±0.09% 1.79 ±1.13%
95.12 ±0.05% 2.96 ±0.03% 72.28 ±1.69% 19.42 ±0.97% 84.25 ±1.03% 5.13 ±0.62% 35.98 ±0.71% 4.51 ±0.52% 79.22 ±1.68% 3.82 ±0.43% 28.41 ±0.69% 6.09 ±0.12% 47.27 ±1.20% 1.95 ±0.18% 92.38 ±1.18% 2.59 ±0.05% 91.47 ±1.24% 6.11 ±0.38%
0.27 ±0.06% 1.79 ±0.59% 0.69 ±0.04% 7.68 ±0.34% 0.68 ±0.07% 5.19 ±0.45% 2.88 ±0.67% 89.10 ±2.98% 0.66 ±0.06% 4.71 ±0.35% 2.71 ±0.56% 90.17 ±3.10% 1.57 ±0.37% 21.34 ±1.99% 0.50 ±0.17% 5.20 ±0.83% 0.47 ±0.06% 3.70 ±0.42%
95.77 ±0.28% 2.18 ±0.80% 76.88 ±1.02% 14.75 ±0.27% 92.09 ±1.02% 2.05 ±1.32% 4.44 ±0.87% 3.57 ±0.22% 90.62 ±1.35% 4.04 ±1.07% 4.03 ±0.14% 3.09 ±0.28% 72.58 ±3.02% 4.51 ±1.39% 89.36 ±1.56% 4.93 ±0.90% 91.63 ±0.16% 4.19 ±0.30%
Annexin V-FITC
Propidium iodide
B
ROS (relative DCFDA Signal to NIH3T3 in Std)
NIH3T3
NIH-RAS
Std
Std+BSO
Std +GSH
Cys1/4
Cys1/4 +BSO
Cys1/8
Cys1/8 +BSO
Not measurable
-Cys
-Cys +GSH
C
Glutathione (relative to NIH3T3 in Std)
GSH
GSH+GSSG
Std
Std +BSO
Cys1/4
Cys1/4 +BSO
Cys1/8
Cys1/8 +BSO
Not measurable
D
Viable cell number (relative to Std)
-Cys
-Cys+GSH 0.08 mM
-Cys+GSH 0.2 mM
-Cys+GSH 0.8 mM
-Cys+GSH 2 mM
-Cys+GSH 4 mM
-Cys+GSH 8 mM
-Cys+GSH 16 mM
NIH3T3
NIH-RAS
E
-Cys+Cys after 72 h
W/o magnification
4X magnification
NIH3T3
NIH-RAS

Figure 2

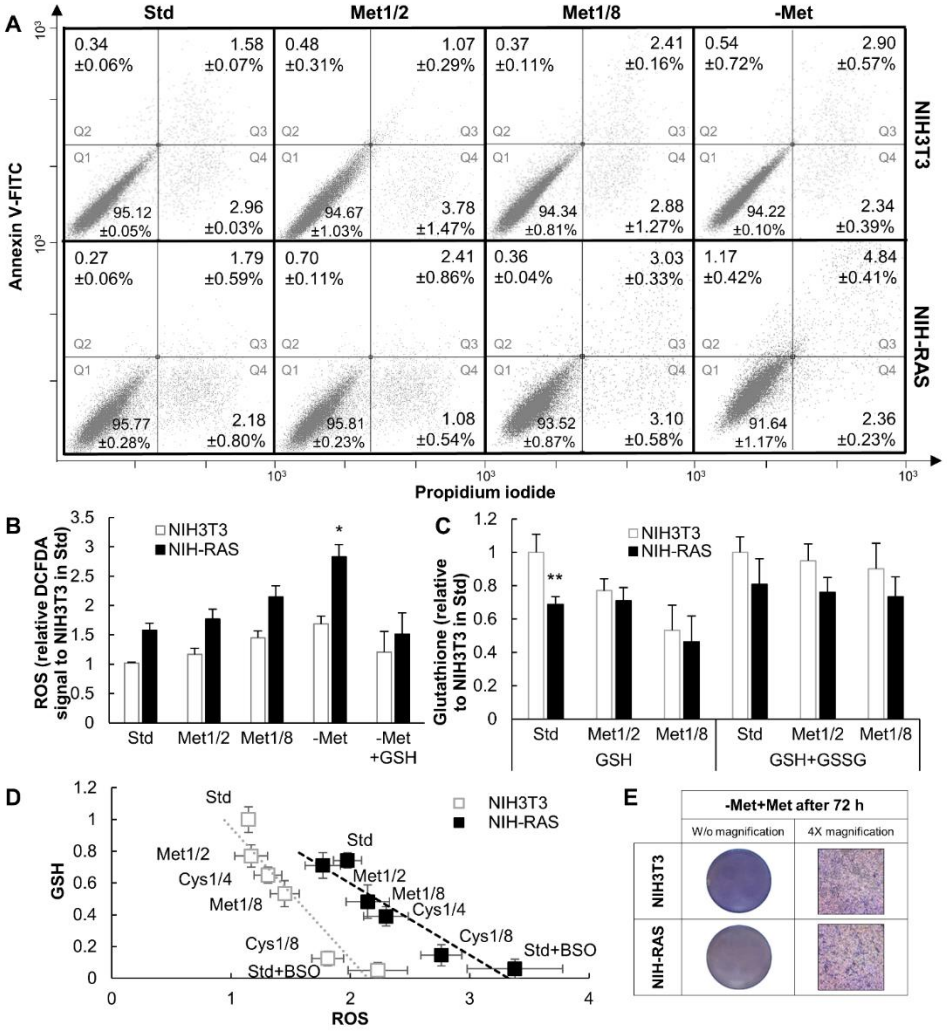
A
Std
Met1/2
Met1/8
-Met
NIH3T3
NIH-RAS
Annexin V-FITC
Propidium iodide
0.34 ±0.06%
1.58 ±0.07%
0.48 ±0.31%
1.07 ±0.29%
0.37 ±0.11%
2.41 ±0.16%
0.54 ±0.72%
2.90 ±0.57%
95.12 ±0.05%
2.96 ±0.03%
94.67 ±1.03%
3.78 ±1.47%
94.34 ±0.81%
2.88 ±1.27%
94.22 ±0.10%
2.34 ±0.39%
0.27 ±0.06%
1.79 ±0.59%
0.70 ±0.11%
2.41 ±0.86%
0.36 ±0.04%
3.03 ±0.33%
1.17 ±0.42%
4.84 ±0.41%
95.77 ±0.28%
2.18 ±0.80%
95.81 ±0.23%
1.08 ±0.54%
93.52 ±0.87%
3.10 ±0.58%
91.64 ±1.17%
2.36 ±0.23%
B
ROS (relative DCFDA signal to NIH3T3 in Std)
NIH3T3
NIH-RAS
Std
Met1/2
Met1/8
-Met
-Met +GSH
C
Glutathione (relative to NIH3T3 in Std)
GSH
GSH+GSSG
D
GSH
ROS
E
-Met+Met after 72 h
W/o magnification
4X magnification

Figure 3

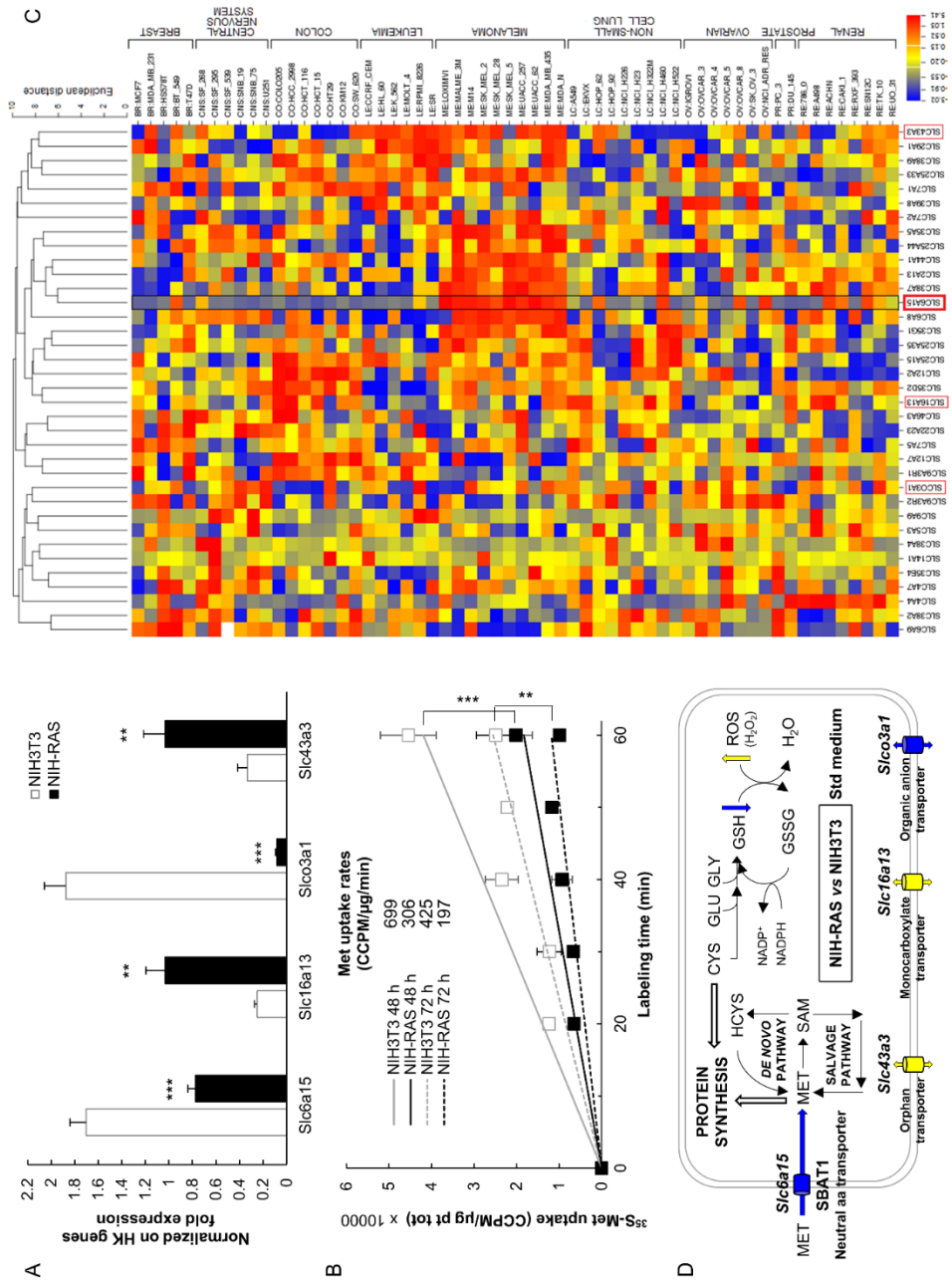
A
Normalized on HK genes
fold expression
NIH3T3
NIH-RAS
Slc6a15
Slc16a13
Slco3a1
Slc43a3
B
35S-Met uptake (CCPM/µg pt tot) x 10000
Labeling time (min)
Met uptake rates
(CCPM/µg/min)
NIH3T3 48 h 699
NIH-RAS 48 h 306
NIH3T3 72 h 425
NIH-RAS 72 h 197
C
Euclidean distance
BREAST
CENTRAL NERVOUS SYSTEM
COLON
LEUKEMIA
MELANOMA
NON-SMALL CELL LUNG
OVARIAN
PROSTATE
RENAL
D
PROTEIN SYNTHESIS
CYS
GLU
GLY
GSH
ROS (H2O2)
H2O
GSSG
NADP+
NADPH
HCYS
DE NOVO PATHWAY
MET
SAM
SALVAGE PATHWAY
NIH-RAS vs NIH3T3
Std medium
Slc6a15
SBAT1
Neutral aa transporter
Slc43a3
Orphan transporter
Slc16a13
Monocarboxylate transporter
Slco3a1
Organic anion transporter

Figure 4

Discussion

Cancer cells show metabolic dependencies that distinguish them from their normal counterparts [14]. Personalized targeting of cancer metabolism that accounts for differences in genetic, epigenetic and environmental factors (i.e., nutrient availability) may lead to major advances in tumor therapy [61]. In this paper we perform nutrient perturbation of the supply of the proteinogenic sulfur-containing amino acids methionine (a potential cysteine precursor) and cysteine (a GSH precursor) of normal, Ras-transformed and reverted mouse fibroblasts to highlight any differential biological response due to the activation state of Ras oncoprotein.

We show that cysteine deprivation causes cell proliferation arrest in both normal and Ras-transformed mouse fibroblasts even in presence of methionine in the culture media. Although databases of metabolic pathway maps, like KEGG ([62,63]), Human Metabolic Atlas ([64]), Reactome ([65]) or Recon2 ([66]) annotate methionine-to-cysteine conversion for all considered cell types, we show that the biosynthetic pathway of cysteine from methionine is not active in mouse fibroblasts (Fig 4D, S1 Fig). In fact, the methionine-to-cysteine pathway may be active only in cells from splanchnic organs, described as important sites of trans-methylation and trans-sulfuration of dietary methionine for cysteine synthesis [36]. These data are in keeping with previous results

demonstrating the dependency from cystine for growth of several human diploid cell lines (human fibroblasts), not able to utilize cystathionine *in lieu* of cystine, likely as a consequence of deficient cystathionase activity [67].

Cysteine deprivation is accompanied by an increase in ROS levels, which could be due to an enhancement of mitochondrial metabolism, and particularly of oxidative phosphorylation-associated proton leakage, induced by energetic stress and increased ATP-demand. This redox unbalance induced by nutritional stress has a pivotal role in up-regulating cellular repair processes and other protective systems (e.g., chaperones) and in driving autophagy, a major mechanism by which starving cells mobilize and reallocate intracellular nutrient resources in order to maintain processes necessary for survival during growth-unfavorable conditions [68].

Cysteine deprivation causes apoptotic cell death. Apoptosis induced by cysteine-withdrawal is essentially due to increased oxidative stress caused by glutathione deprivation. Non-cysteine containing anti-oxidants effectively rescue oxidative stress, but cannot rescue cell death induced by cysteine deprivation. Supplementing reduced glutathione to cysteine-deprived cells not only restores redox homeostasis (and suppresses apoptosis), but also partially restores cell growth, indicating that in mouse fibroblasts GSH can be used as a cysteine reservoir to maintain protein synthesis under nutritional stress. However, high concentrations of GSH

have a toxic effect, stressing the notion that to maximize viability a proper balance between ROS and antioxidants needs to be obtained [54]. Under standard cysteine conditions, severe inhibition of glutathione biosynthesis increases oxidative stress, but has moderate effects on viability. Growth defects induced by cysteine limitation are synergistically increased by inhibiting glutathione synthesis, the more so in NIH-RAS cells, indicating that the growth defects induced by cysteine limitation are largely – though not exclusively – due to cysteine utilization in the synthesis of glutathione. The differential sensitivity of NIH3T3 and NIH-RAS cells to both protective and toxic effects of glutathione may depend on the higher glutathione content of NIH3T3 cells.

The role of cysteine in cancer is controversial. While some authors report that human tumor growth is associated with decreased plasma levels of cysteine and homocysteine [69], more recently other authors demonstrated that antioxidants such as N-acetylcysteine (a direct precursor of cysteine) can accelerate tumor progression by decreasing ROS levels, DNA damage and p53 (a tumor suppressor gene) levels in cancer [70].

The increase in ROS levels under methionine deprivation in both NIH3T3 and NIH-RAS cell lines is not followed by a significant increase in neither apoptosis nor necrosis. While cell growth of normal and Ras-transformed cells was similarly compromised by methionine deprivation, methionine limitation mostly affected NIH-RAS cells.

Some cancers show methionine dependence, a feature firstly noted in xenograft rodents in response to a methionine-free diet [71]. Since then normal cells have been reported to be more resistant to external methionine limitation [34,72]. Methionine dependence might be correlated with inability of methionine-restricted cells to cope with demand for SAM, a major methionine product [34]. This "SAM-checkpoint" may protect cellular integrity and maintain epigenetic stability, since it stops cell cycle progression when intracellular SAM concentrations are insufficient to sustain the methylation reactions necessary for normal cell physiology [34]. Several drugs that target the enzymes that are involved in the post-translational modifications of histones and DNA, cell survival, proliferation and stem cell function [33,73,74] are being evaluated pre-clinically or in early-stage clinical trials [75].

Both a deficiency and an excess of the dietary levels of methionine can result in either genomic instability, which leads to diseases such as cancer, or changes in gene expression, which lead to alterations in metabolism [76], including improvement of hepatic lipid and glucose metabolism and induction of adiposity resistance [76]. Some cancer cells show a high activity of the methionine cycle that promotes chemo-resistance and evasion from apoptosis [77], whereas normal cells are relatively resistant to dietary methionine restriction: therapies to block the methionine cycle in transformed cells may thus represent a safe and effective strategy to

fight cancer [39,77]. Dietary methionine restriction, used alone or in combination with other treatments, impaired cancer growth and carcinogenesis in human patients [78,79] or in rodents [80,81,82]. However, one *caveat* is that methionine restriction must be closely regulated, because methionine is an essential amino acid and a long use of diets extremely poor in methionine could be extremely toxic and cause death. Dietary methionine restriction (achievable in humans with a predominantly vegan diet) may have an additive healthy effect if combined with calorie restriction, by limiting glucose [82]. The potential of methionine depletion in enhancing the anti-cancer effect of chemotherapeutic agents on drug-resistant tumors and cell lines has also been reported [83].

Sensitivity to methionine limitation of mouse fibroblasts and expression of the SBAT1-encoding *Slc6a15* gene are regulated by the activation state of Ras (Fig 4A and S3 Fig), resulting in decreased methionine uptake in NIH-RAS (Fig 4B). Remarkably, expression of the ortholog human gene - *SLC6A15* - is mostly down-regulated in the NCI-60 cells panel, the US National Cancer Institute (NCI) panel of 60 human cancer cell lines grown in culture [84] (Fig 4C). An exception is represented by melanoma cells, in which *SLC6A15* is highly up-regulated. Therefore, the use of methionine uptake as a marker for proliferative activity in substitution of fluoro-deoxyglucose [85,86], or therapeutic use of dietary methionine restriction

would benefit from knowledge of the expression of methionine transporters.

Slc6a15 and its human ortholog belong to a large family (over 450 members) of solute carrier proteins (SLCs) controlling import/export of nutrients, cofactors, ions and many drugs. While many SLCs have not yet well characterized, a quarter of their encoding genes has been associated with human diseases and 26 different SLCs are the targets of known drugs, or drugs in development [87,88]. An increase in amino acid transport may be expected in cancer, most likely as the result of increased amino acid demand for energy, protein synthesis and cell division: surprisingly, S5 Fig shows that SLC-encoding genes down-regulated in NIH-RAS compared to NIH3T3 cells are enriched in genes encoding amino acid transport, particularly of neutral amino acids (e.g. the SBAT1-encoding *Slc6a15* gene).

In conclusion, we show that limitation of sulfur-containing amino acids results in a more dramatic perturbation of the oxidoreductive balance in *K-ras*-transformed cells compared to NIH3T3 cells (Fig 3D). Growth defects induced by cysteine limitation in mouse fibroblasts are largely – though not exclusively – due to cysteine utilization in the synthesis of glutathione, mouse fibroblasts requiring an exogenous cysteine source for protein synthesis. We show for the first time a correlation between Ras-transformation and defects in methionine transport that affect the dependence of *K-ras*-transformed mouse fibroblasts for this amino acid.

Therapeutic regimens of cancer involving modulation of methionine metabolism could be more effective in cells with limited methionine transport capability. To further understand nutrient interactions (such as methionine and glucose restriction), to study the correlation between methionine metabolism and cell signaling and to design a precision medicine approach taking into account the specific nutritional dependencies of a patient's cancer, we consider essential to unravel the underlying networks by using an integrated, Systems Biology approach.

Materials and Methods

Cell culture

Three cells lines have been used in this paper, namely normal NIH3T3 mouse fibroblasts (obtained from the ATCC, Manassas, VA, USA), a K-Ras-transformed normal-derived cell line -that we refer to as NIH-RAS [44,89]- and NIH-RAS cells stably transfected with a pcDNA3-based vector expressing a dominant negative mutant of the Ras-specific guanine nucleotide exchange factor RasGRF1 (RasGRF1W1056E, here simply named GEF-DN) with Ras-sequestering property [44,45,90]. These cell lines proved to be a valid cellular model for studying Ras-dependent transcriptional reprogramming [41], and metabolic rewiring [23,42,43]. Both control and *ras*-transformed NIH3T3 have been passaged a similar number of times, taking care to refreeze the cell lines immediately and to use them for a limited number of passages. The cell lines are periodically assayed to check that the major properties of the cells do not change over time, that the major transformation-related phenotypes are retained and *ras*-dependent (see S2 Fig and accompanying text). The cell lines were routinely grown in Dulbecco's modified Eagle's medium (Invitrogen Inc., Carlsbad, CA, USA) containing 10% newborn calf serum, 4 mM glutamine, 100 U/ml penicillin and 100 mg/ml streptomycin (standard medium), at 37°C in a humidified atmosphere of 5% CO_2. Cells were passaged using trypsin-ethylenediaminetetraacetic acid (EDTA) (Invitrogen Inc., Carlsbad, CA, USA) and maintained in culture before experimental manipulation.

Cell proliferation analysis

Cells were plated at the density of 3000 cells/cm^2 in standard medium and incubated overnight at 37°C and 5% CO_2. After 18 h, cells were washed twice with phosphate-buffered saline (PBS) and, to verify the response to the cysteine or methionine deprivation, cells were incubated in medium without cysteine and methionine (Invitrogen Inc., Carlsbad, CA, USA), possibly supplemented with limiting concentration of cysteine (0.025, 0.05, 0.1 mM) or methionine (0.025, 0.1 mM) (Sigma Aldrich Inc.) or with antioxidants glutathione (0.08, 0.2, 0.8, 2, 4, 16 mM) or MitoTEMPO (10 μM) (Sigma Aldrich Inc.). To measure cell proliferation, cells were treated with trypsin at 0, 3, 6, 24, 30, 48, 54, 72 hours after medium change. Viable (i.e., unstained) cells were counted in a Bürker chamber after staining with 0.5% trypan blue. In amino acid re-feeding and *foci* formation experiments, qualitative evaluation of cell proliferation was obtained by staining with 0.2% Crystal violet (diluted in water from Giemsa Stain 0.4%, Sigma Aldrich Inc.). After 45 minutes of incubation in the dark at RT, cells were washed twice with water, photographed, and counted.

***Foci* formation assay**

Cells were plated at the density of 30 cells/cm^2 in standard medium and incubated overnight at 37°C and 5% CO_2. After 18 h, cells were washed twice with phosphate-buffered saline (PBS) and, to test the ability of

forming *foci* of NIH3T3 and NIH-RAS under nutritional modulation, cells were incubated for 9 days in medium without cysteine and methionine (Invitrogen Inc., Carlsbad, CA, USA), possibly supplemented with limiting concentration of cysteine (0.025, 0.05 mM) or methionine (0.025, 0.1 mM) (Sigma Aldrich Inc.) or with 4 mM reduced glutathione (Sigma Aldrich Inc.). After 9 days, cells were washed with PBS and fixed with paraformaldehyde 4%, then washed with ice-cold PBS and stained with 0.2%. Crystal violet, photographed as described above and the number of *foci* counted.

Determination of intracellular ROS

Intracellular accumulation of H_2O_2 and $O2^{\bullet -}$ was determined after 48 h from medium change with 2',7'-dichlorodihydrofluoresceine diacetate (Sigma Aldrich Inc.). The cells were incubated for 30 minutes at 37°C with H_2DCFDA 10 mM, treated with trypsin, resuspended in PBS supplemented with NCS 10% (Invitrogen Inc., Carlsbad, CA, USA) and acquired by FACScan (Becton-Dickinson), using the Cell Quest software (BD Bioscience). The percentage of ROS-producing cells was calculated for each sample and corrected for autofluorescence obtained from samples of unlabeled cells.

Apoptosis Assay

Cells were plated at the density of 3000 cells/cm^2 in standard medium and incubated overnight at 37°C and 5% CO_2. After 18 h, cells were washed twice with phosphate-buffered saline (PBS) and incubated for 30 hours in medium without cysteine and methionine (Invitrogen Inc., Carlsbad, CA, USA), possibly supplemented with limiting concentrations of cysteine (0.025, 0.05 mM) or methionine (0.025 and 0.1 mM) (Sigma Aldrich Inc.) or with antioxidants glutathione (4 mM) or MitoTEMPO (10 µM) (Sigma Aldrich Inc.). For apoptosis analysis, 1×10^6 cells (adherent and in suspension cells) were collected, stained with Annexin V-FITC (Immunotools, GmbH) and propidium iodide (Sigma Aldrich Inc.) and analyzed by FACScan (Becton-Dickinson) using the FL1 and FL2 channels. Data analysis was performed with Flowing Software.

Determination of glutathione levels

For reduced and total glutathione measurements, cells were plated at the density of 3000 cells/cm^2 in standard medium and incubated overnight at 37°C and 5% CO_2. After 18 h, cells were washed twice with phosphate-buffered saline (PBS) and incubated for 48 h in standard medium or under limitation of cysteine or methionine. Cells were then treated with trypsin, collected, washed twice with PBS and lysed through freeze-and-thaw cycles. Samples were deproteinized with a 5% 5-sulfosalicylic acid solution, centrifuged to remove the precipitated protein and assayed for glutathione. GSH measurement was an optimization of Tietze's enzymatic

recycling method [55], in which GSH is oxidized by the sulfhydryl reagent 5,5'-dithio-bis(2-nitrobenzoic acid) (DTNB) to form the yellow derivative 5'-thio-2-nitrobenzoic acid (TNB), measurable at 412 nm and the glutathione disulfide (GSSG) formed is recycled to GSH by glutathione reductase in the presence of NADPH. The amount of glutathione in the samples was determined through a standard curve of reduced glutathione. Glutathione levels were normalized to protein content measured by Bradford assay (Bio-Rad reagent) on an aliquot of cell extract collected before deiproteinization.

Methionine transport assays

NIH3T3 and NIH-RAS cells were seeded at the density of 3000 cells/cm^2 and incubated overnight at 37°C and 5% CO_2, then medium change was done after 18 h. At 48 h (exponential growth condition) and 72 h (confluent growth condition), standard medium was replaced with 0.4 ml labeling medium (cysteine and methionine-free medium + 0.025 mCi/ml ^{35}S-Met, PerkinElmer), that was removed after 20-40-60 minutes or 30-50-60 minutes at 37°C and 5% CO_2. Cells were then washed once with cold PBS and scraped after adding lysis buffer. Cell lysates were centrifuged and an aliquot spotted on Whatman Glass Microfiber filters (Sigma Aldrich Inc.). To the remaining volume, 1 volume of cold 20% TCA (Sigma Aldrich Inc.) was added and, after 30 minutes in ice, samples were spotted on filters and washed twice with cold 10% TCA and ethanol (Sigma Aldrich

Inc.). Air-dried filters were transferred to vials containing Ultima Gold MV scintillation fluid (PerkinElmer) and radioactivity measured in a beta-counter (Wallac Microbeta Trilux, PerkinElmer). Averages of technical triplicates for cell lysates (representing amino acid uptake) were calculated and the resulting values were normalized on total protein content, measured by using QuantiPro™ BCA Assay Kit (Sigma Aldrich Inc.).

RNA extraction and semi quantitative RT-PCR analysis

Cells were plated at the density of 3000 cells/cm^2 in standard medium and incubated overnight at 37°C and 5% CO_2. After 18 h, cells were washed twice with phosphate-buffered saline (PBS) and incubated for 48 h in standard medium. RNA was then extracted from cells by using the Quick-RNA™ MicroPrep kit (Zymo Research). Total RNA was reverse-transcribed with oligo-dT by using the iScript cDNA Synthesis Kit (Bio-Rad Laboratories). The RT product (0.5 µg) was amplified with primer pairs specific for the genes studied. As internal control of PCR assays, specific primers for 18S and β-actin transcripts were used. Primers used: *Slc6a15* forward: 5'-GCATCGGAAGAATTTCTGAGC-3', reverse: 5'-AGCGACGAATGATGAACACC-3'; *Slco3a1* forward: 5'-GAGTTAGCCTATCCTTGTTG-3', reverse: 5'-GACAGAACATCACCTTACAA-3'; *Slc16a13* forward: 5'-ACCTGAGTATTGGGCTGCTG-3', reverse: 5'-CCATGGTCGGAGTGAAGGT-3'; *Slc43a3* forward: 5'-

CACCTTGTTGACTGGACTCTTG-3', reverse: 5'-CCAGGGTAAAGATGAGTGAGAAC-3'.

Generation of the heat map of solute carrier gene expression profiles in NCI-60 cell lines

The heat map, or Clustered Image Map (CIM), was generated with CIMminer by selecting the one matrix option. The rows of the matrix were the different cell lines and the columns (each representing a solute carrier gene) were clustered according to Average Linkage algorithm and to Euclidean distance measure. Data values were mapped to colors using the quantile method: the weight range of data values was divided into intervals each containing approximately the same number of data points, thus effectively spreading out the color differences between data values that were present in regions with a large number of values.

Supporting Information

S1 Fig. Methionine and cysteine metabolism in mouse fibroblasts. Methionine is partitioned between protein synthesis, *de novo* and recycling pathway, where it is converted to S-adenosylmethionine (SAM). SAM is converted to S-adenosylhomocysteine (SAH) during methylation of DNA and a large range of proteins and other molecules. SAH is then hydrolyzed to homocysteine (Hcy) in a reversible reaction. Under normal conditions, approximately 50% of Hcy is re-methylated to form

methionine that, in most tissues, occurs via methionine synthase. In the trans-sulfuration pathway, Hcy is metabolized to form cystathionine, which is the immediate precursor to cysteine. Besides from methionine, cysteine can be synthesized from serine. The sulfur is derived from methionine, which is converted to homocysteine through the intermediate SAM. Cystathionine beta-synthase then combines homocysteine and serine to form the asymmetrical thioether cystathionine. The enzyme cystathionine gamma-lyase converts the cystathionine into cysteine and alpha-ketobutyrate. The trans-sulfuration pathway is not active in all cells, and in human is active essentially only in cells from splanchnic organs. Here we demonstrated that mouse embryonic fibroblasts are not able to convert methionine into cysteine. For this reason the trans-sulfuration reaction is highlighted in grey.

S1 Table. Mass duplication times under different nutritional perturbations. Mass duplication times (MDT) for NIH3T3 and NIH-RAS under different methionine or cysteine concentrations (possibly supplemented with GSH) were calculated on semi-logarithmic curves represented in Fig 1A-B. Then, Student's *t*-test was performed on linear regression curves for each nutritional condition that allowed cell growth. A = not parallel to linear regression curve of NIH-RAS cells in standard medium (99% CI); B = not parallel to linear regression curve of NIH3T3 cells in standard medium (99.9% CI); C = not parallel to linear regression curve

of NIH-RAS cells in standard medium (99.9% CI); D = not parallel to linear regression curve of NIH3T3 cells in standard medium (99% CI); E = not parallel to linear regression curve of NIH3T3 cells in standard medium (99.9% CI). CI = confidence interval.

S2 Fig. Ras and MAPK activation state and expression levels in cellular models used in the paper: NIH3T3, NIH-RAS, NIH-RAS pGEF-DN and NIH-RAS pcDNA3

Expression levels of Total Ras proteins (A) and MAPKs p42 and p44 (B) in cell lysates of pull down assay. Antibodies directed against Ras (sc259 Santa Cruz), Phospho-p44/42 MAPK (Erk1/2) (Thr202/Tyr204) (Cell Signaling #9101) and p44/42 MAPK (Erk1/2) (Cell Signaling #9102) were used. (C) Ras–GTP eluted from GST–RBD–glutathione–sepharose, pre-incubated with cell lysates. Pull down assay was performed as described in [7]. (D) Quantification of the Ras–GTP amount after normalization over total Ras. Data are normalized over the Ras-GTP/total Ras ratio in NIH3T3 taken equal to 100. Data shown are mean +/- standard deviation of two independent experiments. (E) Morphological analysis of the different cell lines. (F) Phospho-p44/42 MAPK level in cell lysates, determined by ELISA assay performed using PathScan® Phospho-p44/42 MAPK (Thr202/Tyr204) (Cell Signaling). Data shown are mean +/- standard deviation of two independent experiments. (F) 100X magnification of a *focus* generated by NIH-RAS cells in *foci* formation assay shown in Fig 1.

S3 Fig. Over-expression of GEF-DN reverts sensitivity to methionine limitation in NIH-RAS cells and partially rescues the defect in the expression of *Slc6a15* gene encoding methionine transporter SBAT1

(A) Cell proliferation of NIH3T3, NIH-RAS, NIH-RAS pGEF-DN and NIH-RAS pcDNA3 cells grown in media with different concentrations of methionine and counted daily for 72 h of growth under conditions indicated. Plotted data are mean +/- standard deviation. computed from three independent experiments. (B) Relative to t=0 cell proliferation of NIH3T3, NIH-RAS, NIH-RAS pGEF-DN and NIH-RAS pcDNA3 cells grown for 72 h in media with different concentrations of methionine, as indicated in (A). Part of the data in (B) are present in Fig 1D. (C) Semi-quantitative RT-PCR results for NIH3T3, NIH-RAS, NIH-RAS pGEF-DN and NIH-RAS pcDNA3 cells grown for 48 h in standard medium performed in triplicate on genes showing at least a two-fold change between NIH-RAS *vs*. NIH3T3 cells in each of the two Affymetrix independent experiments (S5 Fig). *P<0.05; **P<0.01; ***P<0.001 (Student's *t*-test).

S4 Fig. Cell proliferation and qualitative ROS levels under different methionine concentrations and in cysteine-limiting or -depleted medium (possibly supplemented with antioxidants glutathione and MitoTEMPO or with GSH synthesis inhibitor BSO). For all the experiments, MitoTEMPO and buthionine sulfoximine (BSO) were used at

the concentration of 10 μM and 100 μM. (A-B) Cell proliferation of NIH3T3 and NIH-RAS cells grown in media supplemented with different concentrations of methionine and cysteine with or without antioxidants glutathione or MitoTEMPO and counted after 72 h (A) and 30 h (B) of growth under conditions indicated. Part of the data in (A) are present in Fig 1D. Plotted data are mean +/- standard deviation computed from three independent experiments. *P<0.05 (Student's *t*-test). (C) Cell proliferation of NIH3T3 and NIH-RAS cells under conditions indicated. (D) Qualitative evaluation of ROS levels in NIH3T3 and NIH-RAS cells upon staining with DCFDA and analysis with a fluorescence microscope.

S5 Fig. Solute carriers differentially expressed between NIH3T3 and NIH-RAS cells. Genome-wide transcriptional profiling datasets for NIH3T3 and NIH-RAS cells (available in NCBI GEO database; accession GSM741354-GSM741361 for NIH3T3 cells and GSM741368-GSM741375 for NIH-RAS cells), previously obtained in our laboratory with an MG_U74Av2 Affymetrix Gene Chip [41], were filtered for all genes encoding for solute carriers. Then, to identify genes whose expression was significantly altered in Ras-transformed *versus* normal cells (here represented in bold), a two-fold and a <0.05 cut-offs on Fold Changes and on *p*-values were used, respectively. In this Figure are represented all transporter genes with a fold change ≥2 (about 20% of all transporter genes) irrespective of their *p*-values. Gene Ontology (GO) enrichment based on molecular

function was performed with GoTermFinder (http://go.princeton.edu/cgi-bin/GOTermFinder) and genes encoding for amino acid transporters were colored in magenta, while genes encoding for ion transporters were colored in grey.

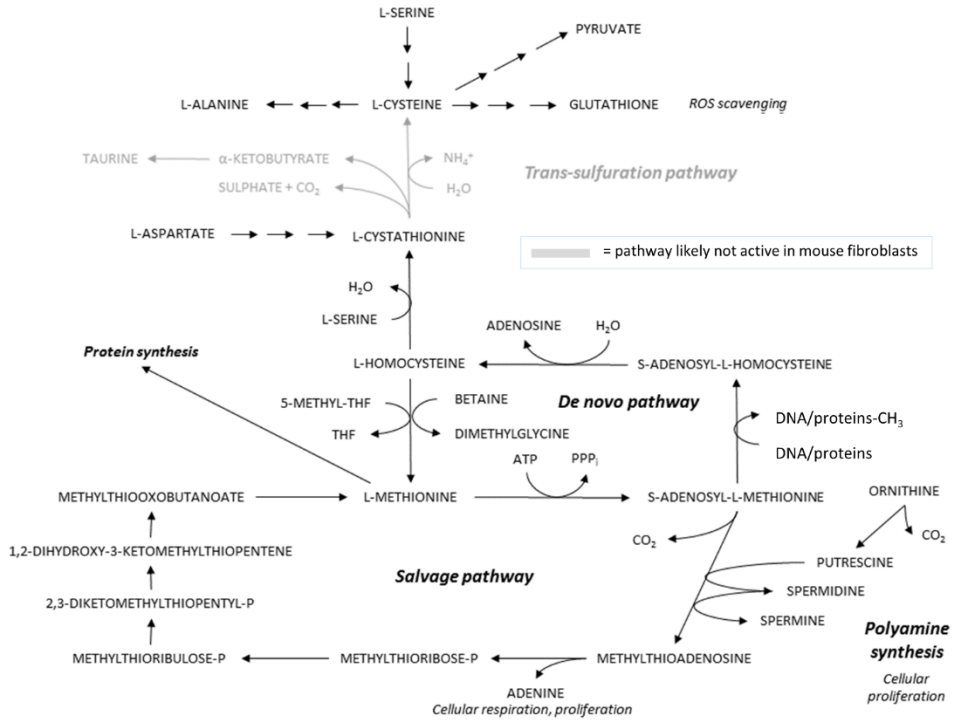

S1 Fig. Methionine and cysteine metabolism in mouse fibroblasts.

	Mass duplication time (MDT) (h)		
Growth condition	**NIH3T3**	**NIH-RAS**	**Student's t-test on linear regression curves (NIH-RAS *vs* NIH3T3)**
Std	25	23	Parallel
Std+GSH	25	23	Parallel
Cys1/2	24	22	Parallel
Cys1/4	27	30[A]	Parallel
Cys1/8	No growth	No growth	-
-Cys	No growth	No growth	-
-Cys+GSH	38[B]	31[C]	Not parallel (99.9% IC)
Met1/2	38[D]	58[E]	Not parallel (95% IC)
Met1/8	No growth	No growth	-
-Met	No growth	No growth	-
-Met+GSH	No growth	No growth	-

S1 Table. Mass duplication times under different nutritional perturbations.

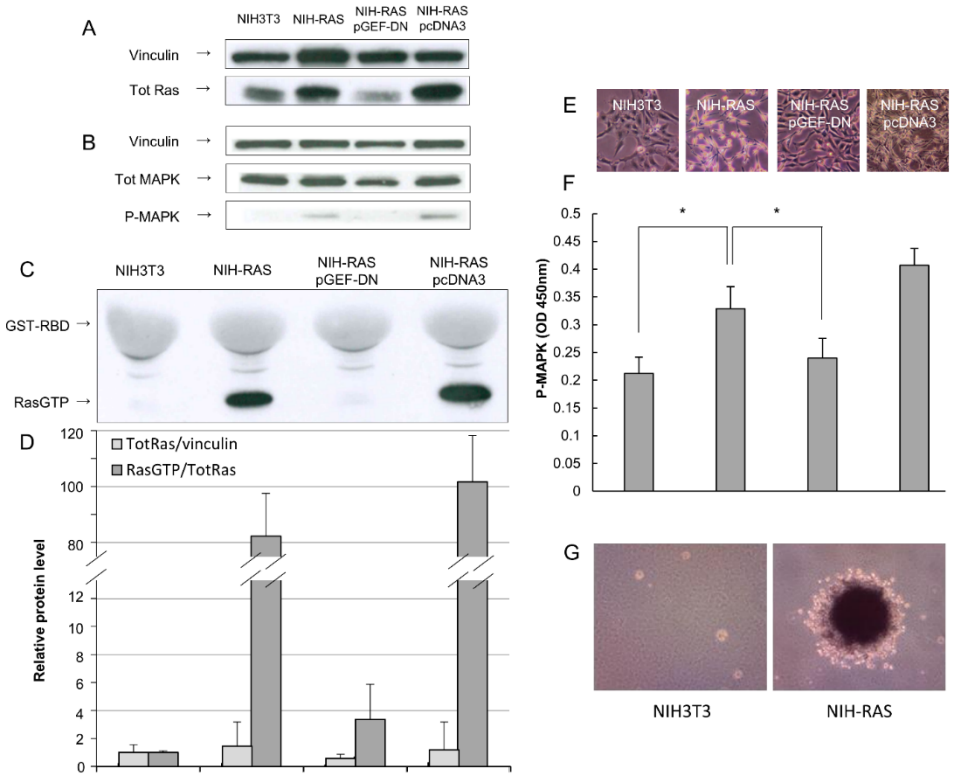

References

Balestrieri et al. (2012). Integrative transcriptional analysis between human and mouse cancer cells provides a common set of transformation associated genes. Biotechnol Adv *30*, 16-29.

Baracca et al. (2010). Mitochondrial Complex I decrease is responsible for bioenergetic dysfunction in K-ras transformed cells. Biochim Biophys Acta *1797*, 314-323.

Bossu et al. (2000). A dominant negative RAS-specific guanine nucleotide exchange factor reverses neoplastic phenotype in K-ras transformed mouse fibroblasts. Oncogene *19*, 2147-2154.

Chiaradonna et al. (2006a). Expression of transforming K-Ras oncogene affects mitochondrial function and morphology in mouse fibroblasts. Biochim Biophys Acta *1757*, 1338-1356.

Chiaradonna et al. (2005). Acquired glucose sensitivity of k-ras transformed fibroblasts. Biochem Soc Trans *33*, 297-299.

Chiaradonna et al. (2006b). Ras-dependent carbon metabolism and transformation in mouse fibroblasts. Oncogene *25*, 5391-5404.

Gaglio et al. (2011). Oncogenic K-Ras decouples glucose and glutamine metabolism to support cancer cell growth. Mol Syst Biol *7*, 523.

Gaglio et al. (2009). Glutamine deprivation induces abortive s-phase rescued by deoxyribonucleotides in k-ras transformed fibroblasts. PLoS One *4*, e4715.

Gaglio et al. (2016). Divergent in vitro/in vivo responses to drug treatments of highly aggressive NIH-Ras cancer cells: a PET imaging and metabolomics-mass-spectrometry study. Oncotarget.

Palorini et al. (2013a). Glucose starvation induces cell death in K-ras-transformed cells by interfering with the hexosamine biosynthesis pathway and activating the unfolded protein response. Cell Death Dis *4*, e732.

Palorini et al. (2013b). Oncogenic K-ras expression is associated with derangement of the cAMP/PKA pathway and forskolin-reversible alterations of mitochondrial dynamics and respiration. Oncogene *32*, 352-362.

Palorini et al. (2013c). Mitochondrial complex I inhibitors and forced oxidative phosphorylation synergize in inducing cancer cell death. Int J Cell Biol *2013*, 243876.

Palorini et al. (2016). Protein Kinase A Activation Promotes Cancer Cell Resistance to Glucose Starvation and Anoikis. PLoS Genet *12*, e1005931.

Pulciani et al. (1985). ras gene Amplification and malignant transformation. Mol Cell Biol *5*, 2836-2841.

Sacco et al. (2012). Novel RasGRF1-derived Tat-fused peptides inhibiting Ras-dependent proliferation and migration in mouse and human cancer cells. Biotechnol Adv *30*, 233-243.

S2 Fig. Ras and MAPK activation state and expression levels in cellular models used in the paper: NIH3T3, NIH-RAS, NIH-RAS pGEF-DN and NIH-RAS pcDNA3.

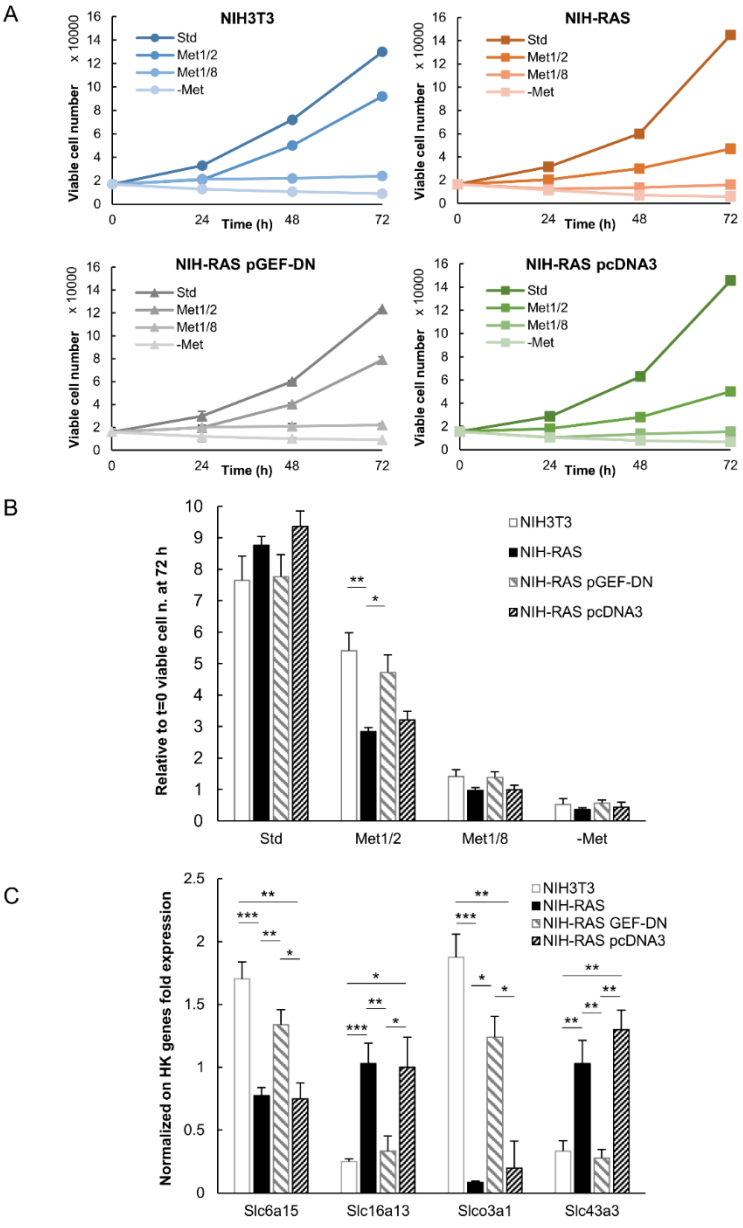

S3 Fig. Over-expression of GEF-DN reverts sensitivity to methionine limitation in NIH-RAS cells and partially rescues the defect in the expression of *Slc6a15* gene encoding methionine transporter SBAT1

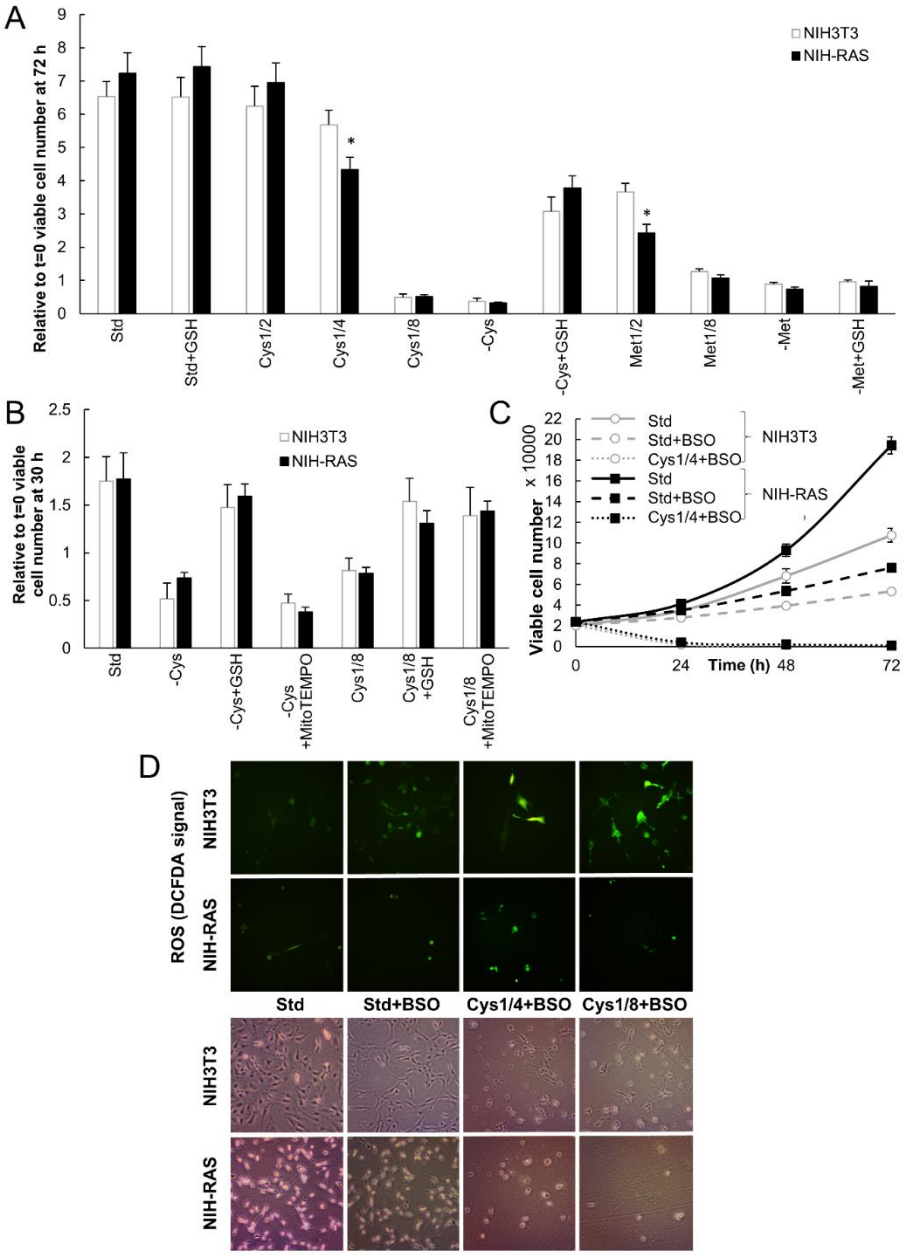

S4 Fig. Cell proliferation and qualitative ROS levels under different methionine concentrations and in cysteine-limiting or -depleted medium (possibly supplemented with antioxidants glutathione and MitoTEMPO or with GSH synthesis inhibitor BSO).

References

1. Downward J (2003) Role of receptor tyrosine kinases in G-protein-coupled receptor regulation of Ras: transactivation or parallel pathways? The Biochemical journal 376: e9-10.
2. Kahn S, Yamamoto F, Almoguera C, Winter E, Forrester K, et al. (1987) The c-K-ras gene and human cancer (review). Anticancer research 7: 639-652.
3. Schubbert S, Shannon K, Bollag G (2007) Hyperactive Ras in developmental disorders and cancer. Nature reviews Cancer 7: 295-308.
4. Sever R, Brugge JS (2015) Signal transduction in cancer. Cold Spring Harbor perspectives in medicine 5.
5. Forbes SA, Bindal N, Bamford S, Cole C, Kok CY, et al. (2011) COSMIC: mining complete cancer genomes in the Catalogue of Somatic Mutations in Cancer. Nucleic acids research 39: D945-950.
6. Adjei AA, Cohen RB, Franklin W, Morris C, Wilson D, et al. (2008) Phase I pharmacokinetic and pharmacodynamic study of the oral, small-molecule mitogen-activated protein kinase kinase 1/2 inhibitor AZD6244 (ARRY-142886) in patients with advanced cancers. Journal of clinical oncology : official journal of the American Society of Clinical Oncology 26: 2139-2146.
7. Sacco E, Spinelli M, Vanoni M (2012) Approaches to Ras signaling modulation and treatment of Ras-dependent disorders: a patent review (2007--present). Expert opinion on therapeutic patents 22: 1263-1287.
8. McCormick F (2015) KRAS as a Therapeutic Target. Clinical cancer research : an official journal of the American Association for Cancer Research 21: 1797-1801.
9. Shima F, Matsumoto S, Yoshikawa Y, Kawamura T, Isa M, et al. (2015) Current status of the development of Ras inhibitors. Journal of biochemistry 158: 91-99.
10. Singh H, Longo DL, Chabner BA (2015) Improving Prospects for Targeting RAS. Journal of clinical oncology : official journal of the American Society of Clinical Oncology 33: 3650-3659.
11. Hanahan D, Weinberg RA (2011) Hallmarks of cancer: the next generation. Cell 144: 646-674.
12. Levine AJ, Puzio-Kuter AM (2010) The control of the metabolic switch in cancers by oncogenes and tumor suppressor genes. Science 330: 1340-1344.
13. Alberghina L, Gaglio D, Gelfi C, Moresco RM, Mauri G, et al. (2012) Cancer cell growth and survival as a system-level property sustained by enhanced glycolysis and mitochondrial metabolic remodeling. Frontiers in physiology 3: 362.
14. Kimmelman AC (2015) Metabolic Dependencies in RAS-Driven Cancers. Clinical cancer research : an official journal of the American Association for Cancer Research 21: 1828-1834.
15. DeBerardinis RJ, Lum JJ, Hatzivassiliou G, Thompson CB (2008) The biology of cancer: metabolic reprogramming fuels cell growth and proliferation. Cell metabolism 7: 11-20.
16. Warburg O (1956) On the origin of cancer cells. Science 123: 309-314.
17. Hsu PP, Sabatini DM (2008) Cancer cell metabolism: Warburg and beyond. Cell 134: 703-707.
18. Ying H, Kimmelman AC, Lyssiotis CA, Hua S, Chu GC, et al. (2012) Oncogenic Kras maintains pancreatic tumors through regulation of anabolic glucose metabolism. Cell 149: 656-670.
19. Weinberg F, Hamanaka R, Wheaton WW, Weinberg S, Joseph J, et al. (2010) Mitochondrial metabolism and ROS generation are essential for Kras-mediated tumorigenicity. Proceedings of the National Academy of Sciences of the United States of America 107: 8788-8793.

20. Baracca A, Chiaradonna F, Sgarbi G, Solaini G, Alberghina L, et al. (2010) Mitochondrial Complex I decrease is responsible for bioenergetic dysfunction in K-ras transformed cells. Biochimica et biophysica acta 1797: 314-323.
21. Brosnan JT (2003) Interorgan amino acid transport and its regulation. The Journal of nutrition 133: 2068S-2072S.
22. DeBerardinis RJ, Mancuso A, Daikhin E, Nissim I, Yudkoff M, et al. (2007) Beyond aerobic glycolysis: transformed cells can engage in glutamine metabolism that exceeds the requirement for protein and nucleotide synthesis. Proceedings of the National Academy of Sciences of the United States of America 104: 19345-19350.
23. Gaglio D, Metallo CM, Gameiro PA, Hiller K, Danna LS, et al. (2011) Oncogenic K-Ras decouples glucose and glutamine metabolism to support cancer cell growth. Molecular systems biology 7: 523.
24. Metallo CM, Gameiro PA, Bell EL, Mattaini KR, Yang J, et al. (2012) Reductive glutamine metabolism by IDH1 mediates lipogenesis under hypoxia. Nature 481: 380-384.
25. Son J, Lyssiotis CA, Ying H, Wang X, Hua S, et al. (2013) Glutamine supports pancreatic cancer growth through a KRAS-regulated metabolic pathway. Nature 496: 101-105.
26. Fendt SM, Bell EL, Keibler MA, Olenchock BA, Mayers JR, et al. (2013) Reductive glutamine metabolism is a function of the alpha-ketoglutarate to citrate ratio in cells. Nature communications 4: 2236.
27. Chen L, Cui H (2015) Targeting Glutamine Induces Apoptosis: A Cancer Therapy Approach. International journal of molecular sciences 16: 22830-22855.
28. Wise DR, Thompson CB (2010) Glutamine addiction: a new therapeutic target in cancer. Trends in biochemical sciences 35: 427-433.
29. Wang Q, Beaumont KA, Otte NJ, Font J, Bailey CG, et al. (2014) Targeting glutamine transport to suppress melanoma cell growth. International journal of cancer 135: 1060-1071.
30. Bhutia YD, Ganapathy V (2015) Glutamine transporters in mammalian cells and their functions in physiology and cancer. Biochimica et biophysica acta.
31. Oda K, Hosoda N, Endo H, Saito K, Tsujihara K, et al. (2010) L-type amino acid transporter 1 inhibitors inhibit tumor cell growth. Cancer science 101: 173-179.
32. Finkelstein JD (1990) Methionine metabolism in mammals. The Journal of nutritional biochemistry 1: 228-237.
33. Lu SC, Mato JM (2008) S-Adenosylmethionine in cell growth, apoptosis and liver cancer. Journal of gastroenterology and hepatology 23 Suppl 1: S73-77.
34. Borrego SL, Fahrmann J, Datta R, Stringari C, Grapov D, et al. (2016) Metabolic changes associated with methionine stress sensitivity in MDA-MB-468 breast cancer cells. Cancer Metab 4: 9.
35. Ingenbleek Y, Kimura H (2013) Nutritional essentiality of sulfur in health and disease. Nutr Rev 71: 413-432.
36. Riedijk MA, van Beek RH, Voortman G, de Bie HM, Dassel AC, et al. (2007) Cysteine: a conditionally essential amino acid in low-birth-weight preterm infants? The American journal of clinical nutrition 86: 1120-1125.
37. Aoyama K, Watabe M, Nakaki T (2008) Regulation of neuronal glutathione synthesis. Journal of pharmacological sciences 108: 227-238.
38. Lu SC (2009) Regulation of glutathione synthesis. Molecular aspects of medicine 30: 42-59.
39. Cavuoto P, Fenech MF (2012) A review of methionine dependency and the role of methionine restriction in cancer growth control and life-span extension. Cancer treatment reviews 38: 726-736.

40. Stipanuk MH (2004) Sulfur amino acid metabolism: pathways for production and removal of homocysteine and cysteine. Annual review of nutrition 24: 539-577.
41. Balestrieri C, Vanoni M, Hautaniemi S, Alberghina L, Chiaradonna F (2012) Integrative transcriptional analysis between human and mouse cancer cells provides a common set of transformation associated genes. Biotechnology advances 30: 16-29.
42. Palorini R, Votta G, Pirola Y, De Vitto H, De Palma S, et al. (2016) Protein Kinase A Activation Promotes Cancer Cell Resistance to Glucose Starvation and Anoikis. PLoS genetics 12: e1005931.
43. Gaglio D, Valtorta S, Ripamonti M, Bonanomi M, Damiani C, et al. (2016) Divergent in vitro/in vivo responses to drug treatments of highly aggressive NIH-Ras cancer cells: a PET imaging and metabolomics-mass-spectrometry study. Oncotarget.
44. Bossu P, Vanoni M, Wanke V, Cesaroni MP, Tropea F, et al. (2000) A dominant negative RAS-specific guanine nucleotide exchange factor reverses neoplastic phenotype in K-ras transformed mouse fibroblasts. Oncogene 19: 2147-2154.
45. Chiaradonna F, Sacco E, Manzoni R, Giorgio M, Vanoni M, et al. (2006) Ras-dependent carbon metabolism and transformation in mouse fibroblasts. Oncogene 25: 5391-5404.
46. Mates JM, Perez-Gomez C, Nunez de Castro I, Asenjo M, Marquez J (2002) Glutamine and its relationship with intracellular redox status, oxidative stress and cell proliferation/death. The international journal of biochemistry & cell biology 34: 439-458.
47. Franco R, Schoneveld OJ, Pappa A, Panayiotidis MI (2007) The central role of glutathione in the pathophysiology of human diseases. Archives of physiology and biochemistry 113: 234-258.
48. Alberghina L, Gaglio D (2014) Redox control of glutamine utilization in cancer. Cell death & disease 5: e1561.
49. Trachootham D, Zhou Y, Zhang H, Demizu Y, Chen Z, et al. (2006) Selective killing of oncogenically transformed cells through a ROS-mediated mechanism by beta-phenylethyl isothiocyanate. Cancer cell 10: 241-252.
50. Sies H (1999) Glutathione and its role in cellular functions. Free radical biology & medicine 27: 916-921.
51. Dickinson DA, Forman HJ (2002) Cellular glutathione and thiols metabolism. Biochemical pharmacology 64: 1019-1026.
52. Wu G, Fang YZ, Yang S, Lupton JR, Turner ND (2004) Glutathione metabolism and its implications for health. The Journal of nutrition 134: 489-492.
53. Estrela JM, Ortega A, Obrador E (2006) Glutathione in cancer biology and therapy. Critical reviews in clinical laboratory sciences 43: 143-181.
54. Poljsak B, Suput D, Milisav I (2013) Achieving the balance between ROS and antioxidants: when to use the synthetic antioxidants. Oxidative medicine and cellular longevity 2013: 956792.
55. Rahman I, Kode A, Biswas SK (2006) Assay for quantitative determination of glutathione and glutathione disulfide levels using enzymatic recycling method. Nature protocols 1: 3159-3165.
56. Pramod AB, Foster J, Carvelli L, Henry LK (2013) SLC6 transporters: structure, function, regulation, disease association and therapeutics. Molecular aspects of medicine 34: 197-219.
57. Takanaga H, Mackenzie B, Peng JB, Hediger MA (2005) Characterization of a branched-chain amino-acid transporter SBAT1 (SLC6A15) that is expressed in human brain. Biochemical and biophysical research communications 337: 892-900.

58. Broer A, Tietze N, Kowalczuk S, Chubb S, Munzinger M, et al. (2006) The orphan transporter v7-3 (slc6a15) is a Na+-dependent neutral amino acid transporter (B0AT2). The Biochemical journal 393: 421-430.
59. Reinhold WC, Sunshine M, Liu H, Varma S, Kohn KW, et al. (2012) CellMiner: a web-based suite of genomic and pharmacologic tools to explore transcript and drug patterns in the NCI-60 cell line set. Cancer research 72: 3499-3511.
60. Weinstein JN, Myers TG, O'Connor PM, Friend SH, Fornace AJ, Jr., et al. (1997) An information-intensive approach to the molecular pharmacology of cancer. Science 275: 343-349.
61. Elia I, Schmieder R, Christen S, Fendt SM (2016) Organ-Specific Cancer Metabolism and Its Potential for Therapy. Handbook of experimental pharmacology 233: 321-353.
62. Kanehisa M, Sato Y, Kawashima M, Furumichi M, Tanabe M (2016) KEGG as a reference resource for gene and protein annotation. Nucleic acids research 44: D457-462.
63. Kanehisa M, Goto S (2000) KEGG: kyoto encyclopedia of genes and genomes. Nucleic acids research 28: 27-30.
64. Pornputtapong N, Nookaew I, Nielsen J (2015) Human metabolic atlas: an online resource for human metabolism. Database : the journal of biological databases and curation 2015: bav068.
65. Fabregat A, Sidiropoulos K, Garapati P, Gillespie M, Hausmann K, et al. (2016) The Reactome pathway Knowledgebase. Nucleic acids research 44: D481-487.
66. Thiele I, Swainston N, Fleming RM, Hoppe A, Sahoo S, et al. (2013) A community-driven global reconstruction of human metabolism. Nature biotechnology 31: 419-425.
67. Eagle H, Washington C, Friedman SM (1966) The synthesis of homocystine, cystathionine, and cystine by cultured diploid and heteroploid human cells. Proceedings of the National Academy of Sciences of the United States of America 56: 156-163.
68. Filomeni G, De Zio D, Cecconi F (2015) Oxidative stress and autophagy: the clash between damage and metabolic needs. Cell death and differentiation 22: 377-388.
69. Al-Awadi F, Yang M, Tan Y, Han Q, Li S, et al. (2008) Human tumor growth in nude mice is associated with decreased plasma cysteine and homocysteine. Anticancer research 28: 2541-2544.
70. Sayin VI, Ibrahim MX, Larsson E, Nilsson JA, Lindahl P, et al. (2014) Antioxidants accelerate lung cancer progression in mice. Science translational medicine 6: 221ra215.
71. Sugimura T, Birnbaum SM, Winitz M, Greenstein JP (1959) Quantitative nutritional studies with water-soluble, chemically defined diets. VIII. The forced feeding of diets each lacking in one essential amino acid. Archives of biochemistry and biophysics 81: 448-455.
72. Cellarier E, Durando X, Vasson MP, Farges MC, Demiden A, et al. (2003) Methionine dependency and cancer treatment. Cancer treatment reviews 29: 489-499.
73. Shiraki N, Shiraki Y, Tsuyama T, Obata F, Miura M, et al. (2014) Methionine metabolism regulates maintenance and differentiation of human pluripotent stem cells. Cell metabolism 19: 780-794.
74. Wellen KE, Thompson CB (2012) A two-way street: reciprocal regulation of metabolism and signalling. Nature reviews Molecular cell biology 13: 270-276.
75. Locasale JW (2013) Serine, glycine and one-carbon units: cancer metabolism in full circle. Nature reviews Cancer 13: 572-583.
76. Ables GP, Hens JR, Nichenametla SN (2016) Methionine restriction beyond life-span extension. Annals of the New York Academy of Sciences 1363: 68-79.
77. Montenegro MF, Sanchez-del-Campo L, Fernandez-Perez MP, Saez-Ayala M, Cabezas-Herrera J, et al. (2015) Targeting the epigenetic machinery of cancer cells. Oncogene 34: 135-143.

78. Epner DE, Morrow S, Wilcox M, Houghton JL (2002) Nutrient intake and nutritional indexes in adults with metastatic cancer on a phase I clinical trial of dietary methionine restriction. Nutrition and cancer 42: 158-166.
79. Ornish D, Weidner G, Fair WR, Marlin R, Pettengill EB, et al. (2005) Intensive lifestyle changes may affect the progression of prostate cancer. The Journal of urology 174: 1065-1069; discussion 1069-1070.
80. Komninou D, Leutzinger Y, Reddy BS, Richie JP, Jr. (2006) Methionine restriction inhibits colon carcinogenesis. Nutrition and cancer 54: 202-208.
81. Caro P, Gomez J, Sanchez I, Naudi A, Ayala V, et al. (2009) Forty percent methionine restriction decreases mitochondrial oxygen radical production and leak at complex I during forward electron flow and lowers oxidative damage to proteins and mitochondrial DNA in rat kidney and brain mitochondria. Rejuvenation research 12: 421-434.
82. Li Y, Liu L, Tollefsbol TO (2010) Glucose restriction can extend normal cell lifespan and impair precancerous cell growth through epigenetic control of hTERT and p16 expression. FASEB journal : official publication of the Federation of American Societies for Experimental Biology 24: 1442-1453.
83. Poirson-Bichat F, Goncalves RA, Miccoli L, Dutrillaux B, Poupon MF (2000) Methionine depletion enhances the antitumoral efficacy of cytotoxic agents in drug-resistant human tumor xenografts. Clinical cancer research : an official journal of the American Association for Cancer Research 6: 643-653.
84. Shoemaker RH, Monks A, Alley MC, Scudiero DA, Fine DL, et al. (1988) Development of human tumor cell line panels for use in disease-oriented drug screening. Progress in clinical and biological research 276: 265-286.
85. Minn H, Clavo AC, Grenman R, Wahl RL (1995) In vitro comparison of cell proliferation kinetics and uptake of tritiated fluorodeoxyglucose and L-methionine in squamous-cell carcinoma of the head and neck. Journal of nuclear medicine : official publication, Society of Nuclear Medicine 36: 252-258.
86. Trencsenyi G, Marian T, Lajtos I, Krasznai Z, Balkay L, et al. (2014) 18FDG, [18F]FLT, [18F]FAZA, and 11C-methionine are suitable tracers for the diagnosis and in vivo follow-up of the efficacy of chemotherapy by miniPET in both multidrug resistant and sensitive human gynecologic tumor xenografts. BioMed research international 2014: 787365.
87. Lin L, Yee SW, Kim RB, Giacomini KM (2015) SLC transporters as therapeutic targets: emerging opportunities. Nature Reviews Drug Discovery 14: 543–560.
88. Cesar-Razquin A, Snijder B, Frappier-Brinton T, Isserlin R, Gyimesi G, et al. (2015) A Call for Systematic Research on Solute Carriers. Cell 162: 478-487.
89. Pulciani S, Santos E, Long LK, Sorrentino V, Barbacid M (1985) ras gene Amplification and malignant transformation. Molecular and cellular biology 5: 2836-2841.
90. Sacco E, Metalli D, Spinelli M, Manzoni R, Samalikova M, et al. (2012) Novel RasGRF1-derived Tat-fused peptides inhibiting Ras-dependent proliferation and migration in mouse and human cancer cells. Biotechnol Adv 30: 233-243.

3.2 Dissecting glutamine roles in promoting proliferation in transformed mouse fibroblasts

Gaia De Sanctis[1,2], Elena Sacco[1,2], Rita Licata[1,2], Marzia Di Filippo[2,3], Riccardo Colombo[2,3], Chiara Damiani[2,3], Daniela Gaglio[2,4], Gianmarco Rinaldi[5,6], Marcella Rocchetti[1], Sarah-Maria Fendt[5,6], Lilia Alberghina[1,2] and Marco Vanoni[1,2*].

[1]Department of Biotechnology and Biosciences, University of Milano-Bicocca, Piazza della Scienza 2, 20126 Milan, Italy
[2]SYSBIO, Centre of Systems Biology, Milan, Italy
[3]Department of Informatics, Systems and Communications, University of Milano-Bicocca, Viale Sarca 336, 20126 Milan, Italy
[4]Institute of Molecular Bioimaging and Physiology, National Research Council (IBFM-CNR), Segrate, Italy
[5]Laboratory of Cellular Metabolism and Metabolic Regulation, Department of Oncology, University of Leuven, Leuven, B-3000, Belgium
[6]Laboratory of Cellular Metabolism and Metabolic Regulation, Vesalius Research Center, VIB, Leuven, B-3000, Belgium

*Corresponding author

E-mail: marco.vanoni@unimib.it

Manuscript in preparation

Abstract

The enhanced growth and survival of K-Ras-transformed cells rely on deep changes in metabolism, including glutamine addiction and increased oxidative stress.

We study glutamine roles in metabolism and redox homeostasis in K-ras-transformed NIH3T3 mouse fibroblasts (NIH-RAS), by complementing glutamine deprivation with dimethyl-α-ketoglutarate (AKG) and nonessential amino acids (NEAA).

The combination AKG+NEAA only partly rescues glutamine deprivation and weakly activates mTOR pathway. This substitution results in low levels of nucleotides and the non-use of reductive carboxylation of AKG –predicted by ENGRO model– to synthesize lipids, whose content is lower due to downregulated expression of genes involved in lipogenesis that correlates with lower NADPH levels.

Thus, in NIH-RAS cells glutamine is essential as a carbon and nitrogen source for biosynthesis (amino acids, nucleotides and glutathione) and as a signaling molecule.

We successfully exploit an integrated, Systems Biology approach to study nutritionally-perturbed transformed cells, pushing forward a system-level understanding of complex diseases like cancer.

Introduction

In the last decades, increasing attention has been directed to the dependency of some cancer cells on the conditionally essential amino acid glutamine [1,2,3,4]. Indeed, during situations of stress, the organism needs glutamine supplementation with the diet to satisfy the increased demand of this amino acid [1,2]. Similarly, rapidly growing cancer cells may display an increased glutamine consumption to sustain their fast proliferation and may die rapidly in the absence of glutamine [3]. As a metabolic precursor, glutamine is used for protein, RNA and DNA biosynthesis. Moreover, through the process known as glutaminolysis, glutamine generates ammonia and glutamate (GLU) that, in turn, can be catabolyzed to α-ketoglutarate (AKG) through either transamination or oxidative deamination. As such, glutamine participates in energy production and cellular redox homeostasis, being a precursor of the antioxidant glutathione [4]. As the carbon skeleton from glutaminolysis can be used for anabolic or anaplerotic processes, tumor cells may be addicted to glutamine as an alternative fuel (which is oxidized to CO_2 for energy production), or because glutamine-derived AKG enters the TCA cycle to replenish metabolic intermediates removed for biosynthesis, particularly NADPH and fatty acids [5]. Alternatively, glutamine can undergo reductive carboxylation (RC), which consists in the reverse conversion of AKG into citrate through mitochondrial and cytosolic isoforms of $NADP^+$/NADPH-dependent isocitrate dehydrogenase.

Subsequent metabolism of glutamine-derived citrate provides both the acetyl-CoA for lipid synthesis and the 4-carbon intermediates needed to produce remaining TCA cycle metabolites and related macromolecular precursors [6].

Besides playing a particularly important role in cell growth and metabolism, glutamine acts as a signaling molecule that ultimately activates a master regulator of protein translation, the mammalian target of rapamycin (mTOR) pathway [7,8]. mTOR is an atypical serine/threonine kinase that integrates several stimuli to regulate cell growth, metabolism, and aging [9]. Indeed, mTORC1 acts by phosphorylating multiple downstream targets, including the p70 ribosome protein S6 kinase (S6K1), that phosphorylates and activates ribosomal protein S6 (rpS6), a component of the 40S ribosomal subunit involved in the regulation of cell size and cell proliferation [10]. Although mTOR-signaling appears to respond most acutely to the essential amino acid leucine, glutamine uptake and export is required for EAA activation of mTORC1 [8,11].

We propose to dissect glutamine roles in cell proliferation by using *K-ras*-transformed NIH3T3 mouse fibroblasts (NIH-RAS) as cellular model, extensively characterized in our laboratory [12,13,14]. We feed glutamine-deprived NIH-RAS with dimethyl-alpha-ketoglutarate (AKG) –a membrane-permeable analogue of alpha-ketoglutarate- as carbon source and nonessential amino acids (NEAA: Pro, Ala, Asp, Asn) as nitrogen source, to reconstitute glutamine and facilitate the understanding of its

roles in sustaining cell growth. In a Systems Biology perspective, we study NIH-RAS cell metabolism with ENGRO metabolic model and *–omics* technologies, highlighting that glutamine owns multiple and unique roles in proliferating cells and may not be substituted by other nutrients, even if contained in its structure. Indeed, we demonstrate that glutamine is necessary to activate mTOR pathway and hence lipogenesis and, above all, to maintain redox homeostasis, allowing NIH-RAS cells to produce lipids through reductive carboxylation of glutamine and to provide a source of nitrogen for nucleotide biosynthesis.

Results

Alpha-ketoglutarate and nonessential amino acids partly rescue glutamine deprivation in NIH-RAS cells

To study nutritional dependency of transformed cells, the first step usually consists in the analysis of physiological readouts, like cell proliferation and viability, under different nutrient perturbations. In this context, we first evaluated parental NIH3T3 and transformed NIH-RAS cell proliferation under glutamine deprivation and we observed that both NIH3T3 and NIH-RAS cell lines are glutamine-addicted, as they die in the absence of this amino acid (**Figure 1C-D**, light blue line). This is in accordance with previous literature data [15].

Given that glutamine is a nitrogen and carbon source, we tried to substitute this amino acid with other nutrients having analogous function. Particularly, when glutamine is available in the medium, it is converted into glutamate and ammonium by glutaminase (GLS), then glutamate is converted into α-ketoglutarate and ammonium either by glutamate dehydrogenase (GDH) or transaminases (**Figure 1A**). As these reactions are reversible, we decided to supplement glutamate (GLU) and ammonium or dimethyl-α-ketoglutarate (AKG) –a membrane-permeable analogue of α-ketoglutarate– and ammonium to glutamine-deprived NIH3T3 and NIH-RAS cells, in order to allow these cells to synthesize glutamine through glutamine synthetase (GS)-catalyzed reaction (**Figure 1B**). As a source of ammonium, we provided NIH3T3 and NIH-RAS with

nonessential amino acids (NEAA: aspartate, asparagine, alanine, proline), since previous experiments demonstrated that supplementing ammonium sulfate or ammonium acetate to NIH3T3 and NIH-RAS cells resulted in cell toxicity and death (data not shown), differently from what happens in yeast.

Supplementing equimolar amounts of GLU (4 mM) to glutamine-depleted NIH3T3 and NIH-RAS did not rescue their growth ability (**Figure 1C-D**, dark green line), as reported by Eagle [16] and, later, by Tardito [17]. Similarly, supplementing NEAA or AKG was ineffective in rescuing growth (**Figure 1C-D**, yellow and light green lines, respectively).

Only co-supplementation of AKG *AND* NEAA (**Figure 1C-D**, red line) or GLU *AND* NEAA (**Figure 1C-D**, dashed burgundy line) restored cell growth and viability, but only in NIH-RAS cells. The apparent mass duplication time (MDT) of NIH-RAS in both these conditions was about 4.5 longer than in standard (STD) medium. Future experiments will clarify whether this reduction originates from all cells growing slower, or to a reduced growth fraction in nutritionally-perturbed conditions.

We measured apoptosis and necrosis of NIH3T3-derived cell lines in STD and –GLN+AKG+NEAA conditions after 54 h from medium change (**Figure 1E**). We found that, in –GLN+AKG+NEAA, neither NIH3T3 nor NIH-RAS cells undergo apoptosis. This is in line with the fact that NIH-RAS cells can proliferate –though with higher mass duplication time- in –

GLN+AKG+NEAA and indicates that NIH3T3 only arrest their proliferation in –GLN+AKG+NEAA without dying.

Due to the low number of NIH3T3 cells grown in –GLN+AKG+NEAA medium and to the ensuing low reliability of experimental results obtainable with such a small cell fraction, we decided to focus our attention on NIH-RAS cells and to analyse different parameters in these cells grown in STD *versus* –GLN+AKG+NEAA medium.

First, we analysed cell dimensions by measuring protein content per cell and we found that NIH-RAS cells are significantly smaller when grown in –GLN+AKG+NEAA medium compared to STD medium (**Figure 1F**). Glutamine-deprived NIH-RAS cells also show slightly higher levels of autophagy, which promotes cellular survival during glutamine starvation (data not shown). However, the differences in autophagy levels between STD and –GLN+AKG+NEAA conditions are mild, likely due to a high basal level of autophagy in NIH-RAS cells compared to the parental NIH3T3 cell line [18]. Further experiments will clarify this aspect by evaluating the presence and the level of autophagy markers.

In the absence of glutamine, NIH-RAS cells may rely more on glucose to produce essential building blocks like amino acids, thus diverting less glucose to lactate. We analysed fresh and spent media to measure glucose consumption (and subsequent lactate production), finding that NIH-RAS grown in –GLN+AKG+NEAA may consume a little less glucose (and produce a little less lactate). However, the differences are minor and

unlikely to be significant. On the contrary, cells grown in –GLN+AKG+NEAA produce and secrete large quantities of glutamate (**Figure 1G**).

Next, we aimed to understand if NIH-RAS cells internalize and consume AKG and NEAA supplemented to the glutamine-free medium. NIH-RAS cells grown in –GLN+AKG+NEAA consume substantial amounts of AKG, Asp and Asn. Little if any consumption of Ala and Pro is detected, suggesting that Asp and Asn may be the only required amino acids to allow growth of NIH-RAS in glutamine-deprived media supplemented with AKG (**Figure 1H**). This conclusion is supported by preliminary results (**Figure 1D**, fuchsia line).

As reported in the Introduction, glutamine also acts as a signaling molecule that ultimately activates mammalian target of rapamycin (mTOR) pathway (**Figure 2C**). Thus, the lack of glutamine in –GLN+AKG+NEAA medium may downregulate mTOR pathway activation, partially accounting for the slower growth of NIH-RAS cells in this medium compared to STD medium.

We confirmed our hypothesis by assaying the activation state of the mTOR pathway, using the level of phosphorylated S6 –a ribosomal protein that acts downstream of mTOR (**Figure 2C**)– in our experimental system and we highlighted a weak mTOR pathway activation in –GLN+AKG+NEAA and also in –GLN+GLU+NEAA conditions (**Figure 2A-B**).

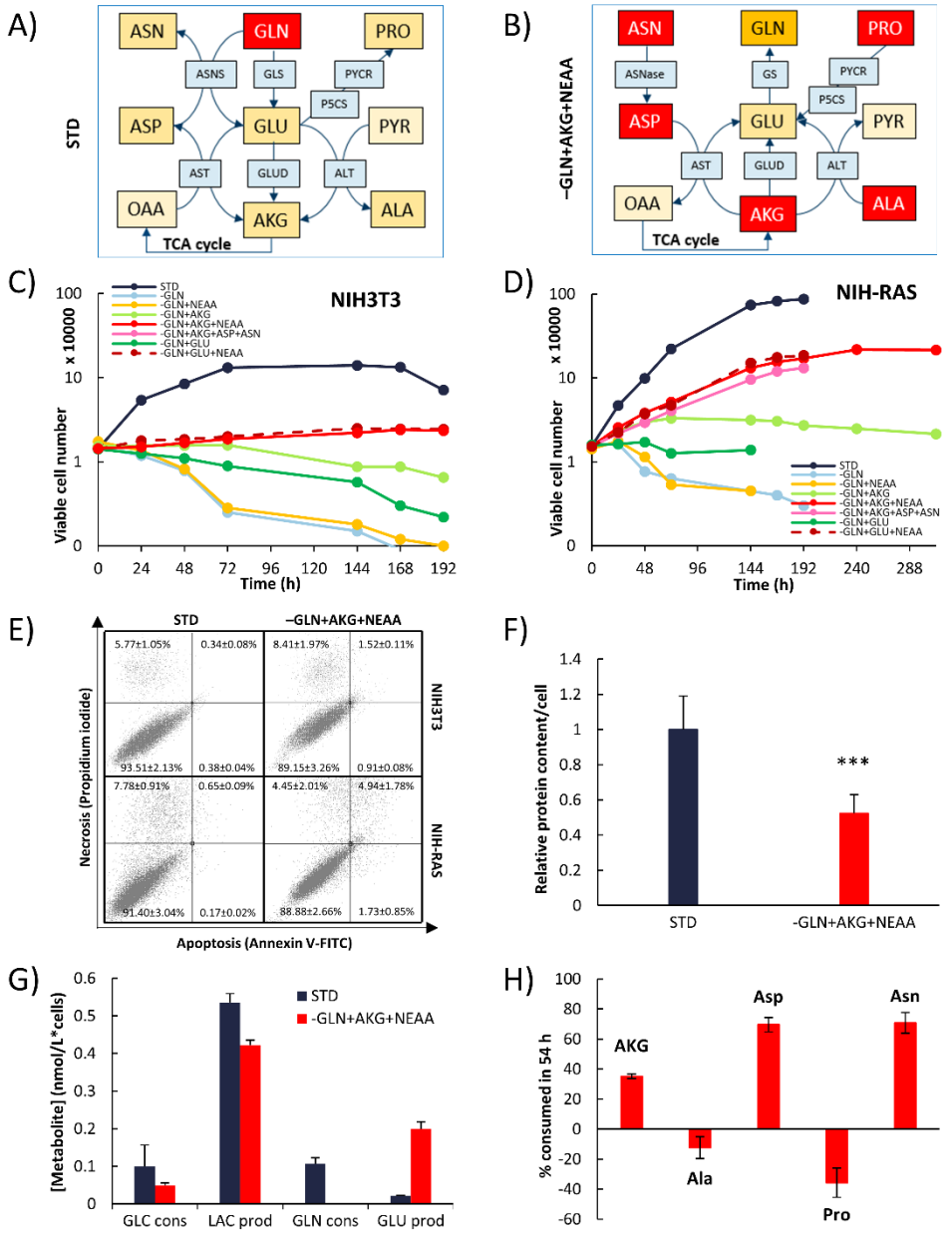

Figure 1 Alpha-ketoglutarate and nonessential amino acids partly rescue glutamine deprivation in NIH-RAS cells. (A-B) Representative scheme of cell metabolism in STD **(A)** and –GLN+AKG+NEAA

(B) *media.* **(C-D)** Growth kinetics of NIH3T3 **(C)** and NIH-RAS **(D)** cells grown under different nutrient conditions as indicated (STD: 4 mM Gln; AKG: 4 mM dm-aKG; NEAA: 4 mM Ala, 4 mM Asp, 4 mM Asn, 4 mM Pro; GLU: 4 mM Glu) and counted daily with trypan blue excluding method (semilog curves). **(E)** Representative dot plots for NIH3T3 and NIH-RAS cells stained with Annexin V-FITC and propidium iodide and analyzed by FACS after 30 h of growth under conditions indicated. **(F)** Cellular size of NIH-RAS cells grown in STD and –GLN+AKG+NEAA, determined by measuring protein content per cell (Bradford assay). **P<0.01 (Student's t-test). **(G)** Glucose and glutamine consumption and lactate and glutamate production under conditions indicated measured with YSI Analyzer. **(H)** AKG and NEAA consumption for NIH-RAS cells after 54 h of growth under conditions indicated. Measurements were made with GC-MS on fresh and spent *media*.

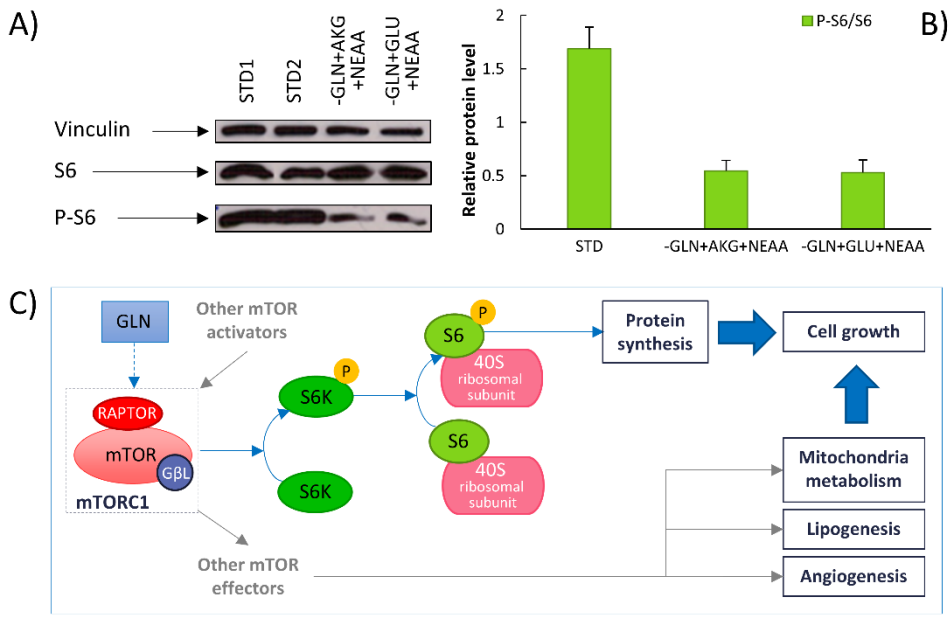

Figure 2 Mammalian target of rapamycin (mTOR) pathway activation is low in glutamine-deprived NIH-RAS supplemented with AKG+NEAA or GLU+NEAA. (A) Expression and phosphorylation of the S6 protein in NIH-RAS cells grown in STD, –GLN+AKG+NEAA and –GLN+GLU+NEAA *media.* For the protein expression, cells were collected at 54 h after medium change and 30 µg of proteins from the total cellular extract were subjected to SDS-PAGE followed

by Western blotting with a specific anti-phosphorylated$^{Ser235/236}$ S6 (P-S6) antibody and an anti-S6 (S6) antibody. **(B)** Quantification of the P-S6 over S6 amounts after normalization over vinculin. Quantitative data were obtained by analyzing Western blot with ImageJ software. **(C)** Schematic overview of mTOR pathway activation by glutamine.

Glutamine-deprived NIH-RAS cells supplemented with AKG+NEAA downregulate the expression of genes involved in lipogenesis

Transcriptomic analysis on NIH-RAS cells grown in STD and in –GLN+AKG+NEAA media revealed that only 115 genes are differentially expressed between the two nutritional conditions (Fold Change >1.5; corrected P value <0.05) (**Figure 3A**). The heat map in **Figure 3A** shows the hierarchical clustering of such differentially expressed genes (DEGs), represented in green if downregulated in NIH-RAS cells grown in –GLN+AKG+NEAA medium, while in red if upregulated. As Panther analysis revealed (**Figure 3C**), most of the DEGs deal with metabolism, especially cholesterol biosynthesis and transport. Other identified DEGs are involved in the response to the oxidative stress induced by nutrient deprivation, like that mediated by p53 signaling pathway, and in cell cycle, like the downregulated Cdkn1a gene.

To integrate transcriptomic data and deepen the aspect of the strong impact on metabolism induced by growth in –GLN+AKG+NEAA medium, a computational analysis was carried out to identify the "reporter metabolites" (**Figure 3D**; see Materials and Methods for the reporter metabolite identification process). Reporter metabolites are those spots

in the metabolism where there is a substantial regulation either to maintain homeostasis (i.e. a constant metabolite level) or adjust the concentration of the metabolite to another level required for proper functioning of the metabolic network. Thus, the identification of reporter metabolites adds knowledge to the pathway analysis shown in **Figure 3C**, as it considers the information on the connectivity and the magnitude of the significance of change for differentially expressed genes. Moreover, reporter metabolite analysis also takes into account genes not differentially expressed, which can exhibit significant coordinated changes when considered together.

Reporter metabolite analysis confirmed that most of the downregulated genes in cells grown in –GLN+AKG+NEAA medium deal with lipid synthesis, especially cholesterol synthesis and transport (**Figure 3D**), which is a process that requires a high amount of NADPH. In this regard, the most relevant reporter metabolite (i.e. to which the highest normalized score is associated) was NADP –either in its reduced or oxidized form- (**Figure 3D**), suggesting potential differences in redox state between NIH-RAS cells grown in STD medium and glutamine-deprived NIH-RAS cells.

To validate transcriptomic data, we first measured lipid and cholesterol levels in STD and –GLN+AKG+NEAA *media*, confirming a lower lipid content (**Figure 4A**) and a reduction of 40% of cholesterol levels under glutamine deprivation (**Figure 4B**).

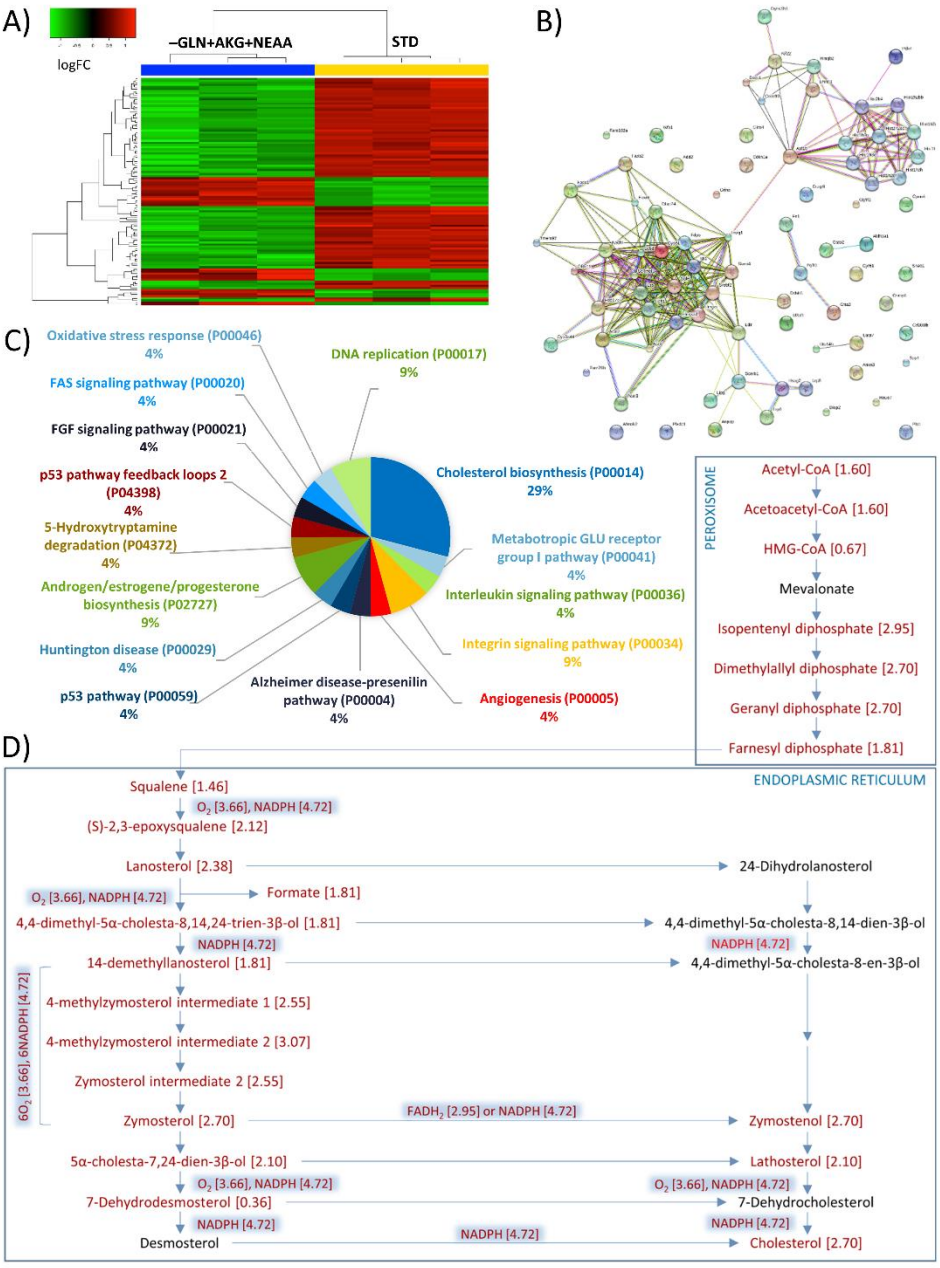

Figure 3 Glutamine-deprived NIH-RAS cells supplemented with AKG+NEAA downregulate the expression of genes involved in lipogenesis. (A) Heat map of significant DEGs (115; FC>1.5;

corrected P value<0.05) in NIH-RAS grown in –GLN+AKG+NEAA *versus* STD *media*. **(B)** STRING analysis of putative interactions between the identified DEGs. **(C)** List of pathways affected by the identified DEGs (Panther analysis). **(D)** Main reporter metabolites (RM) mapped in red on steroid biosynthetic pathway. In parentheses: normalized score for each RM.

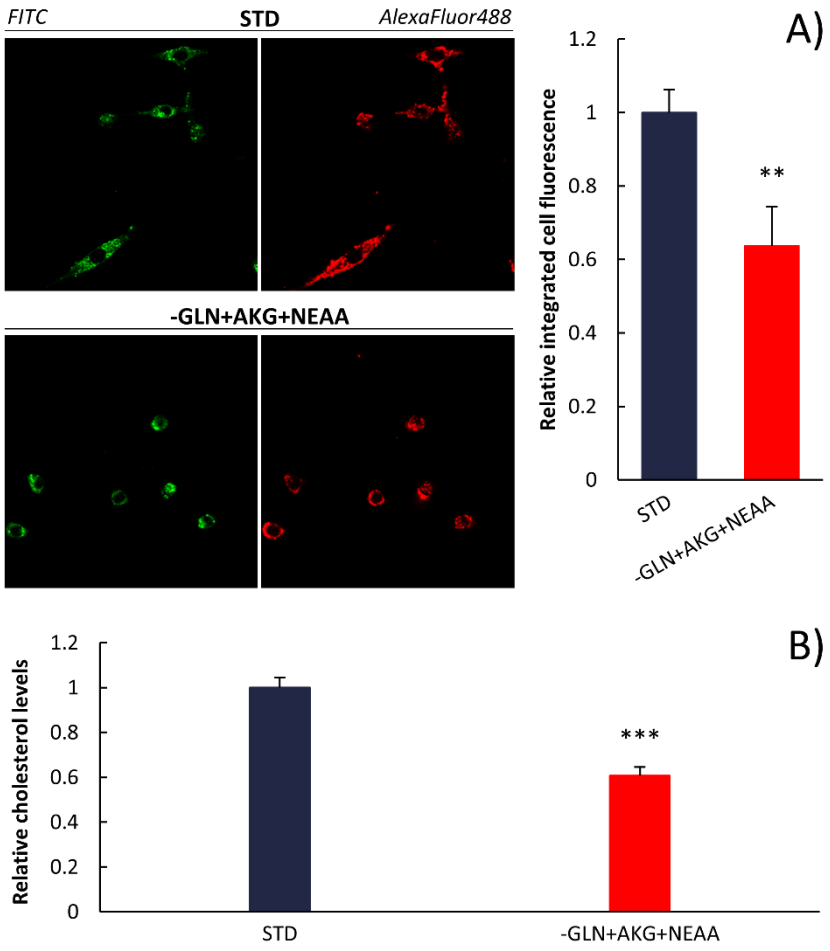

Figure 4 Glutamine-deprived NIH-RAS cells supplemented with AKG+NEAA have a lower lipid and cholesterol content. (A) Nile Red staining of lipids in NIH-RAS cells grown in STD and –GLN+AKG+NEAA *media*. Cells were analyzed with confocal microscope (60X magnification) and photos were taken after exciting with FITC (left) and AlexaFluor488 channels (right). Total cell

fluorescence (i.e. green + red) integrated on cell area was determined using ImageJ software and plotted in the histogram. **(B)** Cholesterol levels in NIH-RAS cells grown in STD and –GLN+AKG+NEAA *media*, measured with Total Cholesterol Assay kit (Cell Biolabs). **P<0.01; ***P<0.001 (Student's t-test).

AKG and NEAA mitigate oxidative stress and redox unbalance induced by glutamine deprivation in NIH-RAS cells

As mentioned above, computational analyses on transcriptomic data suggested that NIH-RAS cells grown in STD and in –GLN+AKG+NEAA *media* may differ in terms of redox potential (**Figure 3D**). Thus, we wanted to explore this aspect, as well as to further validate transcriptomic results.

According to literature data on *K-ras*-transformed cell lines [19], we found that glutamine deprivation enhances oxidative stress in NIH-RAS cells, and supplementation of AKG or NEAA partly decreases ROS levels, especially when combined in the –GLN+AKG+NEAA medium (**Figure 5A**).

Measuring reduced glutathione (GSH) and total glutathione (GSH+GSSG) levels (**Figure 5B-C**), we found that glutamine deprivation leads to decreased GSH and GSH+GSSG levels, due to the lack of glutamate (and ensuing glutathione) precursor glutamine. As seen for ROS levels, supplementation of AKG or NEAA –but above all their combination- partly restores basal GSH and GSH+GSSG levels. According to the role of ROS scavenger that glutathione in the reduced form has [20], we obtained a negative correlation between ROS and GSH levels (**Figure 5D**).

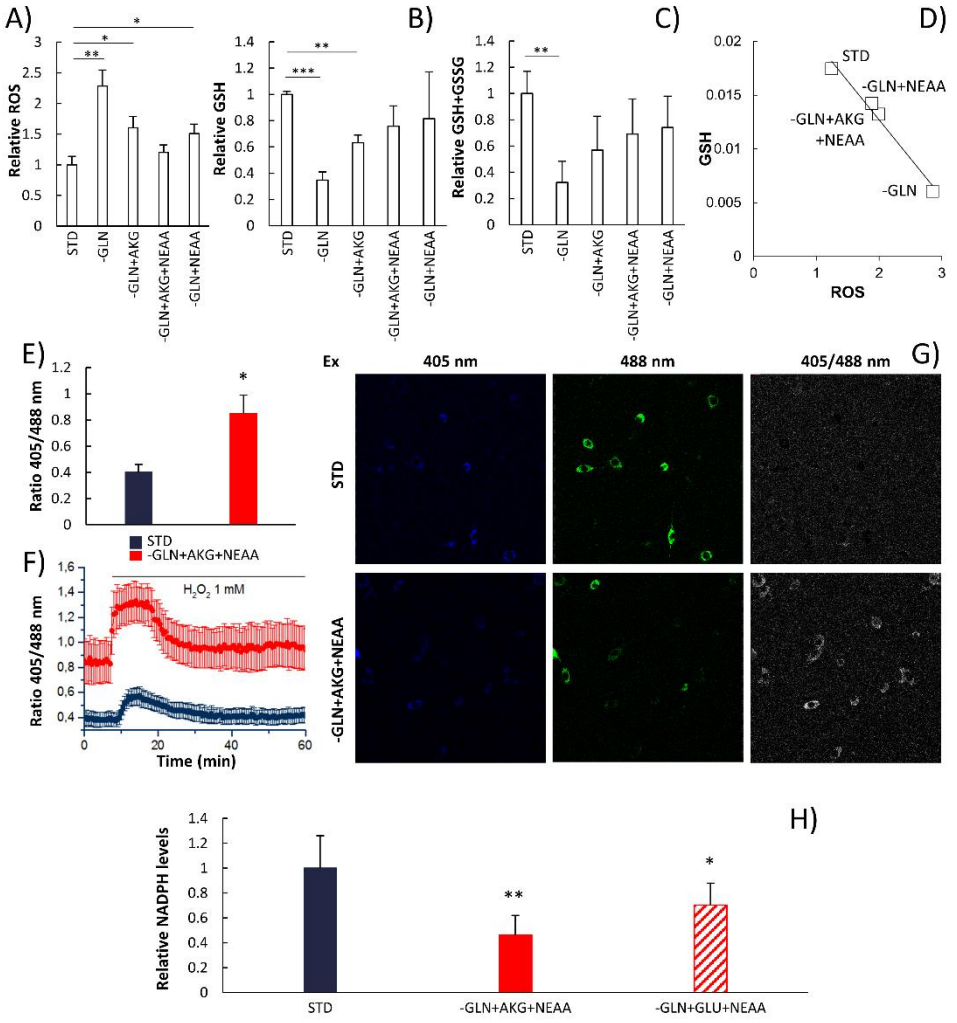

Figure 5 Glutamine-deprived NIH-RAS cells supplemented with AKG+NEAA show increased oxidative stress and redox unbalance. (A) Relative ROS levels in NIH-RAS cells grown for 54 h under conditions indicated as determined by DCFDA (2',7'-dichlorodihydrofluorescein diacetate) staining. Each bar represents the mean of at least three independent experiments with error bars representing the standard deviation. **(B)** Reduced glutathione levels measured after 54 h from medium change as described in [23]. Each bar represents the mean of at least three independent experiments with error bars representing the standard deviations. **(C)** Total glutathione levels measured after 54 h from medium change as described in [23]. Each bar represents the mean of

at least three independent experiments with error bars representing the standard deviations. **(D)** Negative correlation between reduced glutathione levels and ROS levels. **(E-F)** Mitochondrial matrix redox potential (in **(E)**: basal level) in NIH-RAS transfected with Mito-roGFP (ratiometric redox-sensitive GFP), grown in STD and –GLN+AKG+NEAA and time-lapse-analyzed with confocal microscope (Ex: 405 and 485 nm; Em: 510 nm). **(G)** Representative images obtained at confocal microscope during time-lapse analysis of mitochondrial redox potential. Cells were excited at 405 nm (left) and 488 nm (center); the resulting ratio 405/488 nm is reported on the right. **(H)** NADPH levels of NIH-RAS cells grown under conditions indicated as determined with NADP/NADPH Quantitation Kit (BioVision). *P<0.05; **P<0.01; ***P<0.001 (Student's *t*-test).

To further characterize the aspect of redox state in the presence or absence of glutamine, we used a redox-sensitive GFP probe (roGFP) that contains engineered cysteine residues, enabling dithiol formation in response to oxidant stress. This causes reciprocal changes in emission intensity at 510 nm when excited at two different wavelengths (405 and 488 nm): the ratio between the emission intensity obtained by exciting at 405 nm and that obtained by exciting at 488 nm would increase in an oxidizing environment. In detail, we used a plasmid harbouring mitochondrial matrix ro-GFP (Matrix-roGFP; **Figure 5E-G**). We performed *time-lapse* analyses of the fluorescence of roGFP-transfected NIH-RAS cells grown in STD *versus* –GLN+AKG+NEAA media for 54 h (**Figure 5G**), highlighting that the mitochondrial matrix is found in a more oxidizing environment in –GLN+AKG+NEAA *versus* STD medium (**Figure 5E-F**).

As revealed by transcriptomic data and ensuing analyses, NIH-RAS cells grown in –GLN+AKG+NEAA medium downregulate the synthesis of fatty acids and cholesterol, which is a NADPH-requiring process. Therefore,

such downregulation may depend on a lower NADPH content in glutamine-deprived NIH-RAS cells supplemented with AKG+NEAA.

We confirmed that, in glutamine-deprived NIH-RAS cells supplemented with AKG+NEAA, NADPH resulted about 50% lower than in STD (**Figure 5H**). We observed a drop in NADPH levels also for –GLN+GLU+NEAA growth condition, which showed a NADPH content 30% lower than in STD (**Figure 5H**). Thus, we hypothesized that the reaction responsible for the lower NADPH content and redox unbalance in –GLN+AKG+NEAA or –GLN+GLU+NEAA *media* may be the one catalyzed by the mitochondrial enzyme glutamate dehydrogenase (GDH).

Glutamine-deprived NIH-RAS cells supplemented with AKG+NEAA have low levels of nucleotides partly rescued by deoxyribonucleotide supplementation

Glutamine is known to be the nitrogen donor for N-3 and N-9 of the purine nucleobases, adenine and guanine, and for the amino group of guanine (**Figure 6A**). In this context, we wanted to compare nucleotide levels of NIH-RAS cells grown in STD and –GLN+AKG+NEAA media to highlight any difference between the two nutritional conditions.

First, as low energy levels may contribute to the slow growth of glutamine-deprived NIH-RAS cells, we measured ATP content, which was reduced of about 50% in glutamine-deprived NIH-RAS compared to NIH-RAS grown in STD medium (**Figure 6B**).

Previous literature data showed that depletion of deoxyribonucleotides (dNTPs) is the major effect of glutamine limitation, leading to reduced proliferation of NIH-RAS cells, which is rescued by adding these precursors of DNA polymerization to low glutamine medium [15]. Therefore, we measured the level of nucleotides and nucleotide precursors in NIH-RAS cells grown in STD and in –GLN+AKG+NEAA *media*, which resulted lower under glutamine deprivation (**Figure 6C**). Thus, we supplemented dNTPs at 0, 24, 48 and 72 hours to NIH-RAS cells grown in –GLN+AKG+NEAA medium. This supplementation schedule [15] allowed complete recovery of cell growth in the first 72 hours. The incomplete recovery at later time points may depend on nucleotide exhaustion or degradation (**Figure 6D**).

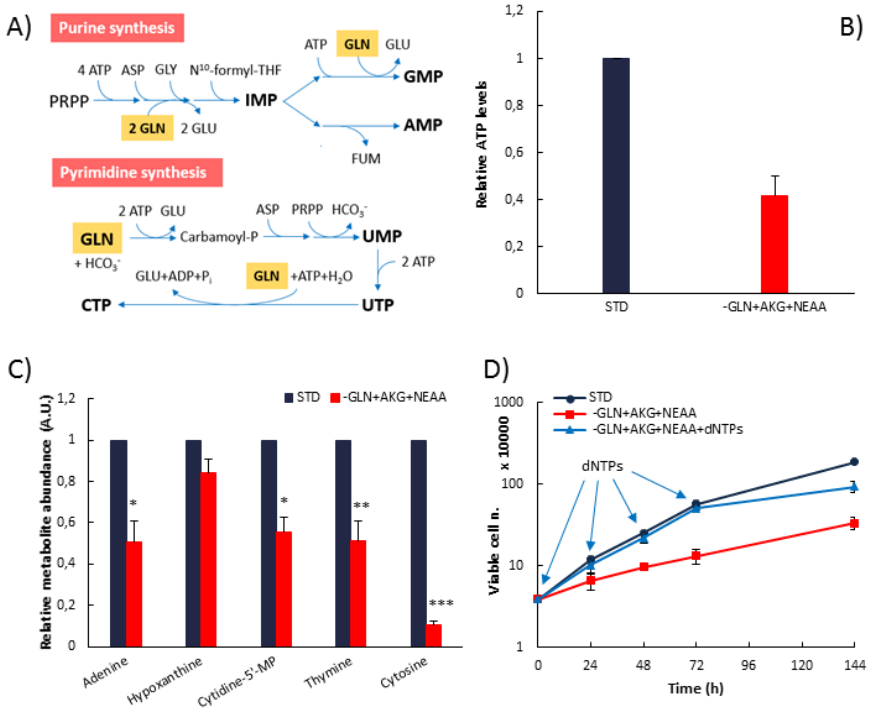

Figure 6 Glutamine-deprived NIH-RAS cells supplemented with AKG+NEAA show low nucleotide levels partly rescued by deoxyribonucleotide supplementation. (A) Glutamine in purine and pyrimidine synthesis. **(B)** Relative ATP levels in NIH-RAS grown in STD and –GLN+AKG+NEAA *media* determined with ATPlite Luminescence Assay System (Perkin Elmer). **(C)** Relative nucleotide abundance of NIH-RAS cells grown in STD and in –GLN+AKG+NEAA, analyzed with GC-MS. **(D)** Nucleotide supplementation in NIH-RAS cells grown in –GLN+AKG+NEAA medium.

Glutamine-deprived NIH-RAS cells do not follow reductive carboxylation of AKG and divert NEAA mainly to glutamate production

We analyzed metabolic profile of NIH-RAS cells grown in STD and in –GLN+AKG+NEAA *media* with GC/MS technology. As **Figure 7A** shows, in –GLN+AKG+NEAA condition the level of amino acids, glutamate, fumarate, malate and lactate is lower than in STD medium, while the level of proline and alanine is higher (**Figure 7A**). Next, we analyzed the fluxome of NIH-RAS cells grown in STD and in –GLN+AKG+NEAA *media* to understand if glucose (another major nutrient source for transformed cells) is diverted to other pathways to sustain growth when cells are glutamine-deprived and to understand if supplements AKG and NEAA under glutamine deprivation follow the same metabolic pathways as glutamine.

First, we provided NIH-RAS cells grown in STD and –GLN+AKG+NEAA *media* with [U-$^{13}C_6$]-glucose, finding that, compared to STD medium, labelled glucose is preferentially converted to serine, glycine and

glutamate in –GLN+AKG+NEAA medium and less converted to lactate (**Figure 7B**).

Then, we provided [U-$^{13}C_5$]-glutamine to NIH-RAS cells grown in STD medium (**Figure 7C**). Compared to what seen for glucose, NIH-RAS cells showed a higher use of glutamine for the synthesis of TCA cycle intermediates and for NEAA biosynthesis (with the exception of glucose-derived alanine), while lactate fully derived from glucose rather than from glutamine.

Likewise, we provided [1-^{13}C]-glutamate -and NEAA- to glutamine-deprived NIH-RAS cells. Strikingly, about 80% of the glutamate was still [1-^{13}C]-labeled, suggesting that glutamate may not be converted to other metabolites under glutamine deprivation (**Figure 7C**).

Finally, we provided NIH-RAS cells grown in –GLN+AKG+NEAA medium either with [^{15}N]-aspartate or with [^{15}N]-asparagine (the only NEAA that enter NIH-RAS cells) to follow their intracellular destiny. While asparagine is not used to synthesize other molecules, aspartate is mainly used to produce glutamate, since 43% of glutamate is ^{15}N-labelled (**Figure 7D**).

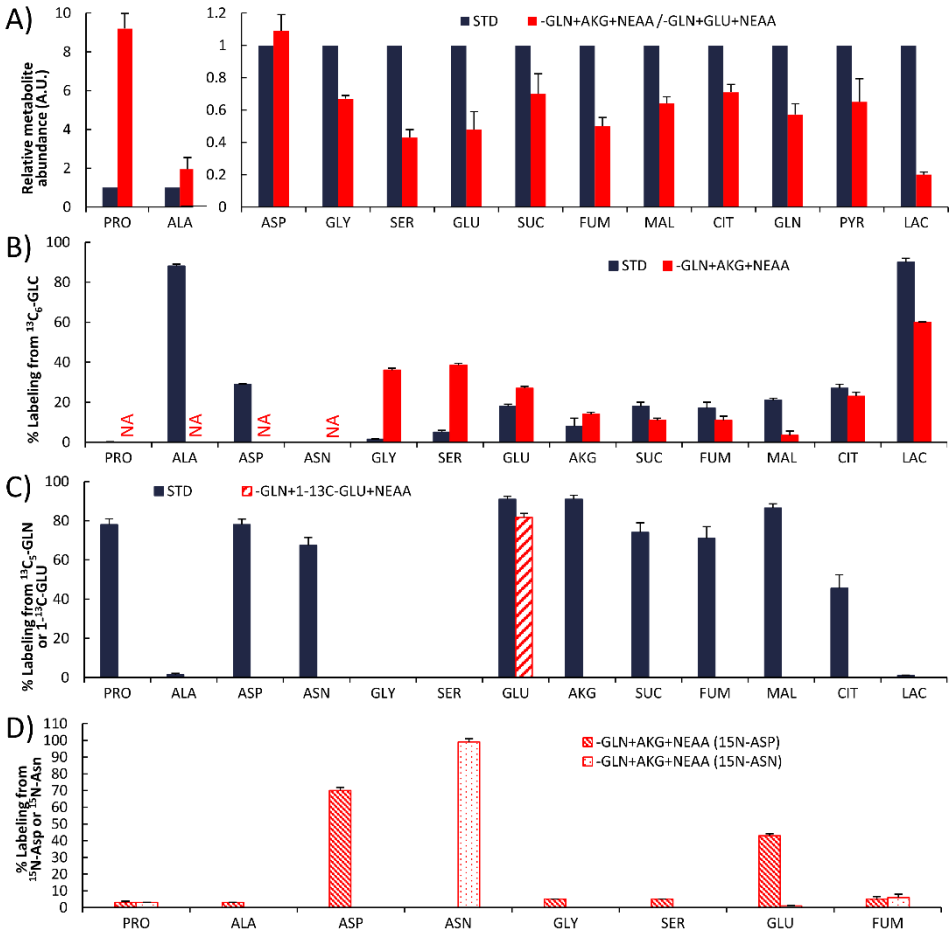

Figure 7 Metabolome and metabolic fluxes of NIH-RAS cells under nutrient perturbation. (A) Metabolic profile of NIH-RAS cells grown in STD and in –GLN+AKG+NEAA for 54 h, analyzed with GC-MS. **(B)** Percentage of metabolite labeling from [U-$^{13}C_6$]glucose in NIH-RAS cells grown in STD and –GLN+AKG+NEAA conditions. The analysis was made with GC-MS on NIH-RAS cells grown for 54 h. NA = not applicable, due to isotope dilution by external addition of NEAAs. **(C)** Percentage of metabolite labeling from [U-$^{13}C_5$]glutamine (for STD medium) or from [1-^{13}C]glutamate (for –GLN+GLU+NEAA medium) analyzed with GC-MS after 54 h of cell growth. **(D)** Percentage of metabolite labeling from [^{15}N]aspartate and from [^{15}N]asparagine in NIH-RAS cells grown for 54 h in –GLN+AKG+NEAA medium, measured with GC-MS.

Previous results on NIH-RAS cell metabolism [21] suggested that glutamine reductive carboxylation (RC) through the aconitase-catalyzed reaction is a marker of the enhanced growth of NIH-RAS cells when compared to their parental NIH3T3 normal cell line. Therefore, we performed a series of Flux Balance Analysis (FBA) simulations on the model on central carbon metabolism ENGRO introduced in [22] by maximizing the backward direction of the aconitase–catalyzed reaction in both STD and –GLN+AKG+NEAA conditions. The aim of the analysis was to investigate the compatibility of the two growth conditions with the possibility of undergo RC. **Figure 8A-B** shows that when the backward direction of aconitase-catalyzed reaction is maximized, NIH-RAS cells grown in –GLN+AKG+NEAA medium are less capable of relying on RC for fatty acid synthesis. Indeed, the aconitase-catalyzed reaction displays a much higher flux value for NIH-RAS cells grown in STD medium than for glutamine-deprived NIH-RAS cells. Furthermore, FBA experiments highlighted that recurring to RC in –GLN+AKG+NEAA growth condition implies a 62%-reduction of biomass synthesis flux with respect to growth in STD medium, according to experimental observations (**Figure 1D**).

To validate computational results, we provided [U-$^{13}C_5$]-glutamine to NIH-RAS cells grown in STD medium (**Figure 8C**), founding that glutamine-derived labeled AKG undergoes both RC and forward TCA cycle. Indeed, both citrate M4 isotopomer (i.e. with 4 labeled carbon atoms, typical of oxidative metabolism) and citrate M5 isotopomer (typical of reductive

metabolism) are generated, in line with previous results [19]. On the contrary, as predicted by ENGRO model, we demonstrated that AKG derived from [1-^{13}C]-glutamate in glutamine-deprived NIH-RAS cells does not follow RC, since neither TCA intermediates nor citrate were labelled (labelled carbon atom is indeed lost as CO_2 in the decarboxylation step from AKG to succinyl-CoA) (**Figure 8D**).

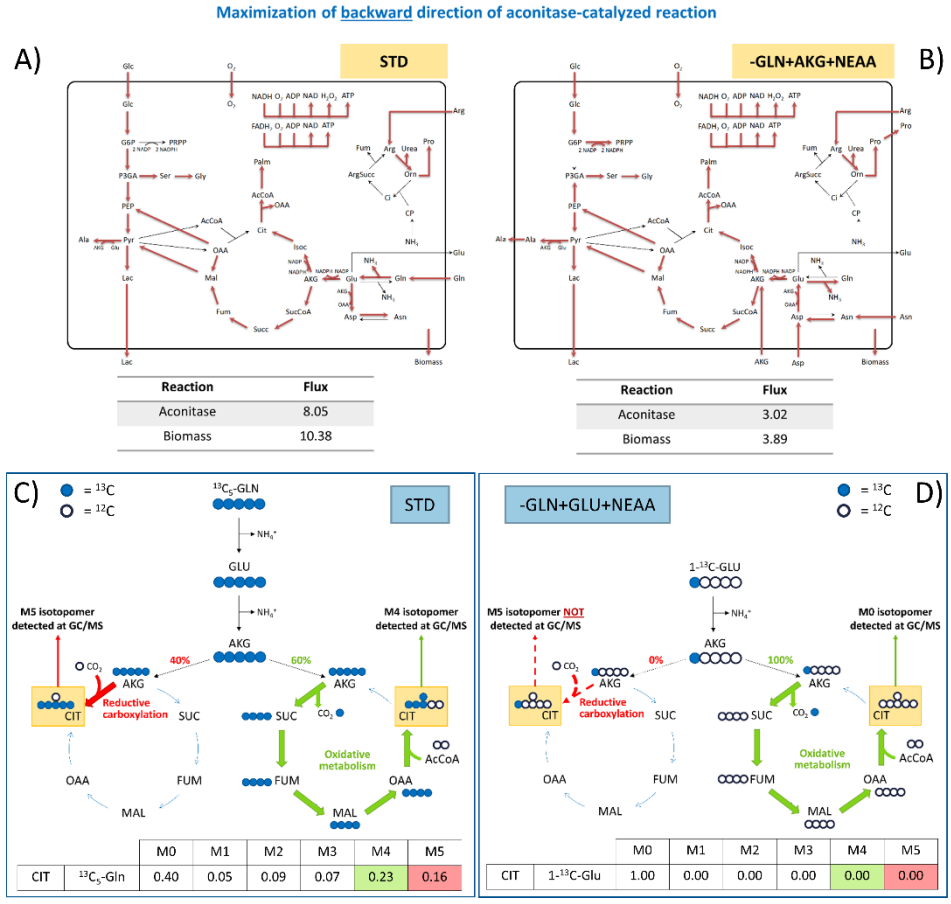

Figure 8 Glutamine-deprived NIH-RAS cells supplemented with AKG+NEAA do not follow reductive carboxylation (RC) pathway. (A-B) Flux balance analysis (FBA) experiments on ENGRO network to maximize the backward direction of the aconitase-catalyzed reactions for NIH-RAS cells grown in STD **(A)** and –GLN+AKG+NEAA **(B)** *media*. **(C)** Map and experimental values of labeling destiny when [U-$^{13}C_5$]glutamine is metabolized both reductively and oxidatively (for STD medium). **(D)** Map and experimental values of labeling destiny when [1-^{13}C]glutamate is metabolized oxidatively (for –GLN+GLU+NEAA medium).

Discussion

Growing cancer cells often depend on glutamine, with some cell lines dying rapidly if they are deprived of this amino acid [3,4].

We show that *K-ras*-transformed mouse fibroblasts are addicted to glutamine, glutamine concentration modulating the transformed phenotype [15].

Alpha-ketoglutarate and ammonium-containing nonessential amino acids, the molecules that constitute glutamine, can only partly restore cell growth when combined upon glutamine deprivation (**Figure 1C-D**).

A likely cause of the partial complementation of glutamine deprivation may lie in altered signaling events, such as the low mTOR activation pathway when glutamine is substituted by AKG+NEAA or GLU+NEAA (**Figure 2A-B**). This result is in accordance with previous literature data [15] in which addition of GLU or AKG failed to rescue mTORC1 activation under glutamine deprivation.

Other key reasons for the partial growth recovery of glutamine-deprived NIH-RAS supplemented with AKG+NEAA are metabolic events that we studied at the biochemical, transcriptional and cellular level. Such events include a reduction in nucleotide synthesis (**Figure 6B-C**) and in fatty acid and lipid synthesis (**Figure 3-4**). Downregulation of lipogenesis, which is a process that requires high amounts of reducing power in the form of NADPH, correlates with the higher oxidative stress evidenced by ratiometric roGFP probes and the lower NADPH levels (**Figure 5**). The

observation that NADPH levels are lower also when glutamine is substituted by GLU+NEAA may reflects a probable missed production of NADPH in the reaction step catalyzed by glutamate dehydrogenase (GDH). Indeed, glutamine-deprived NIH-RAS cells may not need to synthesize AKG from GLU through the GDH-catalyzed reaction when AKG+NEAA are supplemented, while GDH may be inhibited by sirtuin SIRT4 [24], not transcriptionally repressed by weakly active mTORC1, when glutamine-deprived NIH-RAS cells are supplemented with GLU+NEAA. The inhibition of GDH by SIRT4, together with the probable low ATP-dependent glutamine synthase (GS) activity -likely due to the low ATP levels measured under glutamine deprivation (**Figure 6B**)-, could account for the intracellular accumulation of GLU supplemented to glutamine-deprived NIH-RAS cells (**Figure 7C**). Experiments to test GDH and GS activities are needed to clarify this aspect.

A possible connection between mTOR pathway activation state and lipogenesis lies in the fact that the transcriptional program activated by mTOR includes SREBP-1 and the related protein SREBP-2, which regulates transcription of genes in fatty acid and sterol biosynthesis [25,26]. Thus, when mTOR is inactive (or weakly active), SREBP-mediated fatty acid and sterol biosynthesis cannot occur, leading to dowregulated lipid content.

Finally, glutamine-deprived NIH-RAS cells supplemented with AKG precursor GLU and NEAA rely less on reductive carboxylation of AKG (**Figure 8D**), which is an efficient and rapid way to synthesize lipids but

requires high amounts of NADPH to ensure an adequate citrate production [27]. This result was predicted by our model of NIH-RAS cell metabolism ENGRO introduced in [22], which indicated that cells grown in –GLN+AKG+NEAA medium are less capable of relying on reductive carboxylation for fatty acid synthesis (**Figure 8B**).

In our work, we validated some of the above-mentioned observations about NIH-RAS cell behaviour when deprived of glutamine and supplemented with AKG+NEAA, like the rescuing effect of deoxyribonucleotide supplementation on cell growth. We also rationalized some other observations through mathematical models of metabolism, like the lower reliance on reductive carboxylation pathway.

We will need further experiments to extend such validations and to clarify some aspects. First, we would like to deepen our knowledge about the role of mTOR in NIH-RAS cell proliferation when glutamine is substituted with AKG+NEAA, by activating mTOR pathway biochemically or genetically and measuring its possible complementation effect on cell growth. Second, we may want to study the epigenetic state of the genes involved in fatty acid and sterol biosynthesis. Third, we would like to understand how do signalling and metabolic pathways intersect and cross-regulate each other.

Although the extension of our research to human cell lines is required to identify fragile points in the metabolic network of cancer cells, our studies help to elucidate the role of glutamine in the proliferation of glutamine-

addicted cancer cells. Moreover, by integrating metabolic and signaling events, as well as experimental data within metabolic models, such studies may reveal useful in defining clinical protocols that make use of drugs directed against glutamine metabolism [4].

Materials and Methods

Cell culture

Two cell lines have been used in this work, namely normal NIH3T3 mouse fibroblasts (obtained from the ATCC, Manassas, VA, USA) and a K-Ras-transformed normal-derived cell line –that we refer to as NIH-RAS. Both control and ras-transformed NIH3T3 have been passaged a similar number of times, taking care to refreeze the cell lines immediately and to use them for a limited number of passages. The cell lines are periodically assayed to check that the major properties of the cells do not change over time, that the major transformation-related phenotypes are retained and ras-dependent. The cell lines were routinely grown in Dulbecco's modified Eagle's medium (Invitrogen Inc., Carlsbad, CA, USA) containing 10% newborn calf serum (NCS), 4 mM glutamine, 100 U/ml penicillin and 100 mg/ml streptomycin, that we refer to as standard medium (STD), at 37°C in a humidified atmosphere of 5% CO_2. Cells were passaged using trypsin-ethylenediaminetetraacetic acid (EDTA) (Invitrogen Inc., Carlsbad, CA, USA) and maintained in culture before experimental manipulation.

Cell proliferation analysis

Cells were plated at the density of 3000 cells/cm^2 in standard medium and incubated overnight at 37°C and 5% CO_2. After 18 h, cells were washed twice with phosphate-buffered saline (PBS) and, to verify the response to

glutamine deprivation, cells were incubated in medium without glutamine (Invitrogen Inc., Carlsbad, CA, USA), possibly supplemented with dimethyl-2-oxoglutarate (AKG, 4 mM, Sigma Aldrich Inc.) or glutamate (GLU, 4 mM, Sigma Aldrich Inc.) and/or nonessential amino acids (Pro, Ala, Asp, Asn, 4 mM each, Sigma Aldrich Inc.).To measure cell proliferation, cells were treated with trypsin at 0, 24, 48, 54, 72, 144, 168, 192, 240 and 312 hours after medium change. Viable (i.e., unstained) cells were counted in a Bürker chamber after staining with 0.5% trypan blue.

Apoptosis Assay

Cells were plated at the density of 3000 cells/cm^2 in standard medium and incubated overnight at 37°C and 5% CO_2. After 18 h, cells were washed twice with PBS and incubated for 30 hours in medium without glutamine (Invitrogen Inc., Carlsbad, CA, USA), supplemented with dimethyl-2-oxoglutarate (AKG, 4 mM, Sigma Aldrich Inc.) and nonessential amino acids (Pro, Ala, Asp, Asn, 4 mM each, Sigma Aldrich Inc.). For apoptosis analysis, 1×10^6 cells (adherent and in suspension cells) were collected, stained with Annexin V-FITC (Immunotools, GmbH) and propidium iodide (Sigma Aldrich Inc.) and analyzed by FACScan (Becton-Dickinson) using the FL1 and FL2 channels. Data analysis was performed with Flowing Software.

Autophagy assay

Autophagy was determined by using Autophagy Assay Kit (Sigma Aldrich Inc.) following manufacturer's instructions. Briefly, NIH-RAS cells that had to be grown in STD medium were plated at 3000 cells/cm^2, while NIH-RAS cells that had to be grown in –GLN+AKG+NEAA medium were plated at 9000 cells/cm^2 in glass bottom petri dishes, suitable for confocal microscopy, with normal growth medium (STD). After 18 h at 37°C and 5% CO_2, cells were rinsed twice with PBS and medium change was done, by incubating cells for 24 h with STD or –GLN+AKG+NEAA media. Cells were then incubated with the Autophagosome Detection Reagent working solution for 30 minutes in a 37°C in a 5% CO_2 incubator and washed 4 times with wash buffer. Cells were imaged immediately under a confocal microscope with a DAPI channel.

Cell size measurement

NIH-RAS cells were plated at 3000 cells/cm^2 (for 54 h-growth in STD and for 144 h-growth in –GLN+AKG+NEAA) and at 9000 cells/cm^2 (for 54 h-growth in –GLN+AKG+NEAA) in 6-well plates in STD medium and incubated overnight at 37°C and 5% CO_2. After 18 h, cells were washed twice with PBS and incubated for 54 h and 144 h in STD medium or in –GLN+AKG+NEAA medium. Cells were then 1) trypsinized and counted in a Bürker chamber (Trypan blue excluding method) and 2) scraped in lysis buffer to measure protein content with Bradford assay [28]. The resulting

protein content was then normalized on cell number for both nutritional conditions (STD and –GLN+AKG+NEAA) to get the protein content per cell, which is an indicator of cell size.

Determination of intracellular ROS

Intracellular accumulation of H_2O_2 and $O_2^{\bullet-}$ was determined after 54 h from medium change with 2',7'-dichlorodihydrofluoresceine diacetate (Sigma Aldrich Inc.). The cells were incubated for 30 minutes at 37°C with H_2DCFDA 10 mM, treated with trypsin, resuspended in PBS supplemented with NCS 10% (Invitrogen Inc., Carlsbad, CA, USA) and acquired by FACScan (Becton-Dickinson), using the Cell Quest software (BD Bioscience). The percentage of ROS producing cells was calculated for each sample and corrected for autofluorescence obtained from samples of unlabeled cells.

Determination of glutathione levels

For reduced and total glutathione measurements, cells were plated at the density of 3000 cells/cm^2 in standard medium and incubated overnight at 37°C and 5% CO_2. After 18 h, cells were washed twice with PBS and incubated for 54 h in STD medium or in medium without glutamine (Invitrogen Inc., Carlsbad, CA, USA), possibly supplemented with dimethyl-2-oxoglutarate (AKG, 4 mM, Sigma Aldrich Inc.) and/or nonessential amino acids (Pro, Ala, Asp, Asn, 4 mM each, Sigma Aldrich Inc.). Cells were then treated with trypsin, collected, washed twice with PBS and lysed

through freeze-and-thaw cycles. Samples were deproteinized with a 5% 5-sulfosalicylic acid solution, centrifuged to remove the precipitated protein and assayed for glutathione. GSH measurement was an optimization of Tietze's enzymatic recycling method [23], in which GSH is oxidized by the sulfhydryl reagent 5,5'-dithio-bis (2-nitrobenzoic acid) (DTNB) to form the yellow derivative 5'-thio-2-nitrobenzoic acid (TNB), measurable at 412 nm and the glutathione disulfide (GSSG) formed is recycled to GSH by glutathione reductase in the presence of NADPH. The amount of glutathione in the samples was determined through a standard curve of reduced glutathione. Glutathione levels were normalized to protein content measured by Bradford assay (Bio-Rad reagent) on an aliquot of cell extract collected before deproteinization.

Western blot analysis

For the analysis of mTOR pathway protein levels, cells were harvested after 54 h of growth in STD, –GLN+AKG+NEAA or –GLN+GLU+NEAA *media* and disrupted in an appropriated lysis buffer [29]. Thirty microgram of the total cellular extracts were then resolved by SDS-PAGE and transferred to the nitrocellulose membrane, which was incubated overnight with specific antibodies: vinculin from Santa Cruz Biotechnology Inc. (1:10000); S6 Ribosomal Protein (5G10) Rabbit mAb and Phospho-S6 Ribosomal Protein (Ser235/236) Rabbit mAb from Cell Signaling Technology Inc. (1:1000). Protein levels were determined by densitometric scanning and

quantitation with ImageJ software. Data are expressed after normalization to the level of vinculin.

Confocal microscopy analyses of redox potential

Cells were seeded at the density of 3000 cells/cm^2 (for growth in STD medium) and 9000 cells/cm^2 (for growth in –GLN+AKG+NEAA and –GLN+GLU+NEAA media) in glass bottom petri dishes, suitable for confocal microscopy, in STD medium and incubated overnight at 37°C and 5% CO_2. After 18 h, cells were transfected with 2 µg of plasmid harbouring either Cyto-roGFP (engineered GFP able to measure redox potential in cytosol) or Matrix-roGFP (engineered GFP able to measure redox potential in mitochondrial matrix), using Lipofectamine® RNAiMax Reagent (Thermo Fisher Scientific). After 24 h from transfection, medium was changed to STD, -GLN+AKG+NEAA or –GLN+GLU+NEAA (depending on the nutritional condition to be assayed). After 54 h from medium change, cells were analyzed with a Nikon Eclipse Ti-E confocal microscope, equipped with a climate chamber (with CO_2 vent and humidifier), a 405-nm UV diode laser and a 488-nm Ar laser. In detail, time-series experiments were performed by exciting the cells with 405-nm and 488-nm lasers for 7 minutes every 30 seconds (15 loops), using the 40x-oil objective. Then, cells were treated with 100 µM H_2O_2 to become fully oxidized (a procedure necessary to calibrate the microscope) and followed over time for 50 minutes by exciting them at 405 and 488 nm. Finally, the ratio 405:488 nm (i.e. the

ratio between the emission intensity at 510 nm obtained by exciting at 405 nm and that obtained by exciting at 488 nm) was determined for each loop after drawing ROIs (Regions Of Interest) on analyzed fluorescent cells, using NIS-Elements Software (Nikon Instruments).

NADPH levels

The measurement of NADPH levels of NIH-RAS grown in STD, –GLN+AKG+NEAA and –GLN+GLU+NEAA *media* was made using NADP/NADPH Quantification Colorimetric Kit (BioVision), following manufacturer's instructions. Cells were seeded at the density of 3000 cells/cm^2 (for growth in STD medium) and 9000 cells/cm^2 (for growth in –GLN+AKG+NEAA and –GLN+GLU+NEAA *media*) in 150-mm dishes in STD medium and incubated overnight at 37°C and 5% CO_2. After 18 h, cells were washed twice with PBS and incubated for 54 h in STD, –GLN+AKG+NEAA or –GLN+GLU+NEAA *media*. The day of the analysis, cell metabolism was quenched with liquid nitrogen and cells were lysed with NADP/NADPH Extraction Buffer provided with the kit. After following the protocol, NADPH and NADP+NADPH were quantified by reading the absorbance of the samples at 450 nm and comparing it with NADPH standard curve.

Cholesterol levels

Cholesterol levels of NIH-RAS grown in STD and –GLN+AKG+NEAA *media* were measured by using Total Cholesterol Assay Kit, Colorimetric (Cell

Biolabs), following manufacturer's protocol. Cells were seeded at the density of 3000 cells/cm^2 (for growth in STD medium) and 9000 cells/cm^2 (for growth in –GLN+AKG+NEAA medium) in 150-mm dishes in STD medium and incubated overnight at 37°C and 5% CO_2. After 18 h, cells were washed twice with PBS and incubated for 54 h in STD or –GLN+AKG+NEAA *media*. The day of the analysis, cells were lysed with a mixture of chloroform:isopropanol:NP-40 (7:11:0.1) and samples were processed according to the datasheet instructions. Finally, cholesterol levels were assayed by reading the absorbance of the samples at 570 nm and comparing it with cholesterol standard curve.

Lipid content (Nile Red staining)

The neutral lipid dye Nile Red (9-diethylamino-5H-benzo[α]phenoxazine-5-one) was used for lipid staining. The stock solution (1.0 mg/ml) in methanol was stored frozen (−20°C) in dark. Staining was carried out on live cells by adding the dye to a final concentration of 10 ng/ml directly in the culture medium for 5 minutes. Then, the dye was carefully washed out using PBS prior to microscopy. Lipid droplets were then visualized with confocal microscope (Nikon Eclipse Ti-E; 60X magnification) by exciting with FITC (green fluorescence) and AlexaFluor488 (red fluorescence) channels. Total fluorescence (i.e. green+red) per cell was determined by analysing photos with ImageJ software: regions of interest (ROIs) corresponding to each cell were drawn on brightfield images, then ROIs

were superimposed on photos acquired by exciting both with green and red fluorescence. Then, the corrected total cell fluorescence (CTCF) – normalized on cell area– was calculated, after subtracting the mean fluorescence of the background readings, by summing the corrected green and red fluorescence.

RNA extraction and transcriptomic analysis

Cells were plated at the density of 3000 cells/cm^2 in standard medium and incubated overnight at 37°C and 5% CO_2. After 18 h, cells were washed twice with PBS and incubated for 54 h in STD medium or for 144 h in medium without glutamine (Invitrogen Inc., Carlsbad, CA, USA) supplemented with dimethyl-2-oxoglutarate (AKG, 4 mM, Sigma Aldrich Inc.) and nonessential amino acids (Pro, Ala, Asp, Asn, 4 mM each, Sigma Aldrich Inc.). RNA was then extracted from cells by using TriFast™ reagent (EuroGOLD) and generated triplicate samples were stored at -80°C until the analysis. The QC evaluation was performed using Nanodrop and Agilent 2100 Bioanalyzer. Single strand biotinylated cDNA was generated from 200 ng of total RNA using two cycles of cDNA synthesis with the Affymetrix WT PLUS expression Kit. The first cycle-first strand synthesis was performed using an engineered set of random primers that excluded rRNA-matching sequences and included the T7 promoter sequences. After second-strand synthesis, the resulting cDNA was *in vitro* transcribed with the T7 RNA polymerase to generate a cRNA. This cRNA was subjected to a

second cycle-first strand synthesis in the presence of dUTP in a fixed *ratio* relative to dTTP. Single strand cDNA was then purified and fragmented with a mixture of uracil DNA glycosylase and apurinic/apirimidinic endonuclease 1 (Affymetrix) in correspondence of incorporated dUTPs. DNA fragments were then terminally labeled by terminal deoxynucleotidyl transferase (Affymetrix) with biotin. The biotinylated cDNA was hybridized to the Clariom D Arrays (previously known as Mouse GeneChip MTA 1.0 Arrays) containing more than 214000 full-length transcripts. After the hybridization, chips were washed and scanned on the Affymetrix Complete GeneChip® Instrument System, generating digitized image data (DAT) files and CEL files. CEL files were analyzed by R Bioconductor Oligo and Limma Packages, respectively. The full dataset was normalized by using the Robust Multialignment Algorithm (RMA). Results were filtered for a Fold Change ≥1.5. The genes were classified as Differentially Expressed if showed a FDR corrected p-value ≤ 0.05.

Reporter metabolites

Transcriptomic data were mapped on the corresponding enzymes of a genome scale metabolic model adding the *p* value obtained from a Student's *t*-test as a specification of the significance of differential gene expression (and so of the change for each enzyme). Each p_i was then converted to a *Z* score of the enzyme node (Z_{ni}) connected to the enzyme

under investigation, by using the inverse normal cumulative distribution (θ^{-1}).

$$Z_{ni} = \vartheta^{-1}(1-p_i)$$

Thus, each metabolite node in the genome-wide metabolic model (GWMM) was scored based on the normalized transcriptional response of its neighboring enzymes. Dealing with differential data, the normalized transcriptional response has been calculated as size-independent aggregated *Z* scores of the *k* neighboring enzymes.

$$Z_{\text{metabolite}} = (1/\sqrt{k}) \sum Z_{ni}$$

The scoring used to identify reporter metabolites was a test for the null hypothesis "neighbor enzymes of a metabolite in the metabolic graph show the observed normalized transcriptional response by chance". Metabolites with the highest score are defined as reporter metabolites, namely those metabolites around which transcriptional changes occur.

To perform the analyses, the Cobra Toolbox function "reporterMets" was used, which implements under Matlab the reporter metabolites algorithm by Patil and Nielsen [30]. Regarding the input, the Recon 2.2 model [31] was used.

Metabolomics analyses

For metabolite extraction, NIH-RAS cells that had to be grown in STD medium were plated at 3000 cells/cm^2, while NIH-RAS cells that had to be grown in –GLN+AKG+NEAA medium were plated at 9000 cells/cm^2 –in

order to reach the same cell density after 54 h– in 6-well plates with normal growth medium (STD). After 18 h at 37°C and 5% CO_2, cells were rinsed twice with PBS and incubated for 54 h in STD medium or –GLN+AKG+NEAA medium. After 54 h from medium change, cells were quickly rinsed with NaCl 0.9% and quenched with 0.4 ml ice-cold methanol. An equal volume of water was added, and cells were collected by scraping with a pipette tip. Cells were sonicated 5 seconds for 5 pulses at 70% power three times. One volume of chloroform was added, and cells were vortexed at 4°C for 20 min. Samples were centrifuged at 12000 g for 10 min, and the aqueous phase was collected in a new tube and evaporated under airflow at 37°C. Dried polar metabolites were dissolved in 60 µl of 2% methoxyamine hydrochloride in pyridine (Pierce) and held at 40°C for 6 h. After dissolution and reaction, 90 µl of MSTFA (N-Methyl-N-(trimethylsilyl) trifluoroacetamid) was added and samples were incubated at 60°C for 1 h. For cell culture, GC/MS analysis was performed using 6890 GC system combined with 5975BMS system (Agilent Technologies) equipped with a 30-m DB-5MS capillary column operating under electron impact (EI) ionization at 70eV. 1 µl of sample was injected in splitless mode at 250°C, using helium as the carrier gas at a flow rate of 1 ml/min. The GC oven temperature was held at 70°C for 2 min and increased to 325°C at 10°C/min. GC/MS data processing was performed using Agilent MassHunter software and statistical analyses were performed using Mass Profile Professional (MPP) software [32]. Relative

metabolites abundance was carried out after normalization to internal standard norvaline and cell number.

^{13}C tracer analyses

All labeling experiments were performed in media with 10% dialyzed newborn calf serum (NCS) for 54 h. All tracers were purchased from Sigma-Aldrich. For metabolite extraction, NIH-RAS cells that had to be grown in STD medium were plated at 3000 cells/cm^2, while NIH-RAS cells that had to be grown in –GLN+AKG+NEAA medium were plated at 9000 cells/cm^2 –in order to reach the same cell density after 54 h– in 6-well plates with normal growth medium (STD). After 18 h at 37°C and 5% CO_2, cells were rinsed twice with PBS and medium change was done, by incubating cells for 54 h with STD or –GLN+AKG+NEAA media containing dialyzed NCS and the proper tracer ([U-$^{13}C_6$]-glucose, [U-$^{13}C_5$]-glutamine, [1-^{13}C]-glutamate, [^{15}N]-aspartate or [^{15}N]-asparagine). Labeled cell cultures were then washed with 0.9% NaCl and metabolism was quenched in liquid nitrogen and then with -20°C cold 70% methanol. After cell scraping in 70% methanol (containing internal standards norvaline and glutarate), -20°C cold chloroform was added and the samples were vortexed at 4°C to extract metabolites. Phase separation was achieved by centrifugation at 4°C. The methanol-water phase containing polar metabolites was separated and dried using a vacuum concentrator. Dried metabolite samples were stored at −80 °C.

Polar metabolites were derivatized for 90 min at 37 °C with 7.5 µl of 20 mg/ml methoxyamine in pyridine and subsequently for 60 min at 60°C with 15 µl of N-(tert-butyldimethylsilyl)-N-methyl-trifluoroacetamide, with 1% tert-butyldimethylchlorosilane [33] (Sigma-Aldrich). Mass distributions and metabolite concentrations were measured with a 7890A GC system (Agilent Technologies) combined with a 5975C Inert MS system (Agilent Technologies). 1 µl of sample was injected into a DB35MS column in splitless mode using an inlet temperature of 270°C. The carrier gas was helium with a flow rate of 1 ml/min. Upon injection, the GC oven was held at 100°C for 3 min and then ramped to 300°C with a gradient of 2.5°C/min followed by a 5 min after run at 320°C. The MS system was operated under electron impact ionization at 70 eV and a mass range of 100–650 amu was scanned. Mass distributions were extracted from the raw ion chromatograms using a custom Matlab M-file [34]. Mass spectra were corrected for naturally occurring isotopes [35] and for potential metabolite contamination in a blank extraction. All labeling fractions were transformed to a natural abundance corrected mass distribution vector (MDV) [36]. Metabolite levels were determined based on the internal standards norvaline and glutarate, and protein content determined with Pierce™ BCA Protein Assay Kit (Thermo Fisher Scientific) to normalize metabolomics data.

ENGRO metabolic network reconstruction

A metabolic network designed to evaluate the contribution of glucose and glutamine to biomass formation was extracted from the HMR [37] and Recon 2 [38] databases and manually curated. It includes central metabolic pathways and the connected production of building blocks for lipids and protein biosynthesis, together accounting for 80% of the dry cellular biomass [38]. To streamline the analysis of ENGRO emergent properties, unless strictly required by reaction thermodynamics, all metabolites are assumed in the same compartment and linear pathways are lumped into a single reaction. The obtained model is structurally free from thermodynamically infeasible loops, which is a major problem in genome-wide models [39].

Flux Balance Analysis (FBA)

FBA requires a stoichiometric matrix *S* and a set of constraints that impose the upper and lower bound of fluxes. The steady state constraint is defined by the equation $dx/dt = S \cdot v = 0$, where dx/dt are time derivatives of metabolite concentrations represented by the product of the *m*×*n* matrix *S* times the vector of fluxes $v = (v_1, v_2, \dots, v_n)$, where v_i is the flux of reaction *i*, *n* is the number of reactions, and *m* is the number of metabolites. The ensemble of functional states that the system can reach given a boundary condition *I* determines the *feasible solutions space* $\Phi = \Sigma \cap I$. By exploiting linear programming, FBA allows for optimization of

the flux through a weighted sum of fluxes. In particular, the COBRA Toolbox [40] and the GLPK solver were used.

References

1. Mizock BA (2010) Immunonutrition and critical illness: an update. Nutrition 26: 701-707.
2. Lacey JM, Wilmore DW (1990) Is glutamine a conditionally essential amino acid? Nutrition reviews 48: 297-309.
3. Yuneva M, Zamboni N, Oefner P, Sachidanandam R, Lazebnik Y (2007) Deficiency in glutamine but not glucose induces MYC-dependent apoptosis in human cells. The Journal of cell biology 178: 93-105.
4. Altman BJ, Stine ZE, Dang CV (2016) From Krebs to clinic: glutamine metabolism to cancer therapy. Nature reviews Cancer 16: 619-634.
5. Meng M, Chen S, Lao T, Liang D, Sang N (2010) Nitrogen anabolism underlies the importance of glutaminolysis in proliferating cells. Cell cycle 9: 3921-3932.
6. Mullen et al. 2012 Reductive carboxylation supports growth in tumors with defective mitochondria. Nature 481(7381): 385–388
7. Cohen A, Hall MN (2009) An amino acid shuffle activates mTORC1. Cell 136: 399-400.
8. Nicklin P, Bergman P, Zhang B, Triantafellow E, Wang H, et al. (2009) Bidirectional transport of amino acids regulates mTOR and autophagy. Cell 136: 521-534.
9. Duran RV, Oppliger W, Robitaille AM, Heiserich L, Skendaj R, et al. (2012) Glutaminolysis activates Rag-mTORC1 signaling. Molecular cell 47: 349-358.
10. Magnuson B, Ekim B, Fingar DC (2012) Regulation and function of ribosomal protein S6 kinase (S6K) within mTOR signalling networks. Biochemical Journal 441 (1): 1–21.
11. Zheng L, Zhang W, Zhou Y, Li F, Wei H, et al. (2016) Recent Advances in Understanding Amino Acid Sensing Mechanisms that Regulate mTORC1. International journal of molecular sciences 17.
12. Sacco E, Metalli D, Spinelli M, Manzoni R, Samalikova M, et al. (2012) Novel RasGRF1-derived Tat-fused peptides inhibiting Ras-dependent proliferation and migration in mouse and human cancer cells. Biotechnology advances 30: 233-243.
13. Bossu P, Vanoni M, Wanke V, Cesaroni MP, Tropea F, et al. (2000) A dominant negative RAS-specific guanine nucleotide exchange factor reverses neoplastic phenotype in K-ras transformed mouse fibroblasts. Oncogene 19: 2147-2154.
14. Chiaradonna F, Sacco E, Manzoni R, Giorgio M, Vanoni M, et al. (2006) Ras-dependent carbon metabolism and transformation in mouse fibroblasts. Oncogene 25: 5391-5404.
15. Gaglio D, Soldati C, Vanoni M, Alberghina L, Chiaradonna F (2009) Glutamine deprivation induces abortive s-phase rescued by deoxyribonucleotides in k-ras transformed fibroblasts. PloS one 4: e4715.
16. Eagle H, Oyama VI, Levy M, Horton CL, Fleischman R (1956) The growth response of mammalian cells in tissue culture to L-glutamine and L-glutamic acid. The Journal of biological chemistry 218: 607-616.
17. Tardito S, Oudin A, Ahmed SU, Fack F, Keunen O, et al. (2015) Glutamine synthetase activity fuels nucleotide biosynthesis and supports growth of glutamine-restricted glioblastoma. Nature cell biology 17: 1556-1568.
18. Gaglio D, Valtorta S, Ripamonti M, Bonanomi M, Damiani C, et al. (2016) Divergent in vitro/in vivo responses to drug treatments of highly aggressive NIH-Ras cancer cells: a PET imaging and metabolomics-mass-spectrometry study. Oncotarget.
19. Son J, Lyssiotis CA, Ying H, Wang X, Hua S, et al. (2013) Glutamine supports pancreatic cancer growth through a KRAS-regulated metabolic pathway. Nature 496: 101-105.

20. Lu SC (2009) Regulation of glutathione synthesis. Molecular aspects of medicine 30: 42-59.
21. Gaglio D, Metallo CM, Gameiro PA, Hiller K, Danna LS, et al. (2011) Oncogenic K-Ras decouples glucose and glutamine metabolism to support cancer cell growth. Molecular systems biology 7: 523.
22. Damiani C, Colombo R, Gaglio D, Mastroianni F, Pescini D, et al. (2017) The WarburQ effect: glutamine-dependent lactate production allows optimal growth of Complex I compromised tumor cells. Submitted.
23. Rahman I, Kode A, Biswas SK (2006) Assay for quantitative determination of glutathione and glutathione disulfide levels using enzymatic recycling method. Nature protocols 1: 3159-3165.
24. Csibi A, Fendt SM, Li C, Poulogiannis G, Choo AY, et al. (2013) The mTORC1 pathway stimulates glutamine metabolism and cell proliferation by repressing SIRT4. Cell 153: 840-854.
25. Duvel K, Yecies JL, Menon S, Raman P, Lipovsky AI, et al. (2010) Activation of a metabolic gene regulatory network downstream of mTOR complex 1. Molecular cell 39: 171-183.
26. Peterson TR, Sengupta SS, Harris TE, Carmack AE, Kang SA, et al. (2011) mTOR complex 1 regulates lipin 1 localization to control the SREBP pathway. Cell 146: 408-420.26.
27. Alberghina L and Gaglio D (2014) Redox control of glutamine utilization in cancer. Cell Death and Disease 5,e1561.
28. Bradford MM (1976) A rapid and sensitive method for the quantitation of microgram quantities of protein utilizing the principle of protein-dye binding. Analytical biochemistry 72: 248-254.
29. Taylor SJ, Shalloway D (1996) Cell cycle-dependent activation of Ras. Current biology : CB 6: 1621-1627.
30. Patil KR, Nielsen J (2005) Uncovering transcriptional regulation of metabolism by using metabolic network topology. Proceedings of the National Academy of Sciences of the United States of America 102: 2685-2689.
31. Swainston N, Smallbone K, Hefzi H, Dobson PD, Brewer J, et al. (2016) Recon 2.2: from reconstruction to model of human metabolism. Metabolomics : Official journal of the Metabolomic Society 12: 109.
32. Musharraf SG, Mazhar S, Choudhary MI, Rizi N, Atta ur R (2015) Plasma metabolite profiling and chemometric analyses of lung cancer along with three controls through gas chromatography-mass spectrometry. Scientific reports 5: 8607.
33. Fendt SM, Bell EL, Keibler MA, Davidson SM, Wirth GJ, et al. (2013) Metformin decreases glucose oxidation and increases the dependency of prostate cancer cells on reductive glutamine metabolism. Cancer research 73: 4429-4438.
34. Young JD, Walther JL, Antoniewicz MR, Yoo H, Stephanopoulos G (2008) An elementary metabolite unit (EMU) based method of isotopically nonstationary flux analysis. Biotechnology and bioengineering 99: 686-699.
35. Fernandez CA, Des Rosiers C, Previs SF, David F, Brunengraber H (1996) Correction of 13C mass isotopomer distributions for natural stable isotope abundance. Journal of mass spectrometry : JMS 31: 255-262.
36. Buescher JM, Antoniewicz MR, Boros LG, Burgess SC, Brunengraber H, et al. (2015) A roadmap for interpreting (13)C metabolite labeling patterns from cells. Current opinion in biotechnology 34: 189-201.
37. Mardinoglu A, Agren R, Kampf C, Asplund A, Nookaew I, et al. (2013) Integration of clinical data with a genome-scale metabolic model of the human adipocyte. Mol Syst Biol 9: 649.

38. Thiele I, Swainston N, Fleming RM, Hoppe A, Sahoo S, et al. (2013) A community-driven global reconstruction of human metabolism. Nat Biotechnol 31: 419-425.
39. De Martino D, Capuani F, Mori M, De Martino A, Marinari E (2013) Counting and correcting thermodynamically infeasible flux cycles in genome-scale metabolic networks. Metabolites 3: 946-966.
40. Schellenberger J, Que R, Fleming RM, Thiele I, Orth JD, et al. (2011) Quantitative prediction of cellular metabolism with constraint-based models: the COBRA Toolbox v2.0. Nat Protoc 6: 1290-1307.

4. GENERAL DISCUSSION

Compared to normal cells, transformed cells have the ability to continuously proliferate and thus to expand to become tumors. Tumor metabolism is significantly altered to accommodate for the increased metabolic needs for energy generation (bioenergetic) and macromolecule synthesis (biosynthetic) necessary for oncogenic transformation. The Warburg Effect is a central feature of tumor metabolism that consists in the preferential use of glucose and glycolysis for energy generation [235,236,237,238]. The generated lactate contributes to the prominent lactic acidosis in most solid tumors. The causes and functional consequences of this increased glucose uptake and utilization are the subject of many studies. However, glucose deprivation is common in solid tumors, and the extracellular acidosis further restricts the glucose uptake and glycolysis [239,240]. Therefore, recent research efforts have found that, beside glucose, tumor cells also rely on a wide variety of *alternative fuels* to provide various metabolic needs. The consumption and utilization of these alternative fuels are affected by different oncogenic signaling events and/or tumor microenvironmental stresses. The reliance of tumor cells on alternative fuels may present tumor-specific metabolic fragilities, and thus, meaningful therapeutic windows to eradicate tumor cells. Targeting essential tumor metabolism may be particularly interesting for the tumors that have developed resistance to chemotherapeutics or

targeting agents. Indeed, improved understanding of cancer nutrient addictions may allow to better target these metabolic dependencies.

Most mammalian cells have efficient ways to cope with, and therefore survive, nutrient deprivation in their external environments that occurs during pathological adaptations or therapeutic intervention. The success of these mechanisms allows cells to survive nutrient deprivation and preserve the capacity to resume proliferation after the resolution of the metabolic stresses. Thus, addiction to alternative nutrients, as measured by cell death upon deprivation, will only manifest when these adaptive mechanisms fail or are inadequate. During nutrient starvation, cells can resort to autophagy (self-eating) to generate amino acids, lipids and other nutrients by degrading existing macromolecules [241]. In addition, mammalian cells can trigger highly conserved signaling mechanisms in response to nutrient deprivation and other metabolic stresses to control protein translation and transcriptional responses. One of these mechanisms is via mammalian target of rapamycin (mTOR), a conserved Ser/Thr kinase (a part of the mTOR complexes), to regulate cell growth and autophagy. The importance of nutrient sensing and adaptive pathways in cancer biology is clear when considering the high number of tumor suppressors and oncogenes in these pathways that are oncogenic drivers. Employing these nutrient sensing pathways allows many cells (but not all) to adapt to and survive nutrient limitations in their environments.

Generally, alternative fuels become indispensable for cancer-specific nutrient dependencies through several underlying mechanism. First, the enhanced proliferation of tumor cells increases the demands on the quantity of building blocks necessary to synthesize the macromolecules needed for cell growth. Additionally, cancer cells may also require nutrients to maintain pro-growth gene expression programs and redox homeostasis. Second, many mechanisms of oncogenic transformation alter the expression or activities of enzymes critical for the metabolism of essential nutrients. Third, the expression of rate-limiting enzymes themselves may be transcriptionally regulated or affected by the DNA amplifications or deletions that become selected for during cancer progression as they provide survival advantage. Fourth, tumor cells are often exposed to different tumor microenvironmental stresses, including hypoxia, lactic acidosis and glucose deprivation, which further restrict the nutrients and fuels available to the tumor cells. Fifth, tumor cells have different cellular origins and may retain some of the metabolic properties of the original cells that are associated with a particular differentiation program or environmental *milieu*. All of these different factors may contribute to the particular nutrient addictions and metabolic vulnerabilities that different cancer cells develop [242].

Glutamine is the most abundant amino acid in plasma and plays a unique role in the metabolism of proliferating cells. However, the essential role of glutamine in cancer metabolism was not well understood until recent

studies employed modern biochemical and genetic tools. It is now clear that glutamine plays several important metabolic roles, including as a carbon source for energy production, a nitrogen source for biosynthetic reactions, a regulator of lipid generation and a maintainer of redox homeostasis. Glutamine availability and metabolism also tightly intersect with oncogenic mutations and transduction pathways involved in oncogenesis. Therefore, glutamine metabolism is a particularly attractive therapeutic target for the significant number of tumors that appear to be addicted to this nutrient [126,142].

One of the most important metabolic needs of proliferating tumor cells is the biosynthesis of macromolecules for cell division. To support lipid biosynthesis from acetyl-CoA, citrate is exported out of the mitochondria to generate acetyl-CoA in the cytoplasm. As this depletes TCA cycle intermediate metabolites, an additional carbon source is required to replenish the TCA cycle, and this occurs in the process of *anaplerosis*. In most proliferating cells, glutamine serves as an important anaplerotic substrate to generate oxaloacetate that will combine with acetyl-CoA to replenish citrate. Consequently, for many of the cancer cells that are glutamine-addicted, it has a critical role as a carbon source to feed anaplerotic reactions. Additionally, under hypoxia or with mitochondrial dysfunction, glutamine can directly supply the acetyl-CoA needed for lipogenesis by being converted into α-ketoglutarate that can undergo reductive carboxylation to generate isocitrate, which is then converted

into citrate [102,106]. Therefore, the direction of metabolic flux and utilization of glutamine can vary among different tumors with distinct somatic mutations and degrees of hypoxia.

The amido and amino groups of glutamine contribute to the nucleotide synthesis, especially during proliferation. For instance, the cell cycle arrest of K-ras transformed fibroblasts caused by glutamine deprivation could be rescued by addition of deoxyribonucleotides [243]. Interestingly, the expression of glutaminase 1 (GLS1), that encodes the critical enzyme for glutaminolysis into glutamate, is tightly regulated within the cell cycle [244]. The coupling between the degree of glutaminolysis and DNA synthesis likely contributes to glutamine role in supporting DNA synthesis and cell proliferation.

Glutamine can also modulate cellular signaling pathways, including redox homeostasis [245]. Glutamine metabolism is crucial in the synthesis of glutathione (GSH), an endogenous antioxidant constituted by glutamate, cysteine and glycine. High endogenous levels of glutathione render it the predominant cellular anti-oxidant that scavenges reactive oxygen species by donating electrons and becoming oxidized (GSSG). The regeneration of GSH from GSSG requires NADPH, which can be produced by glutamine metabolism through malic enzyme. In addition, glutamine also increases the NADPH/$NADP^+$ ratio and maintains the GSH levels and cellular redox state by being converted to pyruvate [103]. Thus, glutamine metabolism is essential to maintain the GSH level and redox homeostasis.

In addition to glutamine, a wide variety of studies and systems have indicated that amino acid addiction is a common phenomenon of cancer cells that changes significantly among different normal and transformed cells. Exogenous cysteine is essential for several cancer types (glioma [183], prostate [184] and pancreatic [179]), as blocking uptake through the cystine/glutamate antiporter (system Xc^-) reduces viability due to the cell death caused by uncontrolled oxidative stresses [246,247]. Methionine is also essential for maintaining levels of S-Adenosyl methionine (SAM), which is critical for subsequent histone methylation, especially tri-methylation of histone H3 lysine-4 (H3K4me3). Given the potential involvement of HeK4me3 and H3K4 demethylase JARID1B upregulation in prostate cancer [248], methionine restriction may affect the epigenetic landscape and oncogenesis of tumor cells driven by these epigenetic features [157,249].

Cancer cells are highly versatile in obtaining nutrients from the extracellular environment to satisfy their metabolic needs. With the limited availability of glucose, tumor cells resort to the use of various amino acids and other nutrients as alternative fuels to support their continuous survival and proliferation. There is extensive crosstalk and reciprocal metabolite flow between these alternative fuels and the sensing and metabolic pathways of glucose metabolism [250]. The importance of these pathways can be demonstrated by the DNA amplifications or significant up-regulation of many genes involved in the

metabolic adaptations under stresses [251,252]. The huge flexibility in the nutrients that cancer cells are able to successfully metabolize likely reflects both the metabolic demands necessary to support oncogenesis and the survival advantage for cells that have developed the abilities to use such nutrients.

Second, these alternative fuels supply many aspects of tumor biology beyond the bioenergetic and biosynthetic needs. Methionine may be important for the levels of SAM and the proper pattern of histone and DNA methylation. Both glutamine and cysteine are essential for the generation of GSH and maintenance of redox homeostasis. These results indicate an extensive and intricate involvement of metabolic flux into many aspects of tumor biology, which were not previously thought to be fueled by metabolic needs. Thus, the approach of nutrient deprivation, by removing one nutrient at a time, may be applied to a large number of cancer cells with genetic information to uncover, on a systemic level, the linkage of particular oncogenic events with nutrient addictions.

By understanding how oncogenic mutations regulate the uptake and metabolism of the alternative fuels that cancer cells are able to use to support their metabolic needs, we may be able to identify therapeutic targets to eradicate tumors via their metabolic fragilities.

In this regards, mathematical modeling and computational methods have become an indispensable mean to achieve a full understanding of the functioning and to identify the design principles of complex systems.

Interaction-based models and, particularly, constraint-based models are the most widely used for the study of metabolism, although they neglect most of the quantitative and kinetic information.

In order for a model to be useful to experimental biologists, it must be strongly linked with biological data and *ad hoc* experimental measurements during the computational phases of model construction and validation. In Systems Biology, the interaction between experimental biologists and modelers is indeed necessary to understand each other's requirements and to take advantage of the respective expertise. Experimental biologists have to design appropriate laboratory experiments, while modelers should develop appropriate modeling strategies and simulation tools. This interplay is then expected to increase the efficacy and broaden the scope of mathematical models in the study of metabolism, and increase our knowledge of cancer metabolism and its regulatory properties.

5. SUPPLEMENTARY INFORMATION

5.1 Stable isotope tracers to study cancer cell metabolism: assessing utilization of glutamine as an example

As previously explained, to date large-scale analyses of cancer cells include metabolomics and fluxomics, with the aim of understanding posttranscriptional modifications [253,254,255]. Compared to metabolomics, that enables the study of metabolism at the system level through the measurement of metabolite concentrations, fluxomics allows to better characterize metabolic routes through the measurement of fluxes, which describe the actual functionality of an enzyme or pathway [256,257]. Thus, intracellular fluxes for a given system are quantitatively estimated through isotopic tracers and computational algorithms [258,259], being such methods effectively applied to mammalian cells [85,260].

Stable isotope labeling offers a direct readout of intracellular metabolism and can be combined with the known stoichiometry of biochemical pathways to quantify the activity of corresponding enzyme fluxes [261]. Here are described the steps to perform the analysis.

a) Choice of tracer

In isotopic labeling studies, the choice of tracer determines the range of possible labeling metabolite patterns, strongly affecting the observability

and the accuracy of the estimated intracellular fluxes. Usually, [U-$^{13}C_5$] glutamine allows a good evaluation of the total contribution of glutamine in the TCA cycle and lipogenesis [262], while partially labeled glutamine tracers such as [1-^{13}C] and [5-^{13}C]-glutamine are useful to estimate the fraction of glutamine that flows through RC [111].

b) Cell culture

Cell culture is usually performed with commercially available media formulations, such as Dulbecco's modified Eagle medium (DMEM). In stable isotope tracer experiments, special basal media without glucose, glutamine, and/or any other substrate of interest are used, allowing the use of specific ^{13}C-labeled tracer (usually glucose or glutamine). As the culture medium is supplemented with 10% serum (e.g. NCS), which contains many unspecified molecules that may dilute ^{13}C-labeling of intracellular metabolites and interfere in cellular metabolism, in tracer experiments normal serum is replaced by dialyzed serum (typical cut-off: 10000 Da).

c) Measuring extracellular glutamine and glutamate

As mentioned before, different cancer cell lines have distinct patterns of glutamine metabolism and are either glutamine-dependent or -independent. Measuring consumption of glutamine gives an indication of its total use by cells. The concentration of glutamine and glutamate can be measured by numerous ways, among which are enzymatic assay [263],

high-performance liquid chromatography [264] and mass spectrometry-based methods like GC- or LC-MS [265,266]. The YSI Bioanalytical System (YSI Life Science) uses immobilized enzymes to catalyze the corresponding chemical reactions to measure glutamine and glutamate. The analysis is carried out on cells in exponential growth phase and when the culture has reached its metabolic steady state, i.e. all intra- and extracellular fluxes are constant. Then, the specific growth rate, specific uptake rate of glutamine and specific production rate of ammonium can be determined [267].

d) Extraction of intracellular metabolites

While extracellular metabolite measurements only provide information on those metabolites that are consumed or secreted, intracellular metabolite concentrations contain more information on the state of cellular metabolism. However, most intracellular metabolites cannot cross the cell membrane, making necessary the lysis of the cells to release the metabolites. Moreover, due to the differences in the level of polarity among metabolites, it is necessary to apply both polar and nonpolar solvents to extract metabolites after cell lysis. Finally, in the process of cell lysis and metabolite extraction, cells experience highly harsh conditions and the metabolic steady state may be strongly perturbed; therefore, an effective quenching procedure is of utmost importance to rapidly stop all enzymatic activities so that concentration of metabolites is not significantly altered.

e) GC-MS analysis of intracellular metabolites

GC-MS is largely used for the analysis of ^{13}C-labeled intracellular metabolites [268], which are chemically derivatized for better volatility in GC separation and analyzed by electron impact ionization in MS.

Each set of metabolite mass fragments generates ion chromatograms that are integrated to give the resulting mass isotopomer distribution (MID) [269]. The MID is characterized as the fractional abundance of mass isotopomers defined by M0, M1 to Mn. Particularly, M is the base mass of an ion fragment while the following number from 0 to *n* (active carbon number) indicates the mass shift from M. To account for the contribution in the labeling of a metabolite that is derived from only the ^{13}C atoms from ^{13}C isotopic tracers, MIDs need to be corrected for natural isotope abundances [270]. Intracellular metabolites can be identified by searching against libraries of the metabolite's retention time (using the specific GC program) and its characteristic fragmentation pattern.

5.2 Drugs or compounds targeting metabolism under clinical trial or approved by the US Food And Drug Administration (FDA) [271]

Pathways	Target Proteins/Enzymes or Metabolites	Drugs/Compounds	Cancer/Tumor Type	Clinical Trial Status
Signalling proteins and transcription factors				
	mTORC1	Temsirolimus and Everolimus	Metastatic/non-metastatic solid tumors	US FDA approved
		Ridaforolimus and other rapalogues	Pancreatic, endometrial and glioblastoma; lymphoma.	Phase I/II
	mTORC1 and mTORC2	Torin1 and PP242	-	Preclinical
	HIF1α	PX-478	Advanced solid tumor and lymphoma	Phase I
		Acriflavine	-	Preclinical
	Hypoxia	Tirapazamine and other bioreductive compounds	Cervical, SCLC, NSCLC	Phase III
	Hypoxia, VEGF and VEGFR	Bevacizumab	Malignant glioma, NSCLC, ovarian and colorectal	US FDA approved
	IGF1R	Dalotuzumab (MK-0646), BIIB022, AVE1642 *etc.*	Solid tumors of NSCLC, pancreatic, hepatocellular carcinoma (HCC) and metastatic breast cancer	Phase I/II
	PI3K and mTOR	BEZ235, XL765, SF1126 and BGT226	Malignant glioma and NSCLC	Phase I/II
	PI3K	GDC-0941 and PX866	Metastatic breast cancer and non-Hodgkin's lymphoma	Phase I
	AKT	Perifosine and GSK690693	Renal cancer, NSCLC and lymphoma	Phase I/II
	AMPK and Complex I (mitochondrial)	Metformin	Solid tumors and lymphoma	US FDA approved
Metabolic pathway enzymes				
Nucleotide biosynthesis pathway	DNA and RNA synthesis	5-FU, cytarabine and methotrexate	Different types of tumors	US FDA approved
	DNA synthesis	Folate, choline, methionine,		Lab studies
	Methyltransferases	Betaine, selected B vitamins, Flavonoids, EGCG, genistein		Lab studies
	Histone deacetylases (HDAC)	Butyrate, sulforaphane, Allylmercaptan, 3,3-Diindolylmethane		Lab studies
	Histone acetyltranferase	Anacardic acid, garcinol, Curcumin, EGCG, Genistein		
	Acetylation of non-histone proteins	Butyrate, cambinol, Dihydrocoumarin, genistein		

Pathways	Target Proteins/Enzymes or Metabolites	Drugs/Compounds	Cancer/Tumor Type	Clinical Trial Status
Metabolic pathway enzymes				
Glycolysis pathway	GLUT1	Phloretin	Colon cancer and leukemia	-
	GLUT1	WZB117	Lung cancer and breast cancer	-
	GLUT4	Ritonavir	Multiple myeloma	-
	Hexokinase	2-deoxyglucose (2-DG)	Leukemia, cervical cancer, hepatocarcinoma, breast cancer, small lung cancer, lymphoma and prostate cancer	PhaseI/II
	Hexokinase Hexokinase	Lonidamine (LND)	Benign prostatic hyperplasia, leukemia and lymphoma	Phase III
		3-bromopyruvate (3-BrPA)	Leukemia, multiple myeloma, colon cancer and leukemia	Preclinical
	Pyruvate kinase M2 (PKM2)	shRNA	Lung cancer	-
	Pyruvate kinase (PK)	TLN-232	Metastatic melanoma and renal cell carcinoma	Phase II
	Lactate dehydrogenase (LDHA)	Oxamate	Breast cancer	
Pentose phosphate pathway (PPP)	Glucose-6-phosphate dehydrogenase (G6PDH)	Resveratrol	Colon cancer	
	Transketolase (TK)	Oxythiamine (OT)	Colon cancer	
	G6PDH and TK	Avemar	Jurkat T cells (Leukemia)	
	G6PDH, 6PGDH and Transaldolase TA	Combination of arginine and ascorbic acid	Human hepatoma cell lines (HA2T/VGH)	
	G6PDH, also depletion of ribose-5-phosphate (R-5P)	Dehydroepiandrosterone (DHEA)	Indirect study on polycystic ovary syndrome	
TCA cycle	Pyruvate dehydrogenase kinase (PDK3)	siRNA	Cervical cancer and breast cancer	
	Pyruvate dehydrogenase kinase (PDK1)	Dichloroacetate (DCA)	Fibrosarcoma, colon cnacer, lung cancer, squamous cell carcinoma and prostate cancer	
Fatty acid synthesis	FASN	Cerulenin and C75	Breast cancer	
		Orlistat	Breast and pancreatic cancer	Preclinical
	ATP-citrate lyase	SB-204990	-	Preclinical
Amino acid metabolism pathway	Glutamine	Phenylacetate	Brain tumors	Phase II
	Asparagine	Asparaginase and pegasparaginase	Acute lymphoblastic leukaemia (ALL), T-cell lymphoma (TCL) and B-cell lymphoma (BCL)	Phase II/III
	Arginine	Arginine deiminase	Metastatic melanoma and hepatocellular carcinoma	Phase I/II

REFERENCES

1. DeBerardinis RJ, Lum JJ, Hatzivassiliou G, Thompson CB (2008) The biology of cancer: metabolic reprogramming fuels cell growth and proliferation. Cell metabolism 7: 11-20.
2. wwwcancergov.
3. Hanahan D, Weinberg RA (2000) The hallmarks of cancer. Cell 100: 57-70.
4. Davies MA, Samuels Y (2010) Analysis of the genome to personalize therapy for melanoma. Oncogene 29: 5545-5555.
5. Hynes NE, MacDonald G (2009) ErbB receptors and signaling pathways in cancer. Current opinion in cell biology 21: 177-184.
6. Malumbres M, Barbacid M (2003) RAS oncogenes: the first 30 years. Nature reviews Cancer 3: 459-465.
7. Burkhart DL, Sage J (2008) Cellular mechanisms of tumour suppression by the retinoblastoma gene. Nature reviews Cancer 8: 671-682.
8. Sherr CJ, McCormick F (2002) The RB and p53 pathways in cancer. Cancer cell 2: 103-112.
9. Adams JM, Cory S (2007) Bcl-2-regulated apoptosis: mechanism and therapeutic potential. Current opinion in immunology 19: 488-496.
10. Junttila MR, Evan GI (2009) p53--a Jack of all trades but master of none. Nature reviews Cancer 9: 821-829.
11. Lowe SW, Cepero E, Evan G (2004) Intrinsic tumour suppression. Nature 432: 307-315.
12. Blasco MA (2005) Telomeres and human disease: ageing, cancer and beyond. Nature reviews Genetics 6: 611-622.
13. Ferrara N (2009) Vascular endothelial growth factor. Arteriosclerosis, thrombosis, and vascular biology 29: 789-791.
14. Hanahan D, Folkman J (1996) Patterns and emerging mechanisms of the angiogenic switch during tumorigenesis. Cell 86: 353-364.
15. Talmadge JE, Fidler IJ (2010) AACR centennial series: the biology of cancer metastasis: historical perspective. Cancer research 70: 5649-5669.
16. Berx G, van Roy F (2009) Involvement of members of the cadherin superfamily in cancer. Cold Spring Harbor perspectives in biology 1: a003129.
17. Hanahan D, Weinberg RA (2011) Hallmarks of cancer: the next generation. Cell 144: 646-674.
18. Ward PS, Thompson CB (2012) Metabolic reprogramming: a cancer hallmark even warburg did not anticipate. Cancer cell 21: 297-308.
19. DeBerardinis RJ, Chandel NS (2016) Fundamentals of cancer metabolism. Science advances 2: e1600200.
20. Warburg O, Wind F, Negelein E (1927) The Metabolism of Tumors in the Body. The Journal of general physiology 8: 519-530.
21. Vander Heiden MG, Cantley LC, Thompson CB (2009) Understanding the Warburg effect: the metabolic requirements of cell proliferation. Science 324: 1029-1033.
22. Weinhouse S (1955) Oxidative metabolism of neoplastic tissues. Advances in cancer research 3: 269-325.
23. Weinhouse S (1956) On respiratory impairment in cancer cells. Science 124: 267-269.
24. DeBerardinis RJ, Mancuso A, Daikhin E, Nissim I, Yudkoff M, et al. (2007) Beyond aerobic glycolysis: transformed cells can engage in glutamine metabolism that exceeds the

requirement for protein and nucleotide synthesis. Proceedings of the National Academy of Sciences of the United States of America 104: 19345-19350.
25. Daye D, Wellen KE (2012) Metabolic reprogramming in cancer: unraveling the role of glutamine in tumorigenesis. Seminars in cell & developmental biology 23: 362-369.
26. DeBerardinis RJ, Cheng T (2010) Q's next: the diverse functions of glutamine in metabolism, cell biology and cancer. Oncogene 29: 313-324.
27. Lunt SY, Vander Heiden MG (2011) Aerobic glycolysis: meeting the metabolic requirements of cell proliferation. Annual review of cell and developmental biology 27: 441-464.
28. Wise DR, DeBerardinis RJ, Mancuso A, Sayed N, Zhang XY, et al. (2008) Myc regulates a transcriptional program that stimulates mitochondrial glutaminolysis and leads to glutamine addiction. Proceedings of the National Academy of Sciences of the United States of America 105: 18782-18787.
29. Yuneva M, Zamboni N, Oefner P, Sachidanandam R, Lazebnik Y (2007) Deficiency in glutamine but not glucose induces MYC-dependent apoptosis in human cells. The Journal of cell biology 178: 93-105.
30. Altman BJ, Stine ZE, Dang CV (2016) From Krebs to clinic: glutamine metabolism to cancer therapy. Nature reviews Cancer 16: 619-634.
31. Cantor JR, Sabatini DM (2012) Cancer cell metabolism: one hallmark, many faces. Cancer discovery 2: 881-898.
32. Dibble CC, Manning BD (2013) Signal integration by mTORC1 coordinates nutrient input with biosynthetic output. Nature cell biology 15: 555-564.
33. Yuan TL, Cantley LC (2008) PI3K pathway alterations in cancer: variations on a theme. Oncogene 27: 5497-5510.
34. Stine ZE, Walton ZE, Altman BJ, Hsieh AL, Dang CV (2015) MYC, Metabolism, and Cancer. Cancer discovery 5: 1024-1039.
35. Kruiswijk F, Labuschagne CF, Vousden KH (2015) p53 in survival, death and metabolic health: a lifeguard with a licence to kill. Nature reviews Molecular cell biology 16: 393-405.
36. Jiang L, Kon N, Li T, Wang SJ, Su T, et al. (2015) Ferroptosis as a p53-mediated activity during tumour suppression. Nature 520: 57-62.
37. Li T, Kon N, Jiang L, Tan M, Ludwig T, et al. (2012) Tumor suppression in the absence of p53-mediated cell-cycle arrest, apoptosis, and senescence. Cell 149: 1269-1283.
38. Levine AJ, Puzio-Kuter AM (2010) The control of the metabolic switch in cancers by oncogenes and tumor suppressor genes. Science 330: 1340-1344.
39. Alberghina L, Gaglio D, Gelfi C, Moresco RM, Mauri G, et al. (2012) Cancer cell growth and survival as a system-level property sustained by enhanced glycolysis and mitochondrial metabolic remodeling. Frontiers in physiology 3: 362.
40. Kimmelman AC (2015) Metabolic Dependencies in RAS-Driven Cancers. Clinical cancer research : an official journal of the American Association for Cancer Research 21: 1828-1834.
41. Chiaradonna F, Gaglio D, Vanoni M, Alberghina L (2006) Expression of transforming K-Ras oncogene affects mitochondrial function and morphology in mouse fibroblasts. Biochimica et biophysica acta 1757: 1338-1356.
42. Downward J (2003) Role of receptor tyrosine kinases in G-protein-coupled receptor regulation of Ras: transactivation or parallel pathways? The Biochemical journal 376: e9-10.
43. Kahn S, Yamamoto F, Almoguera C, Winter E, Forrester K, et al. (1987) The c-K-ras gene and human cancer (review). Anticancer research 7: 639-652.
44. Schubbert S, Shannon K, Bollag G (2007) Hyperactive Ras in developmental disorders and cancer. Nature reviews Cancer 7: 295-308.

45. Sever R, Brugge JS (2015) Signal transduction in cancer. Cold Spring Harbor perspectives in medicine 5.
46. Forbes SA, Bindal N, Bamford S, Cole C, Kok CY, et al. (2011) COSMIC: mining complete cancer genomes in the Catalogue of Somatic Mutations in Cancer. Nucleic acids research 39: D945-950.
47. Fernandez-Medarde A, Santos E (2011) Ras in cancer and developmental diseases. Genes & cancer 2: 344-358.
48. Takashima A, Faller DV (2013) Targeting the RAS oncogene. Expert opinion on therapeutic targets 17: 507-531.
49. Adjei AA, Cohen RB, Franklin W, Morris C, Wilson D, et al. (2008) Phase I pharmacokinetic and pharmacodynamic study of the oral, small-molecule mitogen-activated protein kinase kinase 1/2 inhibitor AZD6244 (ARRY-142886) in patients with advanced cancers. Journal of clinical oncology : official journal of the American Society of Clinical Oncology 26: 2139-2146.
50. Sacco E, Spinelli M, Vanoni M (2012) Approaches to Ras signaling modulation and treatment of Ras-dependent disorders: a patent review (2007--present). Expert opinion on therapeutic patents 22: 1263-1287.
51. McCormick F (2015) KRAS as a Therapeutic Target. Clinical cancer research : an official journal of the American Association for Cancer Research 21: 1797-1801.
52. Shima F, Matsumoto S, Yoshikawa Y, Kawamura T, Isa M, et al. (2015) Current status of the development of Ras inhibitors. Journal of biochemistry 158: 91-99.
53. Singh H, Longo DL, Chabner BA (2015) Improving Prospects for Targeting RAS. Journal of clinical oncology : official journal of the American Society of Clinical Oncology 33: 3650-3659.
54. Sacco E, Fantinato S, Manzoni R, Metalli D, De Gioia L, et al. (2005) The isolated catalytic hairpin of the Ras-specific guanine nucleotide exchange factor Cdc25Mm retains nucleotide dissociation activity but has impaired nucleotide exchange activity. FEBS letters 579: 6851-6858.
55. Pylayeva-Gupta Y, Grabocka E, Bar-Sagi D (2011) RAS oncogenes: weaving a tumorigenic web. Nature reviews Cancer 11: 761-774.
56. Berndt N, Hamilton AD, Sebti SM (2011) Targeting protein prenylation for cancer therapy. Nature reviews Cancer 11: 775-791.
57. Scheffzek K, Ahmadian MR, Kabsch W, Wiesmuller L, Lautwein A, et al. (1997) The Ras-RasGAP complex: structural basis for GTPase activation and its loss in oncogenic Ras mutants. Science 277: 333-338.
58. Blum R, Jacob-Hirsch J, Amariglio N, Rechavi G, Kloog Y (2005) Ras inhibition in glioblastoma down-regulates hypoxia-inducible factor-1alpha, causing glycolysis shutdown and cell death. Cancer research 65: 999-1006.
59. Chun SY, Johnson C, Washburn JG, Cruz-Correa MR, Dang DT, et al. (2010) Oncogenic KRAS modulates mitochondrial metabolism in human colon cancer cells by inducing HIF-1alpha and HIF-2alpha target genes. Molecular cancer 9: 293.
60. Kikuchi H, Pino MS, Zeng M, Shirasawa S, Chung DC (2009) Oncogenic KRAS and BRAF differentially regulate hypoxia-inducible factor-1alpha and -2alpha in colon cancer. Cancer research 69: 8499-8506.
61. Barata JT, Silva A, Brandao JG, Nadler LM, Cardoso AA, et al. (2004) Activation of PI3K is indispensable for interleukin 7-mediated viability, proliferation, glucose use, and growth of T cell acute lymphoblastic leukemia cells. The Journal of experimental medicine 200: 659-669.

62. Edinger AL, Thompson CB (2002) Akt maintains cell size and survival by increasing mTOR-dependent nutrient uptake. Molecular biology of the cell 13: 2276-2288.
63. Roos S, Jansson N, Palmberg I, Saljo K, Powell TL, et al. (2007) Mammalian target of rapamycin in the human placenta regulates leucine transport and is down-regulated in restricted fetal growth. The Journal of physiology 582: 449-459.
64. Wieman HL, Wofford JA, Rathmell JC (2007) Cytokine stimulation promotes glucose uptake via phosphatidylinositol-3 kinase/Akt regulation of Glut1 activity and trafficking. Molecular biology of the cell 18: 1437-1446.
65. Warburg O (1956) On the origin of cancer cells. Science 123: 309-314.
66. Hsu PP, Sabatini DM (2008) Cancer cell metabolism: Warburg and beyond. Cell 134: 703-707.
67. Ying H, Kimmelman AC, Lyssiotis CA, Hua S, Chu GC, et al. (2012) Oncogenic Kras maintains pancreatic tumors through regulation of anabolic glucose metabolism. Cell 149: 656-670.
68. Weinberg F, Hamanaka R, Wheaton WW, Weinberg S, Joseph J, et al. (2010) Mitochondrial metabolism and ROS generation are essential for Kras-mediated tumorigenicity. Proceedings of the National Academy of Sciences of the United States of America 107: 8788-8793.
69. Baracca A, Chiaradonna F, Sgarbi G, Solaini G, Alberghina L, et al. (2010) Mitochondrial Complex I decrease is responsible for bioenergetic dysfunction in K-ras transformed cells. Biochimica et biophysica acta 1797: 314-323.
70. Nathan C, Cunningham-Bussel A (2013) Beyond oxidative stress: an immunologist's guide to reactive oxygen species. Nature reviews Immunology 13: 349-361.
71. Perry G, Raina AK, Nunomura A, Wataya T, Sayre LM, et al. (2000) How important is oxidative damage? Lessons from Alzheimer's disease. Free radical biology & medicine 28: 831-834.
72. Boonstra J, Post JA (2004) Molecular events associated with reactive oxygen species and cell cycle progression in mammalian cells. Gene 337: 1-13.
73. Sosa V, Moline T, Somoza R, Paciucci R, Kondoh H, et al. (2013) Oxidative stress and cancer: an overview. Ageing research reviews 12: 376-390.
74. Cairns RA, Harris IS, Mak TW (2011) Regulation of cancer cell metabolism. Nature reviews Cancer 11: 85-95.
75. Liou GY, Storz P (2010) Reactive oxygen species in cancer. Free radical research 44: 479-496.
76. Kawanishi S, Hiraku Y, Pinlaor S, Ma N (2006) Oxidative and nitrative DNA damage in animals and patients with inflammatory diseases in relation to inflammation-related carcinogenesis. Biological chemistry 387: 365-372.
77. Trachootham D, Alexandre J, Huang P (2009) Targeting cancer cells by ROS-mediated mechanisms: a radical therapeutic approach? Nature reviews Drug discovery 8: 579-591.
78. Brown NS, Bicknell R (2001) Hypoxia and oxidative stress in breast cancer. Oxidative stress: its effects on the growth, metastatic potential and response to therapy of breast cancer. Breast cancer research : BCR 3: 323-327.
79. Kang DH (2002) Oxidative stress, DNA damage, and breast cancer. AACN clinical issues 13: 540-549.
80. Portakal O, Ozkaya O, Erden Inal M, Bozan B, Kosan M, et al. (2000) Coenzyme Q10 concentrations and antioxidant status in tissues of breast cancer patients. Clinical biochemistry 33: 279-284.
81. Trachootham D, Zhou Y, Zhang H, Demizu Y, Chen Z, et al. (2006) Selective killing of oncogenically transformed cells through a ROS-mediated mechanism by beta-phenylethyl isothiocyanate. Cancer cell 10: 241-252.

82. Irani K, Xia Y, Zweier JL, Sollott SJ, Der CJ, et al. (1997) Mitogenic signaling mediated by oxidants in Ras-transformed fibroblasts. Science 275: 1649-1652.
83. Cook JA, Gius D, Wink DA, Krishna MC, Russo A, et al. (2004) Oxidative stress, redox, and the tumor microenvironment. Seminars in radiation oncology 14: 259-266.
84. Young TW, Mei FC, Yang G, Thompson-Lanza JA, Liu J, et al. (2004) Activation of antioxidant pathways in ras-mediated oncogenic transformation of human surface ovarian epithelial cells revealed by functional proteomics and mass spectrometry. Cancer research 64: 4577-4584.
85. Vizan P, Boros LG, Figueras A, Capella G, Mangues R, et al. (2005) K-ras codon-specific mutations produce distinctive metabolic phenotypes in NIH3T3 mice [corrected] fibroblasts. Cancer research 65: 5512-5515.
86. de Atauri P, Benito A, Vizan P, Zanuy M, Mangues R, et al. (2011) Carbon metabolism and the sign of control coefficients in metabolic adaptations underlying K-ras transformation. Biochimica et biophysica acta 1807: 746-754.
87. Mitsuishi Y, Motohashi H, Yamamoto M (2012) The Keap1-Nrf2 system in cancers: stress response and anabolic metabolism. Frontiers in oncology 2: 200.
88. Kim YR, Oh JE, Kim MS, Kang MR, Park SW, et al. (2010) Oncogenic NRF2 mutations in squamous cell carcinomas of oesophagus and skin. The Journal of pathology 220: 446-451.
89. Singh A, Misra V, Thimmulappa RK, Lee H, Ames S, et al. (2006) Dysfunctional KEAP1-NRF2 interaction in non-small-cell lung cancer. PLoS medicine 3: e420.
90. Solis LM, Behrens C, Dong W, Suraokar M, Ozburn NC, et al. (2010) Nrf2 and Keap1 abnormalities in non-small cell lung carcinoma and association with clinicopathologic features. Clinical cancer research : an official journal of the American Association for Cancer Research 16: 3743-3753.
91. Tsai J, Lee JT, Wang W, Zhang J, Cho H, et al. (2008) Discovery of a selective inhibitor of oncogenic B-Raf kinase with potent antimelanoma activity. Proceedings of the National Academy of Sciences of the United States of America 105: 3041-3046.
92. Ganan-Gomez I, Wei Y, Yang H, Boyano-Adanez MC, Garcia-Manero G (2013) Oncogenic functions of the transcription factor Nrf2. Free radical biology & medicine 65: 750-764.
93. DeNicola GM, Karreth FA, Humpton TJ, Gopinathan A, Wei C, et al. (2011) Oncogene-induced Nrf2 transcription promotes ROS detoxification and tumorigenesis. Nature 475: 106-109.
94. Mitsuishi Y, Taguchi K, Kawatani Y, Shibata T, Nukiwa T, et al. (2012) Nrf2 redirects glucose and glutamine into anabolic pathways in metabolic reprogramming. Cancer cell 22: 66-79.
95. Brosnan JT (2003) Interorgan amino acid transport and its regulation. The Journal of nutrition 133: 2068S-2072S.
96. Eagle H (1955) Nutrition needs of mammalian cells in tissue culture. Science 122: 501-514.
97. Kovacevic Z (1971) The pathway of glutamine and glutamate oxidation in isolated mitochondria from mammalian cells. The Biochemical journal 125: 757-763.
98. Frieden C (1963) Glutamate Dehydrogenase. V. The Relation of Enzyme Structure to the Catalytic Function. The Journal of biological chemistry 238: 3286-3299.
99. Voet D (1995) Biochemistry. John Wiley & Sons, Inc.
100. Young VR, Ajami AM (2001) Glutamine: the emperor or his clothes? The Journal of nutrition 131: 2449S-2459S; discussion 2486S-2447S.
101. Gaglio D, Metallo CM, Gameiro PA, Hiller K, Danna LS, et al. (2011) Oncogenic K-Ras decouples glucose and glutamine metabolism to support cancer cell growth. Molecular systems biology 7: 523.

102. Metallo CM, Gameiro PA, Bell EL, Mattaini KR, Yang J, et al. (2012) Reductive glutamine metabolism by IDH1 mediates lipogenesis under hypoxia. Nature 481: 380-384.
103. Son J, Lyssiotis CA, Ying H, Wang X, Hua S, et al. (2013) Glutamine supports pancreatic cancer growth through a KRAS-regulated metabolic pathway. Nature 496: 101-105.
104. Fendt SM, Bell EL, Keibler MA, Olenchock BA, Mayers JR, et al. (2013) Reductive glutamine metabolism is a function of the alpha-ketoglutarate to citrate ratio in cells. Nature communications 4: 2236.
105. Metallo CM, Gameiro PA, Bell EL, Mattaini KR, Yang J, et al. (2011) Reductive glutamine metabolism by IDH1 mediates lipogenesis under hypoxia. Nature 481: 380-384.
106. Mullen AR, Wheaton WW, Jin ES, Chen PH, Sullivan LB, et al. (2011) Reductive carboxylation supports growth in tumour cells with defective mitochondria. Nature 481: 385-388.
107. Wise DR, Ward PS, Shay JE, Cross JR, Gruber JJ, et al. (2011) Hypoxia promotes isocitrate dehydrogenase-dependent carboxylation of alpha-ketoglutarate to citrate to support cell growth and viability. Proceedings of the National Academy of Sciences of the United States of America 108: 19611-19616.
108. Leonardi R, Subramanian C, Jackowski S, Rock CO (2012) Cancer-associated isocitrate dehydrogenase mutations inactivate NADPH-dependent reductive carboxylation. The Journal of biological chemistry 287: 14615-14620.
109. Gameiro PA, Laviolette LA, Kelleher JK, Iliopoulos O, Stephanopoulos G (2013) Cofactor balance by nicotinamide nucleotide transhydrogenase (NNT) coordinates reductive carboxylation and glucose catabolism in the tricarboxylic acid (TCA) cycle. The Journal of biological chemistry 288: 12967-12977.
110. Fendt SM, Bell EL, Keibler MA, Davidson SM, Wirth GJ, et al. (2013) Metformin decreases glucose oxidation and increases the dependency of prostate cancer cells on reductive glutamine metabolism. Cancer research 73: 4429-4438.
111. Gameiro PA, Yang J, Metelo AM, Perez-Carro R, Baker R, et al. (2013) In vivo HIF-mediated reductive carboxylation is regulated by citrate levels and sensitizes VHL-deficient cells to glutamine deprivation. Cell metabolism 17: 372-385.
112. Nicklin P, Bergman P, Zhang B, Triantafellow E, Wang H, et al. (2009) Bidirectional transport of amino acids regulates mTOR and autophagy. Cell 136: 521-534.
113. Pochini L, Scalise M, Galluccio M, Indiveri C (2014) Membrane transporters for the special amino acid glutamine: structure/function relationships and relevance to human health. Frontiers in chemistry 2: 61.
114. Bode BP (2001) Recent molecular advances in mammalian glutamine transport. The Journal of nutrition 131: 2475S-2485S; discussion 2486S-2477S.
115. Bungard CI, McGivan JD (2004) Glutamine availability up-regulates expression of the amino acid transporter protein ASCT2 in HepG2 cells and stimulates the ASCT2 promoter. The Biochemical journal 382: 27-32.
116. Ritchie JW, Baird FE, Christie GR, Stewart A, Low SY, et al. (2001) Mechanisms of glutamine transport in rat adipocytes and acute regulation by cell swelling. Cellular physiology and biochemistry : international journal of experimental cellular physiology, biochemistry, and pharmacology 11: 259-270.
117. Taylor L, Curthoys NP (2004) Glutamine metabolism: Role in acid-base balance*. Biochemistry and molecular biology education : a bimonthly publication of the International Union of Biochemistry and Molecular Biology 32: 291-304.
118. Wullschleger S, Loewith R, Hall MN (2006) TOR signaling in growth and metabolism. Cell 124: 471-484.

119. Ma XM, Yoon SO, Richardson CJ, Julich K, Blenis J (2008) SKAR links pre-mRNA splicing to mTOR/S6K1-mediated enhanced translation efficiency of spliced mRNAs. Cell 133: 303-313.
120. Kim J, Kundu M, Viollet B, Guan KL (2011) AMPK and mTOR regulate autophagy through direct phosphorylation of Ulk1. Nature cell biology 13: 132-141.
121. Duvel K, Yecies JL, Menon S, Raman P, Lipovsky AI, et al. (2010) Activation of a metabolic gene regulatory network downstream of mTOR complex 1. Molecular cell 39: 171-183.
122. Peterson TR, Sengupta SS, Harris TE, Carmack AE, Kang SA, et al. (2011) mTOR complex 1 regulates lipin 1 localization to control the SREBP pathway. Cell 146: 408-420.
123. Hara K, Yonezawa K, Weng QP, Kozlowski MT, Belham C, et al. (1998) Amino acid sufficiency and mTOR regulate p70 S6 kinase and eIF-4E BP1 through a common effector mechanism. The Journal of biological chemistry 273: 14484-14494.
124. Zheng L, Zhang W, Zhou Y, Li F, Wei H, et al. (2016) Recent Advances in Understanding Amino Acid Sensing Mechanisms that Regulate mTORC1. International journal of molecular sciences 17.
125. Krause U, Bertrand L, Maisin L, Rosa M, Hue L (2002) Signalling pathways and combinatory effects of insulin and amino acids in isolated rat hepatocytes. European journal of biochemistry 269: 3742-3750.
126. Wise DR, Thompson CB (2010) Glutamine addiction: a new therapeutic target in cancer. Trends in biochemical sciences 35: 427-433.
127. Gao P, Tchernyshyov I, Chang TC, Lee YS, Kita K, et al. (2009) c-Myc suppression of miR-23a/b enhances mitochondrial glutaminase expression and glutamine metabolism. Nature 458: 762-765.
128. Cheng T, Sudderth J, Yang C, Mullen AR, Jin ES, et al. (2011) Pyruvate carboxylase is required for glutamine-independent growth of tumor cells. Proceedings of the National Academy of Sciences of the United States of America 108: 8674-8679.
129. Chen L, Cui H (2015) Targeting Glutamine Induces Apoptosis: A Cancer Therapy Approach. International journal of molecular sciences 16: 22830-22855.
130. van den Heuvel AP, Jing J, Wooster RF, Bachman KE (2012) Analysis of glutamine dependency in non-small cell lung cancer: GLS1 splice variant GAC is essential for cancer cell growth. Cancer biology & therapy 13: 1185-1194.
131. Kung HN, Marks JR, Chi JT (2011) Glutamine synthetase is a genetic determinant of cell type-specific glutamine independence in breast epithelia. PLoS genetics 7: e1002229.
132. Rajagopalan KN, DeBerardinis RJ (2011) Role of glutamine in cancer: therapeutic and imaging implications. Journal of nuclear medicine : official publication, Society of Nuclear Medicine 52: 1005-1008.
133. Lieberman BP, Ploessl K, Wang L, Qu W, Zha Z, et al. (2011) PET imaging of glutaminolysis in tumors by 18F-(2S,4R)4-fluoroglutamine. Journal of nuclear medicine : official publication, Society of Nuclear Medicine 52: 1947-1955.
134. Baek S, Choi CM, Ahn SH, Lee JW, Gong G, et al. (2012) Exploratory clinical trial of (4S)-4-(3-[18F]fluoropropyl)-L-glutamate for imaging xC- transporter using positron emission tomography in patients with non-small cell lung or breast cancer. Clinical cancer research : an official journal of the American Association for Cancer Research 18: 5427-5437.
135. Ploessl K, Wang L, Lieberman BP, Qu W, Kung HF (2012) Comparative evaluation of 18F-labeled glutamic acid and glutamine as tumor metabolic imaging agents. Journal of nuclear medicine : official publication, Society of Nuclear Medicine 53: 1616-1624.

136. Baek S, Mueller A, Lim YS, Lee HC, Lee YJ, et al. (2013) (4S)-4-(3-18F-fluoropropyl)-L-glutamate for imaging of xC transporter activity in hepatocellular carcinoma using PET: preclinical and exploratory clinical studies. Journal of nuclear medicine : official publication, Society of Nuclear Medicine 54: 117-123.
137. Koglin N, Mueller A, Berndt M, Schmitt-Willich H, Toschi L, et al. (2011) Specific PET imaging of xC- transporter activity using a (1)(8)F-labeled glutamate derivative reveals a dominant pathway in tumor metabolism. Clinical cancer research : an official journal of the American Association for Cancer Research 17: 6000-6011.
138. Hensley CT, Wasti AT, DeBerardinis RJ (2013) Glutamine and cancer: cell biology, physiology, and clinical opportunities. The Journal of clinical investigation 123: 3678-3684.
139. Ahluwalia GS, Grem JL, Hao Z, Cooney DA (1990) Metabolism and action of amino acid analog anti-cancer agents. Pharmacology & therapeutics 46: 243-271.
140. Hassanein M, Hoeksema MD, Shiota M, Qian J, Harris BK, et al. (2013) SLC1A5 mediates glutamine transport required for lung cancer cell growth and survival. Clinical cancer research : an official journal of the American Association for Cancer Research 19: 560-570.
141. Cardaci S, Rizza S, Filomeni G, Bernardini R, Bertocchi F, et al. (2012) Glutamine deprivation enhances antitumor activity of 3-bromopyruvate through the stabilization of monocarboxylate transporter-1. Cancer research 72: 4526-4536.
142. Wang JB, Erickson JW, Fuji R, Ramachandran S, Gao P, et al. (2010) Targeting mitochondrial glutaminase activity inhibits oncogenic transformation. Cancer cell 18: 207-219.
143. Robinson MM, McBryant SJ, Tsukamoto T, Rojas C, Ferraris DV, et al. (2007) Novel mechanism of inhibition of rat kidney-type glutaminase by bis-2-(5-phenylacetamido-1,2,4-thiadiazol-2-yl)ethyl sulfide (BPTES). The Biochemical journal 406: 407-414.
144. Le A, Lane AN, Hamaker M, Bose S, Gouw A, et al. (2012) Glucose-independent glutamine metabolism via TCA cycling for proliferation and survival in B cells. Cell metabolism 15: 110-121.
145. Thornburg JM, Nelson KK, Clem BF, Lane AN, Arumugam S, et al. (2008) Targeting aspartate aminotransferase in breast cancer. Breast cancer research : BCR 10: R84.
146. Qing G, Li B, Vu A, Skuli N, Walton ZE, et al. (2012) ATF4 regulates MYC-mediated neuroblastoma cell death upon glutamine deprivation. Cancer cell 22: 631-644.
147. Li C, Allen A, Kwagh J, Doliba NM, Qin W, et al. (2006) Green tea polyphenols modulate insulin secretion by inhibiting glutamate dehydrogenase. The Journal of biological chemistry 281: 10214-10221.
148. Yang C, Sudderth J, Dang T, Bachoo RM, McDonald JG, et al. (2009) Glioblastoma cells require glutamate dehydrogenase to survive impairments of glucose metabolism or Akt signaling. Cancer research 69: 7986-7993.
149. Choo AY, Kim SG, Vander Heiden MG, Mahoney SJ, Vu H, et al. (2010) Glucose addiction of TSC null cells is caused by failed mTORC1-dependent balancing of metabolic demand with supply. Molecular cell 38: 487-499.
150. Bhutia YD, Ganapathy V (2015) Glutamine transporters in mammalian cells and their functions in physiology and cancer. Biochimica et biophysica acta.
151. Oda K, Hosoda N, Endo H, Saito K, Tsujihara K, et al. (2010) L-type amino acid transporter 1 inhibitors inhibit tumor cell growth. Cancer science 101: 173-179.
152. De Sanctis G, Spinelli M, Vanoni M, Sacco E (2016) K-Ras Activation Induces Differential Sensitivity to Sulfur Amino Acid Limitation and Deprivation and to Oxidative and Anti-Oxidative Stress in Mouse Fibroblasts. PloS one 11: e0163790.

153. Finkelstein JD (1990) Methionine metabolism in mammals. The Journal of nutritional biochemistry 1: 228-237.
154. Lu SC, Mato JM (2008) S-Adenosylmethionine in cell growth, apoptosis and liver cancer. Journal of gastroenterology and hepatology 23 Suppl 1: S73-77.
155. Borrego SL, Fahrmann J, Datta R, Stringari C, Grapov D, et al. (2016) Metabolic changes associated with methionine stress sensitivity in MDA-MB-468 breast cancer cells. Cancer Metab 4: 9.
156. Sugimura T, Birnbaum SM, Winitz M, Greenstein JP (1959) Quantitative nutritional studies with water-soluble, chemically defined diets. VIII. The forced feeding of diets each lacking in one essential amino acid. Archives of biochemistry and biophysics 81: 448-455.
157. Cellarier E, Durando X, Vasson MP, Farges MC, Demiden A, et al. (2003) Methionine dependency and cancer treatment. Cancer treatment reviews 29: 489-499.
158. Shiraki N, Shiraki Y, Tsuyama T, Obata F, Miura M, et al. (2014) Methionine metabolism regulates maintenance and differentiation of human pluripotent stem cells. Cell metabolism 19: 780-794.
159. Wellen KE, Thompson CB (2012) A two-way street: reciprocal regulation of metabolism and signalling. Nature reviews Molecular cell biology 13: 270-276.
160. Locasale JW (2013) Serine, glycine and one-carbon units: cancer metabolism in full circle. Nature reviews Cancer 13: 572-583.
161. Ables GP, Hens JR, Nichenametla SN (2016) Methionine restriction beyond life-span extension. Annals of the New York Academy of Sciences 1363: 68-79.
162. Montenegro MF, Sanchez-del-Campo L, Fernandez-Perez MP, Saez-Ayala M, Cabezas-Herrera J, et al. (2015) Targeting the epigenetic machinery of cancer cells. Oncogene 34: 135-143.
163. Cavuoto P, Fenech MF (2012) A review of methionine dependency and the role of methionine restriction in cancer growth control and life-span extension. Cancer treatment reviews 38: 726-736.
164. Epner DE, Morrow S, Wilcox M, Houghton JL (2002) Nutrient intake and nutritional indexes in adults with metastatic cancer on a phase I clinical trial of dietary methionine restriction. Nutrition and cancer 42: 158-166.
165. Ornish D, Weidner G, Fair WR, Marlin R, Pettengill EB, et al. (2005) Intensive lifestyle changes may affect the progression of prostate cancer. The Journal of urology 174: 1065-1069; discussion 1069-1070.
166. Komninou D, Leutzinger Y, Reddy BS, Richie JP, Jr. (2006) Methionine restriction inhibits colon carcinogenesis. Nutrition and cancer 54: 202-208.
167. Caro P, Gomez J, Sanchez I, Naudi A, Ayala V, et al. (2009) Forty percent methionine restriction decreases mitochondrial oxygen radical production and leak at complex I during forward electron flow and lowers oxidative damage to proteins and mitochondrial DNA in rat kidney and brain mitochondria. Rejuvenation research 12: 421-434.
168. Li Y, Liu L, Tollefsbol TO (2010) Glucose restriction can extend normal cell lifespan and impair precancerous cell growth through epigenetic control of hTERT and p16 expression. FASEB journal : official publication of the Federation of American Societies for Experimental Biology 24: 1442-1453.
169. Poirson-Bichat F, Goncalves RA, Miccoli L, Dutrillaux B, Poupon MF (2000) Methionine depletion enhances the antitumoral efficacy of cytotoxic agents in drug-resistant human tumor xenografts. Clinical cancer research : an official journal of the American Association for Cancer Research 6: 643-653.

170. Lin L, Yee SW, Kim RB, Giacomini KM (2015) SLC transporters as therapeutic targets: emerging opportunities. Nature Reviews Drug Discovery 14: 543–560.
171. Cesar-Razquin A, Snijder B, Frappier-Brinton T, Isserlin R, Gyimesi G, et al. (2015) A Call for Systematic Research on Solute Carriers. Cell 162: 478-487.
172. Shoemaker RH, Monks A, Alley MC, Scudiero DA, Fine DL, et al. (1988) Development of human tumor cell line panels for use in disease-oriented drug screening. Progress in clinical and biological research 276: 265-286.
173. Minn H, Clavo AC, Grenman R, Wahl RL (1995) In vitro comparison of cell proliferation kinetics and uptake of tritiated fluorodeoxyglucose and L-methionine in squamous-cell carcinoma of the head and neck. Journal of nuclear medicine : official publication, Society of Nuclear Medicine 36: 252-258.
174. Trencsenyi G, Marian T, Lajtos I, Krasznai Z, Balkay L, et al. (2014) 18FDG, [18F]FLT, [18F]FAZA, and 11C-methionine are suitable tracers for the diagnosis and in vivo follow-up of the efficacy of chemotherapy by miniPET in both multidrug resistant and sensitive human gynecologic tumor xenografts. BioMed research international 2014: 787365.
175. Riedijk MA, van Beek RH, Voortman G, de Bie HM, Dassel AC, et al. (2007) Cysteine: a conditionally essential amino acid in low-birth-weight preterm infants? The American journal of clinical nutrition 86: 1120-1125.
176. Aoyama K, Watabe M, Nakaki T (2008) Regulation of neuronal glutathione synthesis. Journal of pharmacological sciences 108: 227-238.
177. Lu SC (2009) Regulation of glutathione synthesis. Molecular aspects of medicine 30: 42-59.
178. Stipanuk MH (2004) Sulfur amino acid metabolism: pathways for production and removal of homocysteine and cysteine. Annual review of nutrition 24: 539-577.
179. Lo M, Wang YZ, Gout PW (2008) The x(c)- cystine/glutamate antiporter: a potential target for therapy of cancer and other diseases. Journal of cellular physiology 215: 593-602.
180. Estrela JM, Ortega A, Obrador E (2006) Glutathione in cancer biology and therapy. Critical reviews in clinical laboratory sciences 43: 143-181.
181. Uren JR, Lazarus H (1979) L-cyst(e)ine requirements of malignant cells and progress toward depletion therapy. Cancer treatment reports 63: 1073-1079.
182. Gout PW, Kang YJ, Buckley DJ, Bruchovsky N, Buckley AR (1997) Increased cystine uptake capability associated with malignant progression of Nb2 lymphoma cells. Leukemia 11: 1329-1337.
183. Chung WJ, Lyons SA, Nelson GM, Hamza H, Gladson CL, et al. (2005) Inhibition of cystine uptake disrupts the growth of primary brain tumors. The Journal of neuroscience : the official journal of the Society for Neuroscience 25: 7101-7110.
184. Doxsee DW, Gout PW, Kurita T, Lo M, Buckley AR, et al. (2007) Sulfasalazine-induced cystine starvation: potential use for prostate cancer therapy. The Prostate 67: 162-171.
185. Bannai S, Kitamura E (1980) Transport interaction of L-cystine and L-glutamate in human diploid fibroblasts in culture. The Journal of biological chemistry 255: 2372-2376.
186. Okuno S, Sato H, Kuriyama-Matsumura K, Tamba M, Wang H, et al. (2003) Role of cystine transport in intracellular glutathione level and cisplatin resistance in human ovarian cancer cell lines. British journal of cancer 88: 951-956.
187. Huang Y, Dai Z, Barbacioru C, Sadee W (2005) Cystine-glutamate transporter SLC7A11 in cancer chemosensitivity and chemoresistance. Cancer research 65: 7446-7454.
188. Narang VS, Pauletti GM, Gout PW, Buckley DJ, Buckley AR (2007) Sulfasalazine-induced reduction of glutathione levels in breast cancer cells: enhancement of growth-inhibitory activity of Doxorubicin. Chemotherapy 53: 210-217.

189. Narang VS, Pauletti GM, Gout PW, Buckley DJ, Buckley AR (2003) Suppression of cystine uptake by sulfasalazine inhibits proliferation of human mammary carcinoma cells. Anticancer research 23: 4571-4579.
190. Alberghina G, Cozzolino R, Fisichella S, Garozzo D, Savarino A (2005) Proteomics of gluten: mapping of the 1Bx7 glutenin subunit in Chinese Spring cultivar by matrix-assisted laser desorption/ionization. Rapid communications in mass spectrometry : RCM 19: 2069-2074.
191. Balestrieri C, Vanoni M, Hautaniemi S, Alberghina L, Chiaradonna F (2012) Integrative transcriptional analysis between human and mouse cancer cells provides a common set of transformation associated genes. Biotechnology advances 30: 16-29.
192. Palorini R, Votta G, Pirola Y, De Vitto H, De Palma S, et al. (2016) Protein Kinase A Activation Promotes Cancer Cell Resistance to Glucose Starvation and Anoikis. PLoS genetics 12: e1005931.
193. Gaglio D, Valtorta S, Ripamonti M, Bonanomi M, Damiani C, et al. (2016) Divergent in vitro/in vivo responses to drug treatments of highly aggressive NIH-Ras cancer cells: a PET imaging and metabolomics-mass-spectrometry study. Oncotarget.
194. Liu X, Powlas J, Shi Y, Oleksijew AX, Shoemaker AR, et al. (2004) Rapamycin inhibits Akt-mediated oncogenic transformation and tumor growth. Anticancer research 24: 2697-2704.
195. Anand N, Murthy S, Amann G, Wernick M, Porter LA, et al. (2002) Protein elongation factor EEF1A2 is a putative oncogene in ovarian cancer. Nature genetics 31: 301-305.
196. Armstrong F, Duplantier MM, Trempat P, Hieblot C, Lamant L, et al. (2004) Differential effects of X-ALK fusion proteins on proliferation, transformation, and invasion properties of NIH3T3 cells. Oncogene 23: 6071-6082.
197. Piestun D, Kochupurakkal BS, Jacob-Hirsch J, Zeligson S, Koudritsky M, et al. (2006) Nanog transforms NIH3T3 cells and targets cell-type restricted genes. Biochemical and biophysical research communications 343: 279-285.
198. Bossu P, Vanoni M, Wanke V, Cesaroni MP, Tropea F, et al. (2000) A dominant negative RAS-specific guanine nucleotide exchange factor reverses neoplastic phenotype in K-ras transformed mouse fibroblasts. Oncogene 19: 2147-2154.
199. Chiaradonna F, Sacco E, Manzoni R, Giorgio M, Vanoni M, et al. (2006) Ras-dependent carbon metabolism and transformation in mouse fibroblasts. Oncogene 25: 5391-5404.
200. Vanoni M, Bertini R, Sacco E, Fontanella L, Rieppi M, et al. (1999) Characterization and properties of dominant-negative mutants of the ras-specific guanine nucleotide exchange factor CDC25(Mm). The Journal of biological chemistry 274: 36656-36662.
201. De Sanctis G, Colombo R, Damiani C, Sacco E, Vanoni M (2016) *Omics and clinical data integration* in *Integration of omics approaches and systems biology for clinical applications*. Wiley.
202. Shoemaker RH (2006) The NCI60 human tumour cell line anticancer drug screen. Nature reviews Cancer 6: 813-823.
203. Rhodes DR, Yu J, Shanker K, Deshpande N, Varambally R, et al. (2004) Large-scale meta-analysis of cancer microarray data identifies common transcriptional profiles of neoplastic transformation and progression. Proceedings of the National Academy of Sciences of the United States of America 101: 9309-9314.
204. Kao J, Salari K, Bocanegra M, Choi YL, Girard L, et al. (2009) Molecular profiling of breast cancer cell lines defines relevant tumor models and provides a resource for cancer gene discovery. PloS one 4: e6146.

205. Ruan X, Li Y, Li J, Gong D, Wang J (2006) Tumor-specific gene expression patterns with gene expression profiles. Science in China Series C, Life sciences 49: 293-304.
206. Ahrens CH, Brunner E, Qeli E, Basler K, Aebersold R (2010) Generating and navigating proteome maps using mass spectrometry. Nature reviews Molecular cell biology 11: 789-801.
207. Wolf-Yadlin A, Sevecka M, MacBeath G (2009) Dissecting protein function and signaling using protein microarrays. Current opinion in chemical biology 13: 398-405.
208. Stevens EV, Posadas EM, Davidson B, Kohn EC (2004) Proteomics in cancer. Annals of oncology : official journal of the European Society for Medical Oncology 15 Suppl 4: iv167-171.
209. Russo G, Zegar C, Giordano A (2003) Advantages and limitations of microarray technology in human cancer. Oncogene 22: 6497-6507.
210. von Eggeling F, Davies H, Lomas L, Fiedler W, Junker K, et al. (2000) Tissue-specific microdissection coupled with ProteinChip array technologies: applications in cancer research. BioTechniques 29: 1066-1070.
211. Maas S (2010) Gene regulation through RNA editing. Discovery medicine 10: 379-386.
212. Weckwerth W (2003) Metabolomics in systems biology. Annual review of plant biology 54: 669-689.
213. Zhang GF, Sadhukhan S, Tochtrop GP, Brunengraber H (2011) Metabolomics, pathway regulation, and pathway discovery. The Journal of biological chemistry 286: 23631-23635.
214. Seppanen-Laakso T, Oresic M (2009) How to study lipidomes. Journal of molecular endocrinology 42: 185-190.
215. Cazzaniga P, Damiani C, Besozzi D, Colombo R, Nobile MS, et al. (2014) Computational strategies for a system-level understanding of metabolism. Metabolites 4: 1034-1087.
216. Cascante M, Marin S (2008) Metabolomics and fluxomics approaches. Essays in biochemistry 45: 67-81.
217. Winter G, Kromer JO (2013) Fluxomics - connecting 'omics analysis and phenotypes. Environmental microbiology 15: 1901-1916.
218. Aon MA, Cortassa S (2015) Systems Biology of the Fluxome. Processes 3: 607-618.
219. Cascante M, Benito A, Mas IM, Centelles JJ, Miranda A, et al. (2014) Fluxomics. Springer International Publishing: 237-250.
220. Kromer JO, Quek LE, Nielsen L (2009) 13C-Fluxomics: A Tool for Measuring Metabolic Phenotypes. Australian Biochemist 40: 17-20.
221. Kitano H (2002) Systems biology: a brief overview. Science 295: 1662-1664.
222. Alberghina L, Westerhoff HV (2005) Systems Biology: Did we know it all along? in Systems Biology: Definitions and Perspectives. Topics in Current Genetics - Springer-Verlag Berlin Heidelberg 13: 3-9.
223. Borodina I, Nielsen J (2005) From genomes to in silico cells via metabolic networks. Current opinion in biotechnology 16: 350-355.
224. Hiller K, Metallo CM (2013) Profiling metabolic networks to study cancer metabolism. Current opinion in biotechnology 24: 60-68.
225. Feist AM, Herrgard MJ, Thiele I, Reed JL, Palsson BO (2009) Reconstruction of biochemical networks in microorganisms. Nature reviews Microbiology 7: 129-143.
226. Soon WW, Hariharan M, Snyder MP (2013) High-throughput sequencing for biology and medicine. Molecular systems biology 9: 640.
227. Hyduke DR, Lewis NE, Palsson BO (2013) Analysis of omics data with genome-scale models of metabolism. Molecular bioSystems 9: 167-174.

228. Thiele I, Palsson BO (2010) A protocol for generating a high-quality genome-scale metabolic reconstruction. Nature protocols 5: 93-121.
229. Jia G, Stephanopoulos G, Gunawan R (2012) Ensemble kinetic modeling of metabolic networks from dynamic metabolic profiles. Metabolites 2: 891-912.
230. Orth JD, Thiele I, Palsson BO (2010) What is flux balance analysis? Nature biotechnology 28: 245-248.
231. Vazquez A, Liu J, Zhou Y, Oltvai ZN (2010) Catabolic efficiency of aerobic glycolysis: the Warburg effect revisited. BMC systems biology 4: 58.
232. Ramakrishna R, Edwards JS, McCulloch A, Palsson BO (2001) Flux-balance analysis of mitochondrial energy metabolism: consequences of systemic stoichiometric constraints. American journal of physiology Regulatory, integrative and comparative physiology 280: R695-704.
233. Lee JM, Gianchandani EP, Papin JA (2006) Flux balance analysis in the era of metabolomics. Briefings in bioinformatics 7: 140-150.
234. Covert MW, Schilling CH, Palsson B (2001) Regulation of gene expression in flux balance models of metabolism. Journal of theoretical biology 213: 73-88.
235. Schwartz L, Seyfried T, Alfarouk KO, Da Veiga Moreira J, Fais S (2017) Out of Warburg Effect: an effective cancer treatment targeting the tumor specific metabolism and dysregulated pH. Seminars in cancer biology.
236. Schwartz L, Supuran CT, Alfarouk KO (2017) The Warburg Effect and the Hallmarks of Cancer. Anti-cancer agents in medicinal chemistry 17: 164-170.
237. Garcia-Heredia JM, Carnero A (2015) Decoding Warburg's hypothesis: tumor-related mutations in the mitochondrial respiratory chain. Oncotarget 6: 41582-41599.
238. Lu J, Tan M, Cai Q (2015) The Warburg effect in tumor progression: mitochondrial oxidative metabolism as an anti-metastasis mechanism. Cancer letters 356: 156-164.
239. Tang X, Lucas JE, Chen JL, LaMonte G, Wu J, et al. (2012) Functional interaction between responses to lactic acidosis and hypoxia regulates genomic transcriptional outputs. Cancer research 72: 491-502.
240. Chen JL, Merl D, Peterson CW, Wu J, Liu PY, et al. (2010) Lactic acidosis triggers starvation response with paradoxical induction of TXNIP through MondoA. PLoS genetics 6: e1001093.
241. Russell RC, Yuan HX, Guan KL (2014) Autophagy regulation by nutrient signaling. Cell research 24: 42-57.
242. Keenan MM, Chi JT (2015) Alternative fuels for cancer cells. Cancer journal 21: 49-55.
243. Gaglio D, Soldati C, Vanoni M, Alberghina L, Chiaradonna F (2009) Glutamine deprivation induces abortive s-phase rescued by deoxyribonucleotides in k-ras transformed fibroblasts. PloS one 4: e4715.
244. Duan S, Pagano M (2011) Linking metabolism and cell cycle progression via the APC/CCdh1 and SCFbetaTrCP ubiquitin ligases. Proceedings of the National Academy of Sciences of the United States of America 108: 20857-20858.
245. Reid MA, Wang WI, Rosales KR, Welliver MX, Pan M, et al. (2013) The B55alpha subunit of PP2A drives a p53-dependent metabolic adaptation to glutamine deprivation. Molecular cell 50: 200-211.
246. Timmerman LA, Holton T, Yuneva M, Louie RJ, Padro M, et al. (2013) Glutamine sensitivity analysis identifies the xCT antiporter as a common triple-negative breast tumor therapeutic target. Cancer cell 24: 450-465.

247. Ishimoto T, Nagano O, Yae T, Tamada M, Motohara T, et al. (2011) CD44 variant regulates redox status in cancer cells by stabilizing the xCT subunit of system xc(-) and thereby promotes tumor growth. Cancer cell 19: 387-400.
248. Xiang Y, Zhu Z, Han G, Ye X, Xu B, et al. (2007) JARID1B is a histone H3 lysine 4 demethylase up-regulated in prostate cancer. Proceedings of the National Academy of Sciences of the United States of America 104: 19226-19231.
249. Vidal AC, Grant DJ, Williams CD, Masko E, Allott EH, et al. (2012) Associations between Intake of Folate, Methionine, and Vitamins B-12, B-6 and Prostate Cancer Risk in American Veterans. Journal of cancer epidemiology 2012: 957467.
250. Li Z, Zhang H (2016) Reprogramming of glucose, fatty acid and amino acid metabolism for cancer progression. Cellular and molecular life sciences : CMLS 73: 377-392.
251. Lucas JE, Kung HN, Chi JT (2010) Latent factor analysis to discover pathway-associated putative segmental aneuploidies in human cancers. PLoS computational biology 6: e1000920.
252. Gatza ML, Kung HN, Blackwell KL, Dewhirst MW, Marks JR, et al. (2011) Analysis of tumor environmental response and oncogenic pathway activation identifies distinct basal and luminal features in HER2-related breast tumor subtypes. Breast cancer research : BCR 13: R62.
253. Metallo CM, Vander Heiden MG (2010) Metabolism strikes back: metabolic flux regulates cell signaling. Genes & development 24: 2717-2722.
254. Laubenbacher R, Hower V, Jarrah A, Torti SV, Shulaev V, et al. (2009) A systems biology view of cancer. Biochimica et biophysica acta 1796: 129-139.
255. Kreeger PK, Lauffenburger DA (2010) Cancer systems biology: a network modeling perspective. Carcinogenesis 31: 2-8.
256. Stephanopoulos G, Vallino JJ (1991) Network rigidity and metabolic engineering in metabolite overproduction. Science 252: 1675-1681.
257. Sauer U (2006) Metabolic networks in motion: 13C-based flux analysis. Molecular systems biology 2: 62.
258. Metallo CM, Walther JL, Stephanopoulos G (2009) Evaluation of 13C isotopic tracers for metabolic flux analysis in mammalian cells. Journal of biotechnology 144: 167-174.
259. Hiller K, Metallo CM, Kelleher JK, Stephanopoulos G (2010) Nontargeted elucidation of metabolic pathways using stable-isotope tracers and mass spectrometry. Analytical chemistry 82: 6621-6628.
260. Munger J, Bennett BD, Parikh A, Feng XJ, McArdle J, et al. (2008) Systems-level metabolic flux profiling identifies fatty acid synthesis as a target for antiviral therapy. Nature biotechnology 26: 1179-1186.
261. Keibler MA, Fendt SM, Stephanopoulos G (2012) Expanding the concepts and tools of metabolic engineering to elucidate cancer metabolism. Biotechnology progress 28: 1409-1418.
262. Yoo H, Stephanopoulos G, Kelleher JK (2004) Quantifying carbon sources for de novo lipogenesis in wild-type and IRS-1 knockout brown adipocytes. Journal of lipid research 45: 1324-1332.
263. Pye IF, Stonier C, McGale HF (1978) Double-enzymatic assay for determination of glutamine and glutamic acid in cerebrospinal fluid and plasma. Analytical chemistry 50: 951-953.
264. Tcherkas YV, Kartsova LA, Krasnova IN (2001) Analysis of amino acids in human serum by isocratic reversed-phase high-performance liquid chromatography with electrochemical detection. Journal of chromatography A 913: 303-308.

265. Darmaun D, Manary MJ, Matthews DE (1985) A method for measuring both glutamine and glutamate levels and stable isotopic enrichments. Analytical biochemistry 147: 92-102.
266. Qu J, Chen W, Luo G, Wang Y, Xiao S, et al. (2002) Rapid determination of underivatized pyroglutamic acid, glutamic acid, glutamine and other relevant amino acids in fermentation media by LC-MS-MS. The Analyst 127: 66-69.
267. Glacken MW, Adema E, Sinskey AJ (1988) Mathematical descriptions of hybridoma culture kinetics: I. Initial metabolic rates. Biotechnology and bioengineering 32: 491-506.
268. Wittmann C (2007) Fluxome analysis using GC-MS. Microbial cell factories 6: 6.
269. Antoniewicz MR, Kelleher JK, Stephanopoulos G (2007) Accurate assessment of amino acid mass isotopomer distributions for metabolic flux analysis. Analytical chemistry 79: 7554-7559.
270. Fernandez CA, Des Rosiers C, Previs SF, David F, Brunengraber H (1996) Correction of 13C mass isotopomer distributions for natural stable isotope abundance. Journal of mass spectrometry : JMS 31: 255-262.
271. Rahman M, Hasan MR (2015) Cancer metabolism and drug resistance. Metabolites 5(4):571-600.

APPENDIX

PLOS ONE

RESEARCH ARTICLE

K-Ras Activation Induces Differential Sensitivity to Sulfur Amino Acid Limitation and Deprivation and to Oxidative and Anti-Oxidative Stress in Mouse Fibroblasts

Gaia De Sanctis[1,2], Michela Spinelli[1,2], Marco Vanoni[1,2], Elena Sacco[1,2]*

1 SYSBIO, Centre of Systems Biology, Milan, Italy, **2** Department of Biotechnology and Biosciences, University of Milano-Bicocca, Piazza della Scienza 2, 20126, Milan, Italy

* elena.sacco@unimib.it

OPEN ACCESS

Citation: De Sanctis G, Spinelli M, Vanoni M, Sacco E (2016) K-Ras Activation Induces Differential Sensitivity to Sulfur Amino Acid Limitation and Deprivation and to Oxidative and Anti-Oxidative Stress in Mouse Fibroblasts. PLoS ONE 11(9): e0163790. doi:10.1371/journal.pone.0163790

Editor: François Blachier, National Institute for Agronomic Research, FRANCE

Received: April 20, 2016

Accepted: September 14, 2016

Published: September 29, 2016

Data Availability Statement: All relevant data are within the paper and its Supporting Information files.

Funding: This work was supported by MIUR grant SysBioNet—Italian Roadmap for ESFRI Research Infrastructures. The funders had no role in study design, data collection and analysis, decision to publish, or preparation of the manuscript.

Competing Interests: The authors have declared that no competing interests exist.

Abstract

Background

Cancer cells have an increased demand for amino acids and require transport even of non-essential amino acids to support their increased proliferation rate. Besides their major role as protein synthesis precursors, the two proteinogenic sulfur-containing amino acids, methionine and cysteine, play specific biological functions. In humans, methionine is essential for cell growth and development and may act as a precursor for cysteine synthesis. Cysteine is a precursor for the biosynthesis of glutathione, the major scavenger for reactive oxygen species.

Methodology and Principal Findings

We study the effect of *K-ras* oncogene activation in NIH3T3 mouse fibroblasts on transport and metabolism of cysteine and methionine. We show that cysteine limitation and deprivation cause apoptotic cell death (cytotoxic effect) in both normal and *K-ras*-transformed fibroblasts, due to accumulation of reactive oxygen species and a decrease in reduced glutathione. Anti-oxidants glutathione and MitoTEMPO inhibit apoptosis, but only cysteine-containing glutathione partially rescues the cell growth defect induced by limiting cysteine. Methionine limitation and deprivation has a cytostatic effect on mouse fibroblasts, unaffected by glutathione. *K-ras*-transformed cells–but not their parental NIH3T3—are extremely sensitive to methionine limitation. This fragility correlates with decreased expression of the *Slc6a15* gene—encoding the nutrient transporter SBAT1, known to exhibit a strong preference for methionine—and decreased methionine uptake.

Conclusions and Significance

Overall, limitation of sulfur-containing amino acids results in a more dramatic perturbation of the oxido-reductive balance in *K-ras*-transformed cells compared to NIH3T3 cells. Growth defects induced by cysteine limitation in mouse fibroblasts are largely–though not

exclusively–due to cysteine utilization in the synthesis of glutathione, mouse fibroblasts requiring an exogenous cysteine source for protein synthesis. Therapeutic regimens of cancer involving modulation of methionine metabolism could be more effective in cells with limited methionine transport capability.

Introduction

Activation of the *K-ras* proto-oncogene [1,2,3,4] has a great incidence in human tumors, as reported in the catalogue of somatic mutations in cancer (COSMIC) [5]. *K-ras* activation occurs in 22% of all tumors, prevalently in pancreatic carcinomas (about 90%), colorectal carcinomas (40–50%), and lung carcinomas (30–50%), as well as in biliary tract malignancies, endometrial cancer, cervical cancer, bladder cancer, liver cancer, myeloid leukemia and breast cancer. K-Ras oncoproteins are important clinical targets for anti-cancer therapy [6] and several strategies have been explored in order to inhibit aberrant Ras signaling, as reviewed in [7,8,9,10].

The acquisition of important hallmark traits of cancer cells, including enhanced cell growth and survival, rely on deep changes in metabolism driven by oncogene activation [11,12,13,14,15]. Oncogenic activation of *K-ras* contributes to the acquisition of the hyper-glycolytic phenotype (also known as Warburg effect, from the pioneering studies of Warburg [16]) due to enhancement in glucose transport and aerobic glycolysis [17,18]. *K-ras* oncogene activation also correlates with down-regulated expression of mitochondrial genes, altered mitochondrial morphology and production of large amount of reactive oxygen species (ROS) associated with mitochondrial metabolism [19,20]. Furthermore, *K-ras* activation allows cells to make extensive anaplerotic usage of glutamine, the more concentrated amino acid in human plasma [21]. In Ras-transformed cells, glutamine is largely utilized through reductive carboxylation that results in a non-canonical tricarboxylic acid cycle (TCA) pathway [19,22,23,24,25,26]. These metabolic changes render Ras-transformed cells addicted to glutamine, and to glutaminolysis, and offer new therapeutic opportunities. Indeed, glutamine metabolism restriction and targeted cancer therapeutics directed against glutamine transporters or glutaminolysis can be used to limit tumor cell proliferation and survival without affecting normal cells [27,28,29].

Besides glutamine transporters, all amino acid transporters are being receiving attention from scientific community as potential drug targets for cancer treatment, given the increased demand of cancer cells for these nutrients to support their enhanced cell growth [30,31]. Selective blockers of these transporters might be effective in preventing the entry of important amino acids into tumor cells, thus essentially starving these cells to death.

Methionine is an essential amino acid required for normal growth and development in mammals [32]. The intracellular level of methionine depends on the balance between synthesis (through the *de novo* synthetic pathway), recycle (through the *salvage* pathway), consumption (in biosynthesis of proteins) and its transport. An important metabolite of methionine is S-adenosylmethionine (SAM), the principal methyl donor in the cell. SAM is required for methylation of DNA, RNA, proteins (including histones [33]) and lipids by the enzymes methyltransferases. Moreover, SAM is involved in biosynthesis of polyamines, which have far-ranging effects on nuclear and cell division, and methionine salvage pathway [34]. SAM gives its activated methyl group in methylation reactions, being converted to S-adenosylhomocysteine, which is reversibly hydrolyzed to homocysteine (S1 Fig). Depending on demand, homocysteine metabolism can be either directed toward the re-methylation pathway to regenerate

methionine (thus increasing methylation potential) or toward antioxidant synthesis in the trans-sulfuration pathway [34]. In the first catabolic step of trans-sulfuration, homocysteine may be condensed to serine to form cystathionine, which in turn may be converted to cysteine [35].

Cysteine is a sulfur-containing, semi-essential proteinogenic amino acid. It can be synthesized in humans to some extent; as such, it is classified as conditionally essential, since it may become temporarily essential when synthesis during rapid growth or critical illness is insufficient [36]. Cysteine is a precursor for the tripeptide glutathione, an important intracellular antioxidant that reduces reactive oxygen species (ROS), thereby protecting cells from oxidative stress [37]. The systemic availability of oral glutathione (GSH) is negligible; so it must be biosynthesized from its constituent amino acids, cysteine, glycine, and glutamic acid, the first being the limiting substrate [38]. Furthermore, cysteine is a precursor for the production of taurine, another antioxidant, and sulfate [39]. At least in liver, glutathione also acts as cysteine storage, from which this amino acid can be mobilized if required to maintain protein synthesis under nutritional stress [40]. Under normal physiological conditions, cysteine can usually be synthesized *de novo* from homocysteine in humans if a sufficient quantity of methionine is available.

Normal mouse fibroblasts (NIH3T3) and their derived cells stably expressing oncogenic K-*ras* mutant (NIH-RAS) proved to be a valid cellular model for studying Ras-dependent transcriptional reprogramming [41] and metabolic rewiring [23,42,43]. The Ras-dependent transformation phenotypes of NIH-RAS cells can be down-regulated by over-expressing a dominant negative mutant of RasGRF1 with Ras sequestering properties, extensively characterized in our laboratory [7,44,45]. We use these cell lines to study the effect of *K-ras* proto-oncogene activation on transport and metabolism of the proteinogenic sulfur amino acids, cysteine and methionine.

We show that cysteine limitation and deprivation increase ROS level and decrease reduced glutathione, eventually leading to apoptotic cell death. Through the complementary use of anti-oxidants glutathione and MitoTEMPO (a cysteine non-containing reducing agent) and inhibitors of *de novo* biosynthesis of reduced glutathione, we show that growth defects induced by cysteine limitation in mouse fibroblasts are largely–though not exclusively–due to cysteine utilization in the synthesis of glutathione and that mouse fibroblasts require an exogenous cysteine source for protein synthesis. Methionine limitation and deprivation is cytostatic and unaffected by glutathione. Limitation of sulfur-containing amino acids perturbs the oxidoreductive balance, particularly in *K-ras*-transformed cells that display selective growth fragility to a moderate reduction in methionine supply. Such nutritional fragility correlates with Ras activation, decreased expression of the *Slc6a15* gene -encoding the methionine transporter SBAT1- and reduced methionine uptake.

Results

Methionine limitation reduces growth of Ras-transformed mouse fibroblasts more than growth of normal cells

First, we analyzed cell proliferation of normal NIH3T3 and Ras-transformed NIH-RAS mouse fibroblasts under standard growth condition (0.2 mM Cys, 0.2 mM Met), limitation (1/8: 0.025 mM; 1/4: 0.05 mM; 1/2: 0.1 mM) and deprivation of cysteine or methionine. Both cell lines were unable to grow in the absence of either methionine or cysteine (Fig 1A and 1B, open squares), demonstrating that both sulfur amino acids are essential for cell proliferation of mouse fibroblasts, which are not able to synthesize neither cysteine nor methionine each from the other.

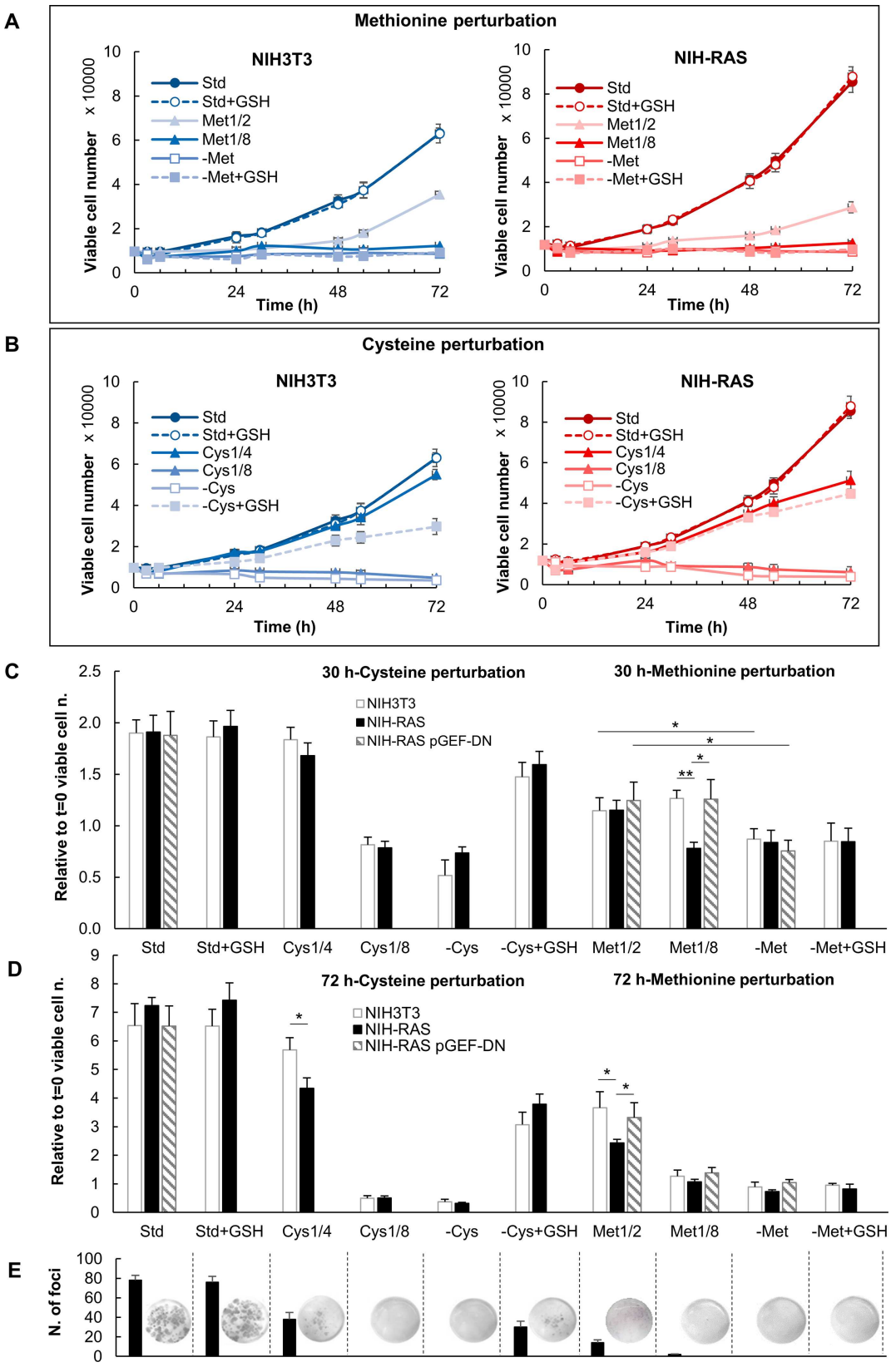
A
Methionine perturbation
NIH3T3
NIH-RAS
Viable cell number x 10000
Time (h)
Std
Std+GSH
Met1/2
Met1/8
-Met
-Met+GSH
B
Cysteine perturbation
NIH3T3
NIH-RAS
Viable cell number x 10000
Time (h)
Std
Std+GSH
Cys1/4
Cys1/8
-Cys
-Cys+GSH
C
30 h-Cysteine perturbation
30 h-Methionine perturbation
NIH3T3
NIH-RAS
NIH-RAS pGEF-DN
Relative to t=0 viable cell n.
Std
Std+GSH
Cys1/4
Cys1/8
-Cys
-Cys+GSH
Met1/2
Met1/8
-Met
-Met+GSH
D
72 h-Cysteine perturbation
72 h-Methionine perturbation
NIH3T3
NIH-RAS
NIH-RAS pGEF-DN
Relative to t=0 viable cell n.
Std
Std+GSH
Cys1/4
Cys1/8
-Cys
-Cys+GSH
Met1/2
Met1/8
-Met
-Met+GSH
E
N. of foci

Fig 1. Proliferation under methionine and cysteine deprivation and limitation. Cell proliferation of NIH3T3 and NIH-RAS cells grown in media supplemented with different concentrations of methionine and glutathione (A) or cysteine and glutathione (B) and counted daily for 72 h of growth under conditions indicated. Plotted data are mean +/- standard deviation computed from at least three independent experiments. (C-D) Cell proliferation of NIH3T3, NIH-RAS and NIH-RAS pGEF-DN cells grown for 30 h (C) and 72 h (D) under conditions indicated. (E) *Foci* formation of NIH-RAS cells grown for 9 days under conditions indicated. *P<0.05; **P<0.01 (Student's *t*-test).

doi:10.1371/journal.pone.0163790.g001

Growth of NIH-RAS cells was more severely inhibited by methionine limitation than that of NIH3T3 cells. In $Met_{1/2}$ condition (Fig 1A and 1B, light triangles, and Fig 1D) the mass duplication time (MTD) of NIH-RAS cells was 1.5 longer than that of NIH3T3 (S1 Table). More stringent methionine limitation ($Met_{1/8}$) resulted in almost complete arrest of cell proliferation of both cell lines (Fig 1A, dark filled triangles, and S1 Table). Fig 1C and 1D show cell proliferation data 30 and 72 hours after methionine limitation, highlighting enhanced sensitivity of transformed NIH3T3 cells to methionine limitation. Note that NIH-RAS cells grown in $Met_{1/2}$ condition are still largely viable after 72 hours, unlike the cells grown in $Met_{1/8}$ condition (Fig 1D). Under methionine limitation NIH-RAS cells were also severely hampered in *foci* formation ability (Fig 1E). Notably the major sensitivity of Ras-transformed cells to methionine limitation was fully reverted by the over-expression of a dominant negative mutant of the Ras-specific guanine nucleotide exchange factor RasGRF1 ($RasGRF1^{W1056E}$, that we refer to as GEF-DN), endowed with Ras sequestering properties (Fig 1C and 1D, S2 and S3 Figs).

All together, these data indicate that Ras hyper-activation enhances sensitivity to methionine limitation in mouse fibroblasts.

As shown in Fig 1B and in S1 Table the cell proliferation behavior under cysteine limitation and deprivation was quite similar in NIH3T3 and NIH-RAS cells. In $Cys_{1/2}$ condition both cell lines grew as well as in standard medium (S4A Fig, S1 Table), while further reduction of cysteine ($Cys_{1/4}$) increased the MDT of both NIH3T3 and NIH-RAS cells, even if slightly more in transformed cells (Fig 1B, S1 Table). Cysteine limitation strongly reduced *foci* formation ability of NIH-RAS cells (Fig 1E).

Cysteine mainly acts as a precursor of glutathione, whose excess mostly affects normal cells

Apoptotic and necrotic cell death can be assayed by FACS after staining with Annexin V-FITC and propidium iodide (PI). After limitation or deprivation of cysteine for 30 hours, apoptotic cells significantly increased in both cell lines, the effect being stronger in cysteine-deprived cells (Fig 2A). Supplementation of cysteine to cells grown for 72 hours in cysteine-free medium did not result in any significant growth recovery, reinforcing the notion that cysteine deprivation exerted a cytotoxic effect (cell death) in both NIH3T3 and NIH-RAS cell lines (Fig 2E).

Glutathione is the most important endogenous antioxidant in mammalian cells, and the major redox buffer responsible for redox homeostasis [46,47]. It acts as a ROS scavenger through its oxidation to GSSG. The reduced form (GSH) is restored at the expenses of NADPH. The intracellular concentration of GSH depends on a dynamic balance between synthesis, consumption rate (metabolism), and its transport.

We measured ROS (by FACS analysis of DCFDA-stained cells, Fig 2B), endogenous total (GSH+GSSG) and reduced (GSH) glutathione levels (by an enzymatic assay, Fig 2C) in NIH3T3 and NIH-RAS cells in standard medium and 48 h after perturbing cysteine metabolism. In keeping with literature data [19,45,48,49], in standard medium NIH-RAS cells showed a 1.7-fold higher ROS level than NIH3T3 (Fig 2B), accompanied by a moderate decrease in total glutathione and a significant decrease in reduced glutathione (Fig 2C). Cysteine limitation and deprivation induced an increase in ROS levels, the effect being stronger in NIH-RAS cells

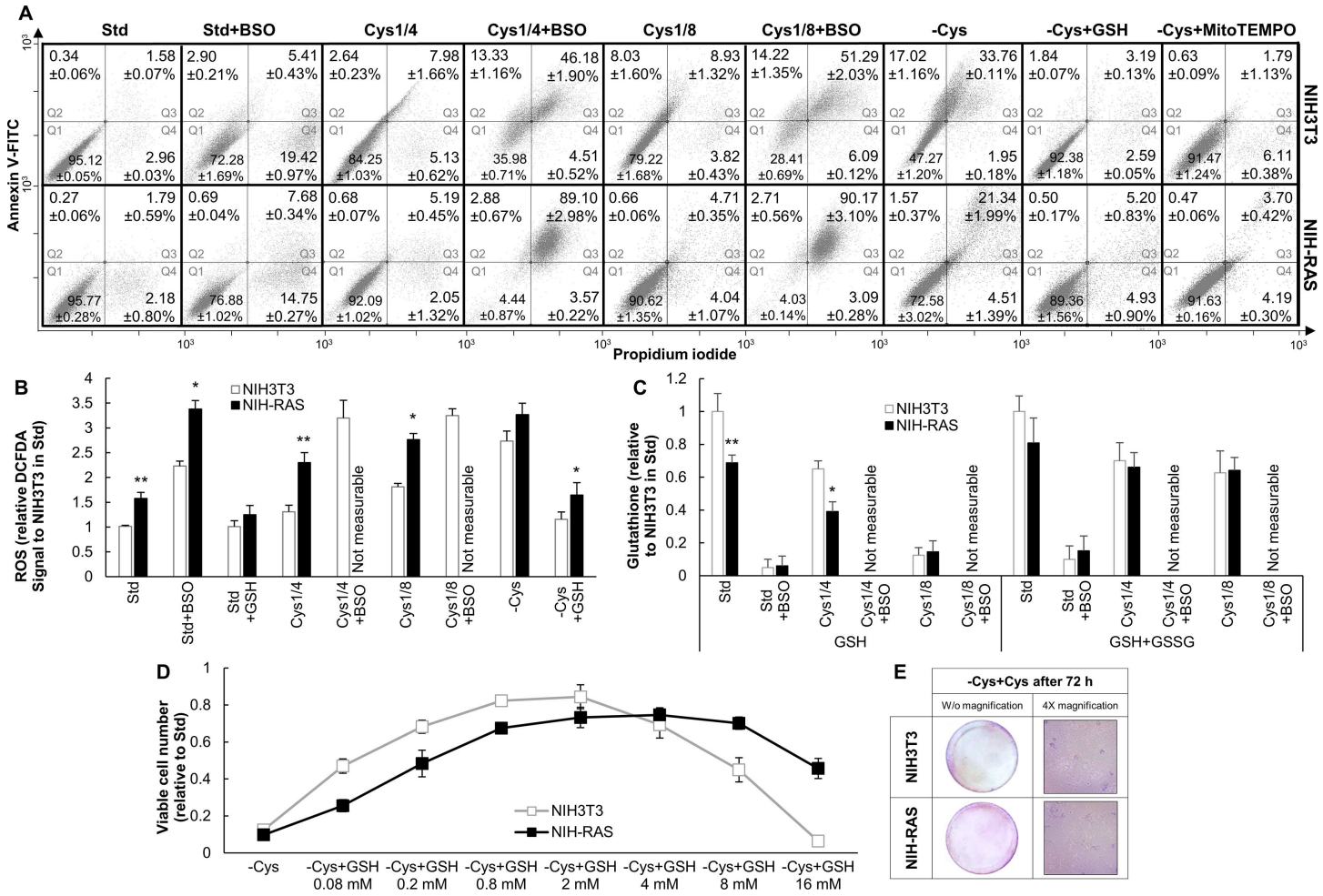

Fig 2. Viability and redox state under cysteine deprivation and limitation. (A) Representative dot plots for NIH3T3 and NIH-RAS cells stained with Annexin V-FITC and propidium iodide and analyzed by FACS after 30 h of growth under conditions indicated. Q1 = quadrant 1, healthy cell; Q2 = quadrant 2, early apoptotic cells; Q3 = quadrant 3, late apoptotic cells; Q4 = quadrant 4, necrotic cells. MitoTEMPO and buthionine sulfoximine (BSO) were used at the concentration of 10 μM and 100 μM, respectively. The values reported for each quadrant are the mean +/- standard deviation of three independent experiments. (B) Relative ROS levels in NIH3T3 and NIH-RAS cells grown for 48 h under conditions indicated as determined by DCFDA (2',7'-dichlorodihydrofluorescein diacetate) staining. Each bar represents the mean of at least three independent experiments with error bars representing the standard deviation. (C) Reduced and total glutathione levels (measured as described in [55]) in NIH3T3 and NIH-RAS cells grown for 48 h under conditions indicated. Each bar represents the mean of at least three independent experiments with error bars representing the standard deviation. (D) Cell proliferation of NIH3T3 and NIH-RAS cells grown for 48 h in cysteine-free medium supplemented with different concentrations of glutathione. Plotted data are mean +/- standard deviation computed from at least three independent experiments. *P<0.05; **P<0.01 (Student's *t*-test). (E) Crystal violet staining of NIH3T3 and NIH-RAS cells plated at the density of 9000 cells/cm^2, grown for 72 h under cysteine deprivation and then for 48 h in standard medium.

doi:10.1371/journal.pone.0163790.g002

(Fig 2B). Under cysteine limitation, total glutathione levels (GSH+GSSG) were lower than in standard condition (Fig 2C), consistently with the notion that cysteine availability is rate-limiting for GSH synthesis [50,51,52,53]. The high cell mortality under cysteine deprivation hindered the measurement of glutathione levels.

To investigate whether mouse fibroblasts are dependent on cysteine for growth, or whether the growth defects are the result of the oxidative stress on the cells, we took two complementary approaches. First, we modulated the oxidative response of cysteine-depleted cells with either cysteine-containing (GSH) or cysteine-non-containing (MitoTEMPO) anti-oxidants. Second, we blocked glutathione *de novo* biosynthesis of standard or cysteine-limited cells with buthionine sulfoximine (BSO), that blocks the activity of gamma-glutamylcysteine synthetase (γ-

GCT) required for the formation of the glutathione precursor gamma-glutamylcysteine from glutamate and cysteine [47].

Supplementing GSH to cysteine-free medium (-Cys+GSH growth condition) partially restored cell proliferation (Fig 1A, 1C and 1D) in both NIH3T3 and NIH-RAS cell lines and the ability to form *foci* in NIH-RAS cells (Fig 1E). Also, supplementation of GSH significantly reduced apoptosis induced by cysteine withdrawal and fully restored ROS levels to basal (Fig 2A and 2B). Compared to NIH3T3, NIH-RAS cells require a higher GSH concentration both to recover cell survival and growth as well as to show the "anti-oxidative stress" (Fig 2D), phenomenon described in [54]. The reduced sensitivity to both positive and negative effects of GSH is most likely the result of the lower GSH content of Ras-transformed cells (Fig 2C). Supplementation of MitoTEMPO in cysteine-free medium reduced apoptosis to the same levels observed after GSH addition (Fig 2A), but could not rescue cell proliferation under cysteine deprivation (S4B Fig).

In both NIH3T3 and NIH-RAS cell lines, BSO treatment severely down-regulated glutathione accumulation (Fig 2C) and reduced proliferation (S4C Fig). Concurrently, both ROS accumulation (Fig 2B) and the fraction of apoptotic cells increased (Fig 2A). These effects appear stronger in NIH-RAS than in NIH3T3 cells. They are dramatically enhanced by growth in limiting cysteine, which results in the death of most cells within 30 h from the treatment (Fig 2A). Cell death in BSO-treated cells grown in the absence of cysteine was essentially caused by oxidative stress, since almost all cells were strongly positive to DCFDA staining, as shown by fluorescence-microscopy analysis (S4D Fig). In these conditions ca 90% and 50% of NIH-RAS and NIH3T3 cells, respectively, are apoptotic after 30 h of treatment (Fig 2A). All together, these data confirm the major dependence of NIH-RAS from cysteine availability for the maintenance of proper GSH levels, redox homeostasis and cell viability, and on the other hand suggest that NIH3T3 cells less recur to the *de novo* synthesis of GSH to maintain redox homeostasis and favorable growth conditions.

Ras-transformed mouse fibroblasts show lower expression of a gene encoding a methionine-transporting solute carrier and reduced methionine uptake than normal cells

Contrary to the behavior of cells perturbed by cysteine limitation or deprivation, methionine perturbation only weakly enhanced apoptosis in cells, slightly more in NIH-RAS cells (Fig 3A). Methionine limitation and deprivation increased ROS levels, methionine limitation having a significantly stronger effect in NIH-RAS cells (Fig 3B). As a likely consequence, GSH levels under limiting methionine were lower than in standard medium (Fig 3C) and inversely correlated with ROS levels (Fig 3D). By contrast, total glutathione levels (GSH+GSSG) under limiting methionine were similar to those found in standard condition, consistently with the presence in the medium of the glutathione precursor cysteine (Fig 3C). The high cell mortality under methionine deprivation hindered the measurement of glutathione levels. These results demonstrated that changes in ROS and reduced glutathione levels under methionine limitation (and, likely, in methionine deprivation) do not depend on alterations in glutathione biosynthesis. It is noteworthy that supplementation of 4 mM GSH to cells growing in methionine-free medium (-Met+GSH growth condition) resulted in decreased ROS levels in both cell lines (Fig 3B), however, neither NIH3T3 nor NIH-RAS cells were able to grow (Fig 1A, 1C and 1D), and NIH-RAS cells did not form *foci* (Fig 1E).

A GSH *versus* ROS plot (Fig 3D) confirms that GSH and ROS levels are inversely correlated (which is not unexpected) and further shows that limitation of sulfur-containing amino acids results in a more dramatic decrease of GSH as a function of ROS concentration in NIH-RAS compared to NIH3T3 cells.

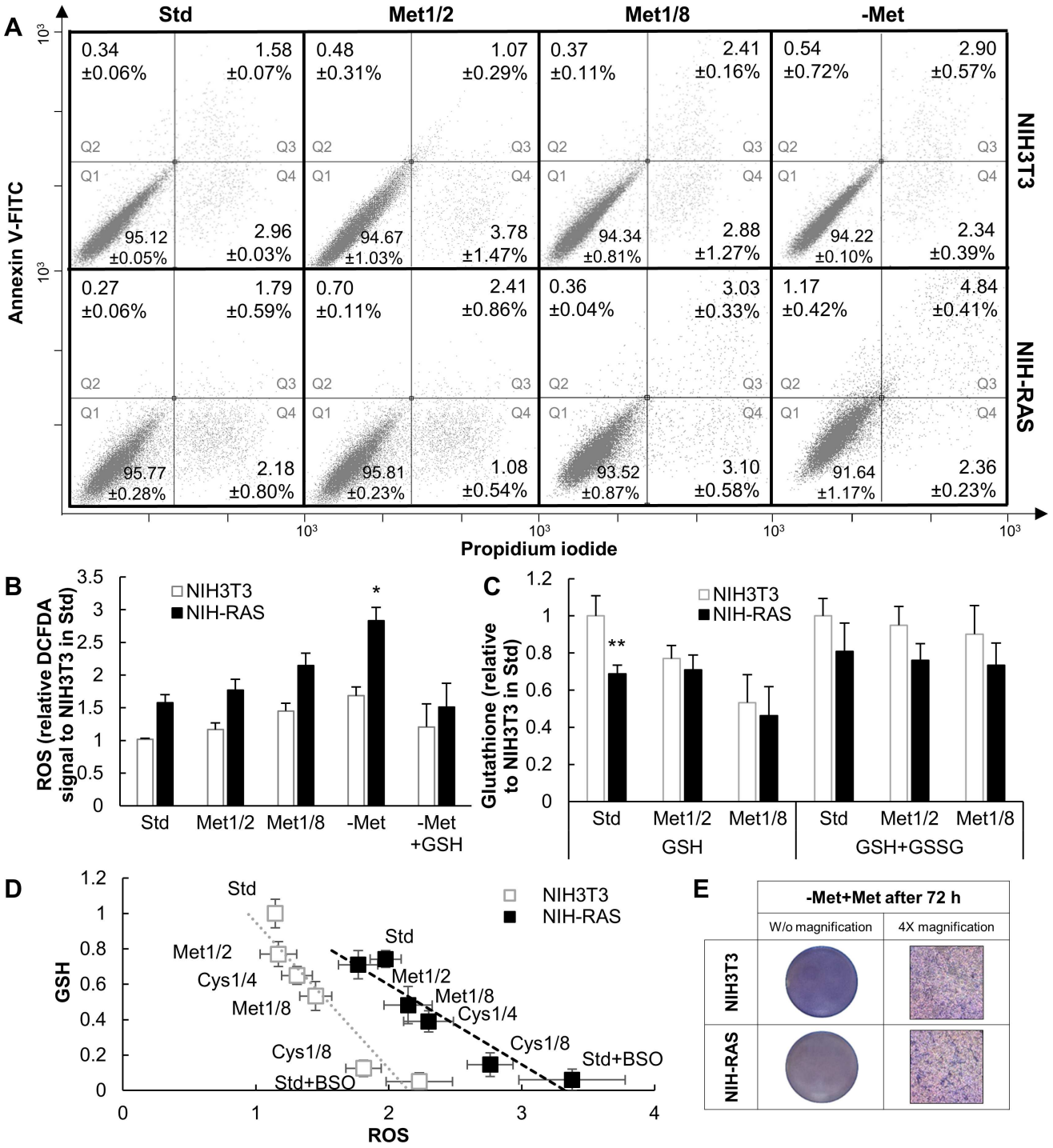

Fig 3. Viability and redox state under methionine deprivation and limitation. (A) Representative dot plots for NIH3T3 and NIH-RAS cells stained with Annexin V-FITC and propidium iodide and analyzed by FACS after 30 h of growth under conditions indicated. Q1 = quadrant 1, healthy cell; Q2 = quadrant 2, early apoptotic cells; Q3 = quadrant 3, late apoptotic cells; Q4 = quadrant 4, necrotic cells. The values reported for each quadrant are the mean +/- standard deviation of three independent experiments. (B) Relative ROS levels in NIH3T3 and NIH-RAS cells grown for 48 h under conditions indicated as determined by DCFDA (2',7'-dichlorodihydrofluorescein diacetate) staining. Each bar represents the mean of at least three independent experiments with error bars representing the standard deviation. (C) Reduced and total glutathione levels (measured as described in [55]) in NIH3T3 and NIH-RAS cells grown for 48 h under conditions indicated. Each bar represents the mean of at least three independent experiments with error bars representing the standard deviation *P<0.05; **P<0.01 (Student's *t*-test). (D) Negative correlation between reduced glutathione levels and ROS levels in NIH3T3 and NIH-RAS cells grown under conditions indicated. Linear regression curves are not parallel with a 99.9% confidence interval; Student's *t*-test. (E) Crystal violet staining of

NIH3T3 and NIH-RAS cells plated at the density of 9000 cells/cm^2, grown for 72 h under methionine deprivation and then for 48 h in standard medium.

doi:10.1371/journal.pone.0163790.g003

Supplementation of methionine to cells grown for 72 hours in methionine-free medium resulted in a significant growth recovery, reinforcing the notion that methionine deprivation exerted a cytostatic effect (arrest of cell proliferation) in both NIH3T3 and NIH-RAS cell lines (Fig 3E).

We analyzed genome-wide transcriptional profiling datasets for NIH3T3 and NIH-RAS cells (available in NCBI GEO database; accession GSM741354-GSM741361 for NIH3T3 cells and GSM741368-GSM741375 for NIH-RAS cells), previously obtained in our laboratory with an MG_U74Av2 Affymetrix Gene Chip [41] to identify the pattern of expression of genes encoding solute carriers [56]. The expression of four of these genes was significantly altered in Ras-transformed *versus* normal cells (S5 Fig). One of these genes is *Slc6a15* that encodes SBAT1, an amino acid transporter exhibiting strong preference for branched chain amino acids and methionine [57,58]. RT-PCR analysis of the expression of these four genes in normal and transformed fibroblasts (Fig 4A) validated Affymetrix results, clearly indicating that in NIH-RAS cells the expression of *Slc6a15* is down-regulated. Notably, over-expression in NIH-RAS cells of the Ras inhibitor GEF-DN determined a significant increase in the expression of *Slc6a15* (S3C Fig). Consistently with the strong, but not always complete reversion of Ras-dependent phenotypes induced by GEF-DN expression [45], up-regulation of *Slc6a15* expression is strong, but possibly not complete compared to NIH3T3 cells. Our data thus indicate that sensitivity to methionine limitation (S3A and S3B Fig) and expression of the SBAT1-encoding *Slc6a15* gene (S3C Fig) are regulated by the activation state of Ras.

To confirm that methionine transport is impaired in NIH-RAS cells as suggested by transcriptional analysis, we assayed methionine uptake in NIH3T3 and NIH-RAS cells by using a ^{35}S-methionine incorporation assay. NIH-RAS cells showed a significantly reduced incorporation of ^{35}S-methionine per unit of protein in both exponential and confluent growth conditions (Fig 4B). The combined transcriptional and biochemical analyses therefore suggest that down-regulation of *Slc6a15* gene expression and ensuing decreased methionine transport activity in Ras-transformed cells could be the reason for their higher sensitivity to methionine limitation.

Discussion

Cancer cells show metabolic dependencies that distinguish them from their normal counterparts [14]. Personalized targeting of cancer metabolism that accounts for differences in genetic, epigenetic and environmental factors (i.e., nutrient availability) may lead to major advances in tumor therapy [61]. In this paper we perform nutrient perturbation of the supply of the proteinogenic sulfur-containing amino acids methionine (a potential cysteine precursor) and cysteine (a GSH precursor) of normal, Ras-transformed and reverted mouse fibroblasts to highlight any differential biological response due to the activation state of Ras oncoprotein.

We show that cysteine deprivation causes cell proliferation arrest in both normal and Ras-transformed mouse fibroblasts even in presence of methionine in the culture media. Although databases of metabolic pathway maps, like KEGG ([62,63]), Human Metabolic Atlas ([64]), Reactome ([65]) or Recon2 ([66]) annotate methionine-to-cysteine conversion for all considered cell types, we show that the biosynthetic pathway of cysteine from methionine is not active in mouse fibroblasts (Fig 4D and S1 Fig). In fact, the methionine-to-cysteine pathway may be active only in cells from splanchnic organs, described as important sites of trans-methylation and trans-sulfuration of dietary methionine for cysteine synthesis [36]. These data are in

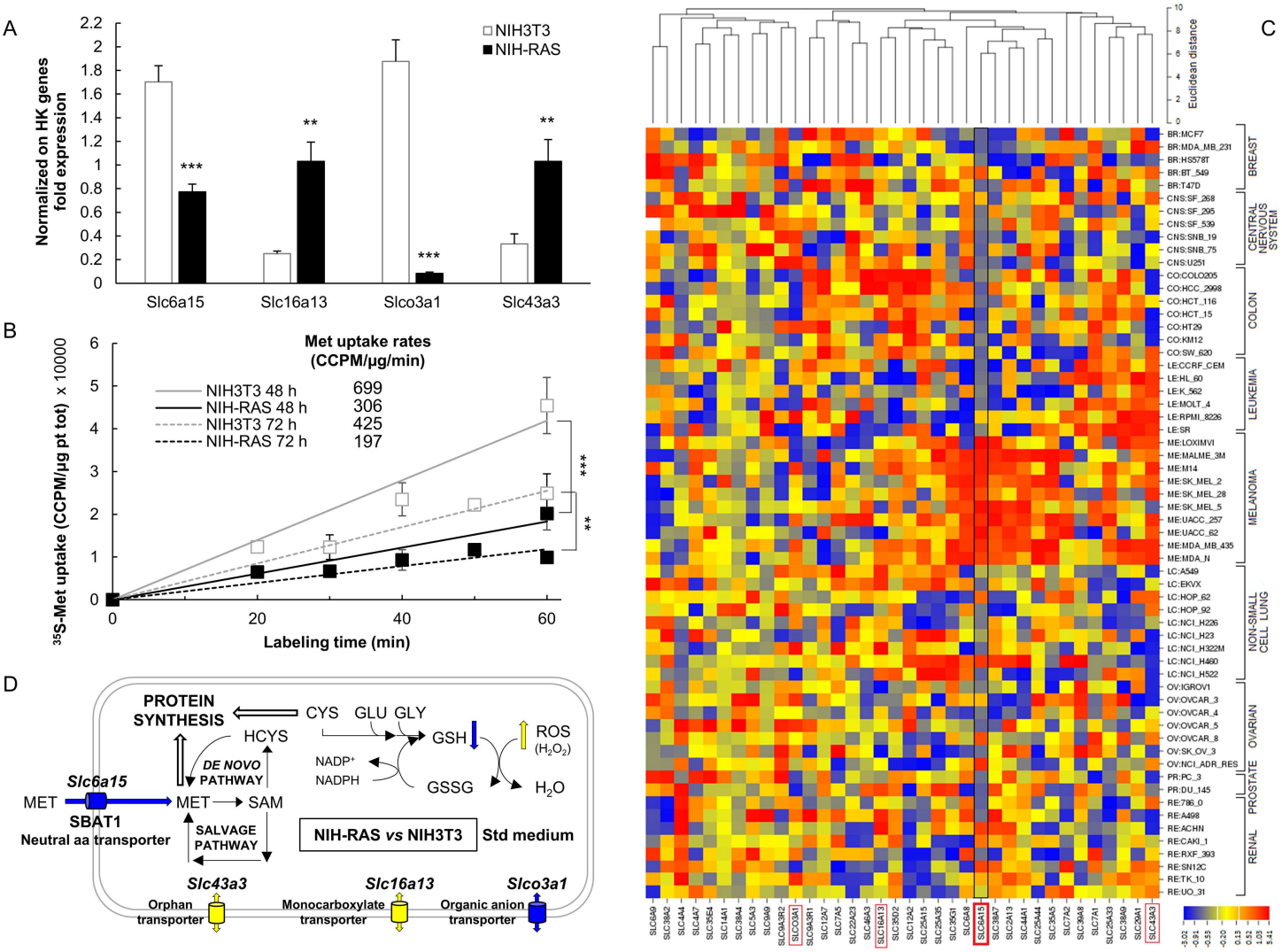

Fig 4. Methionine transport and solute carrier expression in mouse fibroblasts and in NCI-60 panel. (A) Semiquantitative RT-PCR results for NIH3T3 and NIH-RAS cells grown for 48 h in standard medium performed in triplicate on genes showing at least a two-fold change between NIH-RAS *vs* NIH3T3 cells in each of the two Affymetrix independent experiments (S5 Fig). (B) Labeled amino acid (^{35}S-methionine) uptake rate in exponential and confluent cells (48 and 72 h of growth in standard medium, respectively), measured after 20'-40'-60' (for exponential cells) and after 30'-50'-60' (for confluent cells) of labeling with 0.025 mCi/ml ^{35}S-Met. Radioactivity values, expressed as CCPM (corrected counts per minute), were normalized on total protein content and plotted against labeling time. Results are mean +/- standard deviation of three independent experiments. **P<0.01; ***P<0.001 (Student's *t*-test). (C) The mRNA expression data for the NCI-60 human tumor cell lines were retrieved from CellMiner relational database [59]. These expression data were inputted in CIMminer [60] to generate a heat map, as described in Materials and Methods. Here are highlighted the names of the genes whose expression was statistically different between NIH3T3 and NIH-RAS cells, with a particular emphasis on the data related to *SLC6A15* gene. (D) Concept map of cysteine and methionine metabolism in NIH3T3 and NIH-RAS cells.

doi:10.1371/journal.pone.0163790.g004

keeping with previous results demonstrating the dependency from cystine for growth of several human diploid cell lines (human fibroblasts), not able to utilize cystathionine *in lieu* of cystine, likely as a consequence of deficient cystathionase activity [67].

Cysteine deprivation is accompanied by an increase in ROS levels, which could be due to an enhancement of mitochondrial metabolism, and particularly of oxidative phosphorylation-associated proton leakage, induced by energetic stress and increased ATP-demand. This redox unbalance induced by nutritional stress has a pivotal role in up-regulating cellular repair processes and other protective systems (e.g., chaperones) and in driving autophagy, a major

mechanism by which starving cells mobilize and reallocate intracellular nutrient resources in order to maintain processes necessary for survival during growth-unfavorable conditions [68].

Cysteine deprivation causes apoptotic cell death. Apoptosis induced by cysteine-withdrawal is essentially due to increased oxidative stress caused by glutathione deprivation. Non-cysteine containing anti-oxidants effectively rescue oxidative stress, but cannot rescue cell death induced by cysteine deprivation. Supplementing reduced glutathione to cysteine-deprived cells not only restores redox homeostasis (and suppresses apoptosis), but also partially restores cell growth, indicating that in mouse fibroblasts GSH can be used as a cysteine reservoir to maintain protein synthesis under nutritional stress. However, high concentrations of GSH have a toxic effect, stressing the notion that to maximize viability a proper balance between ROS and antioxidants needs to be obtained [54]. Under standard cysteine conditions, severe inhibition of glutathione biosynthesis increases oxidative stress, but has moderate effects on viability. Growth defects induced by cysteine limitation are synergistically increased by inhibiting glutathione synthesis, the more so in NIH-RAS cells, indicating that the growth defects induced by cysteine limitation are largely–though not exclusively–due to cysteine utilization in the synthesis of glutathione. The differential sensitivity of NIH3T3 and NIH-RAS cells to both protective and toxic effects of glutathione may depend on the higher glutathione content of NIH3T3 cells.

The role of cysteine in cancer is controversial. While some authors report that human tumor growth is associated with decreased plasma levels of cysteine and homocysteine [69], more recently other authors demonstrated that antioxidants such as N-acetylcysteine (a direct precursor of cysteine) can accelerate tumor progression by decreasing ROS levels, DNA damage and p53 (a tumor suppressor gene) levels in cancer [70].

The increase in ROS levels under methionine deprivation in both NIH3T3 and NIH-RAS cell lines is not followed by a significant increase in neither apoptosis nor necrosis. While cell growth of normal and Ras-transformed cells was similarly compromised by methionine deprivation, methionine limitation mostly affected NIH-RAS cells.

Some cancers show methionine dependence, a feature firstly noted in xenograft rodents in response to a methionine-free diet [71]. Since then normal cells have been reported to be more resistant to external methionine limitation [34,72]. Methionine dependence might be correlated with inability of methionine-restricted cells to cope with demand for SAM, a major methionine product [34]. This "SAM-checkpoint" may protect cellular integrity and maintain epigenetic stability, since it stops cell cycle progression when intracellular SAM concentrations are insufficient to sustain the methylation reactions necessary for normal cell physiology [34]. Several drugs that target the enzymes that are involved in the post-translational modifications of histones and DNA, cell survival, proliferation and stem cell function [33,73,74] are being evaluated pre-clinically or in early-stage clinical trials [75].

Both a deficiency and an excess of the dietary levels of methionine can result in either genomic instability, which leads to diseases such as cancer, or changes in gene expression, which lead to alterations in metabolism [76], including improvement of hepatic lipid and glucose metabolism and induction of adiposity resistance [76]. Some cancer cells show a high activity of the methionine cycle that promotes chemo-resistance and evasion from apoptosis [77], whereas normal cells are relatively resistant to dietary methionine restriction: therapies to block the methionine cycle in transformed cells may thus represent a safe and effective strategy to fight cancer [39,77]. Dietary methionine restriction, used alone or in combination with other treatments, impaired cancer growth and carcinogenesis in human patients [78,79] or in rodents [80,81,82]. However, one *caveat* is that methionine restriction must be closely regulated, because methionine is an essential amino acid and a long use of diets extremely poor in methionine could be extremely toxic and cause death. Dietary methionine restriction (achievable in humans with a predominantly vegan diet) may have an additive healthy effect if

combined with calorie restriction, by limiting glucose [82]. The potential of methionine depletion in enhancing the anti-cancer effect of chemotherapeutic agents on drug-resistant tumors and cell lines has also been reported [83].

Sensitivity to methionine limitation of mouse fibroblasts and expression of the SBAT1-encoding *Slc6a15* gene are regulated by the activation state of Ras (Fig 4A and S3 Fig), resulting in decreased methionine uptake in NIH-RAS (Fig 4B). Remarkably, expression of the ortholog human gene—*SLC6A15*—is mostly down-regulated in the NCI-60 cells panel, the US National Cancer Institute (NCI) panel of 60 human cancer cell lines grown in culture [84] (Fig 4C). An exception is represented by melanoma cells, in which *SLC6A15* is highly up-regulated. Therefore, the use of methionine uptake as a marker for proliferative activity in substitution of fluoro-deoxyglucose [85,86], or therapeutic use of dietary methionine restriction would benefit from knowledge of the expression of methionine transporters.

Slc6a15 and its human ortholog belong to a large family (over 450 members) of solute carrier proteins (SLCs) controlling import/export of nutrients, cofactors, ions and many drugs. While many SLCs have not yet well characterized, a quarter of their encoding genes has been associated with human diseases and 26 different SLCs are the targets of known drugs, or drugs in development [87,88]. An increase in amino acid transport may be expected in cancer, most likely as the result of increased amino acid demand for energy, protein synthesis and cell division: surprisingly, S5 Fig shows that SLC-encoding genes down-regulated in NIH-RAS compared to NIH3T3 cells are enriched in genes encoding amino acid transport, particularly of neutral amino acids (e.g. the SBAT1-encoding *Slc6a15* gene).

In conclusion, we show that limitation of sulfur-containing amino acids results in a more dramatic perturbation of the oxidoreductive balance in *K-ras*-transformed cells compared to NIH3T3 cells (Fig 3D). Growth defects induced by cysteine limitation in mouse fibroblasts are largely–though not exclusively–due to cysteine utilization in the synthesis of glutathione, mouse fibroblasts requiring an exogenous cysteine source for protein synthesis. We show for the first time a correlation between Ras-transformation and defects in methionine transport that affect the dependence of *K-ras*-transformed mouse fibroblasts for this amino acid. Therapeutic regimens of cancer involving modulation of methionine metabolism could be more effective in cells with limited methionine transport capability. To further understand nutrient interactions (such as methionine and glucose restriction), to study the correlation between methionine metabolism and cell signaling and to design a precision medicine approach taking into account the specific nutritional dependencies of a patient's cancer, we consider essential to unravel the underlying networks by using an integrated, Systems Biology approach.

Materials and Methods

Cell culture

Three cells lines have been used in this paper, namely normal NIH3T3 mouse fibroblasts (obtained from the ATCC, Manassas, VA, USA), a K-Ras-transformed normal-derived cell line -that we refer to as NIH-RAS [44,89]- and NIH-RAS cells stably transfected with a pcDNA3-based vector expressing a dominant negative mutant of the Ras-specific guanine nucleotide exchange factor RasGRF1 (RasGRF1W1056E, here simply named GEF-DN) with Ras-sequestering property [44,45,90]. These cell lines proved to be a valid cellular model for studying Ras-dependent transcriptional reprogramming [41], and metabolic rewiring [23,42,43]. Both control and *ras*-transformed NIH3T3 have been passaged a similar number of times, taking care to refreeze the cell lines immediately and to use them for a limited number of passages. The cell lines are periodically assayed to check that the major properties of the cells do not change over time, that the major transformation-related phenotypes are retained and *ras*-dependent (see S2

Fig and accompanying text). The cell lines were routinely grown in Dulbecco's modified Eagle's medium (Invitrogen Inc., Carlsbad, CA, USA) containing 10% newborn calf serum, 4 mM glutamine, 100 U/ml penicillin and 100 mg/ml streptomycin (standard medium), at 37°C in a humidified atmosphere of 5% CO_2. Cells were passaged using trypsin-ethylenediaminetetraacetic acid (EDTA) (Invitrogen Inc., Carlsbad, CA, USA) and maintained in culture before experimental manipulation.

Cell proliferation analysis

Cells were plated at the density of 3000 cells/cm^2 in standard medium and incubated overnight at 37°C and 5% CO_2. After 18 h, cells were washed twice with phosphate-buffered saline (PBS) and, to verify the response to the cysteine or methionine deprivation, cells were incubated in medium without cysteine and methionine (Invitrogen Inc., Carlsbad, CA, USA), possibly supplemented with limiting concentration of cysteine (0.025, 0.05, 0.1 mM) or methionine (0.025, 0.1 mM) (Sigma Aldrich Inc.) or with antioxidants glutathione (0.08, 0.2, 0.8, 2, 4, 16 mM) or MitoTEMPO (10 μM) (Sigma Aldrich Inc.). To measure cell proliferation, cells were treated with trypsin at 0, 3, 6, 24, 30, 48, 54, 72 hours after medium change. Viable (i.e., unstained) cells were counted in a Bürker chamber after staining with 0.5% trypan blue. In amino acid refeeding and *foci* formation experiments, qualitative evaluation of cell proliferation was obtained by staining with 0.2% Crystal violet (diluted in water from Giemsa Stain 0.4%, Sigma Aldrich Inc.). After 45 minutes of incubation in the dark at RT, cells were washed twice with water, photographed, and counted.

Foci formation assay

Cells were plated at the density of 30 cells/cm^2 in standard medium and incubated overnight at 37°C and 5% CO_2. After 18 h, cells were washed twice with phosphate-buffered saline (PBS) and, to test the ability of forming *foci* of NIH3T3 and NIH-RAS under nutritional modulation, cells were incubated for 9 days in medium without cysteine and methionine (Invitrogen Inc., Carlsbad, CA, USA), possibly supplemented with limiting concentration of cysteine (0.025, 0.05 mM) or methionine (0.025, 0.1 mM) (Sigma Aldrich Inc.) or with 4 mM reduced glutathione (Sigma Aldrich Inc.). After 9 days, cells were washed with PBS and fixed with paraformaldehyde 4%, then washed with ice-cold PBS and stained with 0.2%. Crystal violet, photographed as described above and the number of *foci* counted.

Determination of intracellular ROS

Intracellular accumulation of H_2O_2 and $O2^{\bullet -}$ was determined after 48 h from medium change with 2',7'-dichlorodihydrofluor esceine diacetate (Sigma Aldrich Inc.). The cells were incubated for 30 minutes at 37°C with H_2DCFDA 10 mM, treated with trypsin, resuspended in PBS supplemented with NCS 10% (Invitrogen Inc., Carlsbad, CA, USA) and acquired by FACScan (Becton-Dickinson), using the Cell Quest software (BD Bioscience). The percentage of ROS-producing cells was calculated for each sample and corrected for autofluorescence obtained from samples of unlabeled cells.

Apoptosis Assay

Cells were plated at the density of 3000 cells/cm^2 in standard medium and incubated overnight at 37°C and 5% CO_2. After 18 h, cells were washed twice with phosphate-buffered saline (PBS) and incubated for 30 hours in medium without cysteine and methionine (Invitrogen Inc., Carlsbad, CA, USA), possibly supplemented with limiting concentrations of cysteine (0.025,

0.05 mM) or methionine (0.025 and 0.1 mM) (Sigma Aldrich Inc.) or with antioxidants glutathione (4 mM) or MitoTEMPO (10 μM) (Sigma Aldrich Inc.). For apoptosis analysis, 1×10^6 cells (adherent and in suspension cells) were collected, stained with Annexin V-FITC (Immunotools, GmbH) and propidium iodide (Sigma Aldrich Inc.) and analyzed by FACScan (Becton-Dickinson) using the FL1 and FL2 channels. Data analysis was performed with Flowing Software.

Determination of glutathione levels

For reduced and total glutathione measurements, cells were plated at the density of 3000 cells/cm^2 in standard medium and incubated overnight at 37°C and 5% CO_2. After 18 h, cells were washed twice with phosphate-buffered saline (PBS) and incubated for 48 h in standard medium or under limitation of cysteine or methionine. Cells were then treated with trypsin, collected, washed twice with PBS and lysed through freeze-and-thaw cycles. Samples were deproteinized with a 5% 5-sulfosalicylic acid solution, centrifuged to remove the precipitated protein and assayed for glutathione. GSH measurement was an optimization of Tietze's enzymatic recycling method [55], in which GSH is oxidized by the sulfhydryl reagent 5,5'-dithio-bis (2-nitrobenzoic acid) (DTNB) to form the yellow derivative 5'-thio-2-nitrobenzoic acid (TNB), measurable at 412 nm and the glutathione disulfide (GSSG) formed is recycled to GSH by glutathione reductase in the presence of NADPH. The amount of glutathione in the samples was determined through a standard curve of reduced glutathione. Glutathione levels were normalized to protein content measured by Bradford assay (Bio-Rad reagent) on an aliquot of cell extract collected before deiproteinization.

Methionine transport assays

NIH3T3 and NIH-RAS cells were seeded at the density of 3000 cells/cm^2 and incubated overnight at 37°C and 5% CO_2, then medium change was done after 18 h. At 48 h (exponential growth condition) and 72 h (confluent growth condition), standard medium was replaced with 0.4 ml labeling medium (cysteine and methionine-free medium + 0.025 mCi/ml ^{35}S-Met, PerkinElmer), that was removed after 20-40-60 minutes or 30-50-60 minutes at 37°C and 5% CO_2. Cells were then washed once with cold PBS and scraped after adding lysis buffer. Cell lysates were centrifuged and an aliquot spotted on Whatman Glass Microfiber filters (Sigma Aldrich Inc.). To the remaining volume, 1 volume of cold 20% TCA (Sigma Aldrich Inc.) was added and, after 30 minutes in ice, samples were spotted on filters and washed twice with cold 10% TCA and ethanol (Sigma Aldrich Inc.). Air-dried filters were transferred to vials containing Ultima Gold MV scintillation fluid (PerkinElmer) and radioactivity measured in a beta-counter (Wallac Microbeta Trilux, PerkinElmer). Averages of technical triplicates for cell lysates (representing amino acid uptake) were calculated and the resulting values were normalized on total protein content, measured by using QuantiPro™ BCA Assay Kit (Sigma Aldrich Inc.).

RNA extraction and semi quantitative RT-PCR analysis

Cells were plated at the density of 3000 cells/cm^2 in standard medium and incubated overnight at 37°C and 5% CO_2. After 18 h, cells were washed twice with phosphate-buffered saline (PBS) and incubated for 48 h in standard medium. RNA was then extracted from cells by using the Quick-RNA™ MicroPrep kit (Zymo Research). Total RNA was reverse-transcribed with oligo-dT by using the iScript cDNA Synthesis Kit (Bio-Rad Laboratories). The RT product (0.5 μg) was amplified with primer pairs specific for the genes studied. As internal control of PCR assays, specific primers for 18S and β-actin transcripts were used. Primers used: *Slc6a15*

forward: 5'-GCATCGGAAGAATTTCTGAGC-3', reverse: 5'-AGCGACGAATGATG AACAC C-3'; *Slco3a1* forward: 5'-GAGTTAGCCTA TCCTTGTTG-3', reverse: 5'-GACAGAACATCA CCTTACAA-3'; *Slc16a13* forward: 5'-ACCTGAGTATTGGGCTGCTG-3', reverse: 5'-CCA TGGTCGGAGTGAAGGT-3'; *Slc43a3* forward: 5'-CACCTTGTTGACTGGACTCTTG-3', reverse: 5'-CCAGGGTAAAGATG AGTGAGAAC-3'.

Generation of the heat map of solute carrier gene expression profiles in NCI-60 cell lines

The heat map, or Clustered Image Map (CIM), was generated with CIMminer by selecting the one matrix option. The rows of the matrix were the different cell lines and the columns (each representing a solute carrier gene) were clustered according to Average Linkage algorithm and to Euclidean distance measure. Data values were mapped to colors using the quantile method: the weight range of data values was divided into intervals each containing approximately the same number of data points, thus effectively spreading out the color differences between data values that were present in regions with a large number of values.

Supporting Information

S1 Fig. Methionine and cysteine metabolism in mouse fibroblasts. Methionine is partitioned between protein synthesis, *de novo* and recycling pathway, where it is converted to S-adenosylmethionine (SAM). SAM is converted to S-adenosylhomocysteine (SAH) during methylation of DNA and a large range of proteins and other molecules. SAH is then hydrolyzed to homocysteine (Hcy) in a reversible reaction. Under normal conditions, approximately 50% of Hcy is re-methylated to form methionine that, in most tissues, occurs via methionine synthase. In the trans-sulfuration pathway, Hcy is metabolized to form cystathionine, which is the immediate precursor to cysteine. Besides from methionine, cysteine can be synthesized from serine. The sulfur is derived from methionine, which is converted to homocysteine through the intermediate SAM. Cystathionine beta-synthase then combines homocysteine and serine to form the asymmetrical thioether cystathionine. The enzyme cystathionine gamma-lyase converts the cystathionine into cysteine and alpha-ketobutyrate. The trans-sulfuration pathway is not active in all cells, and in human is active essentially only in cells from splanchnic organs. Here we demonstrated that mouse embryonic fibroblasts are not able to convert methionine into cysteine. For this reason the trans-sulfuration reaction is highlighted in grey.
(PDF)

S2 Fig. Ras and MAPK activation state and expression levels in cellular models used in the paper: NIH3T3, NIH-RAS, NIH-RAS pGEF-DN and NIH-RAS pcDNA3. Expression levels of Total Ras proteins (A) and MAPKs p42 and p44 (B) in cell lysates of pull down assay. Antibodies directed against Ras (sc259 Santa Cruz), Phospho-p44/42 MAPK (Erk1/2) (Thr202/Tyr204) (Cell Signaling #9101) and p44/42 MAPK (Erk1/2) (Cell Signaling #9102) were used. (C) Ras–GTP eluted from GST–RBD–glutathione–sepharose, pre-incubated with cell lysates. Pull down assay was performed as described in [7]. (D) Quantification of the Ras–GTP amount after normalization over total Ras. Data are normalized over the Ras-GTP/total Ras ratio in NIH3T3 taken equal to 100. Data shown are mean +/- standard deviation of two independent experiments. (E) Morphological analysis of the different cell lines. (F) Phospho-p44/42 MAPK level in cell lysates, determined by ELISA assay performed using PathScan® Phospho-p44/42 MAPK (Thr202/Tyr204) (Cell Signaling). Data shown are mean +/- standard deviation of two independent experiments. (F) 100X magnification of a *focus* generated by NIH-RAS cells in

foci formation assay shown in Fig 1.
(PDF)

S3 Fig. Over-expression of GEF-DN reverts sensitivity to methionine limitation in NIH-RAS cells and partially rescues the defect in the expression of *Slc6a15* gene encoding methionine transporter SBAT1. (A) Cell proliferation of NIH3T3, NIH-RAS, NIH-RAS pGEF-DN and NIH-RAS pcDNA3 cells grown in media with different concentrations of methionine and counted daily for 72 h of growth under conditions indicated. Plotted data are mean +/- standard deviation. computed from three independent experiments. (B) Relative to t = 0 cell proliferation of NIH3T3, NIH-RAS, NIH-RAS pGEF-DN and NIH-RAS pcDNA3 cells grown for 72 h in media with different concentrations of methionine, as indicated in (A). Part of the data in (B) are present in Fig 1D. (C) Semi-quantitative RT-PCR results for NIH3T3, NIH-RAS, NIH-RAS pGEF-DN and NIH-RAS pcDNA3 cells grown for 48 h in standard medium performed in triplicate on genes showing at least a two-fold change between NIH-RAS *vs*. NIH3T3 cells in each of the two Affymetrix independent experiments (S5 Fig). $^{*}P<0.05$; $^{**}P<0.01$; $^{***}P<0.001$ (Student's *t*-test).
(PDF)

S4 Fig. Cell proliferation and qualitative ROS levels under different methionine concentrations and in cysteine-limiting or -depleted medium (possibly supplemented with antioxidants glutathione and MitoTEMPO or with GSH synthesis inhibitor BSO). For all the experiments, MitoTEMPO and buthionine sulfoximine (BSO) were used at the concentration of 10 μM and 100 μM. (A-B) Cell proliferation of NIH3T3 and NIH-RAS cells grown in media supplemented with different concentrations of methionine and cysteine with or without antioxidants glutathione or MitoTEMPO and counted after 72 h (A) and 30 h (B) of growth under conditions indicated. Part of the data in (A) are present in Fig 1D. Plotted data are mean +/- standard deviation computed from three independent experiments. $^{*}P<0.05$ (Student's *t*-test). (C) Cell proliferation of NIH3T3 and NIH-RAS cells under conditions indicated. (D) Qualitative evaluation of ROS levels in NIH3T3 and NIH-RAS cells upon staining with DCFDA and analysis with a fluorescence microscope.
(PDF)

S5 Fig. Solute carriers differentially expressed between NIH3T3 and NIH-RAS cells. Genome-wide transcriptional profiling datasets for NIH3T3 and NIH-RAS cells (available in NCBI GEO database; accession GSM741354-GSM741361 for NIH3T3 cells and GSM741368-GSM741375 for NIH-RAS cells), previously obtained in our laboratory with an MG_U74Av2 Affymetrix Gene Chip [41], were filtered for all genes encoding for solute carriers. Then, to identify genes whose expression was significantly altered in Ras-transformed *versus* normal cells (here represented in bold), a two-fold and a <0.05 cut-offs on Fold Changes and on *p*-values were used, respectively. In this Figure are represented all transporter genes with a fold change ≥ 2 (about 20% of all transporter genes) irrespective of their *p*-values. Gene Ontology (GO) enrichment based on molecular function was performed with GoTermFinder (http://go.princeton.edu/cgi-bin/GOTermFinder) and genes encoding for amino acid transporters were colored in magenta, while genes encoding for ion transporters were colored in grey.
(PDF)

S1 Table. Mass duplication times under different nutritional perturbations. Mass duplication times (MDT) for NIH3T3 and NIH-RAS under different methionine or cysteine concentrations (possibly supplemented with GSH) were calculated on semi-logarithmic curves represented in Fig 1A and 1B. Then, Student's *t*-test was performed on linear regression curves

for each nutritional condition that allowed cell growth. A = not parallel to linear regression curve of NIH-RAS cells in standard medium (99% CI); B = not parallel to linear regression curve of NIH3T3 cells in standard medium (99.9% CI); C = not parallel to linear regression curve of NIH-RAS cells in standard medium (99.9% CI); D = not parallel to linear regression curve of NIH3T3 cells in standard medium (99% CI); E = not parallel to linear regression curve of NIH3T3 cells in standard medium (99.9% CI). CI = confidence interval.
(PDF)

Acknowledgments

The Authors wish to acknowledge Prof. Lilia Alberghina for continuous support. The financial support of the MIUR grant SysBioNet—Italian Roadmap for ESFRI Research Infrastructures—to SYSBIO Centre of Systems Biology is gratefully acknowledged.

Author Contributions

Conceptualization: GDS ES MV.

Data curation: GDS ES.

Formal analysis: GDS ES MV.

Funding acquisition: MV.

Investigation: GDS MS.

Project administration: ES MV.

Supervision: ES MV.

Validation: GDS ES.

Visualization: GDS ES MV.

Writing – original draft: GDS ES.

Writing – review & editing: GDS ES MV.

References

1. Downward J (2003) Role of receptor tyrosine kinases in G-protein-coupled receptor regulation of Ras: transactivation or parallel pathways? The Biochemical journal 376: e9–10. doi: 10.1042/BJ20031745 PMID: 14656216
2. Kahn S, Yamamoto F, Almoguera C, Winter E, Forrester K, et al. (1987) The c-K-ras gene and human cancer (review). Anticancer research 7: 639–652. PMID: 3310850
3. Schubbert S, Shannon K, Bollag G (2007) Hyperactive Ras in developmental disorders and cancer. Nature reviews Cancer 7: 295–308. doi: 10.1038/nrc2109 PMID: 17384584
4. Sever R, Brugge JS (2015) Signal transduction in cancer. Cold Spring Harbor perspectives in medicine 5. doi: 10.1101/cshperspect.a006098 PMID: 25833940
5. Forbes SA, Bindal N, Bamford S, Cole C, Kok CY, et al. (2011) COSMIC: mining complete cancer genomes in the Catalogue of Somatic Mutations in Cancer. Nucleic acids research 39: D945–950. doi: 10.1093/nar/gkq929 PMID: 20952405
6. Adjei AA, Cohen RB, Franklin W, Morris C, Wilson D, et al. (2008) Phase I pharmacokinetic and pharmacodynamic study of the oral, small-molecule mitogen-activated protein kinase kinase 1/2 inhibitor AZD6244 (ARRY-142886) in patients with advanced cancers. Journal of clinical oncology: official journal of the American Society of Clinical Oncology 26: 2139–2146. doi: 10.1200/JCO.2007.14.4956 PMID: 18390968

7. Sacco E, Spinelli M, Vanoni M (2012) Approaches to Ras signaling modulation and treatment of Ras-dependent disorders: a patent review (2007—present). Expert opinion on therapeutic patents 22: 1263–1287. doi: 10.1517/13543776.2012.728586 PMID: 23009088
8. McCormick F (2015) KRAS as a Therapeutic Target. Clinical cancer research: an official journal of the American Association for Cancer Research 21: 1797–1801. doi: 10.1158/1078-0432.ccr-14-2662 PMID: 25878360
9. Shima F, Matsumoto S, Yoshikawa Y, Kawamura T, Isa M, et al. (2015) Current status of the development of Ras inhibitors. Journal of biochemistry 158: 91–99. doi: 10.1093/jb/mvv060 PMID: 26100833
10. Singh H, Longo DL, Chabner BA (2015) Improving Prospects for Targeting RAS. Journal of clinical oncology: official journal of the American Society of Clinical Oncology 33: 3650–3659. doi: 10.1200/JCO.2015.62.1052 PMID: 26371146
11. Hanahan D, Weinberg RA (2011) Hallmarks of cancer: the next generation. Cell 144: 646–674. doi: 10.1016/j.cell.2011.02.013 PMID: 21376230
12. Levine AJ, Puzio-Kuter AM (2010) The control of the metabolic switch in cancers by oncogenes and tumor suppressor genes. Science 330: 1340–1344. doi: 10.1126/science.1193494 PMID: 21127244
13. Alberghina L, Gaglio D, Gelfi C, Moresco RM, Mauri G, et al. (2012) Cancer cell growth and survival as a system-level property sustained by enhanced glycolysis and mitochondrial metabolic remodeling. Frontiers in physiology 3: 362. doi: 10.3389/fphys.2012.00362 PMID: 22988443
14. Kimmelman AC (2015) Metabolic Dependencies in RAS-Driven Cancers. Clinical cancer research: an official journal of the American Association for Cancer Research 21: 1828–1834. doi: 10.1158/1078-0432.CCR-14-2425 PMID: 25878364
15. DeBerardinis RJ, Lum JJ, Hatzivassiliou G, Thompson CB (2008) The biology of cancer: metabolic reprogramming fuels cell growth and proliferation. Cell metabolism 7: 11–20. doi: 10.1016/j.cmet.2007.10.002 PMID: 18177721
16. Warburg O (1956) On the origin of cancer cells. Science 123: 309–314. doi: 10.1126/science.123.3191.309 PMID: 13298683
17. Hsu PP, Sabatini DM (2008) Cancer cell metabolism: Warburg and beyond. Cell 134: 703–707. doi: 10.1016/j.cell.2008.08.021 PMID: 18775299
18. Ying H, Kimmelman AC, Lyssiotis CA, Hua S, Chu GC, et al. (2012) Oncogenic Kras maintains pancreatic tumors through regulation of anabolic glucose metabolism. Cell 149: 656–670. doi: 10.1016/j.cell.2012.01.058 PMID: 22541435
19. Weinberg F, Hamanaka R, Wheaton WW, Weinberg S, Joseph J, et al. (2010) Mitochondrial metabolism and ROS generation are essential for Kras-mediated tumorigenicity. Proceedings of the National Academy of Sciences of the United States of America 107: 8788–8793. doi: 10.1073/pnas.1003428107 PMID: 20421486
20. Baracca A, Chiaradonna F, Sgarbi G, Solaini G, Alberghina L, et al. (2010) Mitochondrial Complex I decrease is responsible for bioenergetic dysfunction in K-ras transformed cells. Biochimica et biophysica acta 1797: 314–323. doi: 10.1016/j.bbabio.2009.11.006 PMID: 19931505
21. Brosnan JT (2003) Interorgan amino acid transport and its regulation. The Journal of nutrition 133: 2068S–2072S. PMID: 12771367
22. DeBerardinis RJ, Mancuso A, Daikhin E, Nissim I, Yudkoff M, et al. (2007) Beyond aerobic glycolysis: transformed cells can engage in glutamine metabolism that exceeds the requirement for protein and nucleotide synthesis. Proceedings of the National Academy of Sciences of the United States of America 104: 19345–19350. doi: 10.1073/pnas.0709747104 PMID: 18032601
23. Gaglio D, Metallo CM, Gameiro PA, Hiller K, Danna LS, et al. (2011) Oncogenic K-Ras decouples glucose and glutamine metabolism to support cancer cell growth. Molecular systems biology 7: 523. doi: 10.1038/msb.2011.56 PMID: 21847114
24. Metallo CM, Gameiro PA, Bell EL, Mattaini KR, Yang J, et al. (2012) Reductive glutamine metabolism by IDH1 mediates lipogenesis under hypoxia. Nature 481: 380–384. doi: 10.1038/nature10602 PMID: 22101433
25. Son J, Lyssiotis CA, Ying H, Wang X, Hua S, et al. (2013) Glutamine supports pancreatic cancer growth through a KRAS-regulated metabolic pathway. Nature 496: 101–105. doi: 10.1038/nature12040 PMID: 23535601
26. Fendt SM, Bell EL, Keibler MA, Olenchock BA, Mayers JR, et al. (2013) Reductive glutamine metabolism is a function of the alpha-ketoglutarate to citrate ratio in cells. Nature communications 4: 2236. doi: 10.1038/ncomms3236 PMID: 23900562
27. Chen L, Cui H (2015) Targeting Glutamine Induces Apoptosis: A Cancer Therapy Approach. International journal of molecular sciences 16: 22830–22855. doi: 10.3390/ijms160922830 PMID: 26402672

28. Wise DR, Thompson CB (2010) Glutamine addiction: a new therapeutic target in cancer. Trends in biochemical sciences 35: 427–433. doi: 10.1016/j.tibs.2010.05.003 PMID: 20570523

29. Wang Q, Beaumont KA, Otte NJ, Font J, Bailey CG, et al. (2014) Targeting glutamine transport to suppress melanoma cell growth. International journal of cancer 135: 1060–1071. doi: 10.1002/ijc.28749 PMID: 24531984

30. Bhutia YD, Ganapathy V (2015) Glutamine transporters in mammalian cells and their functions in physiology and cancer. Biochimica et biophysica acta. doi: 10.1016/j.bbamcr.2015.12.017 PMID: 26724577

31. Oda K, Hosoda N, Endo H, Saito K, Tsujihara K, et al. (2010) L-type amino acid transporter 1 inhibitors inhibit tumor cell growth. Cancer science 101: 173–179. doi: 10.1111/j.1349-7006.2009.01386.x PMID: 19900191

32. Finkelstein JD (1990) Methionine metabolism in mammals. The Journal of nutritional biochemistry 1: 228–237. PMID: 15539209

33. Lu SC, Mato JM (2008) S-Adenosylmethionine in cell growth, apoptosis and liver cancer. Journal of gastroenterology and hepatology 23 Suppl 1: S73–77. doi: 10.1111/j.1440-1746.2007.05289.x PMID: 18336669

34. Borrego SL, Fahrmann J, Datta R, Stringari C, Grapov D, et al. (2016) Metabolic changes associated with methionine stress sensitivity in MDA-MB-468 breast cancer cells. Cancer Metab 4: 9. doi: 10.1186/s40170-016-0148-6 PMID: 27141305

35. Ingenbleek Y, Kimura H (2013) Nutritional essentiality of sulfur in health and disease. Nutr Rev 71: 413–432. doi: 10.1111/nure.12050 PMID: 23815141

36. Riedijk MA, van Beek RH, Voortman G, de Bie HM, Dassel AC, et al. (2007) Cysteine: a conditionally essential amino acid in low-birth-weight preterm infants? The American journal of clinical nutrition 86: 1120–1125. PMID: 17921391

37. Aoyama K, Watabe M, Nakaki T (2008) Regulation of neuronal glutathione synthesis. Journal of pharmacological sciences 108: 227–238. doi: 10.1254/jphs.08r01cr PMID: 19008644

38. Lu SC (2009) Regulation of glutathione synthesis. Molecular aspects of medicine 30: 42–59. doi: 10.1016/j.mam.2008.05.005 PMID: 18601945

39. Cavuoto P, Fenech MF (2012) A review of methionine dependency and the role of methionine restriction in cancer growth control and life-span extension. Cancer treatment reviews 38: 726–736. doi: 10.1016/j.ctrv.2012.01.004 PMID: 22342103

40. Stipanuk MH (2004) Sulfur amino acid metabolism: pathways for production and removal of homocysteine and cysteine. Annual review of nutrition 24: 539–577. doi: 10.1146/annurev.nutr.24.012003.132418 PMID: 15189131

41. Balestrieri C, Vanoni M, Hautaniemi S, Alberghina L, Chiaradonna F (2012) Integrative transcriptional analysis between human and mouse cancer cells provides a common set of transformation associated genes. Biotechnology advances 30: 16–29. doi: 10.1016/j.biotechadv.2011.06.013 PMID: 21736933

42. Palorini R, Votta G, Pirola Y, De Vitto H, De Palma S, et al. (2016) Protein Kinase A Activation Promotes Cancer Cell Resistance to Glucose Starvation and Anoikis. PLoS genetics 12: e1005931. doi: 10.1371/journal.pgen.1005931 PMID: 26978032

43. Gaglio D, Valtorta S, Ripamonti M, Bonanomi M, Damiani C, et al. (2016) Divergent in vitro/in vivo responses to drug treatments of highly aggressive NIH-Ras cancer cells: a PET imaging and metabolomics-mass-spectrometry study. Oncotarget. doi: 10.18632/oncotarget.10470 PMID: 27409831

44. Bossu P, Vanoni M, Wanke V, Cesaroni MP, Tropea F, et al. (2000) A dominant negative RAS-specific guanine nucleotide exchange factor reverses neoplastic phenotype in K-ras transformed mouse fibroblasts. Oncogene 19: 2147–2154. doi: 10.1038/sj.onc.1203539 PMID: 10815806

45. Chiaradonna F, Sacco E, Manzoni R, Giorgio M, Vanoni M, et al. (2006) Ras-dependent carbon metabolism and transformation in mouse fibroblasts. Oncogene 25: 5391–5404. doi: 10.1038/sj.onc.1209528 PMID: 16607279

46. Mates JM, Perez-Gomez C, Nunez de Castro I, Asenjo M, Marquez J (2002) Glutamine and its relationship with intracellular redox status, oxidative stress and cell proliferation/death. The international journal of biochemistry & cell biology 34: 439–458. doi: 10.1016/s1357-2725(01)00143-1 PMID: 11906817

47. Franco R, Schoneveld OJ, Pappa A, Panayiotidis MI (2007) The central role of glutathione in the pathophysiology of human diseases. Archives of physiology and biochemistry 113: 234–258. doi: 10.1080/13813450701661198 PMID: 18158646

48. Alberghina L, Gaglio D (2014) Redox control of glutamine utilization in cancer. Cell death & disease 5: e1561. doi: 10.1038/cddis.2014.513 PMID: 25476909

49. Trachootham D, Zhou Y, Zhang H, Demizu Y, Chen Z, et al. (2006) Selective killing of oncogenically transformed cells through a ROS-mediated mechanism by beta-phenylethyl isothiocyanate. Cancer cell 10: 241–252. doi: 10.1016/j.ccr.2006.08.009 PMID: 16959615

50. Sies H (1999) Glutathione and its role in cellular functions. Free radical biology & medicine 27: 916–921. doi: 10.1016/s0891-5849(99)00177-x

51. Dickinson DA, Forman HJ (2002) Cellular glutathione and thiols metabolism. Biochemical pharmacology 64: 1019–1026. doi: 10.1016/s0006-2952(02)01172-3 PMID: 12213601

52. Wu G, Fang YZ, Yang S, Lupton JR, Turner ND (2004) Glutathione metabolism and its implications for health. The Journal of nutrition 134: 489–492. PMID: 14988435

53. Estrela JM, Ortega A, Obrador E (2006) Glutathione in cancer biology and therapy. Critical reviews in clinical laboratory sciences 43: 143–181. doi: 10.1080/10408360500523878 PMID: 16517421

54. Poljsak B, Suput D, Milisav I (2013) Achieving the balance between ROS and antioxidants: when to use the synthetic antioxidants. Oxidative medicine and cellular longevity 2013: 956792. doi: 10.1155/2013/956792 PMID: 23738047

55. Rahman I, Kode A, Biswas SK (2006) Assay for quantitative determination of glutathione and glutathione disulfide levels using enzymatic recycling method. Nature protocols 1: 3159–3165. doi: 10.1038/nprot.2006.378 PMID: 17406579

56. Pramod AB, Foster J, Carvelli L, Henry LK (2013) SLC6 transporters: structure, function, regulation, disease association and therapeutics. Molecular aspects of medicine 34: 197–219. doi: 10.1016/j.mam.2012.07.002 PMID: 23506866

57. Takanaga H, Mackenzie B, Peng JB, Hediger MA (2005) Characterization of a branched-chain amino-acid transporter SBAT1 (SLC6A15) that is expressed in human brain. Biochemical and biophysical research communications 337: 892–900. doi: 10.1016/j.bbrc.2005.09.128 PMID: 16226721

58. Broer A, Tietze N, Kowalczuk S, Chubb S, Munzinger M, et al. (2006) The orphan transporter v7-3 (slc6a15) is a Na+-dependent neutral amino acid transporter (B0AT2). The Biochemical journal 393: 421–430. doi: 10.1042/BJ20051273 PMID: 16185194

59. Reinhold WC, Sunshine M, Liu H, Varma S, Kohn KW, et al. (2012) CellMiner: a web-based suite of genomic and pharmacologic tools to explore transcript and drug patterns in the NCI-60 cell line set. Cancer research 72: 3499–3511. doi: 10.1158/0008-5472.CAN-12-1370 PMID: 22802077

60. Weinstein JN, Myers TG, O'Connor PM, Friend SH, Fornace AJ Jr., et al. (1997) An information-intensive approach to the molecular pharmacology of cancer. Science 275: 343–349. doi: 10.1126/science.275.5298.343 PMID: 8994024

61. Elia I, Schmieder R, Christen S, Fendt SM (2016) Organ-Specific Cancer Metabolism and Its Potential for Therapy. Handbook of experimental pharmacology 233: 321–353. doi: 10.1007/164_2015_10 PMID: 25912014

62. Kanehisa M, Sato Y, Kawashima M, Furumichi M, Tanabe M (2016) KEGG as a reference resource for gene and protein annotation. Nucleic acids research 44: D457–462. doi: 10.1093/nar/gkv1070 PMID: 26476454

63. Kanehisa M, Goto S (2000) KEGG: kyoto encyclopedia of genes and genomes. Nucleic acids research 28: 27–30. doi: 10.1093/nar/28.1.27 PMID: 10592173

64. Pornputtapong N, Nookaew I, Nielsen J (2015) Human metabolic atlas: an online resource for human metabolism. Database: the journal of biological databases and curation 2015: bav068. doi: 10.1093/database/bav068 PMID: 26209309

65. Fabregat A, Sidiropoulos K, Garapati P, Gillespie M, Hausmann K, et al. (2016) The Reactome pathway Knowledgebase. Nucleic acids research 44: D481–487. doi: 10.1093/nar/gkv1351 PMID: 26656494

66. Thiele I, Swainston N, Fleming RM, Hoppe A, Sahoo S, et al. (2013) A community-driven global reconstruction of human metabolism. Nature biotechnology 31: 419–425. doi: 10.1038/nbt.2488 PMID: 23455439

67. Eagle H, Washington C, Friedman SM (1966) The synthesis of homocystine, cystathionine, and cystine by cultured diploid and heteroploid human cells. Proceedings of the National Academy of Sciences of the United States of America 56: 156–163. doi: 10.1073/pnas.56.1.156 PMID: 5229844

68. Filomeni G, De Zio D, Cecconi F (2015) Oxidative stress and autophagy: the clash between damage and metabolic needs. Cell death and differentiation 22: 377–388. doi: 10.1038/cdd.2014.150 PMID: 25257172

69. Al-Awadi F, Yang M, Tan Y, Han Q, Li S, et al. (2008) Human tumor growth in nude mice is associated with decreased plasma cysteine and homocysteine. Anticancer research 28: 2541–2544. PMID: 19035276

70. Sayin VI, Ibrahim MX, Larsson E, Nilsson JA, Lindahl P, et al. (2014) Antioxidants accelerate lung cancer progression in mice. Science translational medicine 6: 221ra215. doi: 10.1126/scitranslmed.3007653 PMID: 24477002

71. Sugimura T, Birnbaum SM, Winitz M, Greenstein JP (1959) Quantitative nutritional studies with water-soluble, chemically defined diets. VIII. The forced feeding of diets each lacking in one essential amino acid. Archives of biochemistry and biophysics 81: 448–455. doi: 10.1016/0003-9861(59)90225-5 PMID: 13638009

72. Cellarier E, Durando X, Vasson MP, Farges MC, Demiden A, et al. (2003) Methionine dependency and cancer treatment. Cancer treatment reviews 29: 489–499. doi: 10.1016/s0305-7372(03)00118-x PMID: 14585259

73. Shiraki N, Shiraki Y, Tsuyama T, Obata F, Miura M, et al. (2014) Methionine metabolism regulates maintenance and differentiation of human pluripotent stem cells. Cell metabolism 19: 780–794. doi: 10.1016/j.cmet.2014.03.017 PMID: 24746804

74. Wellen KE, Thompson CB (2012) A two-way street: reciprocal regulation of metabolism and signalling. Nature reviews Molecular cell biology 13: 270–276. doi: 10.1038/nrm3305 PMID: 22395772

75. Locasale JW (2013) Serine, glycine and one-carbon units: cancer metabolism in full circle. Nature reviews Cancer 13: 572–583. doi: 10.1038/nrc3557 PMID: 23822983

76. Ables GP, Hens JR, Nichenametla SN (2016) Methionine restriction beyond life-span extension. Annals of the New York Academy of Sciences 1363: 68–79. doi: 10.1111/nyas.13014 PMID: 26916321

77. Montenegro MF, Sanchez-del-Campo L, Fernandez-Perez MP, Saez-Ayala M, Cabezas-Herrera J, et al. (2015) Targeting the epigenetic machinery of cancer cells. Oncogene 34: 135–143. doi: 10.1038/onc.2013.605 PMID: 24469033

78. Epner DE, Morrow S, Wilcox M, Houghton JL (2002) Nutrient intake and nutritional indexes in adults with metastatic cancer on a phase I clinical trial of dietary methionine restriction. Nutrition and cancer 42: 158–166. doi: 10.1207/S15327914NC422_2 PMID: 12416254

79. Ornish D, Weidner G, Fair WR, Marlin R, Pettengill EB, et al. (2005) Intensive lifestyle changes may affect the progression of prostate cancer. The Journal of urology 174: 1065–1069; discussion 1069–1070. doi: 10.1097/01.ju.0000169487.49018.73 PMID: 16094059

80. Komninou D, Leutzinger Y, Reddy BS, Richie JP Jr. (2006) Methionine restriction inhibits colon carcinogenesis. Nutrition and cancer 54: 202–208. doi: 10.1207/s15327914nc5402_6 PMID: 16898864

81. Caro P, Gomez J, Sanchez I, Naudi A, Ayala V, et al. (2009) Forty percent methionine restriction decreases mitochondrial oxygen radical production and leak at complex I during forward electron flow and lowers oxidative damage to proteins and mitochondrial DNA in rat kidney and brain mitochondria. Rejuvenation research 12: 421–434. doi: 10.1089/rej.2009.0902 PMID: 20041736

82. Li Y, Liu L, Tollefsbol TO (2010) Glucose restriction can extend normal cell lifespan and impair precancerous cell growth through epigenetic control of hTERT and p16 expression. FASEB journal: official publication of the Federation of American Societies for Experimental Biology 24: 1442–1453. doi: 10.1096/fj.09-149328 PMID: 20019239

83. Poirson-Bichat F, Goncalves RA, Miccoli L, Dutrillaux B, Poupon MF (2000) Methionine depletion enhances the antitumoral efficacy of cytotoxic agents in drug-resistant human tumor xenografts. Clinical cancer research: an official journal of the American Association for Cancer Research 6: 643–653. PMID: 10690550

84. Shoemaker RH, Monks A, Alley MC, Scudiero DA, Fine DL, et al. (1988) Development of human tumor cell line panels for use in disease-oriented drug screening. Progress in clinical and biological research 276: 265–286. PMID: 3051021

85. Minn H, Clavo AC, Grenman R, Wahl RL (1995) In vitro comparison of cell proliferation kinetics and uptake of tritiated fluorodeoxyglucose and L-methionine in squamous-cell carcinoma of the head and neck. Journal of nuclear medicine: official publication, Society of Nuclear Medicine 36: 252–258. PMID: 7830126

86. Trencsenyi G, Marian T, Lajtos I, Krasznai Z, Balkay L, et al. (2014) 18FDG, [18F]FLT, [18F]FAZA, and 11C-methionine are suitable tracers for the diagnosis and in vivo follow-up of the efficacy of chemotherapy by miniPET in both multidrug resistant and sensitive human gynecologic tumor xenografts. BioMed research international 2014: 787365. doi: 10.1155/2014/787365 PMID: 25309926

87. Lin L, Yee SW, Kim RB, Giacomini KM (2015) SLC transporters as therapeutic targets: emerging opportunities. Nature Reviews Drug Discovery 14: 543–560. doi: 10.1038/nrd4626 PMID: 26111766

88. Cesar-Razquin A, Snijder B, Frappier-Brinton T, Isserlin R, Gyimesi G, et al. (2015) A Call for Systematic Research on Solute Carriers. Cell 162: 478–487. doi: 10.1016/j.cell.2015.07.022 PMID: 26232220

89. Pulciani S, Santos E, Long LK, Sorrentino V, Barbacid M (1985) ras gene Amplification and malignant transformation. Molecular and cellular biology 5: 2836–2841. doi: 10.1128/mcb.5.10.2836 PMID: 3915535

90. Sacco E, Metalli D, Spinelli M, Manzoni R, Samalikova M, et al. (2012) Novel RasGRF1-derived Tat-fused peptides inhibiting Ras-dependent proliferation and migration in mouse and human cancer cells. Biotechnol Adv 30: 233–243. doi: 10.1016/j.biotechadv.2011.05.011 PMID: 21620943

Gaia De Sanctis <g.desanctis@campus.unimib.it>

Fwd: Omics book submitted to wiley

marco.vanoni <marco.vanoni@unimib.it> 30 dicembre 2016 19:20
A: gaia <g.desanctis@campus.unimib.it>

--- segue il messaggio inoltrato ---

---------- Messaggio inoltrato ----------
From: izoidakis@bioacademy.gr
To: Katerina Markoska <markoska_kate@yahoo.com>, Lohff.Brigitte@mh-hannover.de, Constantinos Deltas <deltas@ucy.ac.cy>, Daniel Borras <d.borras@genomescan.nl>, Theofilos Papadopoulos <teopapad@gmail.com>, sfilip@bioacademy.gr, Prathibha Reddy <prathibhareddy888@gmail.com>, Claudia Pontillo <pontillo@mosaiques-diagnostics.com>, Agnieszka Latosinska <latosinska@mosaiques.de>, Andy Smith <andyjamessmith6@hotmail.com>, "Gil, Ryan Bruce" <ryan.gil@helmholtz-muenchen.de>, Eleni Ioanna Delatola <eleni.delatola@ucd.ie>, Elena Critselis <ecritselis@bioacademy.gr>, Stella Logotheti <stellalog2002@yahoo.com>, Magdalena Krochmal <magdakro89@gmail.com>, Amel Bekkar <amel.bekkar@isb-sib.ch>, Marco Fernandes <m.fernandes.1@research.gla.ac.uk>, Maria Frantzi <frantzi@mosaiques.de>
Cc: Goce Spasovski <spasovski.goce@gmail.com>, Bart Janssen <b.janssen@genomescan.nl>, joost-peter.schanstra@inserm.fr, "Jankowski, Joachim" <jjankowski@ukaachen.de>, Harald Mischak <mischak@mosaiques-diagnostics.com>, vlahoua@bioacademy.gr, mmakrid@bioacademy.gr, fulvio magni <fulvio.magni@unimib.it>, "Heinzmann, Silke, Dr." <silke.heinzmann@helmholtz-muenchen.de>, Holger Husi <Holger.Husi@glasgow.ac.uk>, Marco Vanoni <marco.vanoni@unimib.it>, Ioannis Xenarios <ioannis.xenarios@isb-sib.ch>, Katryna Cisek <katrynacisek@gmail.com>, franco ferrario <francoferrario49@gmail.com>, Ortiz Arduan Alberto <AOrtiz@fjd.es>
Date: Fri, 23 Dec 2016 16:14:13 +0200
Subject: Omics book submitted to wiley
Dear Colleagues,
The omics book, our "Magnum Opus", was submitted to Wiley today.
You can find all the chapters in the following link

https://www.dropbox.com/sh/iy3xf2tff27i2fi/AABbhQwv4vqODEDivkZVZ0Gia?dl=0

Feel free to read the text and send me comments and suggestions for improvement. The Wiley staff will not begin the publication process before 03/01/2017 so there is still some time for double checking that all is in order.

I would like to thank you all for your hard work.
Together we boldly achieved what no ITN program has done before.
Have a great time during the holidays,
Makis

--
Ieronymos Zoidakis, Ph.D.
Biomedical Research Foundation, Academy of Athens
Department of Biotechnology
Soranou Efessiou 4
11527 Athens
tel. 30-210-6597485
http://www.bioacademy.gr/facility/proteomics

Omics and clinical data integration

Gaia De Sanctis[1,2], Riccardo Colombo[1,3], Chiara Damiani[1,3], Elena Sacco[1,2], and Marco Vanoni[1,2,*]

[1]SYSBIO, Centre of Systems Biology, Piazza della Scienza 2, 20126 Milan, Italy

[2]Department of Biotechnology and Biosciences, University of Milano-Bicocca, Piazza della Scienza 2, 20126 Milan, Italy

[3]Department of Computer Sciences, Systems and Communications, University of Milano-Bicocca, Viale Sarca 336, 20126 Milan, Italy

[*]Address correspondence to: Marco Vanoni e-mail marco.vanoni@unimib.it

TABLE OF CONTENTS

Abstract

Many high-throughput post-genomic (-omic) technologies have been developed to unravel cellular complexity and to investigate biological systems. Each -omic technology (such as genomics, transcriptomics, proteomics or metabolomics) deals with a different layer of cellular or tissue functioning. The integration of two or more -omics connects these different layers, allowing to extract information that would otherwise remain latent if each data set was considered alone. This approach paves the way to the identification of functional emergent properties and their design principles at both the cellular and organismal level. Many diseases are multi-factorial in nature and are affected by the alteration of a large number of gene products whose interaction may profoundly modify the penetrance of the disease and the efficacy of a given therapeutic approach. Ultimately, integration of the knowledge of functional emergent properties will merge with personalized –omic data to generate and constrain mathematical models of the diseased functions allowing to develop personalized medical treatment of multi-factorial diseases.

Keywords

-omic technologies, data integration, multi-factorial diseases, emergent properties, personalized treatment, data visualization, modeling, metabolic diseases, cancer.

Introduction

The various components of a biological system do not act individually, but rather through complex hierarchical, coordinated, dynamical, non-linear interactions of a large number of components (e.g. proteins interacting with DNA, RNA, metabolites and other proteins) that allow the functioning (or dysfunctioning) of the system itself (Langley et al., 2013). Therefore, a biological function generates as an emergent property (Bhalla and Iyengar, 1999) of the system, and is not ascribable or found in its single components, but only in their networking.

High-throughput technologies allow to collect genome-scale comprehensive molecular information – collectively referred to as -omic data – using an increasing number of sophisticated high throughput technologies, including transcriptomics, proteomics (that includes the study of protein level and post-translational modification data at the proteome scale), metabolomics and interactomics. Indeed, our current understanding of biological functions is not limited by availability of vast amounts of data (big data), but rather by our ability to integrate and process them. Systems biology (Kitano, 2002, Alberghina and Westerhoff, 2005) is the conceptual and operative approach needed to extract and integrate information from this huge amount of different omic data. The systems biology approach systematically organizes, integrates and rationalizes the different omic data through statistical analysis, computer aided modeling and visualization. It requires different scientific competencies so to give them structure, improve our understanding of emergent properties and their design principles and gain ability to predict the behavior of a system and to exploit it for applicative purposes (Figure1).

Most common diseases affecting adults, including cardiovascular diseases, cancer and diabetes, are multi-factorial and derive by the interaction of several genetic and environmental factors concurring to phenotype and clinical manifestation (Wruck et al., 2015, Alberghina et al., 2014, Hornberg et al., 2006, Kitano, 2007b, Kitano, 2004). As -omic data become available with ever increasing accuracy and decreased cost, they can be used to guide the choice, design and follow-up of effective therapeutic approaches, allowing to translate systems biology to medicine that aims at tackling the complexity of multi-factorial diseases by means of systematic and integrated approaches for clinical purposes, i.e. to allow a more efficient disease classification and identification of novel therapeutic targets. Post-genomic omic-based systems medicine aims to transform diagnostic and therapeutic strategies being, in the next future, “personalized and predictive”, namely able to suggest the most potentially effective drug for any patient and to eventually foretell if and when a disease will occur and how it will develop (Tanaka, 2010, Hood and Tian, 2012, Auffray and Hood, 2012, Hood et al., 2012, Tian et al., 2012).

Health care systems have nowadays to face considerable challenges connected with the highly variable clinical efficacy of current drugs as well to the huge costs associated with drug discovery, development and clinical trials, inevitably causing economical suffering and high impacts on the financing of the sector. Indeed, a basic problem of the current disease classification system, based on phenotype determination, is that the same phenotype may derive from several disease mechanisms. Thus, a drug directed against one of those mechanisms would not be clinically effective in patients with different underlying mechanisms (Gustafsson et al., 2014).

Let's take breast cancer as an example. During the last 30 years, the definition of a few biomarkers allowed to identify molecular breast cancer subgroups with different clinical characteristics, clinical courses, and sensitivities to existing therapies and allowed to design novel and more effective treatments for patients (Hortobagyi, 2012). Patients with Estrogen Receptor-negative, human Epidermal Growth Factor Receptor 2–positive cancers are currently treated with the monoclonal antibody trastuzumab and have one of the more favorable prognoses of all breast cancer patients. However, trastuzumab is effective only in up to 50% of these patients, possibly because of various resistance mechanisms. As knowledge of the molecular events underlying the ability to respond to trastuzumab treatment increases, novel accurate predictive biomarkers – allowing to identify those patients who will respond to trastuzumab treatment – and/or novel drug targets will be identified. The increased resolution in the classification of these tumors will allow to develop new, highly targeted molecular therapeutics, and at the same time to devise molecular diagnostic tools that will allow to implement a truly personalize medicine.

In this chapter we describe approaches to -omics integration that may uncover information hidden in each individual -omics. Integration of -omic data can be fully exploited if combined with modeling approaches, allowing to develop precision, personalized medicine of patients of multi-factorial diseases, such as cancer.

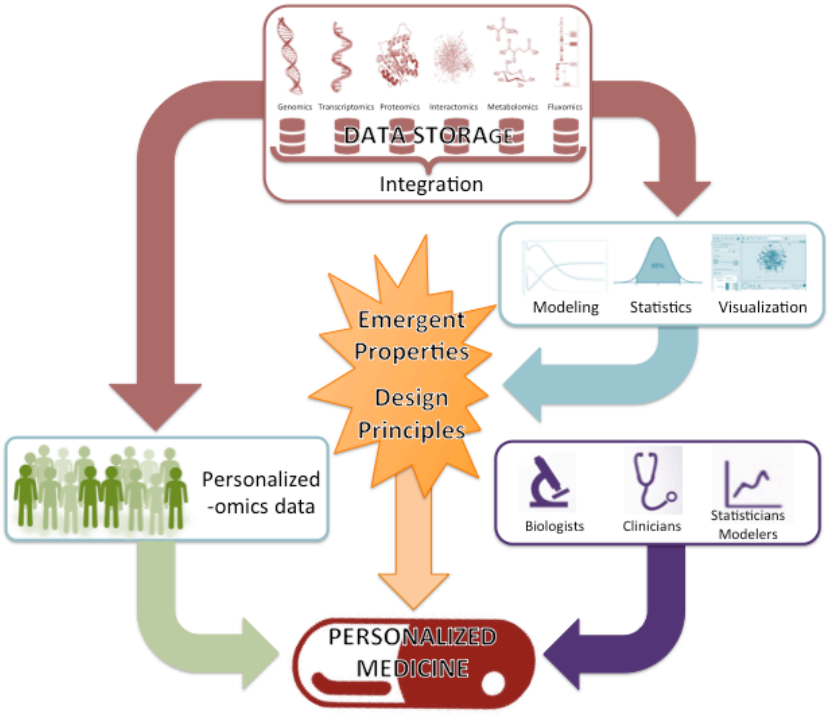

Figure 1 Overview of the systems biology approach towards the realization of personalized medicine. The many different -omic data currently available (reddish box) must be deposited in one or more database in order to systematically organize the information and to facilitate the data integration process. Integrated -omic data are analyzed (light blue box) by means of statistical methods, computer aided modeling and visually represented in order to understand emergent properties and design principles of the biological system (orange cartoon). Personalized -omic data (green box), the knowledge of emergent properties/design principles and different scientific competencies (purple box) will ultimately merge allowing to develop personalized medical treatment of multi-factorial diseases.

Data sources

-omic technologies generate extremely large data sets and a quick Web search can give a first picture of the huge variety of data sources publicly available. Assessing their relevance and quality may be a particularly hard task due to the heterogeneity of representations and notations.

Historically, the Human Genome Project has been the first -omic initiative related to human health. This pioneering study gave rise to a plethora of initiatives paving the way towards the current explosion of data generated by means of different -omic approaches. Focusing exclusively on data sources related to cancer disease, Table 1 describes some of the most relevant repositories of -omic data. Most of the available resources deal with genomic, transcriptomic and proteomic data with some emphasis on cancer-related data. More recent initiatives tend to shed light on the heterogeneity of cancer in terms of genomic mutations and phenotypic differences among the

different tumor subtypes. Table 1 highlights a substantial lack of information on metabolomics, a technology having a great potential to impact clinical practice (e.g. biomarkers for diagnosis, monitoring and definition of new therapeutic targets). In this context, a current challenge is the definition of metabolite resources with comprehensive spectral libraries, various integrative approaches and serious considerations for clinical validation of the identified biomarkers (More et al., 2015).

Data source	Main features	Type of –omic data	Web page	Ref.
Gene Expression Omnibus (GEO)	Repository of gene expression data from more than 2500 studies	Proteomics	http://www.ncbi.nlm.nih.gov/geo/	(Edgar et al., 2002, Barrett et al., 2013)
Ensembl	Sequence data fed into a gene annotation system creating a set of predicted gene locations saved in a MySQL database for subsequent analysis and display.	Genomics	http://www.ensembl.org	(Hubbard et al., 2002)
TRANSFAC database	Data on eukaryotic transcription factors and their miRNAs, binding sites and regulated genes.	Regulomics	http://www.biobase-international.com/product/transcription-factor-binding-sites	(Wingender et al., 1996)
1000 Genomes Project	Generic genetic variants whose frequencies are at least of 1% in the human population by NGS sequencing of genomes from many individuals. The raw and processed data associated with the 1000 resulting genomes are also stored and managed.	Genomics	http://www.1000genomes.org/	(Abecasis et al., 2010, Abecasis et al., 2012)
Encyclopedia of DNA Elements Project (ENCODE)	Integration-based approach aimed at the characterization, for a set of animal models/tissues/cell lines, of the profile of mRNA expression, histone marks and transcription factor binding profiling, DNA methylation, chromatin conformation and the location of active regulatory regions among others.	Genomics Transcriptomics Epigenomics Regulomics	http://genome.ucsc.edu/ENCODE/	(Ecker et al., 2012, ENCODE Project Consortium, 2011, Harrow et al., 2012)
The Cancer Genome Atlas Project (TCGA)	Provides insights into the heterogeneity of different cancer subtypes by creating a map of molecular alterations for every type of cancer at multiple levels. For instance the endometrial carcinoma has been characterized by mRNA, miRNA, protein, DNA methylation, copy number alterations and somatic chromosomal aberrations.	Transcriptomics Regulomics Proteomics Epigenomics Phenomics	http://cancergenome.nih.gov/	(Weinstein et al., 2013)
International Cancer Genome Consortium (ICGC)	Coordinates large-scale cancer genome studies in tumors from 50 cancer types/subtypes of main importance across the globe. More than 25000 cancer genomes are studied at the genomic, epigenomic and transcriptomic levels, to reveal the repertoire of oncogenic mutations, uncover traces of the mutagenic influences, define clinically relevant subtypes for prognosis and therapeutic management and enable the development of new cancer therapies.	Genomic Epigenomic Transcriptomic	https://www.icgc.org/	(Hudson et al., 2010)
Cancer Genome Project (CGP)	Uses the human genome sequence and high-throughput mutation detection techniques to identify somatically acquired sequence variants/mutations and thus genes critical to the development of human cancers.	Genomics Phenomics	http://www.sanger.ac.uk/research/projects/cancergenome/	(Pleasance et al., 2010)
Catalogue of Somatic Mutations in Cancer (COSMIC)	Contains data generated from the ICGC and TCGA studies, the Cancer Genome Project (CGP) and targeted sequencing of the NCI60 cell lines (a panel of 60 human cell lines) in known cancer genes, in addition to information extracted from the literature.	Genomics Phenomics	http://cancer.sanger.ac.uk/cosmic	(Bamford et al., 2004)
Clinical	Has the goal of understanding the molecular	Proteomics	http://proteomics.cancer.gov/prog	(Ellis et al.,

Proteomic Tumor Analysis Consortium (CPTAC)	basis of cancer through the application of proteomic technologies and workflows, systematically identifying proteins that derive from alterations in cancer genomes and related biological processes, and providing this data with accompanying assays and protocols to the public.	Genomics	rams/cptacnetwork	2013, Zhang et al., 2014)
Kyoto Encyclopedia of Genes and Genomes (KEGG)	KEGG contains representations of biological systems. It integrates genetic building blocks of genes and proteins, chemical building blocks of small molecules and reactions, and wiring diagrams of molecular interaction and reaction networks. Thus, KEGG databases are categorized into systems, genomic, chemical and health information.	Many, including Genomics, Proteomics, Interactomics and Metabolomics	http://www.kegg.jp	(Kanehisa and Goto, 2000)
Multi-Omics Profiling Expression Database (MOPED)	Omics expression database that contains over 5 million protein and gene expression records. It links to various protein and pathway databases, including GeneCards, Panther, Entrez, UniProt, KEGG, SEED and Reactome. Protein identifiers are integrated from GeneCards, GI, RefSeq, Locus Tag, UniProt, WormBase and SGD.	Mainly Proteomics and Transcriptomics	http://moped.proteinspire.org (accessible only with valid certificate)	(Kolker et al., 2012, Higdon et al., 2014)
Search Tool for the Retrieval of Interacting Genes/Proteins (STRING)	Database of known and predicted protein interac tions. The interactions include direct (physical) and indirect (functional) associations, derived from genomic context, high-throughput experiments, coexpression and previous knowledge. STRING, currently covering about 10 million proteins from 2031 organisms, quantitatively integrates interaction data from these sources for a large number of organisms and transfers information between these organisms where applicable.	Interactomics	http://string-db.org/	(Snel et al., 2000)
Human Protein Atlas (HPA)	Database of information for almost all human protein-coding genes. Data are available on expression and localization of proteins based on both RNA and protein data.	Proteomics	http://www.proteinatlas.org	(Uhlen et al., 2010)
Human Metabolome Database (HMDB)	Database containing 41,993 metabolite entries, 5,701 protein sequences are linked to these metabolite entries. Each entry has around 110 data fields with 2/3 of the information on chemical/clinical data and the rest regarding enzymatic or biochemical data.	Metabolomics	http://www.hmdb.ca	(Wishart et al., 2007, Wishart et al., 2009, Wishart et al., 2013)
MINT	The database contains experimentally verified protein-protein interactions mined from the scientific literature through human manual curation	Interactomics Bibliomics	http://mint.bio.uniroma2.it/mint/Welcome.do	(Licata et al., 2012)
IntAct	Database of molecular interaction data, here every interaction is derived from literature or submitted directly by the user.	Interactomics	http://www.ebi.ac.uk/intact/	(Orchard et al., 2014)
BioGRID	Repository with interaction data manually curated. It contains 56,300 publications for 1,060,041 protein and genetic interactions, 27,501 chemical associations and 38,559 post-translational modifications	Interactomics Regulomics	http://thebiogrid.org	(Oughtred et al., 2016)

Table 1 Main data sources available for data integration

Integration of different data sources

The definition and the population of a database is by far the most effective way to represent and organize a wide range of data; however, biological databases are affected by the lack of uniformity in types and formats of data sources, mainly due to the lack of a unique standard. Databases of

pathways are an example of this problem. For example, some of the 547 biological pathways reported in Pathguide (http://www.pathguide.org) are similar and redundant but are defined with different boundaries and components. This heterogeneity has to be taken into account when genome analysis methods based on pathways are applied (e.g. in (Menashe et al., 2010, Swaminathan et al., 2012, Sloan et al., 2010, Zhang et al., 2011)). Indeed, the same input data can generate different results if different databases are used for the analysis (Elbers et al., 2009). To overcome these issues, Cantor and colleagues proposed to use multiple databases for each analysis (Cantor et al., 2010) in order to balance divergences among databases and/or to validate similar results obtained from different data sources. Gomez-Cabrero and colleagues, while reviewing data integration in the -omics era, advocate the need to create standards at earlier stages when novel data-type resources are developed (Gomez-Cabrero et al., 2014).

One of the first definitions of database integration has been formulated in the context of the smoothening of redundancies between databases, pointing out the need to access different databases with overlapping content and to connect several of them, as if the user were interacting with one single information system. In general, since 1980's, two main approaches have been defined to efficiently integrate data coming from different sources:

1. **Data warehousing:** Data warehousing consists in the storage of all the data belonging to a certain category from different databases in only one large database, according to the process named ETL (Extract, Transform and Load) (Ponniah, 2004).
2. **Federated approaches:** In contrast to data warehouse, in federated databases data remains in the original data source. The integration consists in mapping data from each source on the federated database; thus, the end user can operate on a simple database. This data storage approach is relevant when the researcher needs updated information or must integrate a large amount of data deriving both from private and public databases (Sheth and Larson, 1990).

The second approach is currently trending in the domain of life sciences. Proving this fact, one of the most common ways to connect data from several biological databases consists in implementing hypertext links between entries of different data sources. As such, link integration approaches represent a connection between web pages, whereas the actual integration method is then carried on by a user or by another application. As a matter of fact, this approach requires a significant amount of manual work in order to integrate data: scientific institutions that maintain biological databases have to face a time-consuming checking process to map the links between entries from distinct data

sources. Therefore, given the high number of databases pertaining to the biological field, only links to the most used ones are typically set. A meaningful example is provided by one of the main search engines for health science databases: Entrez Global Query Cross-Database Search System (http://www.ncbi.nlm.nih.gov/sites/gquery), a tool that is able to retrieve information stored in several sources and regarding bio-molecular sequences, structures and literature references.

Integration of different -omic data

It is becoming more and more evident that the integration of multiple -omic layers is required for a deeper understanding of complex biological entities. To meet this goal, initial attempts of data integration reported in literature analyzed data from individual -omics separately. This phase was then followed by downstream actual integration of previous independent and parallel analyses outcomes. However, this method entails the loss of key emergent properties, which only become apparent by analyzing multiple -omic dataset as a whole and not by studying the system as the sum of its parts (Liu et al., 2013). A first step in the integration of multiple -omic layers is the joining of information deriving from pairs of them. In the following paragraphs, we will illustrate examples of pairwise integration between different -omic data.

Integrating transcriptomics and proteomics

Several studies in model organisms have shown that mRNA and protein expression profiles are often poorly correlated (Yeung, 2011, Ghazalpour et al., 2011, Pascal et al., 2008). Proteins are generally more stable than mRNAs (Schwanhausser et al., 2011), so situations where a protein is still abundant in the near absence of the cognate mRNA may arise. The opposite situation (*i.e.*, low protein level while the corresponding transcript is high) may derive from poor translation of the mRNA. This happens either because the RNA itself is poorly translatable (due, for example, to secondary structures that hamper translation (Hinnebusch, 2014, Stefanovic, 2013) or because of interaction with other molecules, such as the trans-acting factors, RNA-binding proteins (RBPs) and small RNAs that bind to the mRNA and modify its translatability (Szostak and Gebauer, 2013). Among these natural antisense transcripts that regulate gene expression (Nishizawa et al., 2012) are small (19-22 nucleotide) non-protein-coding RNA molecules (microRNAs or miRNAs). miRNAs down-regulate expression of their target mRNAs through specific base pairing that result in decreased translation of the mRNA or leads to mRNA degradation (Ambros, 2004). Although a large number of human miRNAs are reported to be implicated in several developmental and adult disease states (e.g. cancer), many of their mRNA targets and their impact on phenotypes remain

unknown (Nam et al., 2009). Recently, due to the advance of high-throughput and low-cost experimental methods, there has been a huge development of computational methods based on sequence complementarity between the miRNA and the mRNAs (Muniategui et al., 2013).

The utility - and possibly the necessity - of integrating mRNA, miRNA and protein expression in order to obtain a more comprehensive view of the system under study has been recently pointed out (Tebaldi et al., 2012). A possible approach to integration involves the analysis of individual -omic layers separately, whose results are then merged and compared. By way of example, Com and colleagues in a study of gentamycin nephrotoxicity report that transcriptomic and proteomic data were complementary and that their integration provided a more comprehensive picture of the putative nephrotoxicity mechanism of the antibiotic, consistent with histopathological evidence (Com et al., 2012). Although valuable, this approach misses the interconnection between the different –omic layers and may fail to uncover the system-level functional properties. By mapping transcriptomic and proteomic data sets on the protein interaction network and using chronic kidney disease as an example, Perco and colleagues show that such a joint analysis highlights pathways and processes characteristic for the phenotype under analysis that goes unnoticed when the two data sets are analyzed independently (Perco et al., 2010). A similar, network-based methodology for integrative analysis of proteomic and transcriptomic data on psoriasis, showed complementarities between two levels of cellular organization and allowed to identify common regulators - such as the most influential transcription factors and receptors - for two datasets (Piruzian et al., 2010). Imielinski and colleagues identified sub-networks enriched in differentially expressed genes within networks built from proteins differentially expressed in estrogen receptor positive breast cancer tumors (Imielinski et al., 2012) from which a gene expression-based signature biomarker predictive of clinical relapse could be constructed.

Liu and colleagues (Liu et al., 2013) focused on the melanoma sub-set from NCI-60 – a panel of 60 different human cancer cell lines from 9 different tissues. They quantified the additional information provided by their method compared to non-joint approaches and observed that integration and annotation in the analysis of different type of data changed the flow of information, with the joint analysis giving fully relevant molecular information only upon annotation of all mRNA, proteins and miRNA. Particularly, compared to the separate analysis, the joint analysis better described melanogenesis, while the separate analyses failed to identify enrichment in melanin biosynthetic and metabolic processes, both related to the basal melanocyte physiology. A similar algorithm (iCluster) has been used to cross-correlate gene copy number and transcriptional profiling to discover potentially novel cancer breast and lung cancer subtypes by combining weak, consistent alteration patterns across subtypes (Shen et al., 2009).

A final approach worth mentioning exploits the Bayesian framework to infer gene regulatory network form transcriptomics, whose accuracy is extended by combining prior knowledge (Zhang et al., 2007) or protein-protein interaction data (Nariai et al., 2004)..

The reader is referred to Haider and Pal (Haider and Pal, 2013) for a recent comprehensive review detailing other methods for integrating transcriptomic and proteomic networks.

Integrating transcriptomics and interactomics

Analysis of genome-wide expression profiles recently allowed to identify several disease markers (e.g. (Ramaswamy et al., 2003)) exploiting the link between perturbations of a particular phenotype and changes in mRNA levels. In this kind of analysis, each gene is scored for the ability of its expression pattern to discriminate between various classes of disease; subsequently, marker sets are selected based on attributed scores (signature-based approach). However, different marker sets for a specific disease are found among different studies (e.g. (van 't Veer et al., 2002) and (Wang et al., 2005)), likely because changes in expression of the few selected genes may be small compared to those of the downstream effectors, which may vary significantly among patients (Ein-Dor et al., 2005). As such, a better strategy to identify markers would be to combine gene expression measurements over groups of genes that fall within common pathways (Subramanian et al., 2005, Tian et al., 2005, Wei and Li, 2007). Nevertheless, pathway-based analysis (to which gene-set enrichment analysis (GSEA) belongs) has the limitation that there is still no assignment of most human genes to a specific pathway.

A partial solution to these challenges lays in the use of protein–protein interaction (PPI) networks (the interactome) that provide a comprehensive map of functional interactions in the cell and allow the identification of sub-networks (composed by a group of proteins functionally linked to each other) that are significantly dysregulated in a disease of interest. In this regard, the development of a scoring scheme to assess the collective dysregulation of multiple interacting genes (mapped on the corresponding protein on the PPI network) and the development of efficient computational algorithms to search for sub-networks with significant scores represent the main methodological challenges. Commonly, the differential expression of each gene is first scored individually using a standard statistical test (e.g. *t*-test), then sub-network scores are computed as an aggregation of these individual differential expression scores. However, these methods provide limited systems level insights, since they assess the differential expression of functionally related genes individually and cannot capture patterns of coordinated dysregulation. An alternative strategy has been proposed in (Chen and Yuan, 2006). Here, authors illustrate a representation where genes having consistent expression patterns are mapped on PPI networks to form subnetworks that are significantly dysregulated in a disease of interest and may be conserved across multiple species (Sharan et al.,

2005). Chuang and colleagues (Chuang et al., 2007) applied a protein-network-based approach to identify markers of metastasis within gene expression profiles, with the aim of detecting genetic alterations and predicting the probability of metastasis in unknown samples. They show that the network-based method has many advantages compared to earlier analyses of differential expression:

1) The generated subnetworks provided models of the molecular mechanisms underlying metastasis.
2) Though analysis of differential expression usually does not allow detecting genes with known breast cancer mutations (such as KRAS, among others), these genes play a key role in the protein network by interconnecting many expression-responsive genes.
3) Subnetworks are remarkably more reproducible among different breast cancer cohorts than separate marker genes selected without network information.
4) Accuracy in prediction is higher with network-based classification, as demonstrated by selecting markers from one data set and applying them to a second independent data set.

A further evolution of the method, called interactome-transcriptome integration (ITI), consists in the integration of the analysis of several gene expression datasets (multidataset) to extract subnetworks that discriminate breast cancer distant metastasis (Garcia et al., 2012). The method showed increased performance on a vast collection of publicly available data and was validated on two independent breast cancer gene expression datasets (Desmedt et al., 2008, van de Vijver et al., 2002).

For a further dissertation on the essential role for the comprehension of biological systems of the integration between transcriptomics and interactomics (but also with other categories of -omic data, such as genomics, and proteomics), we refer the interested reader to a recent review (Snider et al., 2015) that summarizes strengths and weaknesses of the different approaches.

Integrating transcriptomics and metabolic pathways

In order to better understand the role of differentially transcribed metabolic genes in the context of metabolic pathways, Patil and Nielsen (Patil and Nielsen, 2005) devised a technique of network enrichment whose goal is to identify the "reporter metabolites", i.e. those spots in the metabolism where there is a crucial regulation to maintain homeostasis (i.e., a constant level of the metabolite) or to reset the concentration of the metabolite to a different level required for the correct functioning of the metabolic network. The first step of the procedure consists on mapping differential expression data on the corresponding enzymes of a genome-wide biochemical network (whose reconstruction process is described in the following section) adding a specification of the significance of differential gene expression. In this way, each metabolite node is scored based on

the normalized transcriptional response of its neighboring enzymes. When dealing with differential data, the normalized transcriptional response is calculated as size-independent aggregated Z-scores of the neighboring enzymes. The scoring used to identify reporter metabolites is a test for the null hypothesis hereafter formulated: "Neighbor enzymes of a metabolite in the metabolic graph show the observed normalized transcriptional response by chance". Metabolites with the highest score are defined as reporter metabolites, i.e. those metabolites around which transcriptional changes occur.

All in all, advantages of performing a multi dimensional -omic analysis to obtain more information from human high throughput data instead of analyzing a single -omic data type can be summarized as follows:

1) Integration of multiple data types is a strategy to prevent information loss due to the fact that information on a biological entity (gene, protein, transcript,…) can suggest to refine other -omic analyses in order to fill information gaps or to correct wrong data associations.
2) Different data sources providing information on the same gene or pathway are less likely to produce "false positives".
3) Examination of different levels of regulation by means of an integrated approach is a promising way to unravel the functioning and fine regulation of the biological system under examination.

Readers interested in mathematical aspects of methods for multi-omic data integration may refer to a recent review (Bersanelli et al., 2016). The availability of dedicated servers for the analysis of multi-omic datasets, including trancriptomics, miRNomics, proteomics and genomics may help to spot similarities and differences between the enrichments obtained from different –omics and widen the use of integrative multi-omic analyses (Stockel et al., 2016).

As highlighted in the Introduction, many common diseases such as cancer, diabetes and cardiomyopathy, should be considered as network diseases. If the complexity of the network is not taken into account, we may fail in identifying a potential drug having high efficacy and low toxicity (Kitano, 2007a, Ogilvie et al., 2015, Wierling et al., 2015, Westerhoff, 2015). One of the main reasons of such a poor predictive power is that the exploitation of individual -omic platform does not provide enough information to link drug response with personalized -omic profile. Indeed, a stronger integration of different -omic platforms could validate data and help in clarifying the connections between -omics, as well as accelerate multi-target drug discovery (Leung et al., 2013). Cellular subsystems have been defined by ontologies, such as Gene Ontology (GO). It has been proposed that such a hierarchical structure may guide the organization of -omic data. Interpretation

of this “ontotype” through logical rules generated by machines learning techniques allowed predictions of the growth properties of over 2,000 yeast strains carrying inactivation of two genes and could pave the way for interpretation of the phenotypic properties of complex diseases (Yu et al., 2016). According to similar reasoning an initiative to define the hallmark networks of cancer has been recently launched (Krogan et al., 2015).

As we will see later, a further step, modeling, may be required to fully extract information hidden in -omic data, structure according to mechanistic principles and generate experimentally testable predictions.

Visualization of integrated -omic data

Consistently with the need for -omic data integration approaches, a strong need for tools able to represent them in an effective way has emerged among scientist and clinicians belonging to different communities. To satisfy this need, visual representations of -omic data have been extensively used to give an immediate representation of the complexity beyond the systems, to sum-up relevant information (Suderman and Hallett, 2007) and to help to formulate hypotheses on represented systems.

The recourse to visualization strategies has been motivated by the fact that the human brain has a remarkable capability to process visual information in order to identify patterns (e.g. biochemical pathways) and relevant topological features (e.g. the presence of highly connected nodes called “hubs”) (Bucci et al., 2011). The “visual complexity” of these representations ranges over various orders of magnitude spanning from the description of a small functional units (signal transduction and metabolic pathways, interaction pool of a protein), to the representation, at whole cell/tissue/organism level, of the interactions involving different -omic data.

The development of high-throughput -omic technologies has imposed a change of paradigm for the definition of these representations, shifting from the manual curation and refinement to fully (or partially) automatized procedures exploiting sophisticated software. Even if recent efforts have produced remarkable results (see (Gehlenborg et al., 2010) for an extensive review and Table 2 for a non exhaustive list of relevant and widely used tools for data visualization), in this domain some challenges are still open.

A first challenge is related to the scalability of the methods. Scalability issues are particularly relevant in network representations, an obvious and traditional way to visualize data and their relationships (generally nodes represent entities and edges represent relationships). This type of representation is intuitive and powerful for simple systems, but has also some scalability limitations: when the system size and complexity increases, also the “visual complexity” increases,

and since most of the software make use of standard visualization packages, the most common layout of the network is often a very uninformative "hairball" (Figure 2A) (Suderman and Hallett, 2007)

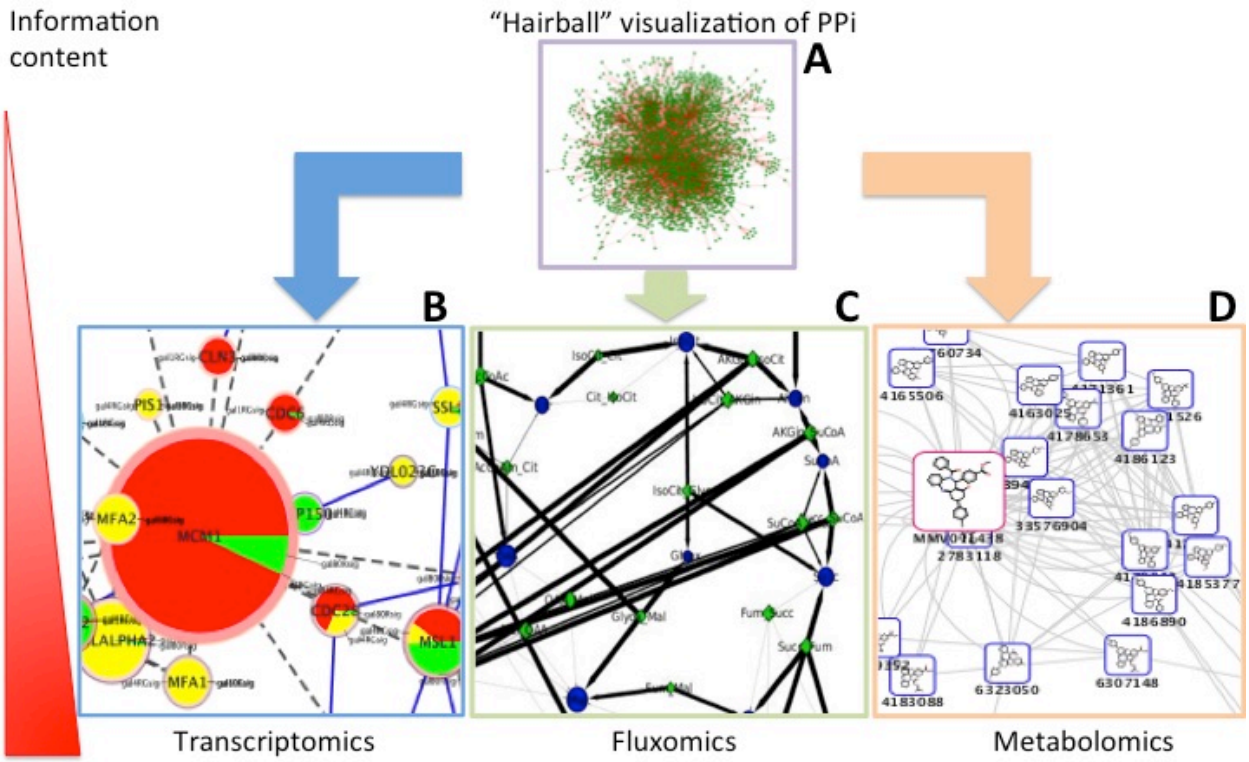

.

Figure 2 From uninformative to meaningful -omic data visualization with Cytoscape: adding data on the network in a rational way improves the information content of the representation. On the top part, an example of hairball layout obtained using data from high-confidence protein-protein interactions (von Mering et al., 2002). On the lower level, examples of -omic data mapped on a network modifying its elements (nodes and edges color/dimension, layout) exploiting Cytoscape apps (Node Chart Plugin for transcriptomics (B), CyFluxViz for fluxomics (C) and chemViz2 for metabolomics (D)).

The wide usage of this primitive layout is mainly due to the lack of knowledge on the inner organization of the network (e.g. cellular localization of elements, molecular functions, structure of protein complexes, etc.), but also to the difficulty of representing the system in a way expected by the user (e.g. the arrangement of metabolic or signaling pathways using an immediately recognizable shape). To move from the uninformative "hairball layout" to a more meaningful representation, several algorithms have been devised to visually organize the network, on the basis of given criteria, such as node degree distribution, geometrical representations (e.g. circles, grids), directionality of the process (hierarchical representations) and physical simulations, modifying both the spatial layout and placing information (i.e. -omic data) on network elements (color/dimension/shape of nodes and edges). In Figure 2, we provide an example of useful -omic

data visualization: in box B, transcriptomic data have been mapped on nodes (genes) using a color code for expression level (red for up-regulation, green for down-regulation, yellow for no change) while slice size in the pie chart is proportional to the number of experiments where the gene has the same expression pattern (up-/down-regulation or no change). In the same graph, node size is proportional to the node degree (i.e. nodes having a large number of connections – hubs – have a larger size). Edges, in box B indicate interactions between proteins encoded by genes represented in nodes, dashed edges indicating a low confidence interaction. In box C, the layout of a metabolic network has been manually defined accordingly to a commonly used representation (in the panel a portion of the TCA cycle). Metabolites are represented with blue nodes having size proportional to the node degree, while reaction nodes are marked with green diamond nodes. Edge thickness is proportional to the value of the flux through a given reaction. In box D, another metabolic network has been represented using a default layout, however metabolite nodes have been represented using boxes inside of which structural formulas are shown; the abundance of every metabolite can be represented here coloring the border of the box accordingly to a color gradient.

A promising way to face visual complexity emerging from -omic size networks, is represented by clustering approaches (e.g. MCODE) that are integrated with network visualization tools and used e.g. to predict higher-order protein complexes from the interaction data. Network clustering is a new kind of clustering method that is performed using correlation networks, in which each node is a gene and each edge indicates co-expression of two genes under a given experimental condition (Figure 3). Available tools include BioLayout Express 3D and Cytoscape.

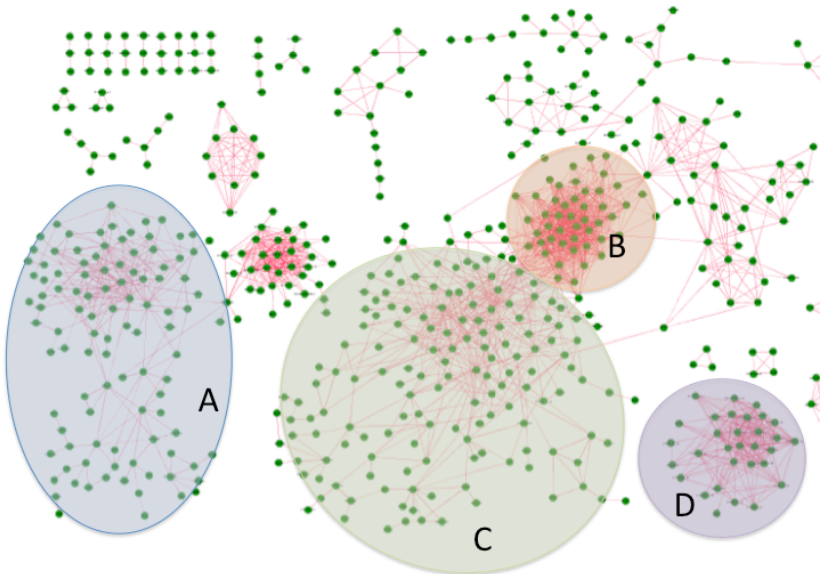

Figure 3 Network showing a clustering of co-expression data using Cytoscape (Dataset from (Prieto et al., 2008)). In the network, genes are mapped as nodes while edges represent the coexpression relation. Identified clusters (isolated groups of nodes highlighted with ellipses) represent different cellular functions, e.g.: A. mitochondrial metabolism, B. ribosome, C. nuclear related metabolism, D. immune response.

A second challenge is connected to the retrieval of desired information and to the network navigation for the exploration of the "surroundings" of a given element, an activity that could generate insights to direct the investigation of the system.

A further challenge can be identified in the enrichment of the visualization by adding further information (e.g. attributes from external sources and database) while maintaining a good readability of the relevant information. In this context, when network enrichment is used to find pathways or networks where genes are significantly over-represented, a valid aid for the interpretation of the results of the analysis is the superimposition on the reference map of the metabolite concentrations or significance levels towards a certain metric by means of dedicated tools, such as MapMan, Pathway Tools Omics Viewer (Figure 4) and ProMeTra.

Figure 4 A cellular overview of the metabolic network of yeast generated with PathwayTools. In this visualization, metabolic reactions are subdivided in pathways (grey boxes), exchange reactions are placed across the border of a rectangle representing the cellular membrane, while reactions not assigned to a specific pathway are grouped on the right side. The metabolic map has been enriched with data (colored nodes) on reporter metabolites (see section "Integrating transcriptomics and metabolic pathways" for a reference on reporter metabolites), the color of the node is set accordingly to the confidence value for the reporter metabolite identification (top left colorbar), the distribution of nodes having a given confidence value is shown on a histogram in the bottom left corner.

Lastly, future perspectives in -omic visualization through networks representations include (1) the exploration of three-dimensional layouts, i.e. multiple networks (representing each one a homogeneous type of data) linked among them to provide a more complete understanding of the system (e.g.: BioLayout Express 3D); (2) combinations of both three-dimensional layouts and temporal descriptions (e.g.: E-Cell 3D); (3) layouts that mix aspects of classic and three dimensional representation (e.g.: Arena3D).

Besides network representations, visualization of -omic data can be performed through complementary approaches that aim at aggregating information and reduce visual complexity. In

particular in the context of transcriptomics (expression profiles), many tools implement scatter plots combined with dimensionality reduction, profile plots, heat maps, dendrograms and clustering.

Visualization tools focused on interaction networks					
Visualization tool	**Main features**	**Functions and compatibility**	**Advantages**	**Web page**	**References**
Arena 3D	Standalone free application. Allows visualizing biological multi-layer networks in 3D.			http://www.arena3d.org/	(Pavlopoulos et al., 2008)
BioLayout Express3D	Layout, visualization and clustering of large scale networks in both 3D and 2D. Supports both unweighted and weighted graphs. Uses a graphic render, so that the size of networks that can be processed is limited.	Highly interactive: it is possible to switch between 2D and 3D representations, zoom in/out, rotate or move the network. Markov Clustering algorithm is incorporated and data are automatically separated in distinct groups. Compatible with Cytoscape.	Offers different analytical approaches to microarray data analysis.	http://www.biolayout.org	(Freeman et al., 2007)
CellDesigner	Structured diagram editor for drawing gene-regulatory and biochemical networks.	Visual Representation of Biochemical Semantics, Direct integration with SBML ODE Solver and Copasi, Linkage to SBW-powered Simulator modules	Intuitive user-interface helps to draw a diagram with the standard SBGN notation	http://www.celldesigner.org	(Funahashi et al., 2008)
Cytoscape	Standalone Java application. Provides 2D representations of large-scale networks (up to hundredth thousands of nodes and edges). Supports directed, undirected and weighted graphs, has powerful visual styles.	Highly interactive: possible zoom in and out and browsing of the network; organization of multiple networks and possibility to compare them; allows to select subsets of nodes/interactions and search for active subnetworks/pathway modules; incorporates statistical analysis of the network. Compatible with other tools. Allows to import mRNA expression profiles, gene functional annotations from GO and KEGG.	Visualization of molecular interaction networks and their integration with gene expression profiles and other data. Allows the manipulation and comparison of multiple networks. Many plug-ins are available for more specialized analysis.	http://www.cytoscape.org	(Shannon et al., 2003)
E-cell 3D	Software platform to model, simulate and analyze complex, heterogeneous and multi-scale biochemical reaction systems.	E-Cell 3D exploits the advanced graphics APIs of MacOS X, however this is the only supported operative system. 3D networks can be navigated using Nintendo Wii remote controller.	Models stored in Systems Biology Markup Language (SBML) XML file can be directly converted to E-Cell 3D.	http://ecell3d.iab.keio.ac.jp/index.html	(Tomita et al., 1999)
iPath	Interactive Pathways Explorer (iPath) is a web-based tool for the visualization, analysis and customization of the various pathways maps.	KEGG based overview maps.	Extensive map customization and data mapping capablities. All maps in iPath can be easily converted to various bitmap and vector graphical formats for easy inclusion in documents or further processing.	http://pathways.embl.de	(Yamada et al., 2011)
MapMan	A user-driven tool that displays large datasets onto diagrams of metabolic pathways or other processes.	Based on Java and hence cross platform.		http://mapman.gabipd.org/	(Thimm et al., 2004)
Medusa	Open source Java application. Provides 2D representation of networks up to a few hundred nodes and edges. Uses non directed, multi-edge connections, allowing the simultaneous representation of more than one connection between two bioentities.	Highly interactive: allows the selection and analysis of subsets of nodes. A text search can be applied to find nodes. Medusa has its own text file format not compatible with other visualization tools or integrated with other data sources.	Shows multi-edge connections, each line representing different concepts of information. It is optimized for PPI data as taken from STRING.	https://sites.google.com/site/medusa3visualization/	(Hooper and Bork, 2005)

Ondex	Standalone freely available open source application. Provides 2D representations of directed, undirected and weighted networks. Handles large scale networks of hundred thousands of nodes and edges and supports bidirectional connections. Different types of data are separating in different disks-circles interconnected between each other.	Various filters allow to selectively add or remove connected nodes from the display. A tree-like sub-graph can be extracted from a given node and the most important nodes at any level can be determined. A filter is available to import microarray expression level data. Data may be imported through many databases, among which are TRANSFAC, Gene Ontology and KEGG.	Ability to combine heterogeneous data types into one network. Suitable for text mining, sequence and data integration analysis.	http://www.ondex.org/	(Koehler et al., 2005, Kohler et al., 2006, Skusa et al., 2005)
Osprey	Standalone application running under a wide range of platforms. Provides 2D representations of directed, undirected and weighted networks. Not efficient for large-scale network analysis but provides various layout options and ways to arrange nodes in different geometric distributions.	Provides several features for functional assessment and comparative analysis of different networks together with network and connectivity filters and dataset superimposing. Also allows to cluster genes by GO Processes. Data can be loaded either by using different text formats or by connecting directly to several databases.	Various filtering capabilities render Osprey a powerful tool for network manipulation. The key feature is the ability to incorporate new interactions into an already existing network.	http://tinyurl.com/osprey1/	(Breitkreutz et al., 2003)
Pajek	Standalone Windows application. Offers 2D and pseudo3D representations, supports single, directed and weighted graphs. Suitable for large scale networks with thousands or million of nodes and vertices. Great variety of layout options. Separates data into layers, allowing the display of hierarchical relationships. Can handle dynamic graphs and reveal how networks change over time.	Highly interactive, many clustering methods. Allows decomposition of a large network into several smaller networks and detection of clusters in them. It has its own input file format, not compatible with commonly used formats; not connected with any biological data sources.	Variety of layout algorithms facilitating exploration and pattern identification within networks.	http://pajek.imfm.si/	(Batagelj and Mrvar, 1998)
PathVisio	Pathway analysis and drawing software to draw edit and analyze biological pathways. Experimental data can be easily visualized on pathways and relevant pathways that are over-represented in a data set can be easily found.	Provides a basic set of features for pathway drawing, analysis and visualization. Additional features are available as plugins.	Plugins extended functionalities and can also be customized for an advanced use.	http://www.pathvisio.org	(Kutmon et al., 2015)
Pathway Tools	A tool to guide the user through creation, editing, querying, visualization, and analysis of Pathway Genome Databases	Wide diffusion in different research communities.	Pathway Tools Omics Viewers allow -omics datasets to be graphically painted onto three system-level diagrams: a diagram of the full metabolic network of the organism, a diagram of the full regulatory network of the organism, and a diagram of the full genome of the organism. It can also depict data from multiple -omic data types simultaneously, such as mixing gene-expression and metabolomics data on one diagram.	http://bioinformatics.ai.sri.com	(Karp et al., 2010)
PIVOT	Java application free for academics. Projects in 2D and uses single non directed lines to show relationships	Allows the expansion of the network, to highlight dense areas of the map, to visualize a subarea of a big network. Many features	Best suited for visualizing PPIs and identifying relationships between them.	http://acgt.cs.tau.ac.il/pivot/	(Orlev et al., 2004)

	between bioentities. No limits in the size of data presented.	help to navigate and interpret the interaction map, and to connect remote proteins to the displayed map through graph-theory algorithms. Configured to work with proteins from human, yeast, *Drosophila* and mouse, links to external web information pages.			
ProMeTra	An open source framework that provides visualization methods for multi-omic datasets.	The integration of genomic and transcriptomic datasets originating from different services.	Format SVG is used to facilitate the visualization of the results of complex functional genomics experiments.	http://fusion.cebitec.uni-bielefeld.de	(Neuweger et al., 2009)
Tulip	Standalone free application. Allows generic visualization of extremely large networks and supports 3D visualization.			http://tulip.labri.fr/TulipDrupal/	(Auber, 2004)
VANTED	Standalone free application. Supports combined visualization of abundance data, networks and pathways.			https://immersive-analytics.infotech.monash.edu/vanted/	(Junker et al., 2006)

Table 2 Visualization tools focused on interaction networks

An interesting cloud-based, community driven resource (GenomeSpace, http://www.genomespace.org) has been recently presented (Qu et al., 2016). Through the implementation of workflows, GenomeSpace aims to make the use of integrative analysis accessible to non-programmers.

Integration of -omic data into models

The statistical and machine learning approaches to data integration illustrated above provide a first attempt to identify the biochemical pathways perturbed in different patients and statistical correlations with drug responses. Identifying recurrent mutations in cancer reveals widespread lineage diversity and mutational specificity, but fails to deliver a system-level understanding of the molecular mechanisms behind the emergence of different phenotypes (Chang et al., 2016). On the other hand, network biology approaches that apply topological and graph theory concepts to biological networks statistically inferred from -omic data or reconstructed according to *a priori* knowledge are important for understanding the structure and properties of the integrated cellular network and its modular structure, with the ultimate aim of understanding its organizational principles (Barabasi et al., 2011). Enrichment of network modules, which integrate -omic data with known or pre-defined molecular scaffolds, allows the identification of the portions of the network that are most active under a given condition (International Cancer Genome Consortium, 2015). Nevertheless, by relying on a static conceptualization of the network, while ignoring its integrated dynamics in state space, also these methods fail to provide a mechanistic understanding of the disease, which would be desirable to reliably predict individual drug response.

The mechanistic understanding of a system requires the integration of these data under mathematical and relational models that can describe dynamically the relationships between their components. Two main computational frameworks allow to predict the phenotype that emerges from a given biological network structure: kinetic modeling and constraint-based modeling.

Kinetic modeling allows estimating the evolution in time of the concentration of each network component in a reacting system (such as metabolites, transcripts or proteins). The transition from one state of the network to the following one is determined by the interaction with the other network components and by rate law equations. The traditional way of modeling the time evolution of the molecular populations in a reacting system is to use ordinary differential equations (ODEs). However, when more appropriate, an approach that considers stochastic fluctuations can be applied.

An example of data integration into kinetic modeling is provided by the kinetic model of glycolysis in yeast (Teusink et al., 2000) and *Plasmodium falciparum* (Penkler et al., 2015). Each glycolytic enzyme was kinetically characterized and the parameters of kinetic equations (for example, Michaelis–Menten) were chosen to best fit the experimental kinetic data; the resulting rate laws incorporated into the model. The difficulty in obtaining kinetic parameters and their appropriateness for *in vivo* situations makes it difficult if not impossible to scale-up traditional kinetic models to large (genome-wide) networks. A recent paper (Bordbar et al., 2015) integrated metabolic profiling data obtained from the plasma of different patients into a whole-cell, metabolic kinetic model of a red blood cell (that includes 55 transport and 87 intracellular reactions). The models allowed to identify individuals at risk for a drug side effect and protective genetic variations, proving the feasibility and usefulness of "personalized" kinetic models, whose use will accelerate discoveries in characterizing individual metabolic variation. Still, routine integration of -omic data into kinetic modeling remains a problematic task that is awaiting improved methodologies.

On the contrary, constraint-based modeling is a framework well suited for metabolic network modeling and multi-omic data integration, which is capable of providing a deeper understanding of metabolic functions than data alone (Hyduke et al., 2013). Constraint-based modeling relies on the idea of excluding phenotypes that do not abide by the imposed constraints, iteratively restricting the space of possible phenotypes until getting the most plausible one(s) (Bordbar et al., 2014). Fundamental assumption of this kind of techniques is a pseudo-steady state for internal metabolites concentrations. As compared to kinetic modeling, constraint-based modeling has the substantial advantage of not requiring any knowledge on kinetic parameters governing reaction rates. Recent developments of constraint-based models account for gene expression reconstructions that use approximate stoichiometric relationships between the level of enzymes and their cognate catalysed

fluxes to compute feasible, optimal and spatially resolved states describing the cellular composition at the molecular level (O'Brien and Palsson, 2015).

Multi-omic data integration into genome-scale constraint-based models

The starting point for multi-omic data integration, within the constraint-based framework, is the description of the entire metabolism of a given organism as a network. This goal is attainable thanks to the increased access to genome sequencing and annotation techniques. Moving from functional gene annotation, a metabolic reaction can be associated to each metabolic gene, that is, the reaction catalyzed by the corresponding enzyme. Once the identified reactions are grouped by metabolite, a genome-wide metabolic network is obtained. According to this paradigm, several genome-wide reconstructions are today available for different organism, from micro-organisms to human. An example is provided by Recon2 (Thiele et al., 2013) and HMR (Mardinoglu et al., 2013), which encompass virtually all the reactions that in principle can occur in human metabolism, and are therefore considered as *generic* reconstructions. Genome-wide generic reconstructions can be customized on specific cell types or tissues (or even patients) by exploiting several kinds of -omic data and appropriate algorithms (for a review see (Yizhak et al., 2015)). The so-obtained *specific* network represents the sub-network that is known to be active in a given cell, according to its transcriptome, proteome, metabolome and fluxome (Agren et al., 2012).

The family of -omic data that can most naturally be incorporated into genome-wide networks is fluxomic data. Constraint based models allow indeed to specify the boundaries for the flux allowed for a given reaction. Constraints on nutrient intake and secretion fluxes (exchange reactions in the constraint-based terminology) are determinant in reducing the space of possible phenotypes.

The incorporation of transcriptome data to further constrain the flux distribution solution space is less straightforward. The main approaches are: (a) the switch approach (e.g. GIMME and iMAT), using on/off reaction fluxes based on threshold expression levels; (b) the valve approach (e.g. E-Flux and PROM): regulate reaction fluxes according to relative gene/protein expressions (Saha et al., 2014). See (Blazier and Papin, 2012) for a recent review.

Paradoxically, metabolite profiling may be the kind of -omic data that can most-difficulty be integrated into genome-wide models (as reviewed in (Topfer et al., 2015)). However, several algorithms, such as the INIT and tINIT (Agren et al., 2014, Agren et al., 2012) have been proposed as an effective strategy to extract the portions of a generic GW model that is active in a given tissue or cell type, according to heterogeneous biological evidence, including metabolome. Based on proteome, or on trascriptome when the former is not available, INIT assigns weights to the reactions in the HMR according to their different levels of evidence in the specific tissue or cell type. A

unitary weight is also assigned to demand reactions (reactions that remove metabolites from the network) according to detected metabolites to impose the capability to accumulate a set of metabolites. An optimization process is then performed with the aim of maximizing as much as possible the reactions fluxes with a high weight (since the corresponding enzymes have a high expression level) while minimizing the others. Reactions that carry flux in the obtained optimal flux distribution are assigned to the tissue or cell specific model.

A more complex approach for integrating quantitative proteomic and metabolomic data with genome-scale metabolic network models, called integrative omics-metabolic analysis (IOMA), was also proposed (Yizhak et al., 2010), which requires a mechanistic model of reaction rates. To evaluate the predictive performance of IOMA, the authors applied it to predict metabolic flux for red blood cells (RBC) for which a detailed kinetic model is available. Remarkably, they demonstrated the advantages in the use of both proteomics and metabolomics to infer metabolic flux, as compared to inputting only one of the sources.
Once an active network is obtained according to the different integration algorithms, Flux Balance Analysis (FBA) is then typically applied to determine the flux distribution that maximizes or minimize a specified objective.

Data integration and human health

The integration of different -omic data, without the aid of computational models, has allowed identifying biomarkers of different human diseases. We focus here on the next step: how integration of data into models may improve system-level understanding of human diseases and in perspective, may help in defining novel drug targets and better therapeutic regimens.

Applications to metabolic diseases

Genome-wide metabolic networks find their natural application in the study of metabolic diseases. In the simplest case, inborn error of metabolism (IEM) can be easily simulated by ‘deleting’ the reaction catalyzed by the enzyme coded by the defecting gene. Metabolic biomarkers can then be predicted by monitoring the change in their feasible exchange flux (Shlomi et al., 2009). Indeed, Recon 2 predicted 54 reported biomarkers for 49 different IEMs, with an accuracy of 77% (Thiele et al., 2013). However, metabolic network modeling has also been successfully applied to the investigation of more complex metabolic diseases, such as diabetes. As an example, the integration of transcriptome data and metabolic pathways, through pathways enrichment analysis has supported the identification of reporter metabolites that allow to distinguish non-alcoholic fatty liver disease from healthy patients (Mardinoglu et al., 2014).

Varemo and colleagues (Varemo et al., 2015) elucidated metabolic alterations in skeletal myocytes associated with type-2 diabetes at a system level, by generating cell-type-specific RNA-sequencing (RNA-seq) data for human myocytes and studying the correlation of this data with proteome data for myocytes from the Human Protein Atlas. Then, the authors constructed a comprehensive myocyte genome-wide model using these data and mapped transcriptional changes related to type-2 diabetes on the myocyte genome-wide model. An extensive transcriptional regulation in type-2 diabetes emerged, particularly around pyruvate oxidation, branched-chain amino acid catabolism and tetrahydrofolate metabolism, connected through the down-regulated dihydrolipoamide dehydrogenase.

Jozefczuk and colleagues (Jozefczuk et al., 2012) analyzed network features of hepatic steatosis, another common metabolic disease. The authors generated gene-set enrichment and over-representation analysis through the pathway database integration system ConsensusPathDB. Network analysis of expression data of steatosis samples *versus* control revealed several pathways and functional modules of the disease, on which a first model prototype of steatosis related processes was developed. The prototype model included a minimal network, comprising a regulatory network (based on the transcription factor SREBF1) linked to a metabolic network of glycerolipid and fatty acid biosynthesis (including the downstream transcriptional targets of SREBF1). As the glutathione pathway was among the pathways enriched in steatosis *versus* control, the authors mapped mRNA expression data to a kinetic model of the glutathione synthesis pathway, focusing on a subset of complete pathways, rather than all genes of the genome. Then, Jozefczuk and co-authors extended this approach to other pathways important for liver regulation and functioning, such as fatty acid biosynthesis, fatty acid metabolism, bile acid pathway, gluconeogenesis, urea cycle, glycolysis, tricarboxylic acid cycle, and glyoxalate shunt. An object-oriented, comprehensive, multi-pathway, multi-tissue *in silico* platform to investigate hepatic metabolism and its associated deregulations has been constructed The SteatoNet model ability to effectively describe biological behavior has been proven by its ability to identify metabolic flux alterations previously identified experimentally in liver patients and animal models (Naik et al., 2014).

Applications to cancer research

Besides metabolic diseases, modeling of metabolic networks finds a large application in cancer research, where alterations in metabolism have been identified as a major hallmark of cancer (Hanahan and Weinberg, 2011, Alberghina et al., 2014, Yizhak et al., 2015). FBA - typically exploited to predict physiologically relevant growth rates or the rate of metabolite production as a function of the underlying biochemical networks (Lewis et al., 2012, O'Brien et al., 2015) - is

particularly useful to investigate the metabolic reprogramming performed by cancer cells (Jerby and Ruppin, 2012). FBA allows to identify, given a specified nutrient availability the distribution of metabolic flux across the various pathways that maximize growth. In fact, enhanced growth indistinctly characterizes cancer cells and can be regarded as their 'purpose'. To this aim, the Human Metabolic Atlas offers a collection of tissue-specific reconstructions for both health and tumor tissues, obtained with the INIT algorithm, starting from the generic human reconstruction HMR and from -omic data in public databases such as the Human Protein Atlas (Uhlen et al., 2010). The Human Metabolic Atlas also includes functional personalized GEMs for six Hepatocellular carcinoma (HCC) patients (Agren et al., 2014). Agren et al. (Agren et al., 2014) identified strong differences among the six HCC patients and simulated the effect of potential antimetabolites, by blocking the reactions that the corresponding metabolite engages in. They identified potential antimetabolites with antiproliferative or cytotoxic effect against HCC tumors for all six patients. Among these potential antimetabolites, they experimentally evaluated the effect of an L-carnitine analog on HepG2 cell proliferation, confirming their genome-scale modeling predictions.

In 2015, Asgari and colleagues (Asgari et al., 2015) used the human metabolic model Recon1 as a scaffold to reconstruct tissue-specific models with the E-Flux method, which maps gene expression data into a genome-wide model by constraining the maximum possible flux through the reactions. Then, through FBA, the authors computed the reaction fluxes between normal and corresponding cancer cells in their subsystems. They found that the distribution of increased and decreased metabolic fluxes was unrelated to the significantly up- and down-regulated metabolic genes of the associated cancer. Thus, they demonstrated that expression pattern of all metabolic genes (and not just significant up- and down-regulated ones) plays a key role in metabolic rewiring of cancer cells. Consistently, rather than differential expression of specific genes, 7 subsystems (out of 13 common to all considered cancer cells) appear to be responsible for the Warburg effect: glutamine metabolism, nucleotides, glycolysis, oxidative phosphorylation, pentose phosphate pathway, TCA cycle and pyruvate metabolism. Therefore, the Warburg effect appears to be a consequence of metabolic adaptation.

GEMs indeed represent a valuable tool to investigate the rationale behind metabolic events associated with cancer like the Warburg effect (Shlomi et al., 2011). In this regard, Shlomi and colleagues inserted a solvent capacity constraint to the genome-scale human metabolic reconstruction Recon1 (Mo et al., 2007) to show how aerobic glycolysis emerges as the best strategy for growth. Along similar lines, (Vazquez, 2010) used a reduced flux balance model of ATP production constrained by the glucose uptake capacity and by the solvent capacity of cell's

cytoplasm, to demonstrate that the Warburg effect is a favorable catabolic state for rapidly proliferating cells with high glucose uptake capacity.

When studying metabolic plasticity and the ability of cells to adapt to changing environmental conditions, "core models" may be a valuable alternative to GEMs by allowing to highlight the more relevant properties of the network (Cazzaniga et al., 2014). Di Filippo and colleagues extracted and manually curated, from the corresponding GEMs in the Human Metabolic Atlas, specific constraint-based core models for liver, breast and lung tumors. A core model reconstructed starting from the original general human metabolic network was used as a reference. The three tumor models showed common metabolic properties reported in different kind of tumors: down regulation of respiratory chain, enhanced glycolytic flux, stimulated utilization of glutamine *via* reductive carboxylation. Metabolic flux distribution among the three tumors was significantly different. Reactions that were present in the reference model, but absent in the tumors models were isolated. Their insertion into the cancer models resulted in a less cancerous phenotype and, vice versa, their deletion from the generic models lead to a more cancerous phenotype. A group of reactions in particular was identified to be critically responsible for the reversion of tumor models towards less cancerous phenotypes (Di Filippo et al., 2016). The group includes the transport of phosphates from cytosol and mitochondrion, whose role for the correct functioning of the respiratory chain was indeed demonstrated in literature (Palmieri, 2004). The metabolic advantages provided by particular metabolic events as compared to alternative phenotypes may also be investigated by comparing ensembles of flux distributions consistent with alternative strategies (Damiani et al., 2014).

The workflow of constraint-based data integration approaches to cancer is schematically illustrated in Figure 5.

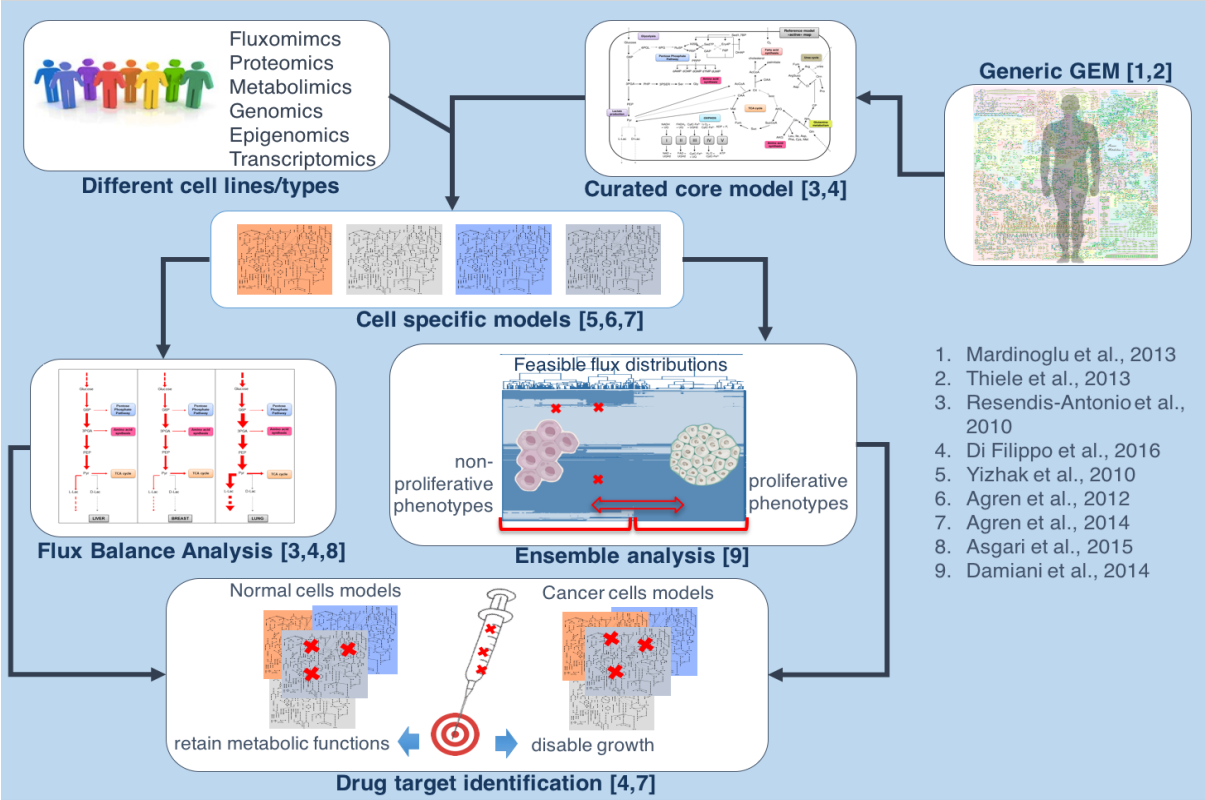

Figure 5 Workflow of constraint-based data integration approaches to cancer. Workflow from the extraction and curation of a model from the generic human metabolic map (top-right box), to its customization according to -omic data (following the arrows downstream of top boxes), to its flux balance analysis to estimate fluxes and other approaches (such as the ensemble approach) to explore the space of possible phenotypes, to the simulation of possible drug targets (bottom box). For each process some references are reported as an example.

Conclusions

Integration of different -omic technologies allows to better extract hidden information in each data set allowing an unprecedented precision in the definition of the molecular phenotype of patient-derived samples. Correlation of these high-resolution molecular phenotypes to the clinical outcome provides precious indications for the development of novel stratification procedures to be used in the choice of the more appropriate therapeutic regimen. Integration of (multi)-omic data into mathematical models of diseased networks – notably metabolic networks – allows *ex-post* examination of patients data collections. These personalized models provided the proof-of-principle of their ability to identify fragility points and to design appropriate personalized therapeutic regimens. As technical improvements and reductions in cost make it easier and easier to collect -omic data and more powerful and efficient computational methods are devised, it will be possible to apply this workflow in real time and use it as a guide in the design of a patient's personalized therapy, enabling the customization of medical care to the specific phenotype of each patient rather than providing a single, conventional treatment.

References

ABECASIS, G. R., ALTSHULER, D., AUTON, A., BROOKS, L. D., DURBIN, R. M., GIBBS, R. A., HURLES, M. E. & MCVEAN, G. A. 2010. A map of human genome variation from population-scale sequencing. *Nature,* 467**,** 1061-73.

ABECASIS, G. R., AUTON, A., BROOKS, L. D., DEPRISTO, M. A., DURBIN, R. M., HANDSAKER, R. E., KANG, H. M., MARTH, G. T. & MCVEAN, G. A. 2012. An integrated map of genetic variation from 1,092 human genomes. *Nature,* 491**,** 56-65.

AGREN, R., BORDEL, S., MARDINOGLU, A., PORNPUTTAPONG, N., NOOKAEW, I. & NIELSEN, J. 2012. Reconstruction of genome-scale active metabolic networks for 69 human cell types and 16 cancer types using INIT. *PLoS computational biology,* 8**,** e1002518.

AGREN, R., MARDINOGLU, A., ASPLUND, A., KAMPF, C., UHLEN, M. & NIELSEN, J. 2014. Identification of anticancer drugs for hepatocellular carcinoma through personalized genome-scale metabolic modeling. *Molecular systems biology,* 10**,** 721.

ALBERGHINA, L., GAGLIO, D., MORESCO, R. M., GILARDI, M. C., MESSA, C. & VANONI, M. 2014. A systems biology road map for the discovery of drugs targeting cancer cell metabolism. *Current pharmaceutical design,* 20**,** 2648-66.

ALBERGHINA, L. & WESTERHOFF, H. V. 2005. Systems Biology: Did we know it all along? in Systems Biology: Definitions and Perspectives. *Topics in Current Genetics - Springer-Verlag Berlin Heidelberg,* 13**,** 3-9.

AMBROS, V. 2004. The functions of animal microRNAs. *Nature,* 431**,** 350-5.

ASGARI, Y., ZABIHINPOUR, Z., SALEHZADEH-YAZDI, A., SCHREIBER, F. & MASOUDI-NEJAD, A. 2015. Alterations in cancer cell metabolism: the Warburg effect and metabolic adaptation. *Genomics,* 105**,** 275-81.

AUBER, D. 2004. Tulip — A Huge Graph Visualization Framework. Graph Drawing Software. *Springer-Verlag Berlin Heidelberg***,** 105-126.

AUFFRAY, C. & HOOD, L. 2012. Editorial: Systems biology and personalized medicine - the future is now. *Biotechnology journal,* 7**,** 938-9.

BAMFORD, S., DAWSON, E., FORBES, S., CLEMENTS, J., PETTETT, R., DOGAN, A., FLANAGAN, A., TEAGUE, J., FUTREAL, P. A., STRATTON, M. R. & WOOSTER, R. 2004. The COSMIC (Catalogue of Somatic Mutations in Cancer) database and website. *British journal of cancer,* 91**,** 355-8.

BARABASI, A. L., GULBAHCE, N. & LOSCALZO, J. 2011. Network medicine: a network-based approach to human disease. *Nature reviews. Genetics,* 12**,** 56-68.

BARRETT, T., WILHITE, S. E., LEDOUX, P., EVANGELISTA, C., KIM, I. F., TOMASHEVSKY, M., MARSHALL, K. A., PHILLIPPY, K. H., SHERMAN, P. M., HOLKO, M., YEFANOV, A., LEE, H., ZHANG, N., ROBERTSON, C. L., SEROVA, N., DAVIS, S. & SOBOLEVA, A. 2013. NCBI GEO: archive for functional genomics data sets--update. *Nucleic acids research,* 41**,** D991-5.

BATAGELJ, V. & MRVAR, A. 1998. Pajek – Program for Large Network Analysis. *Connections,* 21**,** 47-57.

BERSANELLI, M., MOSCA, E., REMONDINI, D., GIAMPIERI, E., SALA, C., CASTELLANI, G. & MILANESI, L. 2016. Methods for the integration of multi-omics data: mathematical aspects. *BMC bioinformatics,* 17 Suppl 2**,** 15.

BHALLA, U. S. & IYENGAR, R. 1999. Emergent properties of networks of biological signaling pathways. *Science,* 283**,** 381-7.

BLAZIER, A. S. & PAPIN, J. A. 2012. Integration of expression data in genome-scale metabolic network reconstructions. *Frontiers in physiology,* 3**,** 299.

BORDBAR, A., MCCLOSKEY, D., ZIELINSKI, D. C., SONNENSCHEIN, N., JAMSHIDI, N. & PALSSON, B. O. 2015. Personalized Whole-Cell Kinetic Models of Metabolism for Discovery in Genomics and Pharmacodynamics. *Cell systems,* 1**,** 283-292.

BORDBAR, A., MONK, J. M., KING, Z. A. & PALSSON, B. O. 2014. Constraint-based models predict metabolic and associated cellular functions. *Nature reviews. Genetics,* 15**,** 107-20.

BREITKREUTZ, B. J., STARK, C. & TYERS, M. 2003. Osprey: a network visualization system. *Genome biology,* 4**,** R22.

BUCCI, E. M., NATALE, M. & POLI, A. 2011. Protein Networks: Generation, Structural Analysis and Exploitation, Systems and Computational Biology - Molecular and Cellular Experimental Systems. *INTECH*.

CANTOR, R. M., LANGE, K. & SINSHEIMER, J. S. 2010. Prioritizing GWAS results: A review of statistical methods and recommendations for their application. *American journal of human genetics,* 86**,** 6-22.

CAZZANIGA, P., DAMIANI, C., BESOZZI, D., COLOMBO, R., NOBILE, M. S., GAGLIO, D., PESCINI, D., MOLINARI, S., MAURI, G., ALBERGHINA, L. & VANONI, M. 2014. Computational strategies for a system-level understanding of metabolism. *Metabolites,* 4**,** 1034-87.

CHANG, M. T., ASTHANA, S., GAO, S. P., LEE, B. H., CHAPMAN, J. S., KANDOTH, C., GAO, J., SOCCI, N. D., SOLIT, D. B., OLSHEN, A. B., SCHULTZ, N. & TAYLOR, B. S. 2016. Identifying recurrent mutations in cancer reveals widespread lineage diversity and mutational specificity. *Nature biotechnology,* 34**,** 155-63.

CHEN, J. & YUAN, B. 2006. Detecting functional modules in the yeast protein-protein interaction network. *Bioinformatics,* 22**,** 2283-90.

CHUANG, H. Y., LEE, E., LIU, Y. T., LEE, D. & IDEKER, T. 2007. Network-based classification of breast cancer metastasis. *Molecular systems biology,* 3**,** 140.

COM, E., BOITIER, E., MARCHANDEAU, J. P., BRANDENBURG, A., SCHROEDER, S., HOFFMANN, D., MALLY, A. & GAUTIER, J. C. 2012. Integrated transcriptomic and proteomic evaluation of gentamicin nephrotoxicity in rats. *Toxicology and applied pharmacology,* 258**,** 124-33.

DAMIANI, C., PESCINI, D., COLOMBO, R., MOLINARI, S., ALBERGHINA, L., VANONI, M. & MAURI, G. 2014. An ensemble evolutionary constraint-based approach to understand the emergence of metabolic phenotypes. *Natural Computing,* 13**,** 321-331.

DESMEDT, C., HAIBE-KAINS, B., WIRAPATI, P., BUYSE, M., LARSIMONT, D., BONTEMPI, G., DELORENZI, M., PICCART, M. & SOTIRIOU, C. 2008. Biological processes associated with breast cancer clinical outcome depend on the molecular subtypes. *Clinical cancer research : an official journal of the American Association for Cancer Research,* 14**,** 5158-65.

DI FILIPPO, M., COLOMBO, R., DAMIANI, C., PESCINI, D., GAGLIO, D., VANONI, M., ALBERGHINA, L. & MAURI, G. 2016. Zooming-in on cancer metabolic rewiring with tissue specific constraint-based models. *Computational biology and chemistry,* 62**,** 60-69.

ECKER, J. R., BICKMORE, W. A., BARROSO, I., PRITCHARD, J. K., GILAD, Y. & SEGAL, E. 2012. Genomics: ENCODE explained. *Nature,* 489**,** 52-5.

EDGAR, R., DOMRACHEV, M. & LASH, A. E. 2002. Gene Expression Omnibus: NCBI gene expression and hybridization array data repository. *Nucleic acids research,* 30**,** 207-10.

EIN-DOR, L., KELA, I., GETZ, G., GIVOL, D. & DOMANY, E. 2005. Outcome signature genes in breast cancer: is there a unique set? *Bioinformatics,* 21**,** 171-8.

ELBERS, C. C., VAN EIJK, K. R., FRANKE, L., MULDER, F., VAN DER SCHOUW, Y. T., WIJMENGA, C. & ONLAND-MORET, N. C. 2009. Using genome-wide pathway analysis to unravel the etiology of complex diseases. *Genetic epidemiology,* 33**,** 419-31.

ELLIS, M. J., GILLETTE, M., CARR, S. A., PAULOVICH, A. G., SMITH, R. D., RODLAND, K. K., TOWNSEND, R. R., KINSINGER, C., MESRI, M., RODRIGUEZ, H. & LIEBLER, D. C. 2013. Connecting genomic alterations to cancer biology with proteomics: the NCI Clinical Proteomic Tumor Analysis Consortium. *Cancer discovery,* 3**,** 1108-12.

ENCODE PROJECT CONSORTIUM 2011. A user's guide to the encyclopedia of DNA elements (ENCODE). *PLoS biology,* 9**,** e1001046.

FREEMAN, T. C., GOLDOVSKY, L., BROSCH, M., VAN DONGEN, S., MAZIERE, P., GROCOCK, R. J., FREILICH, S., THORNTON, J. & ENRIGHT, A. J. 2007. Construction, visualisation, and clustering of transcription networks from microarray expression data. *PLoS computational biology,* 3**,** 2032-42.

FUNAHASHI, A., MATSUOKA, Y., JOURAKU, A., MOROHASHI, M., KIKUCHI, N. & KITANO, H. 2008. CellDesigner 3.5: A Versatile Modeling Tool for Biochemical Networks. *Proceedings of the IEEE,* 96**,** 1254-1265.

GARCIA, M., MILLAT-CARUS, R., BERTUCCI, F., FINETTI, P., BIRNBAUM, D. & BIDAUT, G. 2012. Interactome-transcriptome integration for predicting distant metastasis in breast cancer. *Bioinformatics,* 28**,** 672-8.

GEHLENBORG, N., O'DONOGHUE, S. I., BALIGA, N. S., GOESMANN, A., HIBBS, M. A., KITANO, H., KOHLBACHER, O., NEUWEGER, H., SCHNEIDER, R., TENENBAUM, D. & GAVIN, A. C. 2010. Visualization of omics data for systems biology. *Nature methods,* 7**,** S56-68.

GHAZALPOUR, A., BENNETT, B., PETYUK, V. A., OROZCO, L., HAGOPIAN, R., MUNGRUE, I. N., FARBER, C. R., SINSHEIMER, J., KANG, H. M., FURLOTTE, N., PARK, C. C., WEN, P. Z., BREWER, H., WEITZ, K., CAMP, D. G., 2ND, PAN, C., YORDANOVA, R., NEUHAUS, I., TILFORD, C., SIEMERS, N., GARGALOVIC, P., ESKIN, E., KIRCHGESSNER, T., SMITH, D. J., SMITH, R. D. & LUSIS, A. J. 2011. Comparative analysis of proteome and transcriptome variation in mouse. *PLoS genetics,* 7**,** e1001393.

GOMEZ-CABRERO, D., ABUGESSAISA, I., MAIER, D., TESCHENDORFF, A., MERKENSCHLAGER, M., GISEL, A., BALLESTAR, E., BONGCAM-RUDLOFF, E., CONESA, A. & TEGNER, J. 2014. Data integration in the era of omics: current and future challenges. *BMC systems biology,* 8 Suppl 2**,** I1.

GUSTAFSSON, M., NESTOR, C. E., ZHANG, H., BARABASI, A. L., BARANZINI, S., BRUNAK, S., CHUNG, K. F., FEDEROFF, H. J., GAVIN, A. C., MEEHAN, R. R., PICOTTI, P., PUJANA, M. A., RAJEWSKY, N., SMITH, K. G., STERK, P. J., VILLOSLADA, P. & BENSON, M. 2014. Modules, networks and systems medicine for understanding disease and aiding diagnosis. *Genome medicine,* 6**,** 82.

HAIDER, S. & PAL, R. 2013. Integrated analysis of transcriptomic and proteomic data. *Current genomics,* 14**,** 91-110.

HANAHAN, D. & WEINBERG, R. A. 2011. Hallmarks of cancer: the next generation. *Cell,* 144**,** 646-74.

HARROW, J., FRANKISH, A., GONZALEZ, J. M., TAPANARI, E., DIEKHANS, M., KOKOCINSKI, F., AKEN, B. L., BARRELL, D., ZADISSA, A., SEARLE, S., BARNES, I., BIGNELL, A., BOYCHENKO, V., HUNT, T., KAY, M., MUKHERJEE, G., RAJAN, J., DESPACIO-REYES, G., SAUNDERS, G., STEWARD, C., HARTE, R., LIN, M., HOWALD, C., TANZER, A., DERRIEN, T., CHRAST, J., WALTERS, N., BALASUBRAMANIAN, S., PEI, B., TRESS, M., RODRIGUEZ, J. M., EZKURDIA, I., VAN BAREN, J., BRENT, M., HAUSSLER, D., KELLIS, M., VALENCIA, A., REYMOND, A., GERSTEIN, M., GUIGO, R. & HUBBARD, T. J. 2012. GENCODE: the reference human genome annotation for The ENCODE Project. *Genome research,* 22**,** 1760-74.

HIGDON, R., STEWART, E., STANBERRY, L., HAYNES, W., CHOINIERE, J., MONTAGUE, E., ANDERSON, N., YANDL, G., JANKO, I., BROOMALL, W., FISHILEVICH, S., LANCET, D., KOLKER, N. & KOLKER, E. 2014. MOPED enables discoveries through consistently processed proteomics data. *Journal of proteome research,* 13**,** 107-13.

HINNEBUSCH, A. G. 2014. The scanning mechanism of eukaryotic translation initiation. *Annual review of biochemistry,* 83**,** 779-812.

HOOD, L., BALLING, R. & AUFFRAY, C. 2012. Revolutionizing medicine in the 21st century through systems approaches. *Biotechnology journal,* 7**,** 992-1001.

HOOD, L. & TIAN, Q. 2012. Systems approaches to biology and disease enable translational systems medicine. *Genomics, proteomics & bioinformatics,* 10**,** 181-5.

HOOPER, S. D. & BORK, P. 2005. Medusa: a simple tool for interaction graph analysis. *Bioinformatics,* 21**,** 4432-3.

HORNBERG, J. J., BRUGGEMAN, F. J., WESTERHOFF, H. V. & LANKELMA, J. 2006. Cancer: a Systems Biology disease. *Bio Systems,* 83**,** 81-90.

HORTOBAGYI, G. N. 2012. Toward individualized breast cancer therapy: translating biological concepts to the bedside. *The oncologist,* 17**,** 577-84.

HUBBARD, T., BARKER, D., BIRNEY, E., CAMERON, G., CHEN, Y., CLARK, L., COX, T., CUFF, J., CURWEN, V., DOWN, T., DURBIN, R., EYRAS, E., GILBERT, J., HAMMOND, M., HUMINIECKI, L., KASPRZYK, A., LEHVASLAIHO, H., LIJNZAAD, P., MELSOPP, C., MONGIN, E., PETTETT, R., POCOCK, M., POTTER, S., RUST, A., SCHMIDT, E., SEARLE, S., SLATER, G., SMITH, J., SPOONER, W., STABENAU, A., STALKER, J., STUPKA, E., URETA-VIDAL, A., VASTRIK, I. & CLAMP, M. 2002. The Ensembl genome database project. *Nucleic acids research,* 30**,** 38-41.

HUDSON, T. J., ANDERSON, W., ARTEZ, A., BARKER, A. D., BELL, C., BERNABE, R. R., BHAN, M. K., CALVO, F., EEROLA, I., GERHARD, D. S., GUTTMACHER, A., GUYER, M., HEMSLEY, F. M., JENNINGS, J. L., KERR, D., KLATT, P., KOLAR, P., KUSADA, J., LANE, D. P., LAPLACE, F., YOUYONG, L., NETTEKOVEN, G.,

OZENBERGER, B., PETERSON, J., RAO, T. S., REMACLE, J., SCHAFER, A. J., SHIBATA, T., STRATTON, M. R., VOCKLEY, J. G., WATANABE, K., YANG, H., YUEN, M. M., KNOPPERS, B. M., BOBROW, M., CAMBON-THOMSEN, A., DRESSLER, L. G., DYKE, S. O., JOLY, Y., KATO, K., KENNEDY, K. L., NICOLAS, P., PARKER, M. J., RIAL-SEBBAG, E., ROMEO-CASABONA, C. M., SHAW, K. M., WALLACE, S., WIESNER, G. L., ZEPS, N., LICHTER, P., BIANKIN, A. V., CHABANNON, C., CHIN, L., CLEMENT, B., DE ALAVA, E., DEGOS, F., FERGUSON, M. L., GEARY, P., HAYES, D. N., JOHNS, A. L., KASPRZYK, A., NAKAGAWA, H., PENNY, R., PIRIS, M. A., SARIN, R., SCARPA, A., VAN DE VIJVER, M., FUTREAL, P. A., ABURATANI, H., BAYES, M., BOTWELL, D. D., CAMPBELL, P. J., ESTIVILL, X., GRIMMOND, S. M., GUT, I., HIRST, M., LOPEZ-OTIN, C., MAJUMDER, P., MARRA, M., MCPHERSON, J. D., NING, Z., PUENTE, X. S., RUAN, Y., STUNNENBERG, H. G., SWERDLOW, H., VELCULESCU, V. E., WILSON, R. K., XUE, H. H., YANG, L., SPELLMAN, P. T., BADER, G. D., BOUTROS, P. C., FLICEK, P., GETZ, G., GUIGO, R., GUO, G., HAUSSLER, D., HEATH, S., HUBBARD, T. J., JIANG, T., et al. 2010. International network of cancer genome projects. *Nature,* 464**,** 993-8.

HYDUKE, D. R., LEWIS, N. E. & PALSSON, B. O. 2013. Analysis of omics data with genome-scale models of metabolism. *Molecular bioSystems,* 9**,** 167-74.

IMIELINSKI, M., CHA, S., REJTAR, T., RICHARDSON, E. A., KARGER, B. L. & SGROI, D. C. 2012. Integrated proteomic, transcriptomic, and biological network analysis of breast carcinoma reveals molecular features of tumorigenesis and clinical relapse. *Molecular & cellular proteomics : MCP,* 11**,** M111 014910.

INTERNATIONAL CANCER GENOME CONSORTIUM, M. C. A. P. A. W. G. 2015. Pathway and network analysis of cancer genomes. *Nature methods,* 12**,** 615-21.

JERBY, L. & RUPPIN, E. 2012. Predicting drug targets and biomarkers of cancer via genome-scale metabolic modeling. *Clinical cancer research : an official journal of the American Association for Cancer Research,* 18**,** 5572-84.

JOZEFCZUK, J., KASHOFER, K., UMMANNI, R., HENJES, F., REHMAN, S., GEENEN, S., WRUCK, W., REGENBRECHT, C., DASKALAKI, A., WIERLING, C., TURANO, P., BERTINI, I., KORF, U., ZATLOUKAL, K., WESTERHOFF, H. V., LEHRACH, H. & ADJAYE, J. 2012. A Systems Biology Approach to Deciphering the Etiology of Steatosis Employing Patient-Derived Dermal Fibroblasts and iPS Cells. *Frontiers in physiology,* 3**,** 339.

JUNKER, B. H., KLUKAS, C. & SCHREIBER, F. 2006. VANTED: a system for advanced data analysis and visualization in the context of biological networks. *BMC bioinformatics,* 7**,** 109.

KANEHISA, M. & GOTO, S. 2000. KEGG: kyoto encyclopedia of genes and genomes. *Nucleic acids research,* 28**,** 27-30.

KARP, P. D., PALEY, S. M., KRUMMENACKER, M., LATENDRESSE, M., DALE, J. M., LEE, T. J., KAIPA, P., GILHAM, F., SPAULDING, A., POPESCU, L., ALTMAN, T., PAULSEN, I., KESELER, I. M. & CASPI, R. 2010. Pathway Tools version 13.0: integrated software for pathway/genome informatics and systems biology. *Briefings in bioinformatics,* 11**,** 40-79.

KITANO, H. 2002. Systems biology: a brief overview. *Science,* 295**,** 1662-4.

KITANO, H. 2004. Cancer as a robust system: implications for anticancer therapy. *Nature reviews. Cancer,* 4**,** 227-35.

KITANO, H. 2007a. A robustness-based approach to systems-oriented drug design. *Nature reviews. Drug discovery,* 6**,** 202-10.

KITANO, H. 2007b. The theory of biological robustness and its implication in cancer. *Ernst Schering Research Foundation workshop***,** 69-88.

KOEHLER, J., RAWLINGS, C., VERRIER, P., MITCHELL, R., SKUSA, A., RUEGG, A. & PHILIPPI, S. 2005. Linking experimental results, biological networks and sequence analysis methods using Ontologies and Generalised Data Structures. *In silico biology,* 5**,** 33-44.

KOHLER, J., BAUMBACH, J., TAUBERT, J., SPECHT, M., SKUSA, A., RUEGG, A., RAWLINGS, C., VERRIER, P. & PHILIPPI, S. 2006. Graph-based analysis and visualization of experimental results with ONDEX. *Bioinformatics,* 22**,** 1383-90.

KOLKER, E., HIGDON, R., HAYNES, W., WELCH, D., BROOMALL, W., LANCET, D., STANBERRY, L. & KOLKER, N. 2012. MOPED: Model Organism Protein Expression Database. *Nucleic acids research,* 40**,** D1093-9.

KROGAN, N. J., LIPPMAN, S., AGARD, D. A., ASHWORTH, A. & IDEKER, T. 2015. The cancer cell map initiative: defining the hallmark networks of cancer. *Molecular cell,* 58**,** 690-8.

KUTMON, M., VAN IERSEL, M. P., BOHLER, A., KELDER, T., NUNES, N., PICO, A. R. & EVELO, C. T. 2015. PathVisio 3: an extendable pathway analysis toolbox. *PLoS computational biology,* 11**,** e1004085.

LANGLEY, S. R., DWYER, J., DROZDOV, I., YIN, X. & MAYR, M. 2013. Proteomics: from single molecules to biological pathways. *Cardiovascular research,* 97**,** 612-22.

LEUNG, E. L., CAO, Z. W., JIANG, Z. H., ZHOU, H. & LIU, L. 2013. Network-based drug discovery by integrating systems biology and computational technologies. *Briefings in bioinformatics,* 14**,** 491-505.

LEWIS, N. E., NAGARAJAN, H. & PALSSON, B. O. 2012. Constraining the metabolic genotype-phenotype relationship using a phylogeny of in silico methods. *Nature reviews. Microbiology,* 10**,** 291-305.

LICATA, L., BRIGANTI, L., PELUSO, D., PERFETTO, L., IANNUCCELLI, M., GALEOTA, E., SACCO, F., PALMA, A., NARDOZZA, A. P., SANTONICO, E., CASTAGNOLI, L. & CESARENI, G. 2012. MINT, the molecular interaction database: 2012 update. *Nucleic acids research,* 40**,** D857-61.

LIU, Y., DEVESCOVI, V., CHEN, S. & NARDINI, C. 2013. Multilevel omic data integration in cancer cell lines: advanced annotation and emergent properties. *BMC systems biology,* 7**,** 14.

MARDINOGLU, A., AGREN, R., KAMPF, C., ASPLUND, A., NOOKAEW, I., JACOBSON, P., WALLEY, A. J., FROGUEL, P., CARLSSON, L. M., UHLEN, M. & NIELSEN, J. 2013. Integration of clinical data with a genome-scale metabolic model of the human adipocyte. *Molecular systems biology,* 9**,** 649.

MARDINOGLU, A., AGREN, R., KAMPF, C., ASPLUND, A., UHLEN, M. & NIELSEN, J. 2014. Genome-scale metabolic modelling of hepatocytes reveals serine deficiency in patients with non-alcoholic fatty liver disease. *Nature communications,* 5**,** 3083.

MENASHE, I., MAEDER, D., GARCIA-CLOSAS, M., FIGUEROA, J. D., BHATTACHARJEE, S., ROTUNNO, M., KRAFT, P., HUNTER, D. J., CHANOCK, S. J., ROSENBERG, P. S. & CHATTERJEE, N. 2010. Pathway analysis of breast cancer genome-wide association study highlights three pathways and one canonical signaling cascade. *Cancer research,* 70**,** 4453-9.

MO, M. L., JAMSHIDI, N. & PALSSON, B. O. 2007. A genome-scale, constraint-based approach to systems biology of human metabolism. *Molecular bioSystems,* 3**,** 598-603.

MORE, T., ROYCHOUDHURY, S., GOLLAPALLI, K., PATEL, S. K., GOWDA, H., CHAUDHURY, K. & RAPOLE, S. 2015. Metabolomics and its integration with systems biology: PSI 2014 conference panel discussion report. *Journal of proteomics,* 127**,** 73-9.

MUNIATEGUI, A., PEY, J., PLANES, F. J. & RUBIO, A. 2013. Joint analysis of miRNA and mRNA expression data. *Briefings in bioinformatics,* 14**,** 263-78.

NAIK, A., ROZMAN, D. & BELIC, A. 2014. SteatoNet: the first integrated human metabolic model with multi-layered regulation to investigate liver-associated pathologies. *PLoS computational biology,* 10**,** e1003993.

NAM, S., LI, M., CHOI, K., BALCH, C., KIM, S. & NEPHEW, K. P. 2009. MicroRNA and mRNA integrated analysis (MMIA): a web tool for examining biological functions of microRNA expression. *Nucleic acids research,* 37**,** W356-62.

NARIAI, N., KIM, S., IMOTO, S. & MIYANO, S. 2004. Using protein-protein interactions for refining gene networks estimated from microarray data by Bayesian networks. *Pacific Symposium on Biocomputing. Pacific Symposium on Biocomputing***,** 336-47.

NEUWEGER, H., PERSICKE, M., ALBAUM, S. P., BEKEL, T., DONDRUP, M., HUSER, A. T., WINNEBALD, J., SCHNEIDER, J., KALINOWSKI, J. & GOESMANN, A. 2009. Visualizing post genomics data-sets on customized pathway maps by ProMeTra-aeration-dependent gene expression and metabolism of Corynebacterium glutamicum as an example. *BMC systems biology,* 3**,** 82.

NISHIZAWA, M., OKUMURA, T., IKEYA, Y. & KIMURA, T. 2012. Regulation of inducible gene expression by natural antisense transcripts. *Frontiers in bioscience,* 17**,** 938-58.

O'BRIEN, E. J., MONK, J. M. & PALSSON, B. O. 2015. Using Genome-scale Models to Predict Biological Capabilities. *Cell,* 161**,** 971-87.

O'BRIEN, E. J. & PALSSON, B. O. 2015. Computing the functional proteome: recent progress and future prospects for genome-scale models. *Current opinion in biotechnology,* 34**,** 125-34.

OGILVIE, L. A., WIERLING, C., KESSLER, T., LEHRACH, H. & LANGE, B. M. 2015. Predictive Modeling of Drug Treatment in the Area of Personalized Medicine. *Cancer informatics,* 14**,** 95-103.

ORCHARD, S., AMMARI, M., ARANDA, B., BREUZA, L., BRIGANTI, L., BROACKES-CARTER, F., CAMPBELL, N. H., CHAVALI, G., CHEN, C., DEL-TORO, N., DUESBURY, M., DUMOUSSEAU, M., GALEOTA, E., HINZ, U., IANNUCCELLI, M., JAGANNATHAN, S., JIMENEZ, R., KHADAKE, J., LAGREID, A., LICATA, L., LOVERING, R. C., MELDAL, B., MELIDONI, A. N., MILAGROS, M., PELUSO, D., PERFETTO, L., PORRAS, P., RAGHUNATH, A., RICARD-BLUM, S., ROECHERT, B., STUTZ, A., TOGNOLLI, M., VAN ROEY, K., CESARENI, G. & HERMJAKOB, H. 2014. The MIntAct project--IntAct as a common curation platform for 11 molecular interaction databases. *Nucleic acids research,* 42**,** D358-63.

ORLEV, N., SHAMIR, R. & SHILOH, Y. 2004. PIVOT: protein interacions visualizatiOn tool. *Bioinformatics,* 20**,** 424-5.

OUGHTRED, R., CHATR-ARYAMONTRI, A., BREITKREUTZ, B. J., CHANG, C. S., RUST, J. M., THEESFELD, C. L., HEINICKE, S., BREITKREUTZ, A., CHEN, D., HIRSCHMAN, J., KOLAS, N., LIVSTONE, M. S., NIXON, J., O'DONNELL, L., RAMAGE, L., WINTER, A., REGULY, T., SELLAM, A., STARK, C., BOUCHER, L., DOLINSKI, K. & TYERS, M. 2016. Use of the BioGRID Database for Analysis of Yeast Protein and Genetic Interactions. *Cold Spring Harbor protocols,* 2016**,** pdb prot088880.

PALMIERI, F. 2004. The mitochondrial transporter family (SLC25): physiological and pathological implications. *Pflugers Archiv : European journal of physiology,* 447**,** 689-709.

PASCAL, L. E., TRUE, L. D., CAMPBELL, D. S., DEUTSCH, E. W., RISK, M., COLEMAN, I. M., EICHNER, L. J., NELSON, P. S. & LIU, A. Y. 2008. Correlation of mRNA and protein levels: cell type-specific gene expression of cluster designation antigens in the prostate. *BMC genomics,* 9**,** 246.

PATIL, K. R. & NIELSEN, J. 2005. Uncovering transcriptional regulation of metabolism by using metabolic network topology. *Proceedings of the National Academy of Sciences of the United States of America,* 102**,** 2685-9.

PAVLOPOULOS, G. A., O'DONOGHUE, S. I., SATAGOPAM, V. P., SOLDATOS, T. G., PAFILIS, E. & SCHNEIDER, R. 2008. Arena3D: visualization of biological networks in 3D. *BMC systems biology,* 2**,** 104.

PENKLER, G., DU TOIT, F., ADAMS, W., RAUTENBACH, M., PALM, D. C., VAN NIEKERK, D. D. & SNOEP, J. L. 2015. Construction and validation of a detailed kinetic model of glycolysis in Plasmodium falciparum. *The FEBS journal,* 282**,** 1481-511.

PERCO, P., MUHLBERGER, I., MAYER, G., OBERBAUER, R., LUKAS, A. & MAYER, B. 2010. Linking transcriptomic and proteomic data on the level of protein interaction networks. *Electrophoresis,* 31**,** 1780-9.

PIRUZIAN, E., BRUSKIN, S., ISHKIN, A., ABDEEV, R., MOSHKOVSKII, S., MELNIK, S., NIKOLSKY, Y. & NIKOLSKAYA, T. 2010. Integrated network analysis of transcriptomic and proteomic data in psoriasis. *BMC systems biology,* 4**,** 41.

PLEASANCE, E. D., CHEETHAM, R. K., STEPHENS, P. J., MCBRIDE, D. J., HUMPHRAY, S. J., GREENMAN, C. D., VARELA, I., LIN, M. L., ORDONEZ, G. R., BIGNELL, G. R., YE, K., ALIPAZ, J., BAUER, M. J., BEARE, D., BUTLER, A., CARTER, R. J., CHEN, L., COX, A. J., EDKINS, S., KOKKO-GONZALES, P. I., GORMLEY, N. A., GROCOCK, R. J., HAUDENSCHILD, C. D., HIMS, M. M., JAMES, T., JIA, M., KINGSBURY, Z., LEROY, C., MARSHALL, J., MENZIES, A., MUDIE, L. J., NING, Z., ROYCE, T., SCHULZ-TRIEGLAFF, O. B., SPIRIDOU, A., STEBBINGS, L. A., SZAJKOWSKI, L., TEAGUE, J., WILLIAMSON, D., CHIN, L., ROSS, M. T., CAMPBELL, P. J., BENTLEY, D. R., FUTREAL, P. A. & STRATTON, M. R. 2010. A comprehensive catalogue of somatic mutations from a human cancer genome. *Nature,* 463**,** 191-6.

PONNIAH, P. 2004. Data Warehousing Fundamentals: A Comprehensive Guide for IT Professionals. *Wiley*.

PRIETO, C., RISUENO, A., FONTANILLO, C. & DE LAS RIVAS, J. 2008. Human gene coexpression landscape: confident network derived from tissue transcriptomic profiles. *PloS one,* 3**,** e3911.

QU, K., GARAMSZEGI, S., WU, F., THORVALDSDOTTIR, H., LIEFELD, T., OCANA, M., BORGES-RIVERA, D., POCHET, N., ROBINSON, J. T., DEMCHAK, B., HULL, T., BEN-ARTZI, G., BLANKENBERG, D., BARBER, G. P., LEE, B. T., KUHN, R. M., NEKRUTENKO, A., SEGAL, E., IDEKER, T., REICH, M., REGEV, A., CHANG, H. Y. & MESIROV, J. P. 2016. Integrative genomic analysis by interoperation of bioinformatics tools in GenomeSpace. *Nature methods,* 13**,** 245-7.

RAMASWAMY, S., ROSS, K. N., LANDER, E. S. & GOLUB, T. R. 2003. A molecular signature of metastasis in primary solid tumors. *Nature genetics,* 33**,** 49-54.

SAHA, R., CHOWDHURY, A. & MARANAS, C. D. 2014. Recent advances in the reconstruction of metabolic models and integration of omics data. *Current opinion in biotechnology,* 29**,** 39-45.

SCHWANHAUSSER, B., BUSSE, D., LI, N., DITTMAR, G., SCHUCHHARDT, J., WOLF, J., CHEN, W. & SELBACH, M. 2011. Global quantification of mammalian gene expression control. *Nature,* 473**,** 337-42.

SHANNON, P., MARKIEL, A., OZIER, O., BALIGA, N. S., WANG, J. T., RAMAGE, D., AMIN, N., SCHWIKOWSKI, B. & IDEKER, T. 2003. Cytoscape: a software environment for integrated models of biomolecular interaction networks. *Genome research,* 13**,** 2498-504.

SHARAN, R., SUTHRAM, S., KELLEY, R. M., KUHN, T., MCCUINE, S., UETZ, P., SITTLER, T., KARP, R. M. & IDEKER, T. 2005. Conserved patterns of protein interaction in multiple species. *Proceedings of the National Academy of Sciences of the United States of America,* 102**,** 1974-9.

SHEN, R., OLSHEN, A. B. & LADANYI, M. 2009. Integrative clustering of multiple genomic data types using a joint latent variable model with application to breast and lung cancer subtype analysis. *Bioinformatics,* 25**,** 2906-12.

SHETH, A. P. & LARSON, J. A. 1990. Federated database systems for managing distributed, heterogeneous, and autonomous databases. *ACM Computing Surveys (CSUR),* 22.3**,** 183-236.

SHLOMI, T., BENYAMINI, T., GOTTLIEB, E., SHARAN, R. & RUPPIN, E. 2011. Genome-scale metabolic modeling elucidates the role of proliferative adaptation in causing the Warburg effect. *PLoS computational biology,* 7**,** e1002018.

SHLOMI, T., CABILI, M. N. & RUPPIN, E. 2009. Predicting metabolic biomarkers of human inborn errors of metabolism. *Molecular systems biology,* 5**,** 263.

SKUSA, A., RUEGG, A. & KOHLER, J. 2005. Extraction of biological interaction networks from scientific literature. *Briefings in bioinformatics,* 6**,** 263-76.

SLOAN, C. D., SHEN, L., WEST, J. D., WISHART, H. A., FLASHMAN, L. A., RABIN, L. A., SANTULLI, R. B., GUERIN, S. J., RHODES, C. H., TSONGALIS, G. J., MCALLISTER, T. W., AHLES, T. A., LEE, S. L., MOORE, J. H. & SAYKIN, A. J. 2010. Genetic pathway-based hierarchical clustering analysis of older adults with cognitive complaints and amnestic mild cognitive impairment using clinical and neuroimaging phenotypes. *American journal of medical genetics. Part B, Neuropsychiatric genetics : the official publication of the International Society of Psychiatric Genetics,* 153B**,** 1060-9.

SNEL, B., LEHMANN, G., BORK, P. & HUYNEN, M. A. 2000. STRING: a web-server to retrieve and display the repeatedly occurring neighbourhood of a gene. *Nucleic acids research,* 28**,** 3442-4.

SNIDER, J., KOTLYAR, M., SARAON, P., YAO, Z., JURISICA, I. & STAGLJAR, I. 2015. Fundamentals of protein interaction network mapping. *Molecular systems biology,* 11**,** 848.

STEFANOVIC, B. 2013. RNA protein interactions governing expression of the most abundant protein in human body, type I collagen. *Wiley interdisciplinary reviews. RNA,* 4**,** 535-45.

STOCKEL, D., KEHL, T., TRAMPERT, P., SCHNEIDER, L., BACKES, C., LUDWIG, N., GERASCH, A., KAUFMANN, M., GESSLER, M., GRAF, N., MEESE, E., KELLER, A. & LENHOF, H. P. 2016. Multi-omics enrichment analysis using the GeneTrail2 web service. *Bioinformatics*.

SUBRAMANIAN, A., TAMAYO, P., MOOTHA, V. K., MUKHERJEE, S., EBERT, B. L., GILLETTE, M. A., PAULOVICH, A., POMEROY, S. L., GOLUB, T. R., LANDER, E. S. & MESIROV, J. P. 2005. Gene set enrichment analysis: a knowledge-based approach for interpreting genome-wide expression profiles. *Proceedings of the National Academy of Sciences of the United States of America,* 102**,** 15545-50.

SUDERMAN, M. & HALLETT, M. 2007. Tools for visually exploring biological networks. *Bioinformatics,* 23**,** 2651-9.

SWAMINATHAN, S., SHEN, L., RISACHER, S. L., YODER, K. K., WEST, J. D., KIM, S., NHO, K., FOROUD, T., INLOW, M., POTKIN, S. G., HUENTELMAN, M. J., CRAIG, D. W., JAGUST, W. J., KOEPPE, R. A., MATHIS, C. A., JACK, C. R., JR., WEINER, M. W. & SAYKIN, A. J. 2012. Amyloid pathway-based candidate gene analysis of [(11)C]PiB-PET in the Alzheimer's Disease Neuroimaging Initiative (ADNI) cohort. *Brain imaging and behavior,* 6**,** 1-15.

SZOSTAK, E. & GEBAUER, F. 2013. Translational control by 3'-UTR-binding proteins. *Briefings in functional genomics,* 12**,** 58-65.

TANAKA, H. 2010. Omics-based medicine and systems pathology. A new perspective for personalized and predictive medicine. *Methods of information in medicine,* 49**,** 173-85.

TEBALDI, T., RE, A., VIERO, G., PEGORETTI, I., PASSERINI, A., BLANZIERI, E. & QUATTRONE, A. 2012. Widespread uncoupling between transcriptome and translatome variations after a stimulus in mammalian cells. *BMC genomics,* 13**,** 220.

TEUSINK, B., PASSARGE, J., REIJENGA, C. A., ESGALHADO, E., VAN DER WEIJDEN, C. C., SCHEPPER, M., WALSH, M. C., BAKKER, B. M., VAN DAM, K., WESTERHOFF, H. V. & SNOEP, J. L. 2000. Can yeast glycolysis be understood in terms of in vitro kinetics of the constituent enzymes? Testing biochemistry. *European journal of biochemistry / FEBS,* 267**,** 5313-29.

THIELE, I., SWAINSTON, N., FLEMING, R. M., HOPPE, A., SAHOO, S., AURICH, M. K., HARALDSDOTTIR, H., MO, M. L., ROLFSSON, O., STOBBE, M. D., THORLEIFSSON, S. G., AGREN, R., BOLLING, C., BORDEL, S., CHAVALI, A. K., DOBSON, P., DUNN, W. B., ENDLER, L., HALA, D., HUCKA, M., HULL, D., JAMESON, D., JAMSHIDI, N., JONSSON, J. J., JUTY, N., KEATING, S., NOOKAEW, I., LE NOVERE, N., MALYS, N., MAZEIN, A., PAPIN, J. A., PRICE, N. D., SELKOV, E., SR., SIGURDSSON, M. I., SIMEONIDIS, E., SONNENSCHEIN, N., SMALLBONE, K., SOROKIN, A., VAN BEEK, J. H., WEICHART, D., GORYANIN, I., NIELSEN, J., WESTERHOFF, H. V., KELL, D. B., MENDES, P. & PALSSON, B. O. 2013. A community-driven global reconstruction of human metabolism. *Nature biotechnology,* 31**,** 419-25.

THIMM, O., BLASING, O., GIBON, Y., NAGEL, A., MEYER, S., KRUGER, P., SELBIG, J., MULLER, L. A., RHEE, S. Y. & STITT, M. 2004. MAPMAN: a user-driven tool to display genomics data sets onto diagrams of metabolic pathways and other biological processes. *The Plant journal : for cell and molecular biology,* 37**,** 914-39.

TIAN, L., GREENBERG, S. A., KONG, S. W., ALTSCHULER, J., KOHANE, I. S. & PARK, P. J. 2005. Discovering statistically significant pathways in expression profiling studies. *Proceedings of the National Academy of Sciences of the United States of America,* 102**,** 13544-9.

TIAN, Q., PRICE, N. D. & HOOD, L. 2012. Systems cancer medicine: towards realization of predictive, preventive, personalized and participatory (P4) medicine. *Journal of internal medicine,* 271**,** 111-21.

TOMITA, M., HASHIMOTO, K., TAKAHASHI, K., SHIMIZU, T. S., MATSUZAKI, Y., MIYOSHI, F., SAITO, K., TANIDA, S., YUGI, K., VENTER, J. C. & HUTCHISON, C. A., 3RD 1999. E-CELL: software environment for whole-cell simulation. *Bioinformatics,* 15**,** 72-84.

TOPFER, N., KLEESSEN, S. & NIKOLOSKI, Z. 2015. Integration of metabolomics data into metabolic networks. *Frontiers in plant science,* 6**,** 49.

UHLEN, M., OKSVOLD, P., FAGERBERG, L., LUNDBERG, E., JONASSON, K., FORSBERG, M., ZWAHLEN, M., KAMPF, C., WESTER, K., HOBER, S., WERNERUS, H., BJORLING, L. & PONTEN, F. 2010. Towards a knowledge-based Human Protein Atlas. *Nature biotechnology,* 28**,** 1248-50.

VAN 'T VEER, L. J., DAI, H., VAN DE VIJVER, M. J., HE, Y. D., HART, A. A., MAO, M., PETERSE, H. L., VAN DER KOOY, K., MARTON, M. J., WITTEVEEN, A. T., SCHREIBER, G. J., KERKHOVEN, R. M., ROBERTS, C., LINSLEY, P. S., BERNARDS, R. & FRIEND, S. H. 2002. Gene expression profiling predicts clinical outcome of breast cancer. *Nature,* 415**,** 530-6.

VAN DE VIJVER, M. J., HE, Y. D., VAN'T VEER, L. J., DAI, H., HART, A. A., VOSKUIL, D. W., SCHREIBER, G. J., PETERSE, J. L., ROBERTS, C., MARTON, M. J., PARRISH, M., ATSMA, D., WITTEVEEN, A., GLAS, A., DELAHAYE, L., VAN DER VELDE, T., BARTELINK, H., RODENHUIS, S., RUTGERS, E. T., FRIEND, S. H. & BERNARDS, R. 2002. A gene-expression signature as a predictor of survival in breast cancer. *The New England journal of medicine,* 347**,** 1999-2009.

VAREMO, L., SCHEELE, C., BROHOLM, C., MARDINOGLU, A., KAMPF, C., ASPLUND, A., NOOKAEW, I., UHLEN, M., PEDERSEN, B. K. & NIELSEN, J. 2015. Proteome- and transcriptome-driven reconstruction of the human myocyte metabolic network and its use for identification of markers for diabetes. *Cell reports,* 11**,** 921-33.

VAZQUEZ, A. 2010. Optimal cytoplasmatic density and flux balance model under macromolecular crowding effects. *Journal of theoretical biology,* 264**,** 356-9.

VON MERING, C., KRAUSE, R., SNEL, B., CORNELL, M., OLIVER, S. G., FIELDS, S. & BORK, P. 2002. Comparative assessment of large-scale data sets of protein-protein interactions. *Nature,* 417**,** 399-403.

WANG, Y., KLIJN, J. G., ZHANG, Y., SIEUWERTS, A. M., LOOK, M. P., YANG, F., TALANTOV, D., TIMMERMANS, M., MEIJER-VAN GELDER, M. E., YU, J., JATKOE, T., BERNS, E. M., ATKINS, D. & FOEKENS, J. A. 2005. Gene-expression profiles to predict distant metastasis of lymph-node-negative primary breast cancer. *Lancet,* 365**,** 671-9.

WEI, Z. & LI, H. 2007. A Markov random field model for network-based analysis of genomic data. *Bioinformatics,* 23**,** 1537-44.

WEINSTEIN, J. N., COLLISSON, E. A., MILLS, G. B., SHAW, K. R., OZENBERGER, B. A., ELLROTT, K., SHMULEVICH, I., SANDER, C. & STUART, J. M. 2013. The Cancer Genome Atlas Pan-Cancer analysis project. *Nature genetics,* 45**,** 1113-20.

WESTERHOFF, H. V. 2015. Network-based pharmacology through systems biology. *Drug discovery today. Technologies,* 15**,** 15-6.

WIERLING, C., KESSLER, T., OGILVIE, L. A., LANGE, B. M., YASPO, M. L. & LEHRACH, H. 2015. Network and systems biology: essential steps in virtualising drug discovery and development. *Drug discovery today. Technologies,* 15**,** 33-40.

WINGENDER, E., DIETZE, P., KARAS, H. & KNUPPEL, R. 1996. TRANSFAC: a database on transcription factors and their DNA binding sites. *Nucleic acids research,* 24**,** 238-41.

WISHART, D. S., JEWISON, T., GUO, A. C., WILSON, M., KNOX, C., LIU, Y., DJOUMBOU, Y., MANDAL, R., AZIAT, F., DONG, E., BOUATRA, S., SINELNIKOV, I., ARNDT, D., XIA, J., LIU, P., YALLOU, F., BJORNDAHL, T., PEREZ-PINEIRO, R., EISNER, R., ALLEN, F., NEVEU, V., GREINER, R. & SCALBERT, A. 2013. HMDB 3.0--The Human Metabolome Database in 2013. *Nucleic acids research,* 41**,** D801-7.

WISHART, D. S., KNOX, C., GUO, A. C., EISNER, R., YOUNG, N., GAUTAM, B., HAU, D. D., PSYCHOGIOS, N., DONG, E., BOUATRA, S., MANDAL, R., SINELNIKOV, I., XIA, J., JIA, L., CRUZ, J. A., LIM, E., SOBSEY, C. A., SHRIVASTAVA, S., HUANG, P., LIU, P., FANG, L., PENG, J., FRADETTE, R., CHENG, D., TZUR, D., CLEMENTS, M., LEWIS, A., DE SOUZA, A., ZUNIGA, A., DAWE, M., XIONG, Y., CLIVE, D., GREINER, R., NAZYROVA, A., SHAYKHUTDINOV, R., LI, L., VOGEL, H. J. & FORSYTHE, I. 2009. HMDB: a knowledgebase for the human metabolome. *Nucleic acids research,* 37**,** D603-10.

WISHART, D. S., TZUR, D., KNOX, C., EISNER, R., GUO, A. C., YOUNG, N., CHENG, D., JEWELL, K., ARNDT, D., SAWHNEY, S., FUNG, C., NIKOLAI, L., LEWIS, M., COUTOULY, M. A., FORSYTHE, I., TANG, P., SHRIVASTAVA, S., JERONCIC, K., STOTHARD, P., AMEGBEY, G., BLOCK, D., HAU, D. D., WAGNER, J., MINIACI, J., CLEMENTS, M., GEBREMEDHIN, M., GUO, N., ZHANG, Y., DUGGAN, G. E., MACINNIS, G. D., WELJIE, A. M., DOWLATABADI, R., BAMFORTH, F., CLIVE, D., GREINER, R., LI, L., MARRIE, T., SYKES, B. D., VOGEL, H. J. & QUERENGESSER, L. 2007. HMDB: the Human Metabolome Database. *Nucleic acids research,* 35**,** D521-6.

WRUCK, W., KASHOFER, K., REHMAN, S., DASKALAKI, A., BERG, D., GRALKA, E., JOZEFCZUK, J., DREWS, K., PANDEY, V., REGENBRECHT, C., WIERLING, C., TURANO, P., KORF, U., ZATLOUKAL, K., LEHRACH, H., WESTERHOFF, H. V. & ADJAYE, J. 2015. Multi-omic profiles of human non-alcoholic fatty liver disease tissue highlight heterogenic phenotypes. *Scientific data,* 2**,** 150068.

YAMADA, T., LETUNIC, I., OKUDA, S., KANEHISA, M. & BORK, P. 2011. iPath2.0: interactive pathway explorer. *Nucleic acids research,* 39**,** W412-5.

YEUNG, E. S. 2011. Genome-wide correlation between mRNA and protein in a single cell. *Angewandte Chemie,* 50**,** 583-5.

YIZHAK, K., BENYAMINI, T., LIEBERMEISTER, W., RUPPIN, E. & SHLOMI, T. 2010. Integrating quantitative proteomics and metabolomics with a genome-scale metabolic network model. *Bioinformatics,* 26**,** i255-60.

YIZHAK, K., CHANETON, B., GOTTLIEB, E. & RUPPIN, E. 2015. Modeling cancer metabolism on a genome scale. *Molecular systems biology,* 11**,** 817.

YU, M. K., KRAMER, M., DUTKOWSKI, J., SRIVAS, R., LICON, K., KREISBERG, J., NG, C. T., KROGAN, N., SHARAN, R. & IDEKER, T. 2016. Translation of Genotype to Phenotype by a Hierarchy of Cell Subsystems. *Cell systems,* 2**,** 77-88.

ZHANG, B., WANG, J., WANG, X., ZHU, J., LIU, Q., SHI, Z., CHAMBERS, M. C., ZIMMERMAN, L. J., SHADDOX, K. F., KIM, S., DAVIES, S. R., WANG, S., WANG, P., KINSINGER, C. R., RIVERS, R. C., RODRIGUEZ, H., TOWNSEND, R. R., ELLIS, M. J., CARR, S. A., TABB, D. L., COFFEY, R. J., SLEBOS, R. J. & LIEBLER, D. C. 2014. Proteogenomic characterization of human colon and rectal cancer. *Nature,* 513**,** 382-7.

ZHANG, M., LIANG, L., XU, M., QURESHI, A. A. & HAN, J. 2011. Pathway analysis for genome-wide association study of basal cell carcinoma of the skin. *PloS one,* 6**,** e22760.

ZHANG, Y., DENG, Z., JIANG, H. & JIA, P. 2007. Inferring gene regulatory networks from multiple data sources via a dynamic bayesian network with structural EM, in Data Integration in the Life Sciences. 4544**,** 204–214.